Genome-wide characterization of STAT1 and NFκB-mediated Signal Integration in Vascular Inflammation

doctoral thesis

by

Anna Piaszyk-Borychowska

prepared under supervision of

Prof. dr hab. Johannes A.R. Bluyssen

Department of Human Molecular Genetics
Institute of Molecular Biology and Biotechnology
Faculty of Biology
Adam Mickiewicz University in Poznań

Poznań 2019

Całogenomowa analiza integracji szlaków sygnałowych czynników STAT1 i NFκB w procesie zapalnym naczyń krwionośnych

rozprawa w języku angielskim

ze streszczeniem w języku polskim

Autor:

Anna Piaszyk-Borychowska

przygotowana pod kierunkiem:

Prof. dr hab. Johannes A.R. Bluyssen

Zakład Genetyki Molekularnej Człowieka
Instytut Biologii Molekularnej i Biotechnologii
Wydział Biologii
Uniwersytet im. Adama Mickiewicza w Poznaniu

Poznań 2019

CONTENTS

Chapter 1. Introduction

Unresolved inflammation - a trigger for multiple diseases

Inflammation is an inevitable adaptive process which protects organisms from external microbial infection and internal host tissue damage. Constant exposition towards noxious stimuli results in ongoing process of inflammatory response activation, followed by its resolution, when affected tissues regain their optimal structure and functionality. However, multiple processes like inadequate production of resolution mediators (cytokines, protease inhibitors, reactive oxygen intermediates) or persistent exposition to pro-inflammatory stimuli of exogenous origin, impedes inflammation resolution by immune system components (Nathan and Ding 2010). Therefore, chronic inflammation which cannot be naturally resolved by immune system, may be detrimental and eventually become a major driver of multiple disease types. Indeed, inflammation was shown to play a crucial role in pathogenesis of cancer and aging-related diseases (Grivennikov et al. 2010, Chung et al. 2009, Khansari et al. 2009), neurodegenerative diseases, including Alzheimer's disease (Minghetti 2005, Galasko and Montine 2010), rheumatoid arthritis (Firestein and McInnes 2017), Systemic Lupus Erythematosus (SLE) and Cardiovascular Diseases (CVD) (Manzi and Wasko 2000, Libby 2006), among many others.

Global causes of death

According to World Health Organisation (WHO), in 2016, 41 million people died due to Noncommunicable Diseases (NCD), what accounts for 71% of all deaths world-wide. Among those, 17.9 million people died from CVD, while only 9 million deaths were caused by cancer, 3.8 million by Chronic Respiratory Disease (CRD) and 1.6 million by diabetes (Fig.1.1). Therefore heart and blood vessels disorders, encompassing myocardial infarction, heart failure and stroke, currently remain the leading cause of mortality world-wide (WHO 2018). The dominant cause of CVD is atherosclerosis, characterized as chronic, inflammatory disease of the arteries (Hansson 2005).

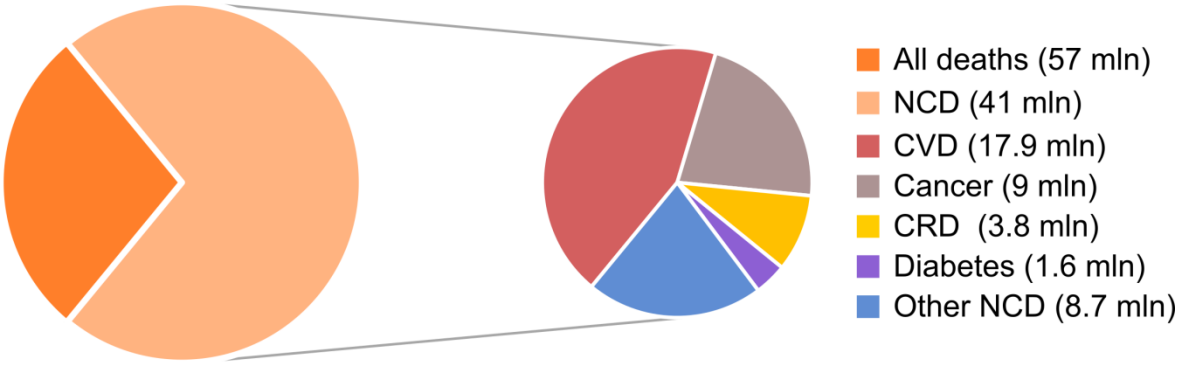

Figure 1. 1. Global causes of death in 2016.

Own interpretation based on *WHO Statistics 2018.*

Structure of the vessel wall

Cardiovascular system consists of the blood vessels which distribute blood containing oxygen, nutrients, hormones as well as waste products and carbon dioxide (CO_2), maintain blood pressure and constant body temperature (van Thiel et al. 2017). In order to perform their functions, healthy vessels represent a specific 3-layered structure: an outer, middle and inner layer, called *tunica adventitia*, *tunica media* and *tunica intima*, respectively (Fig.1.2). The latter one is built of Endothelial Cells (EC) monolayer called 'endothelium' and traces of connective tissue, which together form an even surface allowing for undisturbed blood flow. In the arteries, the inner layer is separated from *tunica media* by an internal elastic membrane, which mediates vascular tone, contraction and permeability for circulating products. The middle layer, mainly consists of smooth muscle fibres and extracellular matrix. *Tunica media* is the thickest layer in the arteries, therefore stabilizes their structure, regulates elasticity, responsiveness to external stimuli as well as modulates blood pressure. External elastic membrane separates *tunica media* and *tunica adventitia*. The most outer layer contains collagen and elastic fibres, small vessels (*vasa vasorum*) and autonomic nerves together with the multiple cell types including fibroblasts and Macrophages (MΦ). *Tunica adventitia* anchors the vessel in the surrounding tissues and provides architectural support (van Thiel et al. 2017). Accordingly, the blood vessels consist of multiple cell types and present complex structure, which supports their functions.

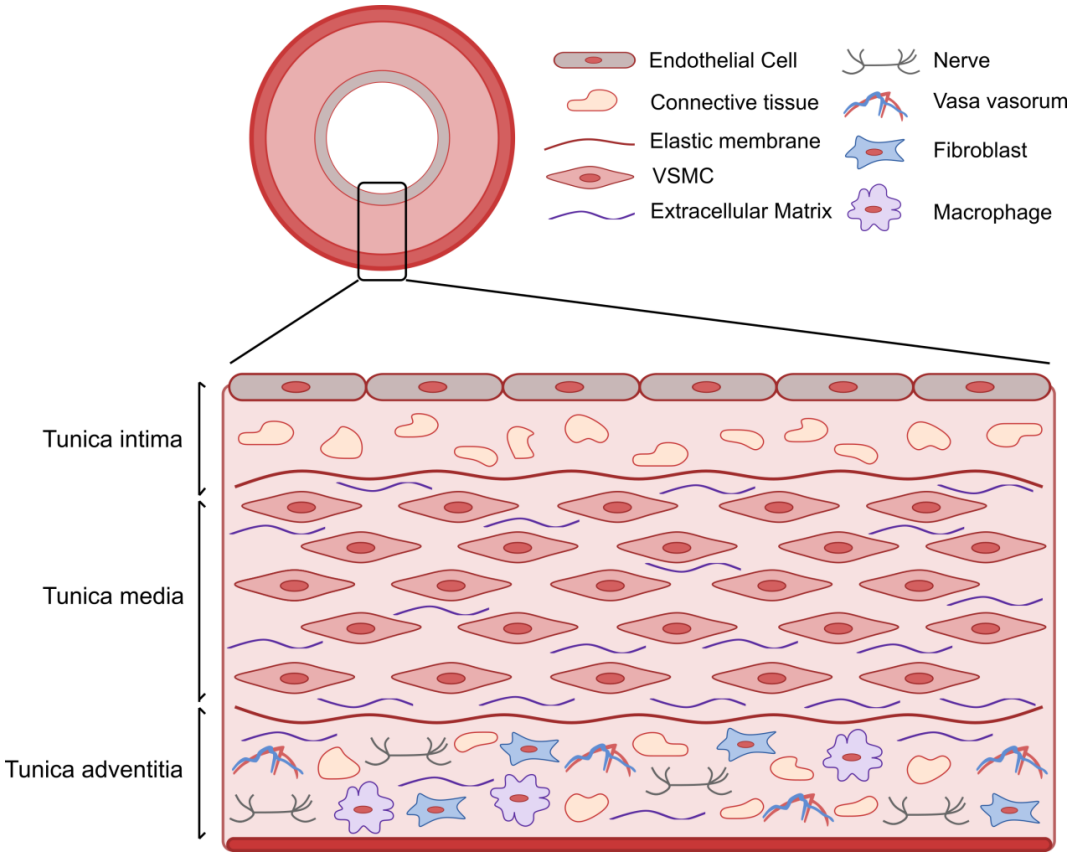

Figure 1. 2. Structure of the artery wall, depicting 3-layered structure.

Paradigms of atherosclerosis pathogenesis

In the presence of vascular pro-inflammatory triggers, arteries homeostasis may be altered, what at very end leads to atherosclerosis development. During past decades there arouse several concepts trying to elucidate the mechanisms driving atherosclerosis, which finally shaped our current view of the disease pathogenesis. One of the first theories, 'encrustation hypothesis', assumed that atherosclerotic lesions are derived from surface deposits and consist of organised thrombi. Yet later proposed 'infiltration theory' contradicted these observations by proposing that plaques have subendothelial composition and result from accumulation of plasma constituents in *intima adventitia*. On the other hand, 'lipid theory' of atherosclerosis ascribed the origin of the disease predominantly to hypercholesterolemia. Development of the latter theory led to the formulation of 'response to injury' model, in which authors proposed that increased levels of circulating lipoproteins, especially oxidized Low-density Lipoprotein (ox-LDL), cause injury of the endothelium, what is a initiating step in atherogenesis [rewieved in: (Monaco and Lutgens 2017)]. Although already suggested in

1856 by Virchow, the latest and constantly examined paradigm finally formulated by Ross in 1999 proposes that atherosclerosis is an inflammatory disorder (Ross 1999).

Consecutive stages of atherosclerotic plaque development

Formation of the atherosclerotic plaque is a gradual process which encompasses a cascade of the following events (Fig.1.3). The very first incident is endothelium activation by injurious stimuli including shear stress, turbulent blood flow, oxidative stress, chronic contact with microbes or endogenous molecules released in response to tissue damage and ox-LDL (Fig.1.3A), which affect EC constitutive functions, including regulation of the vessel wall permeability and maintenance of non-adhesive surface for circulating cells (Sikorski et al. 2012, Manduteanu and Simionescu 2012). Arterial areas which are more prone to the disturbed blood flow, such as branch points or the inner wall of curvatures, were shown to be enriched in EC phenotype presenting elevated expression of pro-atherogenic and decreased expression of athero-protective genes (Gimbrone et al. 2000, Volger et al. 2007). Therefore it seems that these sites are sensitized for further atheroma formation, yet additional pro-inflammatory factors are necessary for subsequent atherosclerosis development. Once injury occurs, EC start to release adhesion molecules (P-selectin, E-selectin, ICAM1, VCAM1) and various cytokines and chemokines (CCL2, CCL5, CXCL8, CX3CL1, CXCL10) (Fig.1.3B), to attract circulating monocytes (Fig.1.3C) and commence a robust inflammatory response (Manduteanu and Simionescu 2012). Following chemotaxis, immune cell precursors adhere to the dysfunctional EC and undergo diapedesis to the vessel intima (Fig.1.3C). In the presence of the differentiation factors including Macrophage-colony Stimulating Factor (M-CSF) and Granulocyte-macrophage Colony-stimulating Factor (GM-CSF), infiltrated monocytes give rise to the various subsets of MΦ and Dendritic Cells (DC), respectively (Fig.1.3D). Intima-resident MΦ and DC ingest the accumulated lipoproteins via scavenger receptors and become cholesterol-laden foam cells (Fig.1.3E). Professional antigen-presenting cells, like MΦ, DC and B cells present foreign antigens for recognition by T helper subsets, including T_H1, T_H2, T_H17 and T_{REG} cells. Various T cells types were detected in the area of atherosclerotic plaques, yet T_H1 cells serve the most pro-atherogenic role (Packard et al. 2008, Witztum and Lichtman 2014, Jonasson et al. 1986). Activated T cells produce pro-inflammatory cytokines, including Interferon gamma (IFNγ), IL6 and IL12, thus contribute to the acceleration of ongoing inflammation in the vessel. IFNγ released in the atheroma activates not only immune

cell precursors, MΦ, DC, but also EC and Vascular Smooth Muscle Cells (VSMC), to secrete pro-inflammatory cytokines and chemokines, matrix metalloproteinases and Reactive Oxygen Species (ROS) (Mallat et al. 2009). In addition, similar pro-inflammatory role has been assigned to IFN alpha(α), predominantly produced by atherosclerotic plaque-resident leukocytes or plasmacytoid DC (Mahlakõiv et al. 2015, Swiecki and Colonna 2011). Oxidative stress promotes modification of circulating LDL. Ox-LDL particles uptake is thought to be one of the crucial pathological events in the nascent atherosclerotic plaques (Moore and Freeman 2006). Immune cells express multiple receptors f.ex. Pattern Recognition Receptors (PRR) (Toll-like Receptors [TLR] and scavenger receptors) and cytokine receptors (interleukin and growth factor receptors) by which they recognize signals from the environment. These signals encompass multiple Pattern-Associated Molecular Patterns (PAMP), released by microorganisms in the host organism and Damage-Associated Molecular Patterns (DAMP), molecules released by damaged and necrotic cells, which are formed under stress condition in the vasculature (f.ex. dyslipidemia, hypertension or diabetes). Upon activation, immune cells release plethora of the pro-inflammatory cytokines and chemokines, which perpetuate inflammation and sustain constant monocytes and T cell infiltration to the atherosclerotic lesion (Fig.1.3F) (Lutgens et al. 2017, Rai and Agrawal 2017). Finally, immune cells undergo necrosis or apoptosis what leads to the formation of atherosclerotic plaque necrotic core (Fig.1.3G), a key component of unstable plaques at the latter stage of the disease (Kavurma et al. 2017). In the inflammatory milieu, VSMC migrating from *tunica intima* as well as *tunica media*, take-up lipoproteins and transform into foam cells alike immune cells, what together with an aberrant migration and proliferation, contributes to the atherosclerosis plaque formation (Fig.1.3H) (Allahverdian et al. 2014). In advanced lesions, VSMC proliferation followed by extracellular matrix synthesis may be entirely beneficial process, leading to formation of the fibrous cap and plaque stabilization. Yet ongoing VSMC apoptosis, cell senescence, collagen and extracellular matrix breakdown, contribute together to fibrous thinning, plaque rupture and increased inflammation (Doran et al. 2008). Consecutive cycles of atheroma rupture and repair result in vessel luminal narrowing and VSMC extracellular calcification in the advanced plaques (Naik et al. 2012). Excessive inflammatory and immune responses, communicated by various vascular and immune cells, contribute to the local inflammation and vascular dysfunction, followed by the atherosclerosis plaque formation on the inside surface of the large and medium-sized arteries. Over time, the atherosclerotic plaque formation results in the narrowing of the artery lumen and finally limited distribution of an oxygen and nutrients to the organs throughout the body.

Furthermore, under certain conditions atherosclerotic plaque may rupture. Released content of the necrotic core forms a blood clot (Fig.1.3I), which may block the blood flow, leading to the life-threatening stage of the disease, myocardial infarction or stroke (Chmielewski et al. 2016).

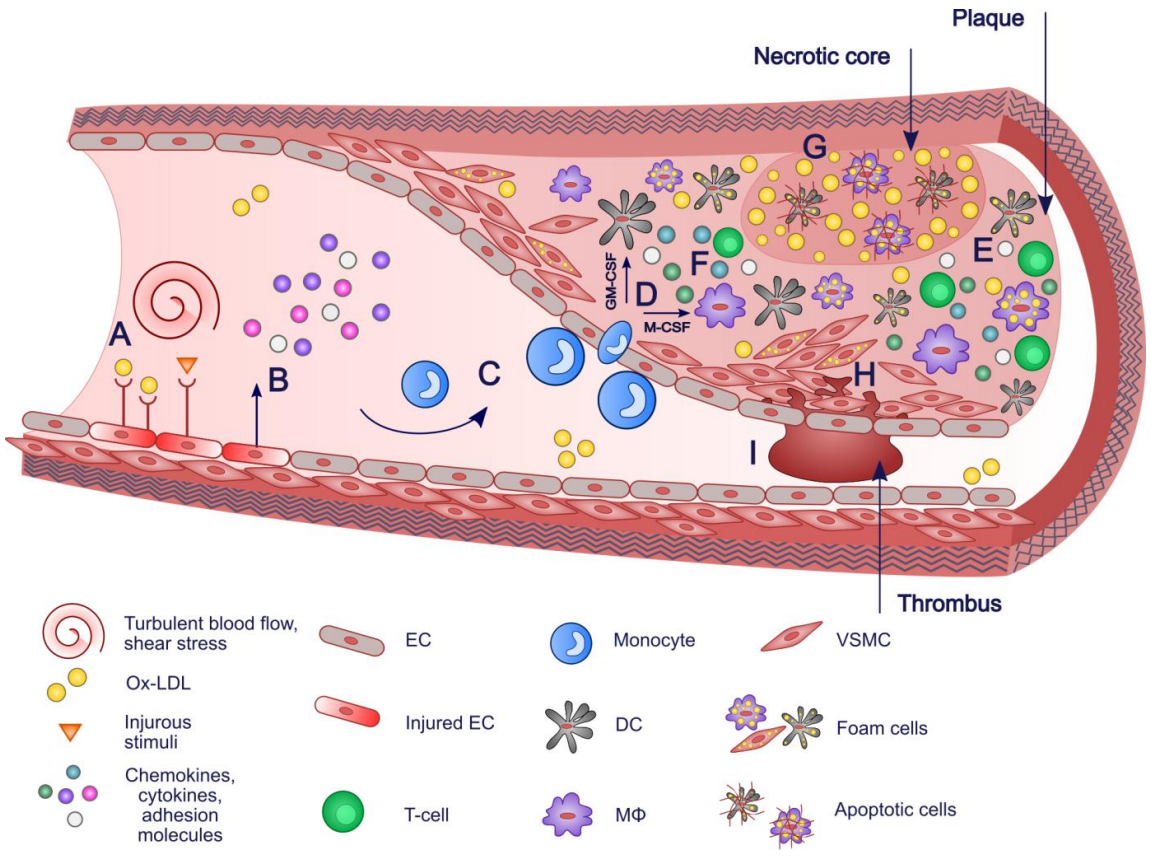

Figure 1. 3. Atherosclerotic plaque progression.

Role of MΦ and VSMC in healthy and inflamed vessel

MΦ are monocyte-derived cells which support tissue functions they reside in by mediating its steady-state homeostasis. As mentioned, these phagocytic cells are equipped with surface-located PRR, which recognize PAMP, to efficiently neutralize spread of invading pathogens, infected cells and cellular debris. In response to harmful external cues, MΦ release plethora of inflammatory cytokines to alert protected cells and prevent excessive inflammation. Importantly, MΦ play a crucial role in mediating tissue healing and repair. Finally, MΦ act at the border of innate and adaptive immunity, by presenting antigens to T

cells (Frodermann and Nahrendorf 2018, Shirai et al. 2015). However, in some circumstances immune system barriers are not sufficient to protect the tissue against intensive inflammation. Such unresolved, prolonged inflammation underlies the pathophysiology of multiple diseases, including CVD (Tabas and Glass 2013). As such, numerous MΦ were detected at initial as well as advanced atherosclerotic plaques and burdened with a major role in potentiating redundant inflammatory response (Hansson and Hermansson 2011). Pathogenic roles of MΦ during vascular inflammation are mainly correlated with secretion of the pro-inflammatory cytokines, including IL1β, IL6, IL8, IL12, IL23, IL27, TNFα, chemokines like MCP1, CCR2, CCL5, CXCL10 and matrix metalloproteinases, MMP1, MMP2, MMP3, MMP8, MMP9 (Shirai et al. 2015). Circulating cytokines activate EC, by inducing expression of VCAM1 and ICAM1, which facilitate subsequent recruitment of immune cells (f.ex. monocytes and leukocytes) to the place of vascular inflammation (Moore et al. 2013). Moreover, cytokines mediate oxidative stress through ROS and reactive nitrogen species, which lead to the damage of membranes, proteins and DNA. NADPH oxidase Nox2 is one of the ROS sources produced by MΦ (Waldo et al. 2008). During later stages of the disease, pro-inflammatory mediators including matrix metalloproteinases, potentiate vascular tissue injury and cell apoptosis, especially of EC and VSMC. This results in the cell matrix degradation, vascular wall weakening and atherosclerotic plaque destabilization (Shirai et al. 2015). Moreover, excessive uptake of lipoprotein-derived cholesterol by MΦ lead to the production of foam cells, which form lipid deposition within the artery, narrowing its lumen and abrogating undisturbed blood flow (Yu et al. 2013).

In a steady-state VSMC together with elastin sheets of extracellular matrix build a muscular, thickest layer of the arteries, called *tunica media*. Together they provide a structure and elasticity of the vessel wall. VSMC main role is to regulate vessel lumen dimension, vessel tone and blood pressure, by repetitive processes of vasodilation (widening of the vessel lumen) and vasoconstriction (narrowing of the vessel lumen) (van Thiel et al. 2017). In a healthy vessel they remain quiescent and do not divide. However exposed to the pro-inflammatory stimuli, VSMC may change their phenotype, morphology and alike MΦ, contribute to the pathophysiology of atherosclerosis, but also restenosis, hypertension, asthma and vascular aneurysms (van Thiel et al. 2017). VSMC are the most abundant cell type identified within the atherosclerotic lesions. In inflamed vessel, injured endothelium release cytokines and growth factors which together with accumulated ox-LDL induce VSMC migration from *tunica media* to the vessel lumen and promote VSMC phenotype switch from

quiescent to synthetic. The latter one is characterized by altered contractile protein expression, high rate of cell proliferation and migration, as well as excessive release of extracellular matrix (Lutgens et al. 2017). Extracellular matrix production plays an important role during vascular repair, thus may stabilize formation of the atherosclerotic cap and protects against the plaque rupture (Lutgens et al. 2017). Additionally, VSMC release multiple pro-inflammatory mediators including cytokines (TNFα or IL1β) and matrix metalloproteinases (MMP9), which together increase synthesis of adhesion molecules, plaque vulnerability, cell migration and proliferation rate (Lin et al. 2008). Moreover, VSMC express LDL receptor, VLDL receptor, CD36, and type I and type II scavenger receptors which promote lipid uptake and induce cell conversion to VSMC-derived foam cells. It was reported that at least 50% of foam cells population identified within human coronary artery plaques were VSMC-derived cells (Allahverdian et al. 2014). Finally, advanced atherosclerotic lesions undergo the process of calcification. VSMC contribute to this process and upon calcification express osteogenic markers, like Bone-Morphogenic Protein-2 (BMP-2), osteopontin, osteonectin and Runx2 (Lutgens et al. 2017).

IFNα, IFNγ and LPS in atherosclerosis pathogenesis

IFN were discovered by Isaacs and Lindenmann in 1957 as cytokines that have an ability to inhibit virus replication (ISAACS and LINDENMANN 1957). Later it became clear, that canonical activity of IFN encompasses plethora of cellular processes from embryonic development, cell differentiation, growth and motility to the inflammatory response, innate and adaptive immunity. Interestingly, since it was proven that atherosclerosis is an inflammation-induced condition, several lines of evidence suggest that type II IFNγ and type I IFNα play a key role in disease pathogenesis.

IFNγ is a sole member of type II IFN, mainly secreted by T cells and MΦ, acting to protect cells against various pathogens (Schroder et al. 2004). In the context of atherosclerosis, IFNγ is indeed mainly derived from T_H1 lymphocytes and activated MΦ, yet also other atheroma interacting cell types were reported to secrete type II IFN, including cytotoxic CD8+ lymphocytes, natural killer cells, B cells and VSMC (Leon and Zuckerman 2005). Crucial role for IFNγ in atherosclerotic lesion development and progression was proven both in Apolipoprotein E (ApoE) and LDL Receptor (LDLR) Knock-out (KO) mouse models (Gupta et al. 1997, Buono et al. 2003). Additionally, aortic SMC exposure to IFNγ,

resulted in increased VCAM1 expression (Li et al. 1993), while IFNγ inhibition was related with ICAM1 down-regulation, followed by reduced neointima formation in the artery (Kusaba et al. 2007). It suggests that IFNγ may prompt initial atherosclerosis onset, by affecting adhesion molecules expression, strictly related with endothelium dysfunction. IFNγ was also associated with accelerated oxidative stress, by increasing NADPH oxidase, known ROS production inducer, expression in MΦ (Casbon et al. 2012). Additionally, IFNγ may affect foam cells formation by modulating cholesterol and lipid trafficking through scavenger receptor SR-A, reported to become up-regulated in VSMC in response to IFN stimulation (Li et al. 1995). Finally, type II IFN was associated with altered VSMC proliferation and migration, which processes are hallmarks of atherosclerotic plaque development (Shimokado et al. 1994).

Type I IFN constitute a large class of IFN, which encompasses IFNα, -β, -ε, -κ, and -ω, all of which share significant structural homology and are secreted by various cell types. The most well-studied type I IFN is IFNα, encoded by 13 homologous genes (Samuel 2001). Alike IFNγ, type I IFN has been linked with atherosclerosis pathogenesis. As such, IFNα stimulation resulted in increased MΦ ox-LDL uptake followed by foam cell formation (Li et al. 2011). Moreover, IFNα decreased the number of endothelial progenitor cells and abrogated the homeostasis between EC apoptosis and repair (Denny et al. 2007, Thacker et al. 2010). These alterations may lead to increased vascular dysfunction, especially in SLE patients who suffer from premature atherosclerosis. In IFNα treated LDLR KO mice there was observed a significant increase in the atherosclerotic plaque area, due to the elevated plasma cholesterol and triglyceride levels (Levy et al. 2003). Others found that IFNβ-IFNAR1-STAT1 signaling increased MΦ-EC association and provided evidence for a role of myeloid type I IFN in the progression of atherosclerosis (Goossens et al. 2010).

TLR belong to the group of receptors that initiate inflammatory signaling in response to the detection of molecules associated with microbial infection (PAMP) or tissue damage (DAMP). Recently, TLR4 has been associated with etiology of CVD. TLR4 was found to be up-regulated in human atherosclerotic lesions with active co-localizing Nuclear Factor-kappa B (NFκB) (Edfeldt et al. 2002). Moreover, increased TLR4 expression was correlated with endothelial dysfunction in cardiac transplant recipients as well as pathology of unstable angina and acute myocardial infarction (Methe et al. 2004, Methe et al. 2005). Additional evidence for TLR4 role in vascular inflammation comes from the animal models. Mice deficient in TLR4 or MyD88 (important signaling adapting molecule) have reduced

atherosclerosis, displayed lower levels of pro-inflammatory cytokines and decreased lipid levels in the plaques (Michelsen et al. 2004). Moreover, in ApoE-deficient mice, TLR4 contributed to an early stage foam cell accumulation and atherosclerosis progression (Higashimori et al. 2011). Worth mentioned, there was found a link between multiple bacterial and viral infections and atherosclerosis pathogenesis. Evidence comes mainly from the animal models of atherosclerosis and associates *Chlamydia pneumoniae, Mycoplasma pneumoniae, Helicobacter pylori, Enterobacter hormaechei* infection with vascular dysfunction [reviewed in: (Campbell and Rosenfeld 2015)].

IFNα and IFNγ Signaling Pathways and their Mediators - STAT and IRF

IFN mediate downstream effects via Janus Kinase/Signal Transducers and Activators of Transcription (JAK-STAT) signaling pathway (Fig.1.4A-H). Crucial mediators of this signaling cascade are STAT and IFN Regulatory Factors (IRF).

STAT belong to a family of Transcription Factors (TF) that consists of seven members: STAT1, STAT2, STAT3, STAT4, STAT5α, STAT5β and STAT6, presenting highly evolutionary conserved structure. As such, STAT proteins are built of 7 conserved domains, including N-terminal domain (N), coiled-coil domain (CC), DNA-binding domain (DBD), linker domain (L), Src Homology 2 domain (SH2), tyrosine phosphorylation site (Y) and transcriptional activation domain (TAD). The N is mostly involved in STAT dimer formation. The CC facilitates an interaction with non-STAT TF, like IRF9, and transcriptional complexes nuclear translocation. The DBD is crucial for directing STAT binding to cognate motifs in the target gene promoters. The L mediates the proper conformation of adjacent STAT protein domains. The most evolutionary conserved domain, SH2, is necessary for STAT binding to cognate receptor by association with phospho-tyrosine residues. Moreover it mediates formation of STAT active dimer. By cause of phosphorylation, preserved tyrosine is exposed and mediates an interaction with SH2 domain in the partner STAT protein. The TAD is the least conserved domain among STAT and participates in the recruitment of General Transcription Machinery (GTM) elements in STAT-specific manner, therefore regulates gene transcription (Blaszczyk et al. 2016, Ihle 2001, Schindler et al. 2007, Schindler and Plumlee 2008).

IRF family is represented by 9 proteins in mammalian cells (IRF1 to 9). They all share a highly conserved DBD, characterized by a helix-loop-helix motif with five tryptophan repeats. Three of these repeats recognize DNA sequences they contact with. DBD domains are very similar among all IRF and recognize common DNA motifs. IRF were shown to bind to IFN-Stimulated Response Element (ISRE), a consensus site identified mainly in the promoters of IFNα-induced genes. Ability of IRF to modulate stimuli-dependent gene transcriptional activation depends not only on their ability to recognize specific DNA binding sequences in target gene regulatory regions, but also on their interactions with other IRF or non-IRF TF, like STAT (Paun and Pitha 2007). IRF3 and IRF7 mediate expression of IFN I, while IRF9 in a form of ISGF3 complex (pSTAT1/pSTAT2 heterodimer associated with IRF9) participates in the regulation of the downstream IFNα-dependent gene expression (Ozato et al. 2007). Additionally, IRF1 and IRF8 are crucial mediators of IFN II-mediated gene activation (Gough et al. 2008).

As mentioned, STAT and IRF mediate IFN-dependent signaling pathways. IFNα binds to the receptor composed of IFNAR1/IFNAR2 subunits associated with Janus kinases JAK1 and TYK2 (Fig.1.4A). Similarly, IFNγ-specific receptor consists of IFNGR1/IFNGR2 subunits connected with JAK1 and JAK2 kinases (Fig.1.4B). Upon ligand binding to its cognate receptor, JAK are brought into close proximity to allow auto-phosphorylation. Once activated, kinases phosphorylate specific tyrosine residues in the cytoplasmic region of the receptor, creating docking sites for STAT family members (Fig.1.4C-D) (Kiu and Nicholson 2012, Wesoly et al. 2007). Receptor-bound STAT are tyrosine phosphorylated, in a JAK-dependent manner, allowing for STAT homo- and heterodimerization (Fig.1.4E-G). Next, STAT dissociate from the receptor and translocate into the nucleus. In the canonical IFN I signaling pathway, IFNα-stimulation results in formation of STAT1/STAT2 heterodimers which after subsequent interaction with IRF9 form ISGF3 complex binding to ISRE, with the consensus sequence of AGTTTCNNTTTCC (Darnell et al. 1994). On the other hand, IFNγ-activated canonical pathway results in formation of stable STAT1 homodimers, known as γ-activated Factor (GAF), which bind to IFNγ-activated Sequence (GAS), consensus sequence: NTT(C/A)(C/T)(C/T)N(T/G)AAA, present in the promoters of Interferon-stimulated Genes (ISG) (Decker et al. 1989) (Fig.1.4H). Among IFNγ-activated genes in STAT1-dependent way there are IRF1 and IRF8 TF, which act in a delayed manner, thus may sustain the first wave of IFN-dependent signaling. IRF1 can form homodimers binding to ISRE element in target gene promoters, while IRF8 cannot bind DNA alone. Therefore it dimerizes with IRF1

or other binding partners, like MΦ-specific TF PU.1, activating ISRE or ISRE-like elements (Wesoly et al. 2007). Additionally, IRF1 collaborates with STAT1 to activate IFNγ-responsive genes, like *GBP1/2* and *gp91phox* (Ramsauer et al. 2007, Kumatori et al. 2002).

Although IFNα mainly induces formation of ISGF3 complex, while IFNγ predominantly activates formation of STAT1 homodimers, relevance of other non-canonical complexes in IFN signaling was reported. Hence, STAT1 may regulate IFNα-dependent gene expression not only in a form of canonical ISGF3, but also as GAF complex. Others demonstrated in IFNα stimulated MΦ, that the presence of TAD domain and its phosphorylation on Ser727 were inevitable for STAT1-dependent activation of *Mx*, a target gene for ISGF3, but also *Irf1* regulated by STAT1 homodimers (Pilz et al. 2003). Additionally, alternative STAT1/STAT2 heterodimer formed upon IFNα stimulation was involved in transcriptional activation of *Irf1* in U2A cells lacking IRF9 (Li et al. 1996). Moreover, PCR-assisted binding site selection procedure revealed that STAT1/STAT2 could participate in the transcriptional activation of the subset of IFNα-activated ISG containing GAS-like site in gene promoters (Ghislain et al. 2001). There is also accumulating evidence for a role of STAT2 homodimers coupled with IRF9 (ISGF3-like complex) in transcriptional activation of IFNα-induced ISRE-containing genes (Bluyssen and Levy 1997). Type I IFN-dependent ISG expression in STAT1 depleted cells was later observed among others by Kraus et al., Poat et al. and Błaszczyk et al. (Kraus et al. 2003, Poat et al. 2010, Blaszczyk et al. 2015). On the other hand, type II IFN stimulation of primary Mouse Embryonic Fibroblasts (MEF) resulted in non-canonical ISGF3 complex formation and ISRE-containing gene expression. In support of a potential role for STAT2 in IFNγ driven gene expression, IFN-dependent STAT2 phosphorylation and subsequent ISGF3 formation was detected in MEF alike (Zimmermann et al. 2005, Matsumoto et al. 1999). Whatsmore, although presenting lower ISRE-binding affinity in comparison to ISGF3, an alternative complex of STAT1 homodimers (GAF) associated with IRF9 (STAT1/STAT1-IRF9) was formed after IFNγ stimulation, leading to the elevated gene expression in STAT2 independent manner (Bluyssen et al. 1995, Kimura et al. 1996). Similar observations were made in IFNγ-stimulated 2fTGH cells, proving STAT1/STAT1-IRF9 complex role in the regulation of *CXCL10* expression (Majumder et al. 1998). Involvement of non-canonical transcriptional complexes activated by IFNα and IFNγ in JAK-STAT signaling pathway is illustrated in Fig.1.4G-H.

Therefore, different IFNα- and/or IFNγ-induced STAT-IRF TF complexes work together in a combinatorial manner to rapidly induce the expression of hundreds of genes that

amplify inflammatory response, exert antimicrobial activities and initiate development of acquired immunity. Importantly, IFN I or IFN II activate overlapping, but also distinct pools of transcriptional complexes. F.ex. IFNα stimulation results in predominant formation of ISRE-recruited ISGF3 motifs, while IFNγ induces GAF enrollment to GAS sites. Consequently, IFN seem to activate distinct group of genes, to mediate either IFNα- or IFNγ-specific effects. On the other hand, there could be observed an overlap in the induced transcriptional targets activated by these two IFN types. Although the mechanisms underlying transcriptional regulation of the individual genes activated by IFNα and IFNγ were thoroughly studied since the 80s, hitherto no comprehensive genome-wide comparison between transcriptional effects of these two IFN was performed. Remarkably, identification of IFN-dependent TF-DNA interactions and associated chromatin modifications would be crucial for full understanding of transcriptional regulation of pro-inflammatory genes involved in the pathogenesis of diseases, such as atherosclerosis.

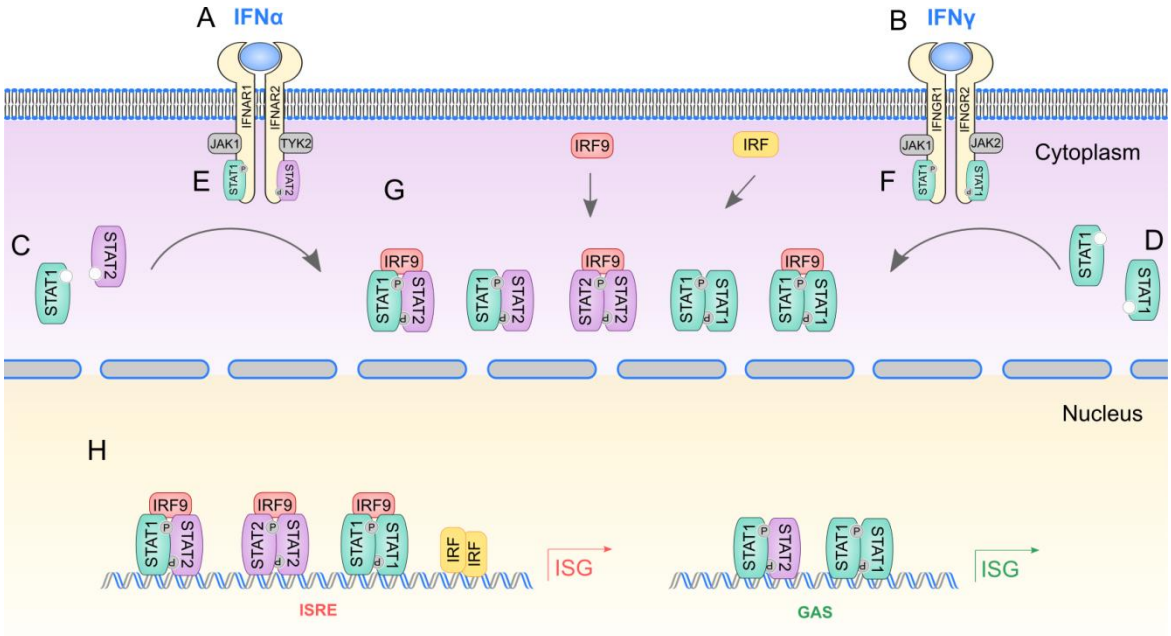

Figure 1. 4. JAK-STAT-mediated signaling in response to IFNα and IFNγ.

(A) IFNα binds to type I IFN receptor composed of IFNAR1/IFNAR2 subunits. **(B)** IFNγ binds to type II IFN receptor built of IFNGR1/IFNGR2 subunits. **(C/D)** Cytoplasmic pool of unphosphorylated STAT1 and STAT2 bind to docking sites created by IFN receptor-specific Janus kinases. **(E)** JAK1/TYK2 kinases are associated with type I IFN receptor, while **(F)** JAK1/JAK2 kinases are connected with type II IFN receptor and phosphorylate specific tyrosine residues in cytoplasmic receptor domains. **(G)** In response to IFN there are formed STAT1 homodimers (GAF), STAT1-

STAT2 heterodimers, IRF9 containing complexes, STAT1/STAT2-IRF9 (ISGF3), STAT2/STAT2-IRF9 (ISGF3-like) and STAT1/STAT1-IRF9 as well as IRF dimers, including IRF1 and/or IRF8. **(H)** Next, assembled complexes are translocated to the nucleus, where ISGF3, ISGF3-like, STAT1/STAT1-IRF9 and IRF dimer complexes are directed to ISRE, while STAT1-STAT2 heterodimers and GAF complexes to GAS binding sites, resulting in transcriptional activation of multiple ISG.

Signal Integration between IFN and LPS

Multiple studies unraveled existence of interactions between signaling pathways which not only share, but also differ in the pool of activating triggers and downstream effectors. Such startling cooperation was reported to exist between JAK-STAT and TLR4-dependent pathways, which by sharing universal TF, including STAT1, NFκB and IRF, together play a major role in mediating the immune and pro-inflammatory response. Moreover, STAT1 has been identified as an important mediator in the biological response to TLR4, in the context of vascular inflammation (Chmielewski et al. 2014). Priming-induced Signal Integration (SI) between IFN and TLR4-activators is reflected by significantly elevated pro-inflammatory gene transcriptional activation in response to pre-stimulation with IFN followed by subsequent lipopolysaccharide (LPS) treatment, as compared to the effect induced by these two stimuli alone. In this context, SI relies on collaborating STAT1-containing complexes ISGF3 and GAF with NFκB, recruited to ISRE/NFκB or GAS/NFκB composite binding sites present in activated gene promoters.

In the first wave of SI, JAK-STAT pathway becomes activated by IFNα or IFNγ. It leads to formation of STAT- and IRF-containing transcriptional complexes, ISGF3 and GAF (Fig.1.5A). TLR4 pathway, activated in the second wave of stimulation, may be activated by viruses, bacteria, protozoa and fungi-derived PAMP, like bacterial endotoxin, lipooligosaccharides or LPS, as well as DAMP, exemplified by β-defensin, high-mobility group protein 1, heat shock proteins and heparin (Peri and Calabrese 2014). LPS binding to homodimeric TLR4 receptor is followed by an interaction of its TIR domains with the proper adapter molecules: MyD88 and TRAM. Finally it leads to transcriptional activation of a number of TF, including members of NFκB and IRF families (Fig.1.5B), which work in a combinatorial manner to rapidly induce gene expression, including type I IFN, pro-inflammatory cytokines, chemokines and cell surface molecules (Hertzog et al. 2003, Kawai and Akira 2010). Next, activated transcriptional complexes are translocated to the nucleus and bind to cognate binding motifs ISRE, GAS and NFκB present in the gene promoters to induce

Inflammatory Gene Expression (IGE) (Fig.1.5C). Several pro-inflammatory genes that are up-regulated in the initial wave of immediate early gene expression, function in feed forward transcriptional loops. One of the important examples is type I IFN. Its IRF3-dependent expression induces a secondary wave of STAT1- and STAT2-dependent ISG up-regulation (Fig.1.5D). As mentioned before, IFNγ stimulation results in activation of IRF1 and IRF8 which act to sustain initial wave of IFN-dependent signaling (Fig.1.5D). Thus combined action of transcriptional complexes (ISGF3, GAF, IRF) activated during 1st wave of stimulation with IFN, sensitizes cells for the 2nd wave of stimulation (NFκB, IRF) and finally leads to increased IGE, in comparison to the transcriptional effect induced by single JAK-STAT or TLR4 pathway (Fig.1.5E).

Rel TF family consists of 5 (RelA/p65, RelB, c-Rel, p50 [NFκB1] and p52 [NFκB2]) members, containing a Rel homology domain (RHD) used for TF DNA binding and C-terminal TAD which allows for transcription initialization. Importantly, the latter domain is characteristic just for RelA, RelB, and c-Rel family members. Before NFκB1 and NFκB2 become functional they are cleaved to the active p50 and p52 subunits, respectively (Aggarwal 2003). Abovementioned NFκB TF are forming both canonical and non-canonical NFκB complexes, kept inactive in the cytoplasm through association with IκB inhibitory proteins, which mask the nuclear localization signal. There were identified 5 main IκB proteins, IκBα, IκBβ, IκBγ, p105 and p100, IκBα being the most abundant. Stimuli-dependent IκB kinase complex (Iκκ complex which consists of Iκκα, Iκκβ, and Iκκγ/NEMO) activation, leads to phosphorylation, ubiquitination, and finally rapid degradation of IκBs by the 26S proteasome (Gilmore 2006, Strickland and Ghosh 2006). Activation of Iκκ complex is either caused by PRR, TNF receptor- or CD40-related receptor families. Further, free NFκB dimers can translocate to the nucleus, bind to cognate 9-10 bp DNA binding motifs, which have a great amount of variability (5′-GGGRNWYYCC-3′) and activate target gene transcription of over 400 genes involved in immune response, growth, inflammation, carcinogenesis and apoptosis (Hayden and Ghosh 2012, Strickland and Ghosh 2006). Remarkably, the major NFκB complex involved in the regulation of pro-inflammatory gene expression is RelA/p65 and p50 heterodimer. Although both p65/p50 heterodimer subunits contact DNA, only p65 contains TAD to directly interact with the basal transcription apparatus (Zhong et al. 1998).

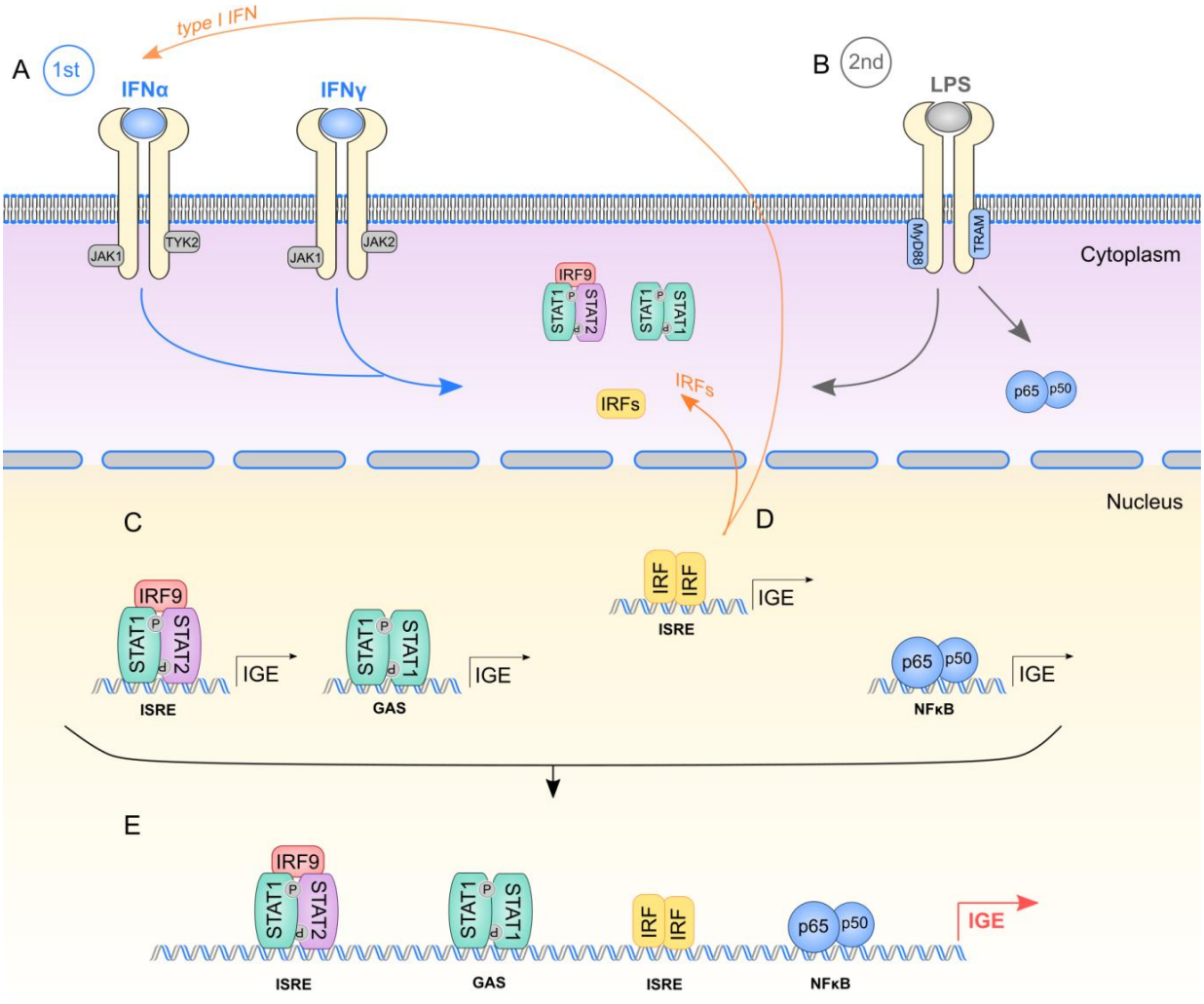

Figure 1. 5. SI between JAK-STAT and TLR-4 signaling pathways.

(A) In 1st wave of stimulation, JAK-STAT pathway is activated by IFNα and IFNγ, resulting in formation of canonical STAT- and IRF-containing transcriptional complexes. **(B)** During 2nd wave of stimulation, TLR4 is activated by LPS, leading to STAT, IRF and NFκB (p65/p50 heterodimers) transcriptional activation. **(C)** Activated TF are translocated to the nucleus and bind to cognate binding sites ISRE, GAS and NFκB present in the gene promoters, activating IGE. **(D)** Some of the activated genes may act in feed forward loops. As such IRF may either act in order to sustain 2nd wave of IFN-dependent gene expression (IRF1, IRF8) or stimulate type I IFN expression (IRF3) to induce a secondary wave of STAT1- and STAT2-dependent ISG expression. **(E)** Combined action of TF activated during 1st wave of stimulation sensitizes cells for the 2nd wave of stimulation and finally leads to increased IGE, in comparison to the transcriptional effect induced by single JAK-STAT or TLR4 pathway. Thus collaboration between ISGF3, GAF, IRF and NFκB results in robust SI-dependent pro-inflammatory gene expression. Due to lack of the evidence for a role of other non-canonical complexes in SI-dependent gene expression, Fig.1.5 depicts potential function only of GAF, ISGF3, IRF and NFκB TF.

Transcriptional regulation of many pro-inflammatory genes, including *Nos2*, *CXCL9*, *CXCL10* and *CXCL11* was shown to rely on SI between IFNγ and TLR4-activators (Farlik et al. 2010, Kleinert et al. 2003, Proost et al. 2004, Tamassia et al. 2007). By sharing universal TF like STAT, IRF and NFκB, which act in a form of ISGF3, GAF and NFκB p65/p50 complexes, JAK-STAT and TLR4 pathways together supply a platform for increased expression of pro-inflammatory genes after combined stimulation in comparison to activation by single IFN or LPS. One of the proposed mechanisms explaining functional cooperation between IFNγ and TLR4 assumes that type II IFN-activated STAT1 enhances positive signaling, due to increased STAT1 phosphorylation. Importantly, it was shown that STAT1 could become phosphorylated not only in response to IFN, but also LPS, what makes it a relevant mediator of SI between JAK-STAT and TLR4 pathways. Indeed, it was shown that TLR-dependent induction enhanced STAT1 activity and the subsequent activities of IFNγ (Hu et al. 2008). On the other hand, STAT1 cooperation with other TF, like IRF or NFκB, was shown to be necessary for SI-dependent gene transcriptional activation and serves additional aspect of SI underlying mechanism. As such, STAT1 could cooperate with NFκB to increase expression of *CXCL10* and *Nos2* (Ganster et al. 2005, Clarke et al. 2010). Additionally, IRF1 cooperated with NFκB to transcriptionally regulate expression of the same genes, *Cxcl10* and *Nos2* (Negishi et al. 2006, Ohmori and Hamilton 2001). Moreover, Zhao et al. reported that combined MΦ stimulation with IFNγ and LPS resulted in *IL1*, *IL6*, *IL12* and *TNFα* synergistic activation in an IRF8-dependent manner (Zhao et al. 2006). Similarly, IRF8 has been involved in IFNγ and LPS-mediated *CCL5* transcriptional activation (Liu and Ma 2006). These findings suggest that transcriptional synergism between IFNγ and TLR4 is mediated in immune cells by precise collaboration between STAT1, NFκB and IRF. New aspect of SI between IFN and LPS was recently highlighted by Qiao and colleagues. They revealed that recruitment of IFNγ-activated STAT1 and IRF1 correlated with an increased H3K27Ac mark deposition at *TNF*, *IL6* and *IL12B* gene regulatory regions. Therefore TF-dependent chromatin priming increased and prolonged recruitment of TLR4-induced NFκB, but also RNA Polymerase II (PolII). Consequently, this STAT1-dependent mechanism of chromatin remodeling resulted in increased transcription of the pro-inflammatory genes (Qiao et al. 2013).

Although various mechanisms underlying SI between IFNγ and TLR4 have been proposed, it is not clear how this phenomenon is mediated on the level of transcriptional cooperation between TF complexes in atheroma interacting VSMC and how it could affect

vital aspects of vascular inflammation. Moreover, there arises a question if there exist and what mechanism could underlie the potential SI between type I IFN and TLR4. Hitherto, no comprehensive studies were performed to address these issues.

Role of STAT1 and NFκB in gene transcriptional repression

Body tissues are constantly exposed to the numerous external cues, including pro-inflammatory mediators. Thus cognate signaling pathways have to be either activated or remain silent, together allowing for an optimal change in ongoing transcriptional programmes regulating tissue homeostasis. As previously described, various mechanisms of gene activation in response to pro-inflammatory IFN or TLR4-activators were widely studied and associated with vascular inflammation. Importantly, priming-induced SI between IFN and TLR4, which relies on collaboration between STAT1-containing transcriptional complexes ISGF3 or GAF and NFκB, was associated with robust pro-inflammatory gene up-regulation. In contrast, this phenomenon was not previously studied in the context of gene repression scenarios. However there exist some reports which could support the concept of the involvement of STAT1 and NFκB in gene transcriptional down-regulation.

Wang et al. demonstrated correlation between STAT1 recruitment to *Skp2* promoter and subsequent gene repression. This in turn resulted in stabilization of antiproliferative and tumor-suppressing $p27^{Kip1}$ in Ras-transformed MEF, implying a potential antitumor STAT1 activity (Wang et al. 2010). In the other study, STAT1 was shown to be sufficient to regulate IFNγ-dependent down-regulation of *ABC1* in MΦ-derived foam cells, suggesting that the pathological role of IFNγ in atherosclerosis depends on STAT1, also in the context of gene suppression (Wang et al. 2002). It was reported, that apoptosis following ischaemia/reperfusion injury is associated with altered *Bcl-2* and *Bcl-x* expression in STAT1-dependent manner. IFNγ treatment of U3A-ST1 cells resulted in *Bcl-2* and *Bcl-x* anti-apoptotic gene down-regulation, which effect was abrogated in STAT1-deficient cells (Stephanou et al. 2000). Moreover this observation was corroborated by the results obtained by others, when combined treatment of murine beta-cell line NIT-1 with TNFα and IFNγ resulted in *Bcl-2* repression, accompanied by enhanced STAT1 activation. This effect of *Bcl-2* down-regulation could not be observed in siRNA-mediated STAT1 KO or upon STAT1 inhibition with fludarabine (Cao et al. 2015). Other Bcl-2 family gene representative, *Bax* was down-regulated by p73 in STAT1-dependent manner in MEF (Soond et al. 2007). In the other study, IFNγ down-regulated hypoxia-induced *CXCR4* expression was also

dependent on STAT1 (Hiroi et al. 2009). Involvement of STAT1 in IFNγ-driven gene repression might rely on the synthesis of specific signaling inhibitors. As such, Suppressor Of Cytokine Signaling 1 (SOCS1) induction was necessary for IFNγ-mediated inhibition of IL4-induced gene expression in STAT1-dependent mechanism (Venkataraman et al. 1999). Ramana et al. reported that IFNγ inhibited cell growth by suppressed *c-myc* expression in Wild-type (WT) but not in STAT1-depleted MEF. The regulatory mechanism possibly involves STAT1 competition for CBP/p300 transcriptional co-activator (Ramana et al. 2000). Indeed such mechanism of STAT1-mediated gene repression in response to IFNγ was reported to be crucial for Colony Stimulating Factor-1 (CSF1)-induced MΦ scavenger receptor gene suppression. STAT1 competed with AP-1/ETS factors for limiting amounts of CBP and p300 to mediate gene down-regulation (Horvai et al. 1997). Besancon et al. reported that IFNγ, but not IFNα/β, caused *CFTR* transcriptional repression in HT-29 and T84 colon-derived epithelial cell lines. Remarkably, potential involvement of STAT1 in *CTFR* down-regulation was not addressed in this study (Besançon et al. 1994). Others shown that IFNα administration against human bladder cancer cells in mice *in vivo,* caused down-regulation of angiogenesis-related genes *bFGF* and *MMP9*. Similarly, it was not reported if IFNα-related gene repression was dependent on STAT1 (Slaton et al. 1999). On the other hand, Wu et al. studied the mechanism of IFNα-dependent repression of *VEGF* in MHCC97 cells. They reported that IFNα could down-regulate *VEGF* by HIF-1α repression via inhibition of PI3 kinase and MAP kinase signaling pathways (Wu et al. 2005). Interestingly Oliveira et al. observed the repressory effect of IFNβ on *IL8* in TNFα-treated human fibroblasts. They proved that NFκB enhancer element was responsible for mediating gene inhibition, possibly as a result of basal NFκB activity in untreated cells (Oliveira et al. 1994). As mentioned previously, altered *Bcl-2* gene expression is related with an apoptosis in the pathology of multiple inflammatory diseases. Except STAT1, down-regulation of *Bcl-2* was shown to be mediated by NFκB activation in *H. pylori*-infected gastric epithelial cells, what correlated with inhibited apoptosis (Chu et al. 2011). Moreover, in Jurkat cells treated with TNFα, *IL4* transcription was down-regulated in NFκB-dependent manner and suppressed in RelA-overexpressing cells (Casolaro et al. 1995). In the other study, LPS diminished Sp1 activity in WT mice, what correlated with increased activity of NFκB. Sp1 protein was degraded by Sp1-degrading enzyme (LISPDE) activated in LPS-NFκB-dependent manner. LPS-mediated Sp1 repression was abrogated in NFκB/p50 KO mice (Ye et al. 2015).

Thus, there are several reports providing proof for the involvement of predominantly IFNγ-activated STAT1 in gene transcriptional repression. At the same time, there is limited

evidence for such connection between IFNα-activated STAT1 or LPS/TNFα-induced NFκB. Hence, we could speculate that IFNγ/STAT1-driven gene down-regulation may serve an important regulatory role in multiple inflammatory diseases, with priming-induced SI being important component of the disease pathophysiology. Based on the abovementioned data and general mechanisms of gene transcriptional regulation, widely studied in the context of other transcriptional repressors, we could anticipate on the potential mechanism of STAT1-NFκB-dependent gene down-regulation. In the most simple scenario STAT1 and/or NFκB acting as a repressor could displace TF positively acting on gene expression, competing for an access to the same or overlapping binding sites. By removing an activator, STAT1 and/or NFκB would determine gene down-regulation (Fig.1.6A). Alternatively, STAT1 and/or NFκB could mediate expression of signaling inhibitors or an activator-degrading enzyme and it this way reverse gene activation (Fig.1.6B). Other potential mechanism involves competition between negatively acting STAT1 and/or NFκB and other positively acting TF for limiting amounts of a co-activator, f.ex. CBP/p300 (Fig.1.6C). Hitherto the most advanced concept assumes that gene repression scenarios are mainly imprinted in the chromatin structure, shaped by the processes of DNA methylation, histone modifications and chromatin remodeling. Together it establishes a 'histone code' regarding gene transcriptional status (Kouzarides 2007). The most widely spread epigenetic modification associated with gene transcriptional repression is deacetylation - histone deacetylase (HDAC)-dependent process of acethyl group removal from lysine residues on histone tails (presumably histone H3 lysines 9 and 14, and H4 lysine 5) which results in DNA condensation, imposing closed, not transcription-friendly chromatin structure (Arnosti 2004). Thus STAT1 and/or NFκB could be necessary for the recruitment of the enzymes (f.ex. HDAC), which would deposit repressive histone marks (Fig.1.6D). Importantly, it is tempting to speculate that STAT1- and NFκB-containing transcriptional complexes would act mutually to induce gene transcriptional repression, alike in the mechanism characterized in the context of priming-induced SI-dependent gene up-regulation. On the other hand, gene suppression could be predominantly mediated by one of these TF, f.ex. STAT1 activated in the first wave of signaling. Moreover, functionality of the proposed STAT1-NFκB-dependent mechanisms of gene transcriptional down-regulation will require experimental validation.

Although gene transcriptional activation was broadly correlated with the course of diseases, like cancer, CVD or neurodegenerative diseases, such data is barely available in case of gene repression and limited to single gene studies, rather than comprehensive genome-wide

reports. Therefore it will be challenging to further characterize the regulatory mechanisms driving transcriptional gene repression in response to the pro-inflammatory cues and translate it to the pathophysiology of various disorders.

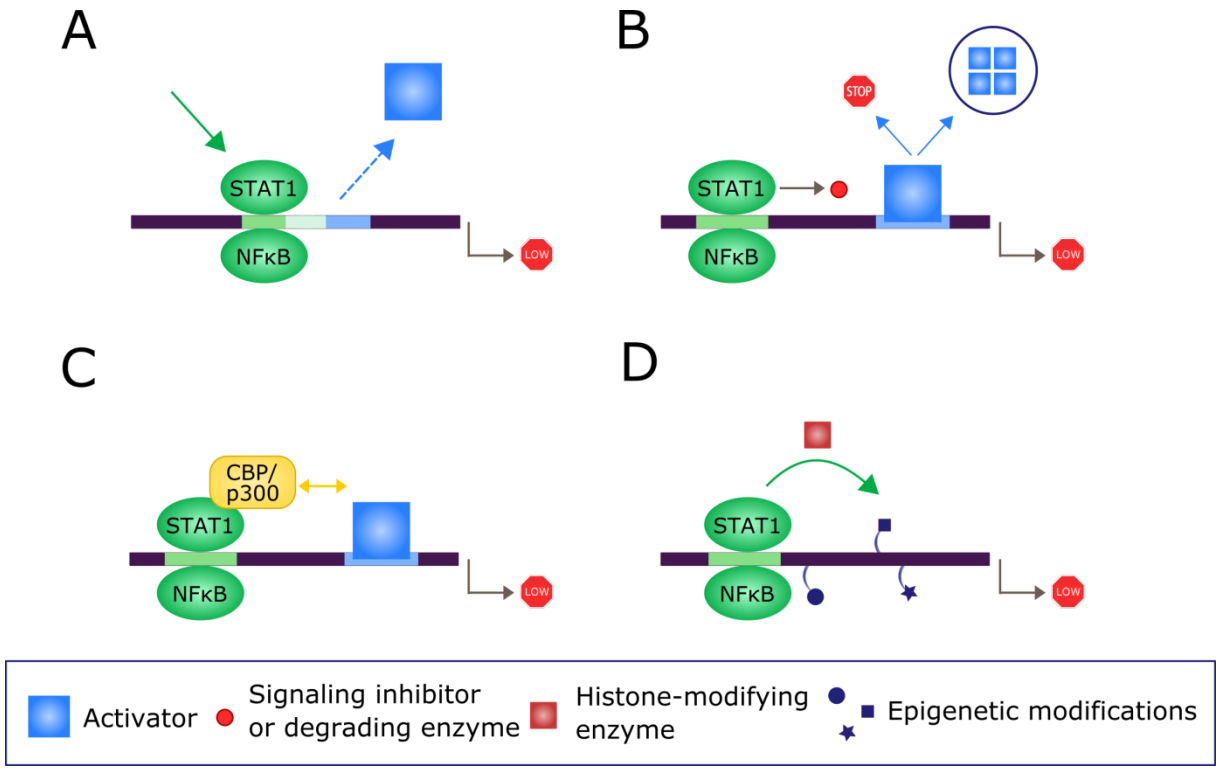

Figure 1. 6. Hypothetical mechanisms of STAT1-NFκB-dependent gene transcriptional repression.

(A) STAT1 and/or NFκB acting as a repressor displaces an activator, competing for an access to the same or partially overlapping binding sites. **(B)** STAT1 and/or NFκB induces expression of signaling inhibitors or an activator-degrading enzyme to reverse gene activation. **(C)** STAT1 and/or NFκB competes with positively acting TF for limiting amounts of a co-activator (f.ex. CBP/p300). **(D)** STAT1 and/or NFκB acting as a repressor recruits histone-modifying enzymes (f.ex. HDAC) to introduce histone tails modifications and establish loci-specific 'histone code' determining chromatin accessibility or hindrance for interacting TF and GTM.

Role of STAT, IRF and NFκB in the establishment of cell type-specific transcriptional responses to pro-inflammatory cues

Every living organism is built by the multiple specialized cell types which share the same genome, yet exhibit uniquely tailored functions to ensure tissue homeostasis. Genomic

DNA carries all the inevitable information determining cell type-specific developmental programs and responses to the external signals. This information is deciphered by a pool of TF, binding to 6-12bp-long DNA sequences, which composition does not vary between cell types, being highly evolutionary conserved (Spitz and Furlong 2012). However it was shown that in general TF recognize and efficiently bind to less than a few percent of their potential binding sites distributed across the genome and these TF cistromes display high cell type-specificity (Zaret and Carroll 2011). Notably, the differences are observed mainly in promoter-distal located sites, which seem to be a place of TF co-localization in cell type-specific manner (Heinz et al. 2010, Kwon et al. 2009, Palii et al. 2011). In this context, particular attention has been paid to enhancers, small DNA segments of a few hundred bp, which contain multiple binding site clusters for sequence-specific TF (Levine 2010). Out of millions of potential enhancers only a small subset is activated in a cell type-specific manner, resulting from hierarchical binding of TF in the context of nucleosome remodeling.

In the eukaryotic cells, ~200bp DNA segments are wrapped around an octamer of the four core histones and form a nucleosome (Cutter and Hayes 2015). This organisation provides a steric barrier, which prevents an access for any DNA-transacting proteins. Therefore, inactive enhancers are hidden in the regions of condensed chromatin, what prevents TF binding. This chromatin barrier can be overcame by 'Pioneer' Factors (PF) which, accompanied by collaborating co-activators, chromatin-modifying and remodeling enzymes, possess an exclusive ability to establish an open chromatin regions and prime enhancers with histone H3 lysine 4 mono- (H3K4me1) and di-methylation (H3K4me2) for future activation. By initiating the process of cell type-specific regulatory region selection, this factors serve as Lineage-Determining TF (LDTF). In response to various external stimuli, including pro-inflammatory stimuli, Signal-Dependent TF (SDTF) are further recruited to their cognate binding sites, usually present in a close proximity to pre-bound PF. These binding events are associated with the following recruitment of Mediator complex and histone modifying enzymes which remove (f.ex. H3K27me3) or deposit (f.ex. H3K27ac) respective histone marks, together proceeding gene transcriptional activation [rewieved in: (Zhang and Glass 2013, Shlyueva et al. 2014, Spitz and Furlong 2012)].

Hierarchical cooperation between cell type-unique LDTF and SDTF, exemplified by STAT, IRF and NFκB induced by IFN and TLR4-activators, was the most well characterized for immune cells, especially MΦ, but also DC, T cells and B cells. Among others, PU.1 and IRF8 are the most important MΦ LDTF which set up a pool of MΦ-specific enhancers that

are accessible for transcriptional control by SDTF and response to pro-inflammatory stimuli, like IFN or LPS. Stimuli-activated STAT, IRF and NFκB mediate cooperation with GTM and further gene transcriptional activation in cell type-specific manner. Interestingly, it was reported that genes pre-bound by PU.1 and IRF8 will associate with IRF1 and IRF8 in IFNγ-treated MΦ. In contrast, solitary PU.1 pre-binding will direct only IRF1 recruitment upon IFNγ treatment. Moreover, both gene groups present high overlap with recruited STAT1 (Langlais et al. 2016). Additionally, PU.1 and STAT1 collaboration in the establishment of cell type-specific gene expression was reported by Aittomaki et al. by showing that expression of FcγRI cell-type specific receptor requires DNA-binding as well as the transactivation functions of both PU.1 and STAT1 (Aittomäki et al. 2004). Moreover, MΦ-specific IFNγ-dependent *Fgl2/Fibroleukin* expression was driven by collaboration between the composite *cis* elements Sp1/Sp3 and STAT1/PU.1 (Liu et al. 2006). Qiao et al. outlined that synergistic activation of *TNF*, *IL6* and *IL12B* by IFNγ and TLR was mediated by STAT1, IRF1 and NFκB which binding correlated with PU.1 pre-binding (Qiao et al. 2013). In myoblasts, cell type-specific factor GATA4 was able to recruit STAT1 and cooperate through direct physical interaction (Wang et al. 2005). Also other STAT except STAT1 could collaborate with LDTF to determine cell type-specific gene expression in various cell types. F.ex. IRF4 and STAT3 recruitment to closely positioned binding motifs was necessary for IL21-dependent *Prdm1*, *Socs3*, *Bcl3* and *Tha1* expression in T cells (Kwon et al. 2009). In the other study, Pai et al. demonstrated that GATA3 collaboration with STAT5 and STAT6 was crucial for cytokine-induced development of CD4+ cells and T_H2 cells differentiation (Pai et al. 2004). Moreover, GATA3 and STAT6 were essential for an establishment of an open chromatin configuration in the regulatory regions of the cytokine-encoding genes in T_H2 cells (Spilianakis and Flavell 2004).

Ifnb is an example of the gene which stays under control of LDTF interacting with IRF and/or NFκB. The gene is constitutively bound by PU.1 and IRF8 in MΦ, while stimulation with LPS or viral infection induces recruitment of IRF3 and/or IRF7 together with NFκB to gene promoter, followed by chromatin remodeling and modifying enzymes (Agalioti et al. 2000). Saliba et al. reported that MΦ stimulation with LPS resulted in RelA-assisted IRF5 binding to a non-canonical PU.1/ISRE motif and transcriptional regulation of a subset of MΦ-specific inflammatory genes (Saliba et al. 2014). Genome-wide location analysis revealed that TNFα treatment-dependent NFκB (p65) binding was directed by PU.1 and C/EBPα in THP-1 cells, but not in HeLa cells (Jin et al. 2011).

Among crucial LDTF for DC identity, there were identified PU.1 and C/EBP, alike in MΦ, yet it is not clear if these TF occupy the same genomic regions in the two cell types. DC stimulation with LPS revealed, that immediate and delayed gene expression is determined by distinct master regulators. As such, IRF4, JUNB, ATF3, EGR2, MAFf or IRF4, JUNB, ATF3, determined immediate versus delayed gene expression, respectively. Moreover, late induced gene cluster was predominantly bound by STAT1 and STAT2, while early induced gene cluster was characterized by RelA and Egr1 recruitment, proving that a specific combination of LDTF shapes DC-specific transcriptional gene activation (Garber et al. 2012).

Therefore, STAT, IRF and NFκB family members play crucial roles in determining various cell type-specific transcriptional programmes in response to the pro-inflammatory cues, by hierarchical cooperation with LDTF, which direct SDTF to genome-wide cognate binding sites in a cell type-specific manner. Interestingly, although such concept is widely appreciated as a general mechanism elucidating basis of cell type-specific gene expression, especially in case of immune cells, there is limited evidence for a similar LDTF and SDTF cooperation determining VSMC identity. Identification of the mechanism determining VSMC-specific gene expression could help to identify potential therapeutical targets and inhibition strategies to fight against vascular inflammatory diseases in the future.

Thus, based on the abovementioned concept, we propose a hypothetical STAT1-dependent model of VSMC-specific gene expression regulation, as compared to MΦ, in response to the pro-inflammatory cues. In untreated MΦ, cell type-specific enhancers are pre-selected by known LDTF PU.1 and IRF8 (Fig.1.7A). In untreated VSMC, regulatory regions are bound be cell type-specific PF of unknown identity (Fig.1.7B). Upon stimulation with pro-inflammatory cue, like IFNγ, SDTF (f.ex. STAT1) are recruited to their cognate motifs present in the regulatory regions of MΦ- or VSMC-specific genes. This allow for PolII recruitment and further transcriptional gene activation in cell type-specific manner (Fig.1.7C-D).

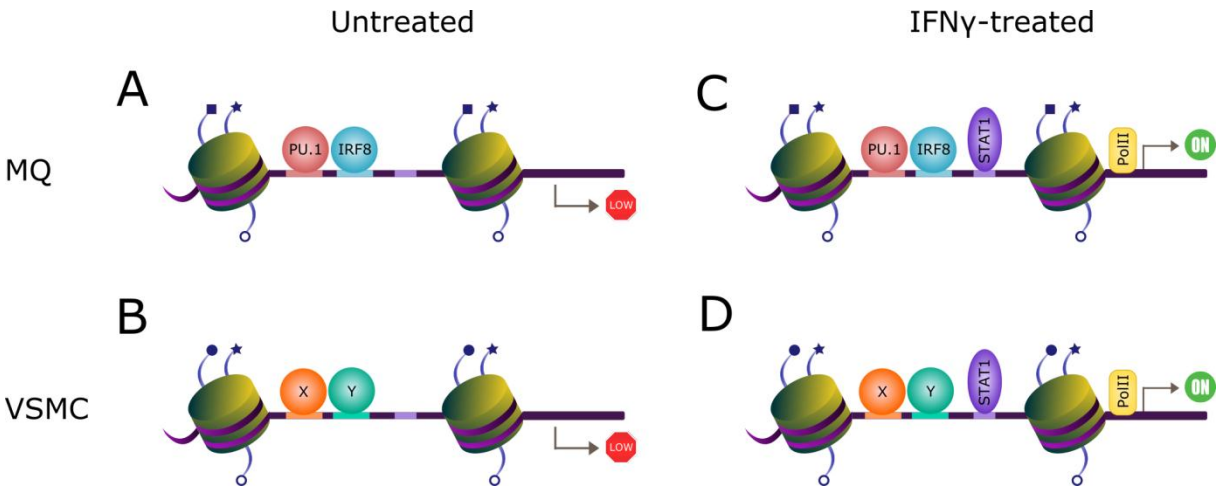

Figure 1. 7. Potential mechanism of STAT1-dependent MQ- and VSMC-specific gene transcriptional regulation in response to IFNγ.

(A) In untreated MΦ, cell type-specific enhancers are bound by PU.1 and IRF8. **(B)** In untreated VSMC cell type-specific regulatory regions are bound by unknown LDTF. IFNγ treatment results in activation of SDTF, including STAT1, which can be recruited to their cognate motifs present in the regulatory regions of cell type-specific genes, pre-bound by PF **(C)** in MΦ **(D)** or VSMC. Hierarchical cooperation between LDTF and SDTF allow for further PolII recruitment and gene transcriptional activation in cell type-specific manner.

Scope of the thesis

In **Chapter 2** we introduce the concept of priming-induced SI between IFN and TLR4 in VSMC, non-immune atheroma-interacting cells, resulting in robust expression of pro-inflammatory genes. Data presented in this chapter provide evidence for a novel mechanism of SI-gene expression, in which STAT1-containing transcriptional complexes collaborate with NFκB on closely spaced GAS/ISRE and NFκB DNA motifs, in the regions of open chromatin. We propose that the same molecular mechanism underlie this phenomenon both in VSMC, as well as MΦ and DC. Results presented in this chapter were published in *Frontiers of Immunology*: Signal Integration of IFN-I and IFN-II With TLR4 Involves Sequential Recruitment of STAT1-Complexes and NFκB to Enhance Pro-inflammatory Transcription (Piaszyk-Borychowska et al. 2019).

In **Chapter 3** we develop a concept of IFNγ and LPS SI-dependent pro-inflammatory gene suppression. We present the results of genome-wide analysis confirming recruitment of STAT1 and/or NFκB to the regulatory regions of down-regulated genes and show gene expression dependence on STAT1 in STAT1 KO VSMC. Finally, we propose a potential mechanism of IFNγ+LPS-mediated gene repression, in which STAT1 and/or NFκB-dependent repressive histone mark deposition would correlate with the recruitment of transcriptional co-repressors or removal of transcriptional co-activators.

Data presented in **Chapter 4** disclose a role of STAT1 in IFNγ-dependent VSMC-specific gene expression. We present evidence that a known mechanism driving MΦ-unique gene expression, which relies on hierarchical collaboration between cell type-specific LDTF and stimuli-dependent SDTF in the context of an open chromatin, could be functional also in VSMC. Thus, we anticipate on potential VSMC-unique LDTF which could bind to the regions of condensed chromatin and initiate its relaxation to allow subsequent IFNγ-dependent STAT1 recruitment in cell type-specific manner.

Chapter 5 summarizes results presented in the thesis and discuss potential applications in the context of the development of new diagnostics or therapeutical targets in CVD.

Chapter 2. Signal Integration of IFN I and IFN II with TLR4 involves sequential recruitment of STAT1-complexes and NFκB to enhance pro-inflammatory transcription

Introduction

Atherosclerosis is a chronic inflammatory disease characterized by a plaque formation on the inside surface of the large and medium-sized arteries. Over time, the plaque build-up results in narrowing of the blood vessel lumen and finally limited distribution of an oxygen and nutrients to organs in the entire organism. The disease process is initiated by excessive inflammatory and immune responses to an early endothelium injury, communicated by various vascular and immune cells, including VSMC, MΦ and DC. Among crucial signaling paths being excessively activated in response to the vascular injury, there were identified JAK-STAT and TLR4 pathways. Accordingly, IFNα, IFNγ and LPS triggering these signaling cascades, have been reported as key components of atherogenesis (Whitman et al. 2000, Thacker et al. 2012, Lu et al. 2013).

Stimulation with IFNα and IFNγ results in JAK-dependent phosphorylation of STAT1, which further dissociates from the receptor and translocates to the nucleus to activate transcription of multiple ISG. Predominantly IFNγ, and to lesser extent IFNα, leads to formation of STAT1 homodimers, known as GAF, which bind to GAS sites, present in ISG promoters (Decker et al. 1989). IFNα induces formation of STAT1/STAT2 heterodimers which after subsequent interaction with IRF9 form ISGF3 complex recruited to ISRE present in the distinct group of ISG promoters (Darnell et al. 1994). Limited evidence supports a role of ISGF3, as well as other non-canonical transcriptional complex STAT1-IRF9, in IFNγ-driven gene expression of ISRE-containing genes (Bluyssen et al. 1996, Matsumoto et al. 1999, Rauch et al. 2015). Therefore two IFN types, IFNα and IFNγ, seem to utilize partially mutual, but also distinct STAT1-containing transcriptional complexes to activate specific target gene sets, which reflect IFN functional similarities or differences.

LPS-dependent activation of TLR4 receptor results in an activation of various TF, exemplified by STAT1, NFκB and IRF (Hertzog et al. 2003, Kawai and Akira 2010), driving together inflammatory gene expression. Several of the early activated target genes, including IFNα, act in feed forward transcriptional loops, to stimulate and sustain a secondary wave of STAT1-, STAT2- and finally NFκB-dependent gene expression.

Therefore, JAK-STAT and TLR4 pathways are sharing a pool of universal TF, like STAT1, NFκB and IRF, which together supply a platform for the increased expression of multiple pro-inflammatory genes. What more, it was shown that to some extent pro-inflammatory gene expression rely on a priming-induced SI between IFN and TLR4-activators. This phenomenon is reflected by drastically elevated gene transcriptional activation in response to IFNγ pre-treatment followed by LPS stimulation, in comparison to treatment with these two stimuli alone. In this context SI relies on STAT1-containing transcriptional complexes ISGF3 and GAF with NFκB, collaborating on ISRE/NFκB or GAS/NFκB binding sites present in ISG promoters. Priming-induced SI was initially described for MΦ and DC (Schroder et al. 2006, Hu et al. 2007, Hu et al. 2008, Hu and Ivashkiv 2009), as a potential way for these cells to activate prompt and robust pro-inflammatory response. Yet it was not investigated in the other atheroma-interacting cell types, like VSMC or EC. Interestingly, expression of the *Nos2* gene in MΦ in response to stimulation with IFNα/LPS behaved similar as after IFNγ/LPS (Meraz et al. 1996), suggesting existence of a functional and mechanistic overlap between different IFN types. However, the role of SI between IFNα and LPS, in the context of IFN-dependent priming, has not been studied before.

Therefore in the current study we aimed at characterizing the mechanism of priming-induced SI between IFNα, IFNγ and LPS in vascular cells as compared to immune cells, by performing comprehensive transcriptome analysis and genome-wide STAT1 and p65 (NFκB) recruitment analysis in response to these stimuli.

Material and Methods

Primary VSMC, MΦ and DC isolation

Mice. WT mice (strain background C57BL/6) were obtained from Charles River Laboratories. STAT1, STAT2 and IRF9 KO mice (strain background C57BL/6) were kindly provided by Thomas Decker (Department of Microbiology, Immunobiology and Genetics, University of Vienna). Before animals handling and performing procedures leading to tissue or bone-marrow isolation, mice were euthanized by cervical dislocation under isoflurane anaesthesia. Animals were handled according to good animal practice as defined by the relevant national and local animal welfare organisations. Performed experimental procedures did not require any medical ethical approval in accordance with the local legislation and institutional requirements.

VSMC. Primary VSMC were isolated from WT, STAT1 KO, STAT2 KO and IRF9 KO mice aortas by enzymatic digestion protocol established by Kobayashi et al. (Kobayashi et al. 2005). Aortas were dissected out and carefully cleaned from a remnant fat and connecting tissue by gentle scrapping. Further, aortas were washed with Ethanol (EtOH) and Phosphate Buffered Saline (PBS), cut into rings and incubated with digestion mix consisting of DMEM (11, IITD PAN Wrocław) supplemented with 1:100 L-glutamine (X0550, BioWest), 1:100 antibiotic/antimycotic solution (A5955, Sigma-Aldrich), 0.09 mg/ml Elastase I (E1250, Sigma Aldrich) and 0.5mg/ml Collagenase I (C1639, Sigma-Aldrich), for 3 hours in 37˚C. After digestion cell suspension was centrifuged and reconstituted in a fresh cell culture media: DMEM (11, IITD PAN Wrocław) supplemented with 20% FBS (10500-064, Thermo Fisher Scientific [TFS]), 1:100 L-glutamine (X0550, BioWest) and 1:100 antibiotic/antimycotic solution (A5955, Sigma-Aldrich). Cells were left undisturbed on 6-well plate for a 4-5 days, since wells got confluent and cells could be split for future experiments. Expression of VSMC marker genes: *α-smooth muscle actin*, *calponin* and *smoothelin*, measured by Real-Time Polymerase Chain Reaction (RT-PCR) (Fig.2.1) was used to assess a homogeneity of cell culture (primers listed in Table 2.1).

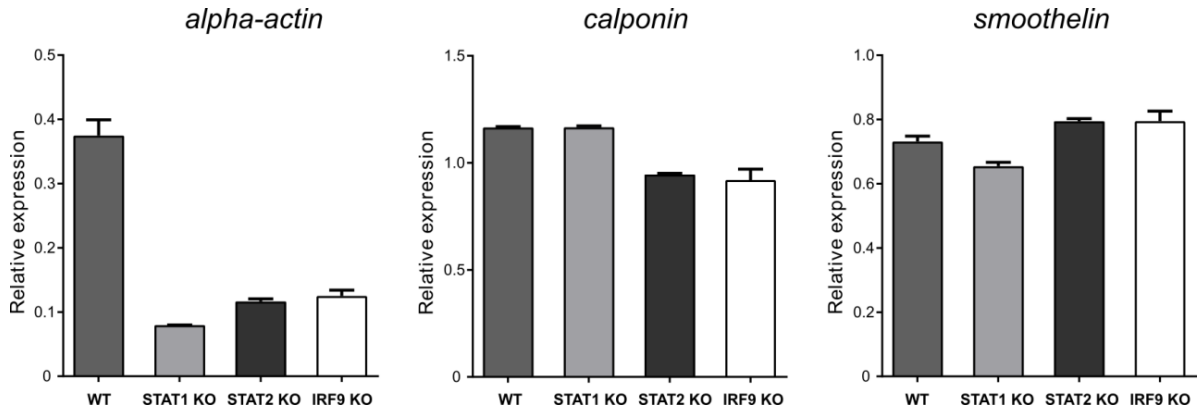

Figure 2. 1. Relative expression (over β-actin) of VSMC marker genes.

Alpha-actin, calponin and smoothelin enrichment in untreated WT, STAT1 KO, STAT2 KO and IRF9 KO VSMC examined by RT-PCR.

MΦ. Freshly isolated femur and tibia form WT mice were cleaned from a remnant muscle tissue by scrapping, put in EtOH 70% for 30 seconds and kept in ice-cold PBS until next procedure steps. Bothe ends of the bones were cut and bone-marrow was flushed into a falcon tube. Obtained suspension was centrifuged for 5 minutes, 1500rpm. Cell pellet was lysed in ACK buffer (0.15M NH_4Cl [A9434, Sigma-Aldrich], 10nM $KHCO_3$ [237205, Sigma-Aldrich], 0.1mM $Na_2EDTAx2H_20$ [E5134, Sigma-Aldrich], pH 7.2-7.4). Next, monocyte cells were purified through a Ficoll-Paque gradient (17-1440, GE Healthcare). Afterwards primary MΦ were differentiated in DMEM medium (11960044, TFS) supplemented with 30% L929 conditioned medium (containing M-CSF), 15% FBS (F7524, Sigma-Aldrich) and 1:100 antibiotic/antimycotic solution (A5955, Sigma-Aldrich) for 5 days. MΦ culture maturation was evaluated with flow cytometry: F4/80 positive cells were considered as desired cell phenotype.

DC. Freshly isolated femur and tibia form WT mice were cleaned from a remnant muscle tissue by scrapping, put in EtOH 70% for 30 seconds and kept in ice-cold PBS until next procedure steps. Bothe ends of the bones were cut and bone-marrow was flushed into a falcon tube. Obtained suspension was centrifuged for 5 minutes, 1500rpm. Cell pellet was lysed in ACK buffer (0.15M NH_4Cl [A9434, Sigma-Aldrich], 10nM $KHCO_3$ [237205, Sigma-Aldrich], 0.1mM $Na_2EDTAx2H_20$ [E5134, Sigma-Aldrich], pH 7.2-7.4). Next, primary DC were differentiated in RPMI1640 medium (R5886, Sigma-Aldrich) containing 200U/ml GM-CSF (315-03, PeproTech), 10% FBS (F7524, Sigma-Aldrich), 1:100 antibiotic/antimycotic solution (A5955, Sigma-Aldrich), 2mM L-glutamine (67513, Sigma-Aldrich) and 50μM β-

ME (31350-010, TFS) for 6 days according to modified Lutz et al. protocol (Lutz et al. 1999). DC culture maturation was evaluated with flow cytometry: CD11c and CD11b double positive cells were considered as desired cell phenotype.

Primary VSMC, MΦ and DC cell culture and treatment

VSMC. WT, STAT1 KO, STAT2 KO and IRF9 KO VSMC were cultured in DMEM complete medium (11, IITD PAN Wrocław) supplemented with 10% FBS (10500-064, TFS), 1:100 L-glutamine (X0550, BioWest) and 1:100 antibiotic/antimycotic solution (A5955, Sigma-Aldrich). On the day before treatment, DMEM complete medium was exchanged into 2% FBS containing DMEM starving medium. After 24 hours, VSMC were treated with: single stimulus: 1000U/ml of IFNα (IF009, Merck Millipore) or 10ng/ml of IFNγ (PMC4031, TFS) for 8 hours or 1μg/ml of LPS (L4391, Sigma-Aldrich) for 4 hours. To further study the effect of IFN priming on LPS signaling, VSMC were first treated with IFNα or IFNγ for 8 hours followed by LPS stimulation for 4 hours, at concentrations listed above. Described treatment strategy (using single or combined stimuli, depending on experimental set up) is presented in Figure 2.2 and was applied in RT-PCR, Western blot, Co-IP, RNA-seq, ChIP-PCR and ChIP-seq experiments performed in this study.

MΦ. Differentiated WT MΦ were immediately placed in serum free medium (12065074, TFS) for 24 hours and further treated with single stimulus: 1000U/ml of IFNα (IF009, Merck Millipore) or 10ng/ml of IFNγ (PMC4031, TFS) for 8 hours or 10ng/ml of LPS (L4391, Sigma-Aldrich) for 4 hours; and combined stimuli: first treated with IFNα or IFNγ for 8 hours followed by LPS stimulation for another 4 hours, at abovementioned concentrations. Described treatment strategy is presented in Figure 2.2 and was applied in RNA-seq experiment.

DC. Differentiated WT DC were immediately placed in 2% FBS (F7524, Sigma-Aldrich) containing RMPI1640 (R5886, Sigma-Aldrich) with added 1:100 antibiotic/antimycotic solution (A5955, Sigma-Aldrich) and 50μM β-ME (31350-010, TFS), for 24 hours. Afterwards, cells were subjected for treatment with single stimulus as follows: 1000U/ml of IFNα (IF009, Merck Millipore) or 10ng/ml of IFNγ (PMC4031, TFS) for 8 hours or 10ng/ml of LPS (L4391, Sigma-Aldrich) for 4 hours; and combined stimuli: first treated with IFNα or IFNγ for 8 hours followed by LPS stimulation for another 4 hours, at abovementioned concentrations. Described treatment strategy is presented in Figure 2.2 and was applied in RNA-seq experiment.

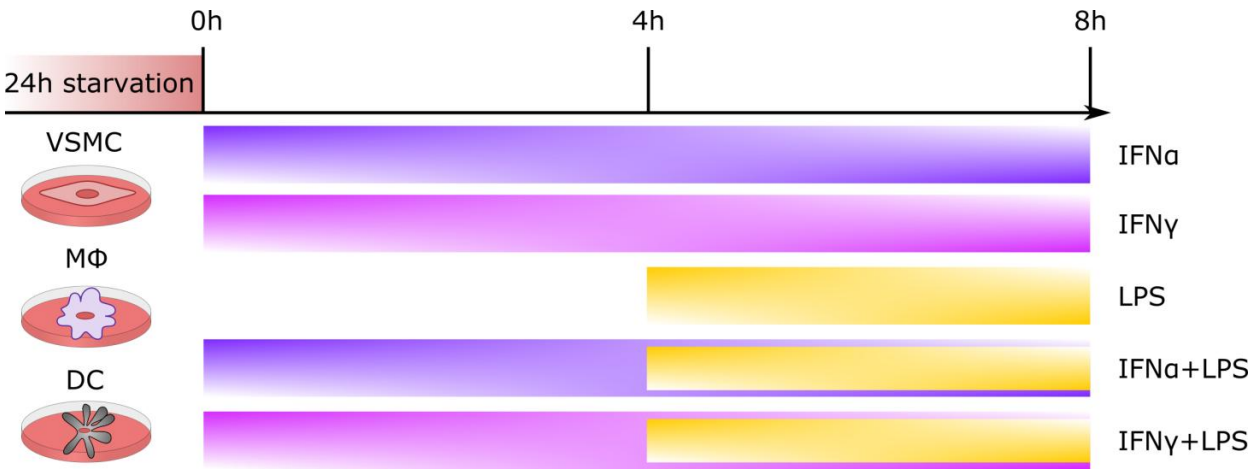

Figure 2. 2. Scheme presenting VSMC, MΦ and DC treatment strategy.

Gene Ontology (GO)

Lists of up-regulated (FC≥2) genes in three analysed cell types (VSMC, MΦ and DC) after combined treatment with IFNα+LPS (579 genes) and IFNγ+LPS (536 genes) resulting from RNA-seq experiment were subjected to GO analysis. Online available Protein ANalysis THrough Evolutionary Relationships (PANTHER) resource (Mi et al. 2017) was applied to identify statistically overrepresented GO terms for two mapped gene lists. Resource available a *Mus musculus* gene list was used as a Reference List and a GO Biological Process Complete was selected as an Annotation Data Set. Fisher's exact test and False Discovery Rate for correction were applied during statistical analysis. GO terms selected for further comparison between IFNα+LPS and IFNγ+LPS-dependent gene lists were chosen as representative terms reflecting biological functions involved in immune, inflammatory, defence and stress response. From obtained results, only GO terms with p-value of less than 0.05 were considered as significantly enriched.

Promoter analysis

Lists of up-regulated (FC≥2) genes in three analysed cell types (VSMC, MΦ and DC) after combined treatment with IFNα+LPS (579 genes) and IFNγ+LPS (536 genes) resulting from RNA-seq experiment were subjected to a promoter analysis. Two gene lists were screened for the over-represented conserved Transcription Factor Binding Sites (TFBS) for STAT1 (GAS and ISRE) and NFκB (NFκB) present in the region of -950bp/+50bp to the nearest gene Transcription Start Site (TSS). The promoter analysis were performed using pSCAN webserver (Zambelli et al. 2009). Following JASPAR Profiles for STAT1 and NFκB sites

were utilized: GAS – MA0137.2, MA0137.3, ISRE – MA0652.1, MA0137.1, MA0.517.1 and NFκB – MA0105.1, MA0105.3. Applied threshold of matrix similarity score for potential GAS/ISRE and NFκB binding site was selected as ≥ 0.85 and ≥ 0.90, respectively.

RNA isolation and RT-PCR

RNA isolation. Total RNA from WT VSMC, WT MΦ, WT DC, STAT1 KO VSMC, STAT2 KO VSMC and IRF9 KO VSMC was isolated with GeneMATRIX Universal RNA Purification Kit (E3598, EURx) following the manufacturer's instructions. Purified total RNA concentration was measured using NanoDrop 2000 spectrophotometer (TFS).

Reverse transcription. 1μg of RNA was used to synthesize complementary DNA (cDNA). First, desired amount of RNA was suspended in Nuclease-Free Water (NFW) up to 8μl and mixed with DNAseI-buffer solution (EN0521, TFS) up to 10ul. Mixture was incubated for 30 minutes at 37°C in order to remove any traces of DNA. Immediately after incubation samples were placed on ice and 1μl of 50mM EDTA (EN0521, TFS) was added to each sample in order to inactivate DNAseI (10 minutes, 65°C). Random hexamers (1μl, 100μM, [SO142, TFS]) were added to the reaction, to randomly attach to mRNA and prime it for extension by DNA polymerase (5 minutes, 65°C). Finally, reaction mix consisting of: 0.75μl of 10mM dNTPs (10297018, TFS), 9.75μl of NFW, 0.5μl of RiboLock RNase Inhibitor 40U/μl (EO0381, TFS), 3μl of 5x RT buffer and 1μl of RevertAid Reverse Transcriptase (200U/μl, [EP0442, TFS]) was added, resulting in a total reaction volume of 30μl. Reverse transcription was performed in C1000 Touch Thermal Cycler (Bio-Rad) for 10 minutes at 25°C, 1h at 42°C and then 10 minutes at 70°C. Obtained cDNA was stored at -20°C or diluted and proceeded for RT-PCR analysis.

RT-PCR. Transcript quantification was performed by RT-PCR with Maxima SYBR Green/ROX qPCR Master Mix (K0223, TFS) on the CFX Connect Thermal Cycler System (Bio-Rad). Per reaction, 3μl of 25x diluted cDNA was mixed with 5μl of Maxima SYBR (K0223, TFS), 1.2μl of forward and reverse primers mix and 0.8μl of NFW. RT-PCR was performed with the following cycle conditions: 10 minutes at 95°C, followed by 40 cycles of: 10 seconds denaturation step at 95°C and 1 minute primer annealing step at 60°C, then 15 seconds at 95°C, 5 seconds at 55°C and 1 minute 95°C was done as final amplification step and a melt curve stage. Target gene levels were normalized to *β-actin* (*β-Actb*). Transcripts levels were determined with the formula: Q = 2^(-ΔCt) where ΔCt = Ct target of interest – Ct housekeeping gene, or with the formula: Q = 2^(-ΔΔCt) where ΔΔCt =ΔCt control – ΔCt

sample. Results are presented as mean ± SEM for three independent biological repeats and compared by two-way ANOVA and unpaired two-tailed student T-test using GraphPad Prism v.7 software. The sequences of the primers are listed in Table 2.1.

Table 2. 1. List of primers used for RT-PCR analysis in Chapter 2.

Gene name	Primer sequence	
	Forward	Reverse
Calponin	ACGGCTTGTCTGCTGAAGTA	AAGATGTCGTGGGGTTTCAC
Cxcl10	TCTGAGTGGGACTCAAGGGAT	AGGCTCGCAGGGATGATTTC
Cxcl9	CTTTTCCTCTTGGGCATCATCT	GCAGGAGCATCGTGCATTC
Ifit1	AGAGCAGAGAGTCAAGGCAGGT	TGGTCACCATCAGCATTCTCTCCCA
Irf7	GGAGCTTGGATCTACTGTGGG	GCCCAGCATTTTCTCTTGCC
Mx2	AGACACTGAGTACCCAACTGA	TCTTTCTCTCCTAGGCCCGT
Nos2	ATGTGATGTTTGCTTCGGACA	CAGCTGGGCTGTACAAACCTT
Oas2	TGTCTGAAGCAGATTGCGGT	CATAGGAGCCACCCTTAGCC
Smoothelin	AGAACTGGCTACACTCTCAAC	GGGTCCAATGTGTGTGCTG
α-Actb	CAACTGGTATTGTGCTGGACT	GAAAGATGGCTGGAAGAGAGT
β-Actb	CCACACCCGCCACCAGTTCG	TAGGGCGGCCCACGATGGAG

Protein isolation and Western blot analysis

VSMC WT cell were suspended in 5ml of ice cold PBS and centrifuged for 5 minutes at 400 rcf (Centrifuge 5430R, Eppendorf). Cell pellets were incubated on ice with Radio Immuno Precipitation Assay (RIPA) buffer (50mM Tris-HCl, pH=8.0 [Invitrogen, 15568025], 150mM NaCl [Sigma-Aldrich, S9888], 1% Nonidet-40 [Bio-Shop, NON505], 0.5% sodium deoxycholate [Bio-Shop, DCA333], 0.1% SDS [Bio-Shop, SDS001], 1% protease inhibitor cocktail [Sigma-Aldrich, P8340], 1% EDTA [TFS, 15575-038], 0.1% PMSF [Sigma-Aldrich, 93482]) for 30 minutes and vortexed every 10 minutes. Collected protein extracts were put in -80˚C and stored overnight. Protein concentrations were measured using Bicinchoninic Acid (BCA) kit (23227, Pierce). 60µg of protein was heated in Bolt LDS buffer (B0008, Invitrogen) in 70˚C for 10 minutes and loaded on Blot 4-12% Bis-Tris Plus Gels (Invitrogen, NW04120BOX). Proteins were electrophoresed for 45 minutes, 165V. Separated proteins were transferred to PVDF membrane (pore size: 0.45µm, 1231325, GVS North America) using kuroGEL Semi-dry transfer system (VWR), 25V for 12 minutes. Western blot experiments were performed using SNAP ID Protein Detection System (Merck Millipore).

Membranes were blocked either with 0.125% non-fat dry milk or with 1% BSA in TBS-Tween (TBS-T) for 15 minutes. Afterwards, membranes were incubated with primary antibodies:

- total(t)STAT1 for 1 hour (CST, 14994, D1K9Y) 1:500,
- phospho(p)STAT1 for 1 hour (CST, 7649, D4A7) 1:500,
- tSTAT2 for 1 hour (CST, 72604, D9J7L) 1:400,
- pSTAT2 for 1 hour (Merck Millipore, 07-224) 1:500,
- IRF1 for 1.5 hour (CST, 8478, D5E4) 1:300,
- IRF9 for 1 hour (CST, 28845, D9I5H) 1:500,
- tp65 for 1 hour (CST, 6956, L8F6) 1:500,
- tubulin for 10 minutes (Merck Millipore, 04-1117, EP1332Y) 1:2000,

and next with secondary HRP-conjugated antibodies:

- anti-rabbit for 15 minutes (A9169, Sigma-Aldrich) 1:20000,
- anti-mouse for 15 minutes (A9044, Sigma-Aldrich) 1:20000.

Antibody-antigen complexes were visualized by Enhanced Chemiluminescence (ECL) using Luminata Forte HRP Substrate (WBLUF0500, Merck Millipore) and detected with G:Box System (Syngene). Image Studio Lite software (LI-COR Biosciences) was used for Western blot quantification.

Co-immunoprecipitation

VSMC WT cell were washed twice with 10ml of ice-cold PBS on 10cm plate and lysed for 10 minutes in 200µl of co-IP buffer (1% NP-40 [NON505, Bio-Shop], 150mM NaCl [S9888, Sigma-Aldrich], 1mM EDTA [15575-038, TFS], 50mM Tris HCl pH 7.5 [15567027, Invitrogen], 10% Glycerol [GLY001, Bio-Shop]) supplemented with protease inhibitors. Next cells were scraped from plates and incubated in eppendorf tubes for additional 20 minutes, for total 30 minutes of lysis. Cell lysates were centrifuged for 15 minutes at 14 000 rpm at 4˚C (Centrifuge 5430R, Eppendorf) and collected to fresh tubes. Protein extracts were immunoprecipitated with:

- IRF1 (CST, 8478, D5E4) 1:100 and
- IRF9 (CST, 28845, D9I5H) 1:100 antibodies

overnight at 4°C. Immunocomplexes were isolated with Dynabeads Protein A/G (10008D[A], 10009D[G], TFS) saturated with 1% BSA (A3059, Sigma-Aldrich), by gentle rocking for 3h

at 4°C. Beads were washed 3 times with ice-cold co-IP buffer and once with Tris-EDTA buffer. Attached proteins were retrieved in Bolt LDS buffer (B0008, Invitrogen) for 10 minutes at 90°C and loaded on Blot 4-12% Bis-Tris Plus Gels (Invitrogen, NW04120BOX). Proteins were separated by electrophoresis (165V, 45 minutes) and transferred to PVDF membrane (pore size: 0.45µm, 1231325, GVS North America) using kuroGEL Semi-dry transfer system (VWR), 25V for 12 minutes. Immunocomplexes were analysed by Western blot (described in Material and Methods section, Protein isolation and Western blot analysis) with:

- tSTAT1 (CST, 14994, D1K9Y) 1:500 and
- tSTAT2 (CST, 72604, D9J7L) 1:400 antibodies.

RNA-seq experimental procedure

Total RNA from primary WT VSMC, WT MΦ and WT DC treated as described previously (Material and Methods section, Primary VSMC, MΦ and DC cell culture and treatment) was isolated using GeneMATRIX Universal RNA Purification Kit (E3598, EURx). RNA-seq libraries were prepared from at least three biological replicates using a TruSeq RNA Library Preparation kit (RS-122, Illumina) according to the manufacturer's protocol. Briefly, 1µg of total RNA was used for mRNA purification and subsequent fragmentation. This matrix was utilized for first and second strand of cDNA synthesis. Next, 3' ends were adenylated and adapters ligated, finally end product was amplified by PCR. Libraries were quantified by Qubit fluorometer (TFS) and DNA quality was assessed with Agilent High Sensitivity DNA kit (5067-4626, Agilent Technologies). Libraries were sequenced with Illumina HiScanSQ sequencer. To validate the quality of RNA-seq dataset, *Cxcl9, Cxcl10 and Nos2* transcripts were quantified using cDNA isolated from WT VSMC, WT MΦ and WT DC, treated with IFN and LPS (described in Material and Methods section, RNA isolation and RT-PCR) and Results section, Figure 2.6).

Chromatin Immunoprecipitation (ChIP)-seq experimental procedure

ChIP was carried out as previously described (Siersbæk et al. 2012), with minor modifications. WT and STAT1 KO VSMC treated as described above (Material and Methods section, Primary VSMC, MΦ and DC cell culture and treatment) were double cross-linked with 0.5M DSG (80424, Sigma-Aldrich) for 45 minutes and 1% formaldehyde (28906, TFS) for 10 minutes, directly on cell culture plates. Glycine (G7126, Sigma-Aldrich) at 125mM final concentration was added to stop cross-linking process. After fixation, nuclei were

isolated with ChIP Lysis Buffer (1% Triton X-100 [TRX777, Bio-Shop], 0.1% SDS [SDS001, Bio-Shop], 150mM NaCl [S9888, Sigma-Aldrich], 1mM EDTA [15575-038, TFS] and 20mM Tris, pH 8.0 [15568-025, TFS]). Chromatin was sonicated with Diagenode Bioruptor Plus to generate fragments of 100-2000bp. Next, chromatin was centrifuged for 10 minutes at 12 000rcf, 4°C to remove any cellular debris and subjected to overnight immunoprecipitation at 4°C with:

- tSTAT1 (Santa Cruz, sc-346),
- pSTAT1 (CST, 7649, D4A7),
- tSTAT2 (CST, 72604, D9J7L),
- pSTAT2 (Merck Millipore, 07-224),
- IRF1 (CST, 8478, D5E4),
- IRF9 (CST, 28845, D9I5H),
- tp65 (CST, 6956, L8F6),
- RNA Polymerase II (Merck Millipore, 05-623, CTD4H8),
- Acetyl-Histone H3 (Lys27) (CST, 8173, D5E4) and
- Tri-Methyl-Histone H3 (Lys27) (CST, 9733, C36B11) antibodies.

Dynabeads Protein A/G (10008D[A], 10009D[G], TFS) were added and incubated for 6h at 4°C with rotation to extract antibody coupled DNA-protein complexes. After, beads were washed at 4°C, once with IP Wash Buffer 1 (1% Triton X-100 [TRX777, Bio-Shop], 0.1% SDS [SDS001, Bio-Shop], 150 mM NaCl [S9888, Sigma-Aldrich], 1mM EDTA [15575-038, TFS], 20mM Tris, pH 8.0 [15568-025, TFS], 0.1% NaDOC [DCA33, Bio-Shop]), twice with IP Wash Buffer 2 (1% Triton X-100 [TRX777, Bio-Shop], 0.1% SDS [SDS001, Bio-Shop], 500mM NaCl [S9888, Sigma-Aldrich], 1mM EDTA [15575-038, TFS], 20mM Tris, pH 8.0 [15568-025, TFS] and 0.1% NaDOC [DCA33, Bio-Shop]), once with IP Wash Buffer 3 (0.25M LiCl [1056790256, Sigma-Aldrich], 0.5% NP-40 [NON505, Bio-Shop], 1mM EDTA [15575-038, TFS], 20mM Tris, pH 8.0 [15568-025, TFS], 0.5% NaDOC [DCA33, Bio-Shop]) and two times with TE buffer (10mM EDTA [15575-038, TFS] and 200mM Tris, pH 8.0 [15568-025, TFS]). DNA-protein complexes were eluted by 30 minutes incubation in Elution Buffer (1%SDS [SDS001, Bio-Shop], 0.1M NaHCO3 [S5761, Sigma-Aldrich]) and de-cross-linked with 0.2M NaCl (S9888, Sigma-Aldrich) at 65°C overnight. DNA was purified with MinElute PCR Purification kit (28006, Qiagen) and quantified with Qubit fluorometer (TFS). ChIP-seq libraries were prepared from two biological replicates (for tSTAT1 and tp65 IP) using TruSeq ChIP Library Preparation kit (IP-202, Illumina) according to the manufacturer's

instructions. Briefly, 5ng of DNA was taken for libraries preparation. After ends repair, 3' ends were adenylated and indexed adapter sequences were ligated. Ligation products were amplified in PCR reaction. Libraries quantification was performed by Qubit fluorometer (TFS) and the quality was assessed with Agilent High Sensitivity DNA kit (5067-4626, Agilent Technologies). Libraries were sequenced with Illumina HiSeq 2500 sequencer. STAT1 and p65 binding (ChIP-seq) in the regulatory regions of several genes was validated by number of ChIP-PCR experiments performed for selected target genes. All ChIP-PCR assays were performed in biological duplicates with primers listed in Table 2.2.

Table 2. 2. List of primers used for ChIP-PCR analysis in Chapter 2.

Gene name	Binding site	Primer sequence	
		Forward	Reverse
Ccl5	ISRE/NFκB	CTGCAGCCAAAGAAACCGAAA	ACACAGTCATGGGGAAACCC
Cxcl10_1	ISRE/NFκB	AGTTTCCCTCCCTGAGTCCT	ACAAGCAATGCCCTCGGTTT
Cxcl10_2	GAS/ISRE/NFκB	TAACTGCGAGTGAGCACAGA	TAGGACATTGGACAGAGCGG
Gbp6_1	ISRE	AGAGAGAAGGAGTTAAAAGAAATCACA	CATGGCCTATTTTATTTTACTTTCAGT
Gbp6_2	NFκB	AAGTGTGCTTCTCTCAGGGG	TGGTTCCTGCTTTAGAAAACACAT
Gbp7	GAS/ISRE/NFκB	AGGAGCTGGCACATTTCTGT	TTGCCTGCACTTAGTTGTGG
Ifit1	ISRE/NFκB	GATTTCAGTGGAGAATGCAGTAGG	GTGTGCTCTTTTCAGTCAGCAGT
Irf1	GAS/NFκB	CTTCGCCGCTTAGCTCTACA	TGAAAGCACGTCCTACCTCG
Irf7	ISRE	TGGTAGGCATGGAGACAGTG	AAACGAAACTGCATCTCAGGA
Mx2	ISRE	TTCCCCAAGAACCAGAGAAA	CCTCTCTCCCTGTTGCCTTT
Oas2	ISRE	AACACAGCCAAGCCTAGGAA	GCTAGCTGGAAGCAAACACAC
Saa1	NFκB	TGTGCATAGTGTCTGGGGAAA	ACAATTAGTGGAAGTGGCCCG
Serpina3i	GAS/NFκB	CTGGGGAAATGTGGTCTGTGTT	TCTGGGCTCTGATGGGAAAAG
Steap4	GAS/NFκB	ATCTCTCTGCCCCTCTAGGC	CCCGCTTGATTTCGCAAGAG

RNA-seq data analysis

RNA-seq raw sequence reads analysis were performed using Strand NGS software. After initial pre-alignment Quality Control (QC), sequencing reads were aligned to the mouse mm10 (GRCm38) genome assembly using internal Strand NGS aligner which follows the Burrows-Wheeler Alignment (BWA) approach. Normalization of aligned reads was performed using DESeq package. The data of RNA-seq can be found at the NCBI GEO DataSets, with the accession number GSE120807. Gene lists used for identification of differentially expressed genes (Fold change (FC), FC≥2: up-regulated) were first filtered based on their normalized signal intensity values, with lower cut-off value >8. Afterwards, FC values were calculated for these genes across all treatment conditions and the resulting lists of

up-regulated genes were used for the further downstream analysis. 18 lists (3 cell types: VSMC, MΦ, DC x 6 conditions: control, IFNα, IFNγ, LPS, IFNα+LPS, IFNγ+LPS) of differentially expressed genes were compared and visualized by Venn diagrams generated with BioVenn web tool (Hulsen et al. 2008). FC values represented as log2 transformed values referring to 579 and 536 commonly up-regulated genes in VSMC and immune cells after combined treatment with IFNα+LPS and IFNγ+LPS, respectively, were visualised by a heatmap generated in GraphPad Prism v.7 software.

ChIP-seq data analysis

The primary analysis of STAT1 and p65 ChIP-seq raw data was carried out using ChIP-seq analysis command line pipeline established by Barta (Barta 2011). Sequencing reads were aligned to the mouse mm10 (GRCm38) genome assembly using the BWA tool (v0.7.10) (Li and Durbin 2009). Further, bam files were created by SAMTools (v0.1.19) (Li and Durbin 2009) and converted by makeTagDirectory (HOMER v4.2 Hypergeometric Optimization of Motif EnRichment) (Heinz et al. 2010). Genome coverage (bedgraph) files were created by makeUCSCfile.pl (HOMER) (Heinz et al. 2010) and subsequently transformed to tiled data files (tdfs) using Integrative Genomics Viewer (IGV) tools (Thorvaldsdóttir et al. 2013). Peaks prediction was performed with MACS2 (v2.0.10) (q-value≤0.01) (Zhang et al. 2008). Artefacts were removed according to the blacklist of ENCODE (Consortium 2012). BedTools (v2.23.0) (Quinlan and Hall 2010) were utilized for following intersections, subtractions, and merging of the predicted peaks (bed files). Finally, tdf files were visualized and genomic snapshots were taken with IGV2.3 (Robinson et al. 2011). The closest gene for each STAT1 and p65 ChIP-seq peak was identified by annotatePeaks.pl (HOMER). TF motifs were identified using two steps procedure. First, using publicly available motif files all known motifs were identified genome-wide by scanMotifGenomeWide.pl (HOMER). Second, the intersection between the identified motifs and peaks using intersectBed (bedtools) was determined. *ChIP-seq bioinformatic analysis was performed by Lajos Széles and Attila Csermely (Department of Biochemistry and Molecular Biology, University of Debrecen).* Sequencing data was submitted to NCBI GEO DataSets under accession number GSE120806.

Read Distribution (RD) plot preparation

For all STAT1 and p65 ChIP-seq peaks occupancy values (expressed as Reads Per Kilobase Million, RPKM) were calculated. The peaks were clustered using k-means clustering (n=10) based on the binding pattern of STAT1 and p65 in 6 samples (control, IFNα, IFNγ, LPS,

IFNγ+LPS, IFNα+LPS). Normalized tag counts for RD histograms were generated by HOMER and subsequently visualized with Java TreeView. *Graph was prepared based on the bioinformatic analysis performed by Lajos Széles and Attila Csermely (Department of Biochemistry and Molecular Biology, University of Debrecen).*

Peak distribution plot (histogram) preparation

Distances between STAT1 and the closest p65 ChIP-seq peaks summits were calculated using Phyton. Histogram plots were generated by annotatePeaks.pl from HOMER (with option-size 2000 and -hist 25) and visualized by R using package ggplot2. *Graph was prepared based on the bioinformatic analysis performed by Lajos Széles and Attila Csermely (Department of Biochemistry and Molecular Biology, University of Debrecen).*

Integrative RNA-seq and ChIP-seq analysis

Consensus STAT1 (GAS, ISRE) and p65 (NFκB) motifs available in HOMER database were used for re-mapping analysis. GAS – motif273, ISRE – motif140, NFκB – motif208 (Motif logos in Results section, Figure 2.10A-C) were re-mapped to STAT1 and p65 peaks detected after WT VSMC stimulation with IFNα+LPS and IFNγ+LPS. Lists of GAS, ISRE and NFκB re-mapped genomic regions were filtered according to the motif distance from the closest annotated gene TSS (-/+100kb) and according to Motif Score Threshold (MST) (GAS - MST 6, ISRE - MST 6, NFκB - MST 7). Next, gene lists resulting from transcriptome analysis, 579 and 536 commonly up-regulated genes in VSMC and immune cells after treatment with IFNα+LPS and IFNγ+LPS, respectively, were overlapped with lists of STAT1 and p65 ChIP-seq genomic regions containing re-mapped motifs. Distribution of consensus motifs occupied by STAT1 and p65 across the genome was classified into 7 categories of genomic locations: promoter/TSS (-1kb to +100bp), introns, intergenic, exon, 5' UTR, 3' UTR and TTS. Re-mapped motifs distribution was plotted by the percentage of total number of occupied GAS, ISRE and NFκB binding sites under treatment with IFNα+LPS or IFNγ+LPS.

Results

Commonly up-regulated genes in vascular and immune cells unravel mechanistic and functional overlap of priming-induced SI between IFNα or IFNγ and LPS

In the attempt to characterize the regulatory mechanism of priming-induced SI between IFNα or IFNγ and LPS, we examined genome-wide transcriptional responses of VSMC as compared to MΦ and DC upon IFNα (8h), IFNγ (8h) or LPS (4h) alone, and after combined treatment (IFNα 8h+LPS 4h; IFNγ 8h+LPS 4h) using RNA-seq. As such, IFNα stimulation increased expression of 666 genes in VSMC, 1753 in MΦ and 1061 in DC, while IFNγ changed expression of 752 genes in VSMC, 1630 in MΦ and 437 in DC. LPS stimulation resulted in elevated expression of 445 genes in VSMC, 1272 in MΦ and 1485 in DC (Fig.2.3 and Fig.2.4A). Cell pre-treatment with IFN, followed by stimulation with LPS increased the number of up-regulated genes to 952 and 878 in VSMC, 2045 and 2185 in MΦ, 1848 and 1628 in DC, after combined treatment with IFNα+LPS or IFNγ+LPS, respectively (Fig.2.3 and Fig.2.4B). Therefore, the potency of VSMC transcriptional responses to applied pro-inflammatory stimuli, reflected by the number of up-regulated genes, was lower in comparison to MΦ and DC. Yet the enhanced effect of IFNα and LPS or IFNγ and LPS, demonstrated by increased number of activated genes in response to combined treatment in comparison to single ones, appeared to be present in all three cell types (Fig.2.3). The effect of priming-induced SI is reflected not only by the increased number of up-regulated genes, but also by increased average gene expression after IFNα+LPS or IFNγ+LPS in comparison to single treatments, in all three cell types (Fig.2.3).

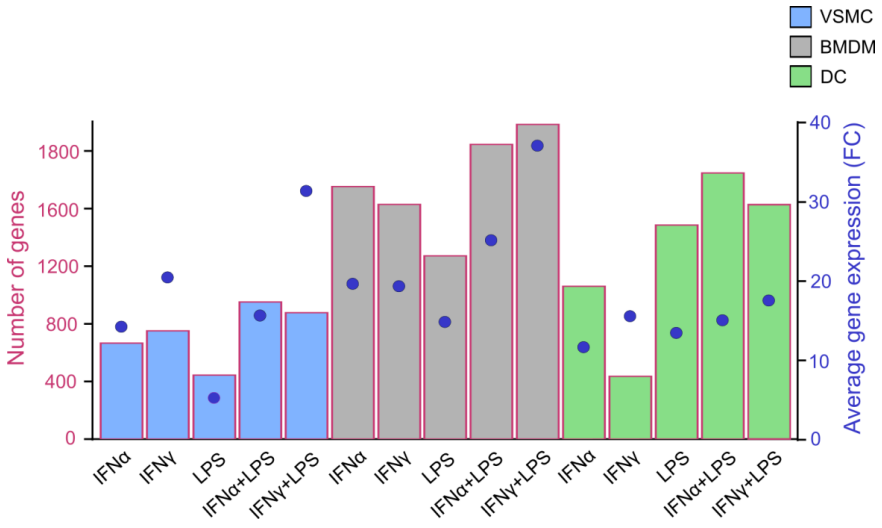

Figure 2. 3. Gene expression levels in vascular and immune cells in response to IFN and LPS. (Figure description on the next page)

Number of up-regulated genes (FC≥2) in response to IFNα(8h), IFNγ(8h), LPS(4h), IFNα(8h)+LPS(4h) and IFNγ(8h)+LPS(4h) in VSMC (blue bars), MΦ (grey bars) and DC (green bars) identified by RNA-seq. Average gene expression (FC) is marked by a blue dot.

Next, we compared the gene expression profiles of the different cell types exposed to the individual or combined stimuli, to identify the commonly up-regulated genes as a result of the interaction between IFNα and LPS or between IFNγ and LPS. Although individual cell types differed in their responsiveness to these stimuli, we identified substantial groups of commonly expressed genes resulting from treatment with both IFN and LPS (Fig.2.4A-B). Not surprisingly, the overlap between MΦ and DC response was stronger in comparison to the overlap between VSMC and immune cells, especially in response to LPS and combined treatments with IFN and LPS (Fig.2.4A-B). Yet, 579 genes were commonly up-regulated in VSMC, MΦ and DC after combined treatment with IFNα+LPS (Fig.2.4B), as compared to 427 genes for IFNα and 249 for LPS alone (Fig.2.4A). Likewise, 536 genes were commonly expressed after combined treatment with IFNγ+LPS (Fig.2.4B), as compared to 219 genes for IFNγ alone (Fig.2.4A). Since we were aiming at SI mechanism characterization in VSMC as compared to immune cells, these two gene groups (579 commonly expressed IFNα+LPS-induced and 536 commonly expressed IFNγ+LPS-induced genes) were selected for further analysis.

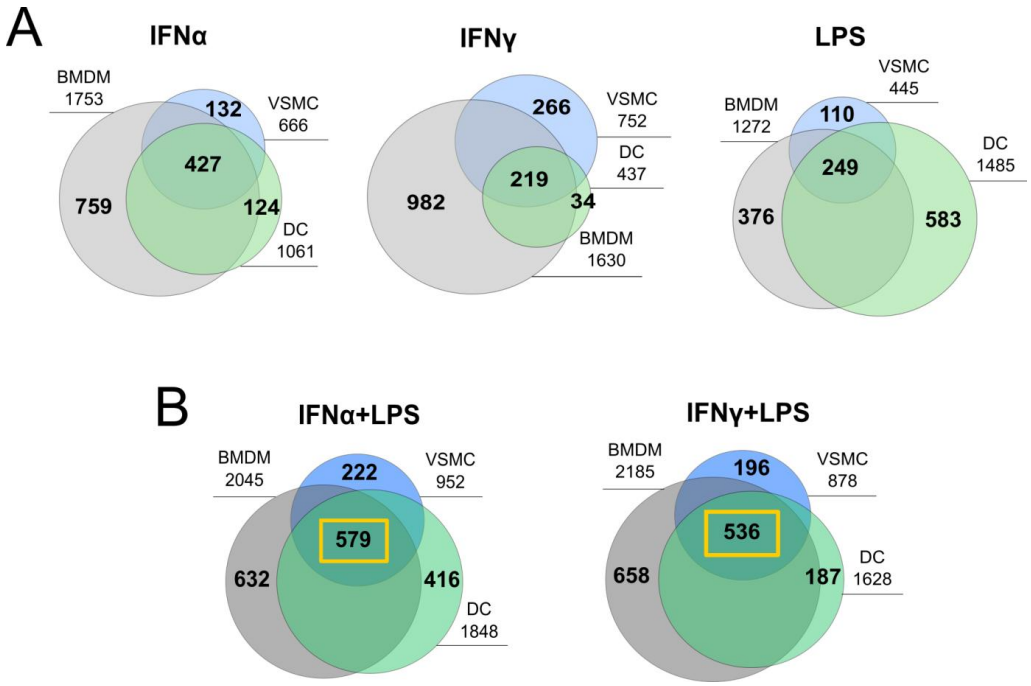

Figure 2. 4. Characterization of gene up-regulation patterns in vascular and immune cells in response to IFN and LPS. (Figure description on the next page)

Venn diagrams presenting overlap between lists of up-regulated genes (FC≥2) in response to **(A)** IFNα(8h), IFNγ(8h), LPS(4h), **(B)** IFNα(8h)+LPS(4h) and IFNγ(8h)+LPS(4h) in VSMC (blue circles), MΦ (grey circles) and DC (green circles) resulting from RNA-seq. Commonly induced genes after combined treatment with IFNα(8h)+LPS(4h) and IFNγ(8h)+LPS(4h) between vascular and immune cells are marked by yellow frames.

Heatmaps present the expression pattern of the commonly 579 IFNα+LPS and 536 IFNγ+LPS up-regulated genes in vascular and immune cells treated by the single or combined stimuli. Increasing brightness of red colour on the heatmap correlates with increasing gene expression levels. Thus, these analysis predicted greater similarity between VSMC and MΦ than between VSMC and DC (Fig.2.5A). Especially, the response of VSMC and MΦ was more directed towards IFNγ, whereas that of DC was primarily dependent on LPS. On the other hand MΦ and DC responses to IFNα were more potent in comparison to VSMC. The heatmaps in Figure 2.5A also illustrate the potential effect of priming-induced SI in vascular and immune cells after combined treatment with IFNα+LPS or IFNγ+LPS, demonstrated by higher gene expression levels as compared to single stimuli. After comparing the overall range and distribution of the common gene expression after single or combined stimulation (Fig.2.5B), in VSMC, MΦ and DC the effect of SI was clearly visible in the presented box plots. The median gene expression after combined treatment with IFNα+LPS and IFNγ+LPS in VSMC and MΦ was significantly increased in comparison to single stimuli. Yet noticed, this SI effect was much less pronounced in DC, what is a consequence of high responsiveness of these cells to single LPS stimulation (Fig.2.5B).

Table 2.3 and 2.4 offer insight in the top-30 of 579 IFNα+LPS and 536 IFNγ+LPS commonly up-regulated genes and illustrate the way of response to IFNα+LPS and IFNγ+LPS in VSMC. Genes affected by SI (reflected by increased gene expression levels under pre-stimulation with IFN followed by LPS in comparison to the sum of the FC values after single treatments) are marked with an asterisk (Table 2.3-4). Strikingly, there exists a significant overlap between the top-30 genes activated by IFNα+LPS and IFNγ+LPS (gene names marked in blue in Table 2.3-4). Comparing the entire lists of 579 IFNα+LPS and 536 IFNγ+LPS commonly up-regulated genes, confirmed this observation and resulted in identification of 64.21% overlap between gene lists, presented on Venn diagram in Figure 2.5C.

To validate the quality of our RNA-seq dataset several gene expression was examined by RT-PCR. Among these genes were *Cxcl9, Cxcl10* and *Nos2*, which expression levels in

VSMC treated with LPS, IFNγ, IFNγ+LPS, IFNα and IFNα+LPS are depicted in Figure 2.6. Measured expression rates correlated with FC values resulting from RNA-seq presented in Table 2.3-4, confirming the credibility of our dataset.

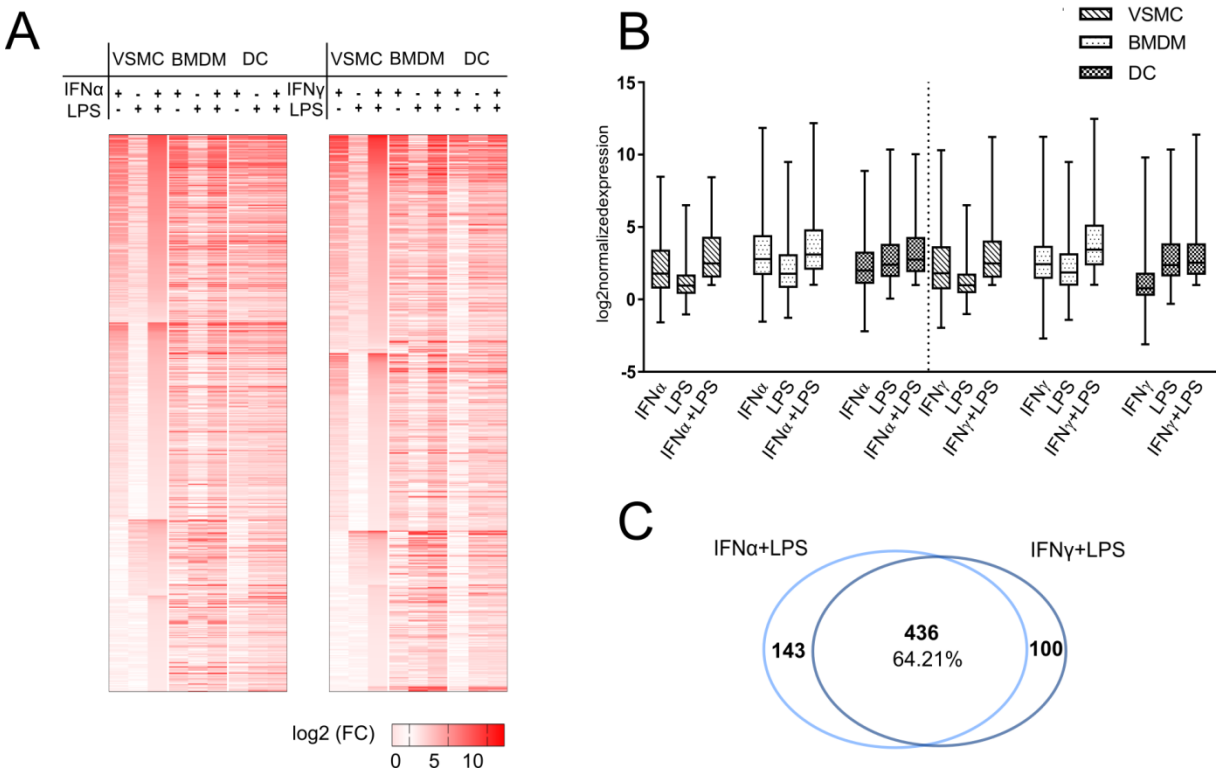

Figure 2. 5. Mechanistic and functional characteristics of common gene expression between VSMC and immune cells in response to IFNα+LPS and IFNγ+LPS.

(A) Heatmaps presenting expression patterns of commonly up-regulated, 579 IFNα(8h)+LPS(4h)- and 536 IFNγ(8h)+LPS(4h)-activated genes in VSMC, MΦ and DC resulting from RNA-seq. Three main columns of each heatmap plot represent one specific treatment condition: IFNα(8h), IFNγ(8h), LPS(4h), IFNα(8h)+LPS(4h) or IFNγ(8h)+LPS(4h). Increasing brightness of red colour correlates with a higher gene expression level (gene expression is presented as log2 FC in comparison to control). **(B)** Box-plots demonstrating gene expression levels (presented as log2 FC in comparison to control) of commonly up-regulated genes after single IFNα(8h), IFNγ(8h), LPS(4h) and combined treatment in VSMC, MΦ and DC. The line within each box represents the median and the lower and upper boundaries of each box indicate first and third quartiles, respectively. **(C)** Venn diagram showing intersection between the lists of commonly up-regulated genes by IFNα(8h)+LPS(4h) and IFNγ(8h)+LPS(4h) from RNA-seq, showing 64.21% overlap.

Table 2. 3. Representative top-30 genes commonly up-regulated (FC≥2) by IFNα+LPS in VSMC, MΦ and DC, reflecting SI between IFNα and LPS in VSMC.

No.	IFNα+LPS induced common genes	VSMC			Binding site		
		IFNα	LPS	IFNα+LPS	GAS	ISRE	NFκB
1	F830016B08Rik*	196,8	6,4	345,9	•	•	-
2	Ifi44	356,3	4,4	343,7	-	•	-
3	Cxcl10*	75,9	4,6	312,1	•	•	•
4	BC023105*	187,1	19,9	289,2	-	-	-
5	Nos2*	4,9	90,9	287,1	•	•	•
6	Gm4955*	209,5	5,4	260,2	-	-	-
7	Gm15725	294,6	2,9	259,8	-	-	-
8	Iigp1*	179,7	9,2	242,3	•	•	-
9	Gm4951*	178,6	6,9	233,4	•	•	-
10	Gbp9*	78,8	22,9	215,9	-	•	•
11	Gbp11*	62,1	13,6	196,5	•	•	-
12	Apod	213,7	2,2	194,9	-	•	•
13	Gm4841*	99,8	9	181,4	•	•	-
14	Gbp4*	36,4	16,4	162	•	•	•
15	Gm14446	164,5	1,8	157,8	-	-	-
16	Mx1*	128,8	3,3	155,9	-	•	•
17	Ifit1*	113,3	11,1	153,6	-	•	-
18	Gm12250*	94,8	3,6	142,3	•	•	-
19	Gm4902*	126,5	3,8	139,3	-	-	-
20	Tnfsf10*	35,8	3,2	128,9	•	•	•
21	Usp18*	96,3	8,9	127,5	-	•	•
22	Gbp1*	91,7	17,5	125,5	-	•	-
23	Gbp6*	36,9	23,5	117,2	•	•	•
24	Gbp10*	35,6	21,1	115,2	-	•	•
25	Ch25h*	3,5	19,6	112,6	•	•	•
26	Tgtp2	114,2	2,6	110,7	•	•	-
27	Gm6904*	94,9	2,6	107,8	-	•	-
28	Zbp1*	95,5	5,8	106,3	•	•	•
29	Saa3*	5,1	66,6	105,7	•	-	•
30	Phf11*	100,2	3,2	105,7	-	-	-

Gene expression levels were presented as FC relative to control in VSMC. SI genes (FC IFNα+LPS> FC IFNα + FC LPS) were marked by an asterisk (*). Overlapping genes between IFNα+LPS- and IFNγ+LPS-induced commonly up-regulated genes (Table 2.4) were colour-coded by blue. Presence of GAS, ISRE or NFκB binding sites in the promoters of listed genes was indicated by a dot (•).

Table 2. 4. Representative top-30 genes commonly up-regulated (FC≥2) by IFNγ+LPS in VSMC, MΦ and DC, reflecting SI between IFNγ and LPS in VSMC.

No.	IFNγ+LPS induced common genes	VSMC			Binding site		
		IFNγ	LPS	IFNγ+LPS	GAS	ISRE	NFκB
1	Cxcl9*	82,2	4	2380,5	•	-	•
2	F830016B08Rik*	1272,1	6,4	2306,6	•	•	•
3	Gm4841*	1087,3	9	1650,3	•	•	•
4	Nos2*	1,8	90,9	933,3	•	•	•
5	BC023105*	600,8	19,9	909,4	-	-	-
6	Gbp4*	304,3	16,4	795,8	•	•	•
7	Iigp1*	687,7	9,2	779,3	•	•	-
8	Ubd*	95,6	5,8	655,1	•	•	•
9	Gbp10*	315,9	21,1	588,2	•	•	•
10	Gbp9*	304,8	22,9	586,1	-	•	•
11	Gbp6*	266,1	23,5	555,3	•	•	•
12	Serpina3f*	200,1	13	529,6	•	•	•
13	Gbp11*	302,3	13,6	482,7	•	•	-
14	Gm12250	502,9	3,6	477,8	•	•	-
15	Gbp8*	215,5	12,9	405,2	•	•	•
16	Ciita	704,4	2	376,5	•	•	•
17	Cxcl10*	49,8	4,6	364,9	•	•	•
18	Gbp1*	295	17,5	364,8	-	•	-
19	Gja4*	82,3	1,6	329,9	•	•	•
20	Gm4951*	300,1	6,9	327,2	•	-	-
21	Batf2*	191,4	3,1	298,4	•	•	-
22	Lcn2*	3,8	36,5	289,2	-	-	•
23	Gbp2*	219,7	13,4	284,4	-	•	•
24	Igtp	328,8	5,3	274,1	•	•	-
25	Tgtp2	261,9	2,6	262,5	•	•	-
26	Gm5970*	183,1	2,3	236,1	-	-	-
27	Ccl8*	115,8	18,6	231,4	•	•	•
28	Tgtp1*	216,7	2,4	222,4	•	•	•
29	Gbp5*	67,7	9,2	211,5	•	•	•
30	Saa3*	4,2	66,6	196,1	•	-	•

Gene expression levels were presented as FC relative to control in VSMC. SI genes (FC IFNγ+LPS> FC IFNγ + FC LPS) were marked by an asterisk (*). Overlapping genes between IFNγ+LPS- and IFNα+LPS-induced commonly up-regulated genes (Table 2.3) were colour-coded by blue. Presence of GAS, ISRE or NFκB binding sites in the promoters of listed genes was indicated by a dot (•).

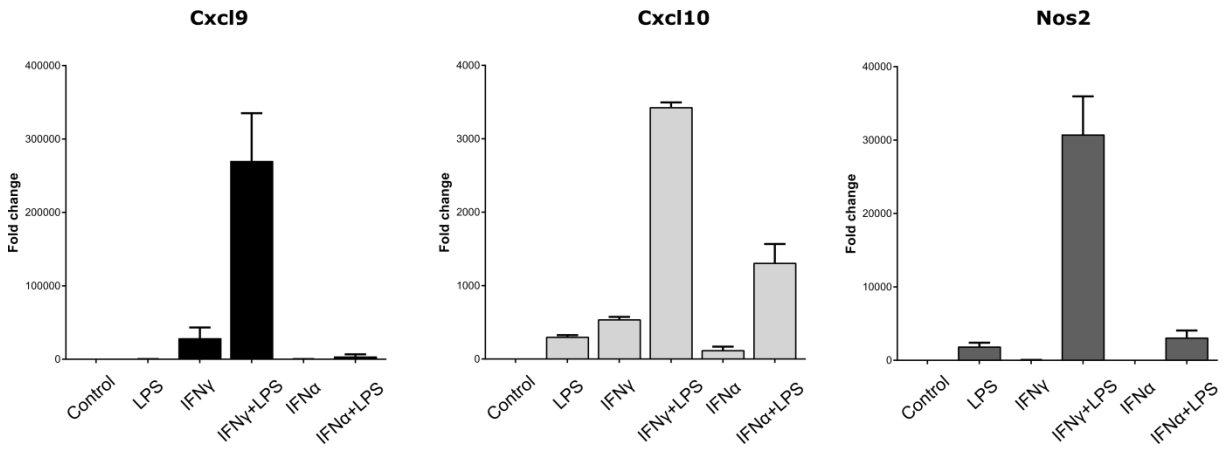

Figure 2. 6. Cxcl9, Cxcl10 and Nos2 relative expression levels (over β-Actin) in VSMC treated with LPS, IFNγ, IFNγ+LPS, IFNα and IFNα+LPS determined by RT-PCR.

Next, we performed GO analysis using 579 IFNα+LPS- and 536 IFNγ+LPS-induced commonly expressed genes as input lists. Among significantly enriched GO terms we identified categories including stress, immune and inflammatory response, regulation of cell proliferation and migration, as well as cell adhesion and chemotaxis, cell death and apoptosis, response to lipid and ROS metabolic process, which together reflect biological functions related with vascular inflammation. These results suggest the existence of the functional overlap between VSMC and immune cells, mediated by the interaction of both IFNα and IFNγ with LPS, what results in the execution of cell-type-common biological responses (Fig.2.7A).

In order to identify potential TF coordinating transcriptional regulation of IFNα+LPS- and IFNγ+LPS-driven genes, we subsequently performed *in silico* promoter analysis on the same gene lists (579 IFNα+LPS- and 536 IFNγ+LPS-induced commonly expressed genes), screening for the presence of GAS, ISRE or NFκB binding sites in the proximal gene promoters (-950 to +100bp). The predicted representation of individual or combined GAS, ISRE or NFκB consensus binding sites is depicted in Figure 2.7B. Examined gene promoter regions contained either single GAS site (89 IFNα+LPS genes and 85 IFNγ+LPS genes) or rather combinations of potential GAS-ISRE (98 IFNα+LPS genes and 91 IFNγ+LPS genes), GAS-NFκB (68 IFNα+LPS genes and 66 IFNγ+LPS genes) or GAS-ISRE-NFκB (92 IFNα+LPS genes and 88 IFNγ+LPS genes) binding sites. Together, this strongly implicates the cooperative involvement of STAT1 together with IRF and NFκB, in the transcriptional regulation of IFNα and LPS or IFNγ and LPS-activated genes in VSMC, in analogy to MΦ and DC.

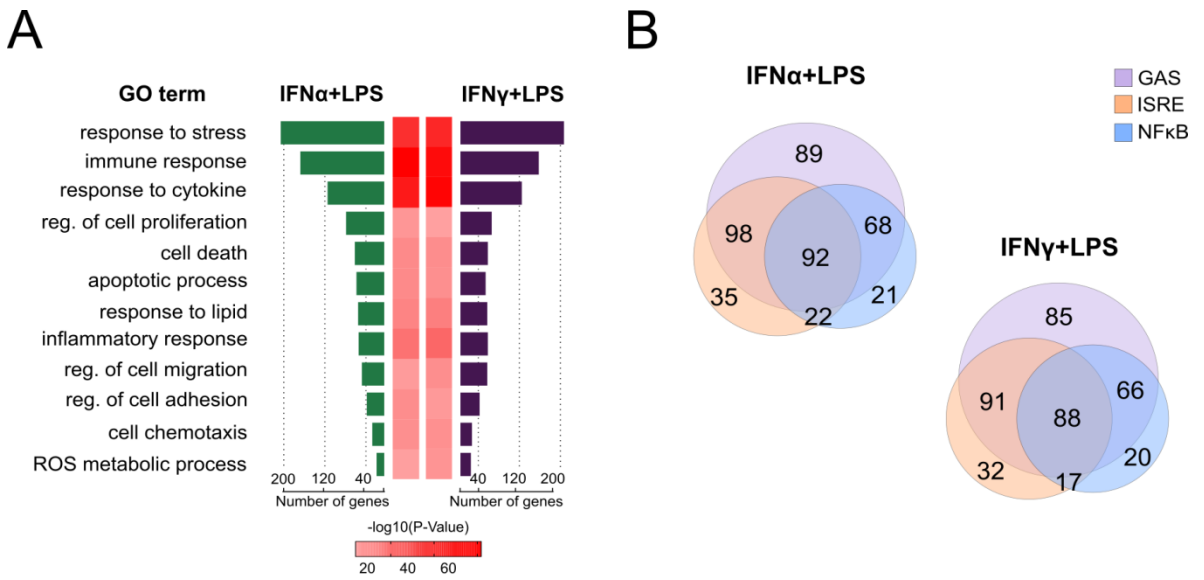

Figure 2. 7. GO and promoter analysis of commonly up-regulated genes by IFNα+LPS and IFNγ+LPS.

(A) GO analysis of commonly IFNα(8h)+LPS(4h)- and IFNγ(8h)+LPS(4h)-activated genes in VSMC and immune cells (RNA-seq) revealed a strong enrichment for terms reflecting pro-inflammatory and pro-atherogenic biological functions. P-value<0.05. **(B)** Venn diagram presenting distribution of promoter located (-950bp/+100bp) GAS, ISRE and NFκB binding sites among commonly up-regulated genes between VSMC, MΦ and DC by IFNα(8h)+LPS(4h) and IFNγ(8h)+LPS(4h) from RNA-seq experiment.

Genome-wide binding of STAT1 and p65 in response to IFNα+LPS and IFNγ+LPS is mediated through comparable single and combined GAS/ISRE/NFκB binding modes

Next we aimed to further address the mechanism of priming-induced SI between type I or II IFN and TLR4-activator LPS. Based on abovementioned *in silico* transcriptome analysis we anticipated on existence of regulatory overlap between IFNα and IFNγ potentially driven by STAT1 and p65, in the context of priming-induced SI. To obtain further proof for this assumption we characterized the genome-wide recruitment of STAT1 and NFκB (p65) to the regulatory regions of commonly up-regulated genes in response to IFNα+LPS and IFNγ+LPS. ChIP-seq with STAT1 and p65 antibodies was performed on chromatin from VSMC exposed to the following treatment conditions: untreated, IFNα (8h), IFNγ (8h) or LPS (4h) alone, or combined treatment (IFNα 8h+LPS 4h; IFNγ 8h+LPS 4h), described in detail in Material and Methods, section: Primary VSMC, MΦ and DC cell culture and treatment.

Peak calling ChIP-seq *in silico* analysis (MACS algorithm) revealed STAT1 and p65 binding pattern upon different treatment conditions. As such, Figure 2.8A reveals that

stimulation with IFNγ resulted in dramatic increase in the number of called STAT1 peaks, which effect was slightly increased upon IFNγ+LPS. Similarly, IFNα and IFNα+LPS stimulation resulted in almost equally increased number of peaks, while LPS-dependent effect on STAT1 recruitment was rather limited (Fig.2.8A). In contrast, the number of p65 called peaks was mainly elevated upon stimulation with single LPS. Treatment with IFNα and IFNγ resulted in comparable number of p65 occupied regions, which effect was moderately elevated upon combined stimulation with IFNα+LPS or IFNγ+LPS in comparison to single IFN, yet slightly lowered in comparison to LPS only (Fig.2.8A). Peak scores calculated for top 1000 STAT1 and p65 peaks upon treatment with IFN and LPS are depicted in Figure 2.8B. Each box represents the range of peak score values, with the median value represented by the horizontal line within the box. Additionally the average peak score value was marked by a red cross. Number of STAT1 and p65 called peaks pattern analysis resembles this of top 1000 peak scores analysis. Thus, the highest STAT1 peak scores could be identified upon stimulation with IFNγ and IFNγ+LPS or IFNα and IFNα+LPS (Fig.2.8B). In case of p65, stimulation with LPS, IFNα+LPS and IFNγ+LPS resulted in comparable high average peak scores (Fig.2.8B). Therefore, these analysis reveals variable influence of IFN and LPS treatment on STAT1 and p65 recruitment to the gene regulatory regions.

To further study potentially distinct and comparable recruitment pattern of STAT1 and p65 upon stimulation with IFN and LPS, we performed clustering analysis of STAT1 and p65 occupied regions in our ChIP-seq experiments. RD plot represents STAT1 and p65 binding regions visualised as tag counts (blue lines on the graph) (Fig.2.9). This analysis clearly indicates that genome-wide binding of STAT1 and p65 under treatment with IFN and LPS could co-localize or be TF-exclusive. Therefore, in Cluster 7 there is visible clear STAT1-p65 co-binding within the same genomic regions after stimulation with IFNα+LPS or IFNγ+LPS, reflected by increased blue colour intensity (Fig.2.9). On the other hand, sole STAT1 binding could be observed in Cluster 2 and 8, while p65 exclusive recruitment was observed within the regions ascribed to Cluster 1 and 9 (Fig.2.9).

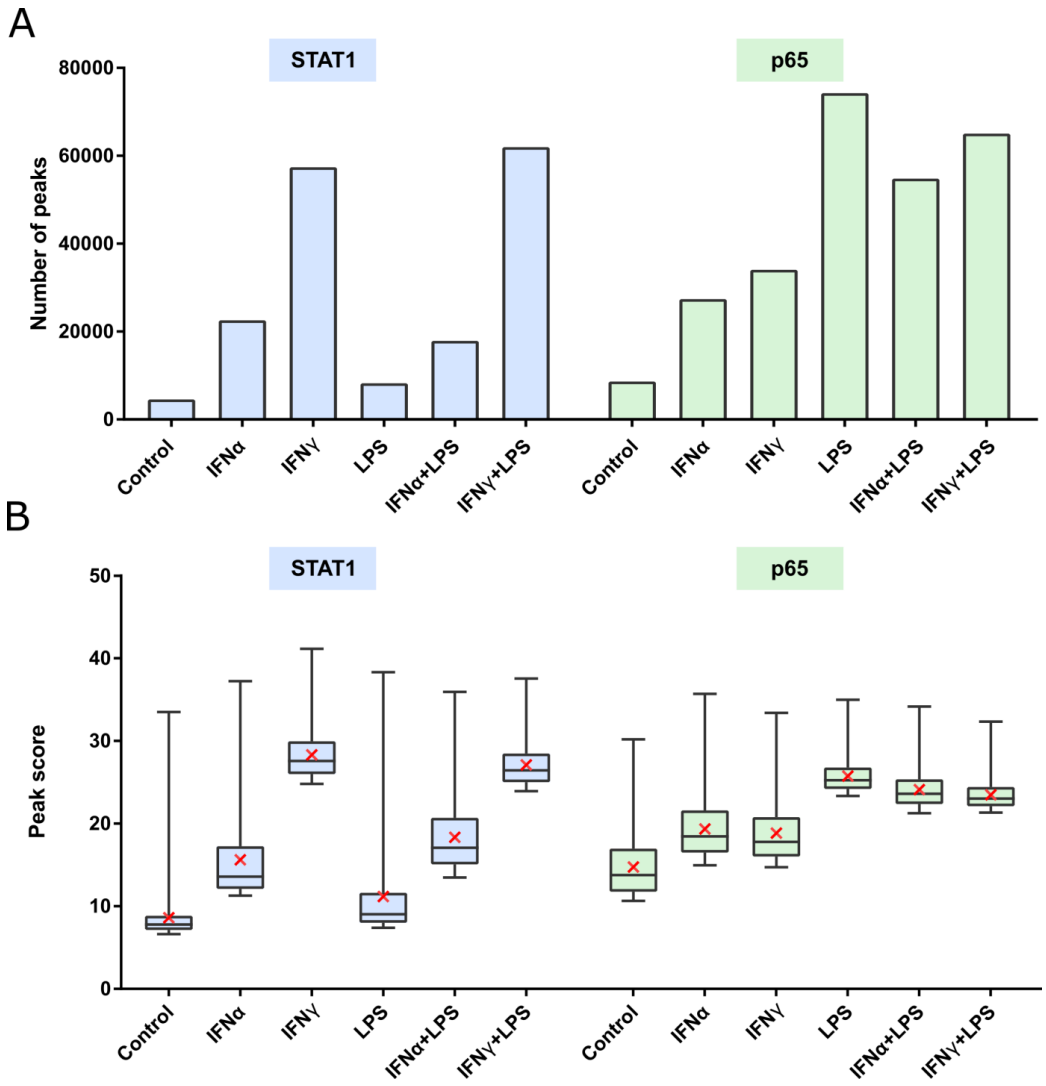

Figure 2. 8. STAT1 and p65 ChIP-seq peak calling analysis in VSMC treated with IFN and LPS.

(A) Number of called peaks (MACS algorithm) in STAT1 (blue bars) and p65 (green bars) ChIP-seq experiments in VSMC stimulated with IFNα(8h), IFNγ(8h), LPS(4h), IFNα(8h)+LPS(4h) and IFNγ(8h)+LPS(4h). **(B)** Distribution of STAT1 (blue boxes) and p65 (green boxes) ChIP-seq peak score values (MACS algorithm) upon VSMC treatment with IFNα(8h), IFNγ(8h), LPS(4h), IFNα(8h)+LPS(4h) and IFNγ(8h)+LPS(4h). The line within each box represents the median and the lower and upper boundaries of each box indicate first and third quartiles, respectively. The average peak score value was marked by a red cross for each treatment condition.

Subsequently, we aimed to characterize the distribution of genome-wide binding of STAT1 and p65 to the genomic regions within STAT1-p65 co-binding regions and STAT1- or p65-solely bound regions. Hence GAS, ISRE and NFκB consensus binding sequences (Fig.2.10A-C) for STAT1 and p65 were re-mapped to the genomic regions occupied by these two TF and overlapped with the lists of 579 IFNα+LPS and 536 IFNγ+LPS commonly up-regulated genes resulting from previous RNA-seq analysis (Fig.2.4B).

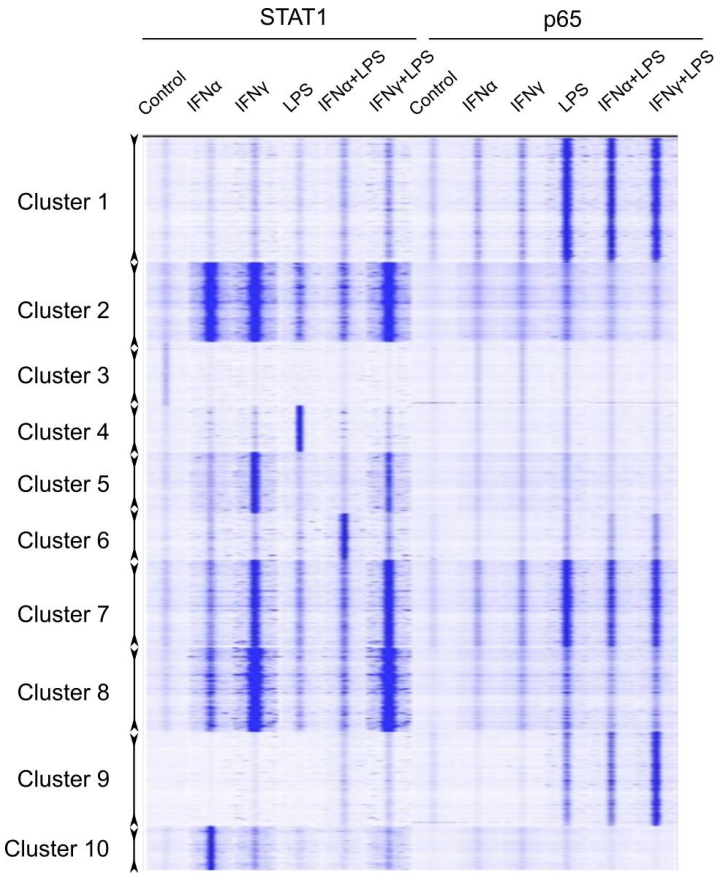

Figure 2. 9. Genome-wide recruitment of STAT1 and p65 to the regulatory regions of commonly up-regulated IFNα+LPS- and IFNγ+LPS-induced genes.

RD plot for STAT1 and p65 ChIP-seq peaks clustered (k-means clustering) based on binding pattern across control, IFNα(8h), IFNγ(8h), LPS(4h), IFNα(8h)+LPS(4h), IFNγ(8h)+LPS(4h) treatment conditions in VSMC. Identified clusters are marked as Cluster(C)1-10. *Graph was prepared based on the bioinformatic analysis performed by Lajos Széles and Attila Csermely (Department of Biochemistry and Molecular Biology, University of Debrecen).*

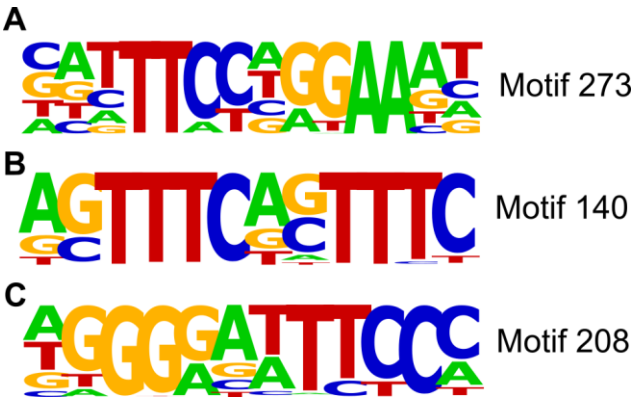

Figure 2. 10. HOMER Motif Logos used for re-mapping analysis in STAT1 and p65 ChIP-seq experiments.

(A) Logo (motif 273) representing GAS binding sequence. **(B)** Logo (motif 140) representing ISRE binding sequence. **(C)** Logo (motif 208) representing NFκB-p65 binding sequence.

STAT1 and p65 re-mapping analysis revealed presence of multiple GAS or ISRE and NFκB binding sites, respectively, distributed genome-wide in the regulatory regions of commonly up-regulated genes. This result correlated with previously presented *in silico* promoter analysis (Fig.2.7B), which predicted the presence of multiple STAT1 and NFκB candidate binding sites in the promoters these genes. Great majority of single GAS, ISRE (STAT1 solely occupied) and NFκB (p65 solely occupied) binding sites, were identified within intronic (28-32.3%), intergenic (24.9-39.6%) and promoter (23.4-38.1%) regions of IFNα+LPS- and IFNγ+LPS-responsive genes (Fig.2.11A). Alike, genomic sites of STAT1-p65 co-binding were predominantly present in intronic (29.9-32.8%), intergenic (37.2-37.8%) and promoter (17.2-26.1%) regions (Fig.2.11A). Additionally, STAT1 and p65 recruitment could be detected to lesser extent (if the percentage was lower than 5% the value was not outlined on the graph) within genomic regions including TTS, exons, 5'UTR and 3'UTR, as depicted in Figure 2.11A.

Next we intended to determine how many IFNα+LPS- and IFNγ+LPS-induced genes were characterized by: (1) STAT1 or p65 recruitment to solitary GAS, ISRE or NFκB sites, respectively, but also (2) STAT1-p65 co-binding to GAS-NFκB, ISRE-NFκB or GAS-ISRE-NFκB composite sites. By this comparison we could define gene groups, which represented different STAT1 and p65 recruitment patterns to their cognate motifs present in gene regulatory regions. Based on these gene groups we delineated so-called STAT1 and p65 'binding modes' (Fig.2.11B), including 'single' binding mode (STAT1 binding to GAS and/or ISRE; p65 to NFκB) or 'co-binding' mode (STAT1 binding to GAS and/or ISRE+p65 to NFκB). Hence, as shown in Figure 2.11B several 'single' STAT1 and p65 binding mode representatives were characterized. In detail, among IFNα+LPS-dependent genes, we identified: 6 solitary GAS-, 81 solitary ISRE-, 85 solitary NFκB-, and 51 GAS-ISRE-containing genes (Fig.2.11B). In case of IFNγ+LPS-induced genes, there were distinguished: 17 solitary GAS-, 45 solitary ISRE-, 28 solitary NFκB- and 53 GAS-ISRE-containing genes (Fig.2.11B). Furthermore, STAT1-p65 'co-binding' mode example genes could be characterized. As such, IFNα+LPS-activated genes were divided into three STAT-p65 'co-binding' modes represented by: 23 GAS-NFκB, 94 ISRE-NFκB and 99 GAS-ISRE-NFκB genes (Fig.2.11B). For IFNγ+LPS-responsive genes three STAT1-p65 'co-binding' modes representatives were identified alike: 40 GAS-NFκB, 59 ISRE-NFκB and 178 GAS-ISRE-NFκB genes (Fig.2.11B).

Additionally, Figure 2.11B offers insight into the overlap between different STAT1 and p65 binding modes upon stimulation with IFN and LPS. Substantial overlap was identified between genes representing NFκB-only (15.9%) and GAS-only (13%) modes, but surprisingly also ISRE-only (29.4%) mode (Fig.2.11B). It is known that stimulation with IFNα as well as IFNγ results in GAF complexes formation and their subsequent recruitment to GAS sites in ISG promoters. Therefore identification of 13% overlap between IFNα+LPS and IFNγ+LPS-induced genes containing solitary GAS site was understandable. Yet 29.4% overlap within ISRE-only mode between type I and type II IFN-dependent responses was very surprising, since limited evidence supports a role of ISGF3 in IFNγ-dependent gene transcriptional activation. Similarly, within STAT1-p65 'co-binding' mode gene we could observe significant overlap between IFNα and IFNγ-induced reponse: GAS-ISRE (32.7%), GAS-NFκB (11.1%), ISRE-NFκB (21.6%) and GAS-ISRE-NFκB genes (29.6%) (Fig.2.11B).

A

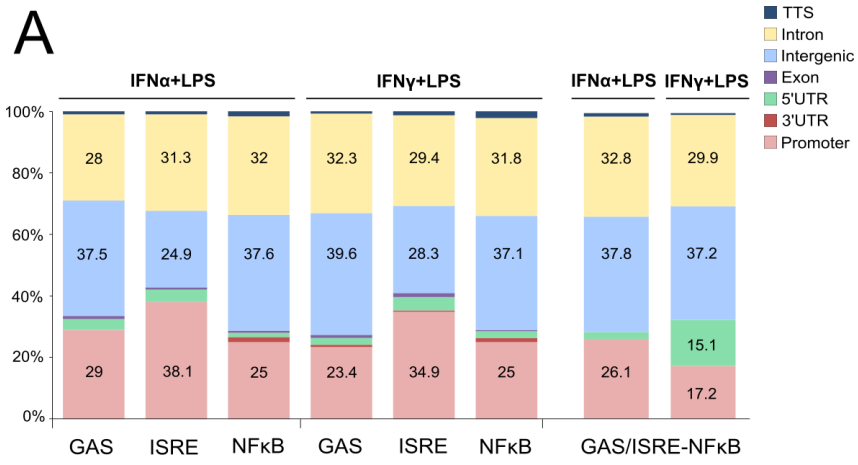

B

Binding mode	IFNα+LPS	IFNγ+LPS	Overlap [%]
GAS	6	17	13,0
ISRE	81	45	29,4
NFκB	85	28	15,9
GAS-ISRE	51	53	32,7
GAS-NFκB	23	40	11,1
ISRE-NFκB	94	59	21,6
GAS-ISRE-NFκB	99	178	29,6

Figure 2. 11. Genome-wide role of STAT1 and p65 in transcriptional regulation of commonly up-regulated IFNα+LPS- and IFNγ+LPS-induced genes.

(A) Global distribution of STAT1 (GAS and ISRE) and p65 (NFκB) occupied binding sites identified by ChIP-seq re-mapping analysis. STAT1 and p65 recruitment was classified in 7 genomic locations (colour-coded with the mapping provided in the legend): promoter/TSS (-1kb to +100bp), introns,

intergenic, exon, 5’ UTR, 3’ UTR and TTS. Re-mapped motifs distribution was plotted by the percentage of total number of occupied GAS, ISRE and NFκB binding sites present in the regulatory regions of commonly up-regulated IFNα(8h)+LPS(4h)- and IFNγ(8h)+LPS(4h)-induced genes in VSMC. **(B)** Representation of STAT1 and p65 occupied binding sites identified by ChIP-seq re-mapping analysis, representing 'single' modes (STAT1 binding to GAS and/or ISRE; p65 binding to NFκB) or 'co-binding' modes (STAT1 binding to GAS and/or ISRE together with p65 to NFκB). Table depicts number of the genes within each STAT1/p65 binding mode among IFNα(8h)+LPS(4h)- and IFNγ(8h)+LPS(4h)-induced genes together with percentage overlap between the two distinct treatment conditions.

Together, these results suggest that it exists a common genome-wide mechanism of priming-induced SI between IFNα and LPS or IFNγ and LPS in VSMC. This mechanism potentially involves collaboration of ISGF3 and GAF with NFκB, which recruitment to composite ISRE/NFκB or GAS/NFκB binding sites would result in SI-dependent transcriptional gene activation.

STAT1-containing complexes ISGF3 and potentially STAT1-IRF9 mediate transcription of ISRE-containing genes in response to both IFN I and IFN II

Since we observed a striking overlap between IFNα- and IFNγ-dependent transcriptional responses within ISRE-only (45 genes) and ISRE-NFκB 'co-binding' mode (59 genes) (Fig.2.11B), we decided to take a closer look and examine a potential mechanism of ISRE-containing gene expression regulation. Among these two gene groups there were identified classical ISRE-containing genes, from which we selected *Ifit1, Mx2, Oas2, Cxcl10* and *Irf7* for further analysis. Closer promoter analysis of these genes indeed confirmed the presence of solitary ISRE (or ISRE-NFκB) binding sites and simultaneous absence of GAS motif.

Thus, as expected all selected ISRE-containing genes were predominantly responsive to IFNα and less to IFNγ (Fig.2.12A). Moreover, in case of *Ifit1, Mx2* and *Cxcl10* there could be observed an effect of SI manifested by increased FC values after combined treatment with IFNα+LPS and IFNγ+LPS in comparison to single stimuli (Fig.2.12A).

As commonly accepted, STAT, IRF and NFκB TF mediate gene transcription in response to IFN and LPS. Therefore next, we performed Western blot analysis for tSTAT1, pSTAT1, tSTAT2, pSTAT2, IRF1, IRF9 and p65 protein. Moderate increase in STAT1 and STAT2 phosphorylation in response to IFNα+LPS and IFNγ+LPS, as compared to the

individual ones, correlated with expression values of ISRE-containing genes presented in Figure 2.12A. Ratios between pSTAT1/tSTAT1 and pSTAT2/tSTAT2 are depicted in Figure 2.12B. Protein enrichment pattern observed upon stimulation with IFN and LPS will be discussed along the text.

A

Gene name	Fold change				
	IFNα	IFNγ	LPS	IFNα+LPS	IFNγ+LPS
Ifit1	113,3	40,1	11,1	153,6	59,2
Mx2	68,2	8,3	3,7	86,0	13,0
Oas2	41,9	19,1	2,6	46,8	18,8
Cxcl10	75,9	49,8	4,6	312,1	364,9
Irf7	58,6	15,4	3,4	50,1	13,0

B

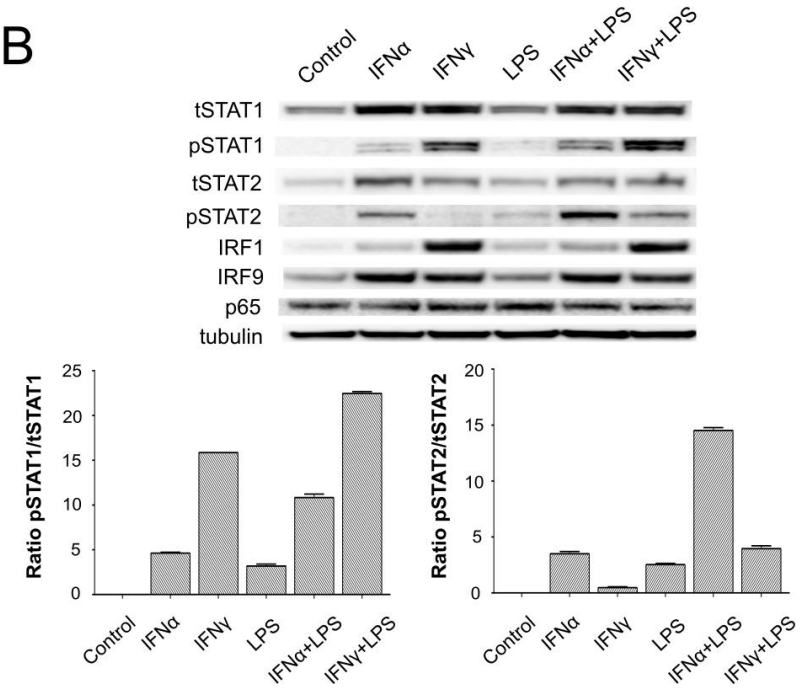

Figure 2. 12. ISRE-containing gene transcriptional regulation upon IFNα and IFNγ treatment.

(A) Gene expression levels (presented as FC in comparison to control) of *Ifit1*, *Mx2*, *Oas2*, *Cxcl10* and *Irf7* genes, resulting from RNA-seq: VSMC untreated or treated with IFNα(8h), IFNγ(8h), LPS(4h), IFNα(8h)+LPS(4h), IFNγ(8h)+LPS(4h). **(B)** Upper panel. Western blot analysis of protein extracts isolated from VSMC untreated or treated with IFNα(8h), IFNγ(8h), LPS(4h), IFNα(8h)+LPS(4h), IFNγ(8h)+LPS(4h). tSTAT1, pSTAT1, tSTAT2, pSTAT2, IRF1, IRF9, p65 and tubulin protein levels were assessed by Western blot analysis. n=3, one representative blot is presented. Lower panel. Western blot quantification bars represent mean quantification of pSTAT1/tSTAT1 and pSTAT2/tSTAT2 ratio (normalized to tubulin). Mean ± s.e.m., n=3;

To further examine the role of STAT1 in transcriptional regulation of ISRE-containing genes we analysed its binding within promoter regions of *Ifit1*, *Mx2*, *Oas2*, *Cxcl10* and *Irf7*. Worth mentioned, it was previously reported that *Cxcl10* gene expression depends on two distinct regulatory regions, of which the proximal one has a solitary ISRE site (Rauch et al. 2015). Thus in this part of our study the proximal region was selected for further examination of IFN-dependent STAT1 recruitment. Treatment with both single IFN, alike combined treatment with LPS, resulted in STAT1 binding to ISRE-motifs in *Ifit1*, *Mx2*, *Oas2*, *Cxcl10* and *Irf7* gene promoters (Fig.2.13A). This surprising observation was further validated by quantitative ChIP-PCR, which indeed confirmed significant recruitment of tSTAT1 to ISRE-containing regions of all 5 genes, especially upon stimulation with IFNγ, but also IFNα (Fig.2.13B). Moreover binding pattern of pSTAT1 mirrored that of tSTAT1 and was essentially elevated upon treatment with both IFN (Fig.2.13B). Furthermore, IFNα and IFNγ driven pSTAT1 recruitment reflected pSTAT1 protein levels previously examined by Western blot under the same treatment conditions (Fig.2.12B).

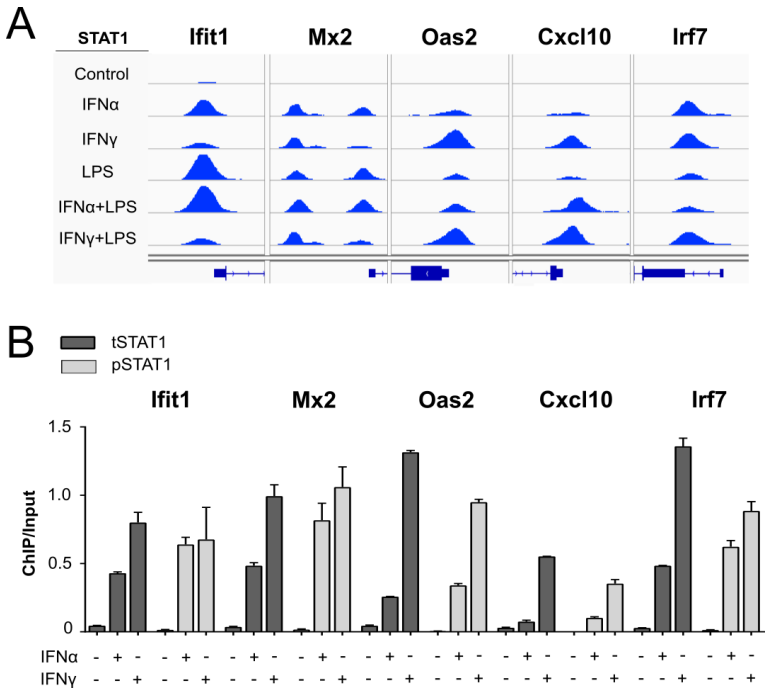

Figure 2. 13. STAT1 recruitment to the regulatory regions of ISRE-containing genes under stimulation with type I and II IFN.

(A) Representative views of STAT1 ChIP-seq peaks detected in the promoter regions of *Ifit1*, *Mx2*, *Oas2*, *Cxcl10* and *Irf7* genes, containing solitary ISRE binding sites, in untreated or IFNα(8h), IFNγ(8h), LPS(4h), IFNα(8h)+LPS(4h), IFNγ(8h)+LPS(4h)-stimulated VSMC. STAT1 peaks were mapped onto the mouse reference genome mm10 and visualized using the IGV genome browser.

(B) VSMC were untreated or treated with IFNα(8h) and IFNγ(8h), chromatin was isolated and immunoprecipitated with tSTAT1 and pSTAT1 antibodies. ChIP-PCR validation of tSTAT1 and pSTAT1 binding to ISRE motif present in the promoters at *Ifit1*, *Mx2*, *Oas2*, *Cxcl10* and *Irf7* genes was performed. Mean ± s.e.m., n=2. Primers are listed in Table 2.2.

Likewise we analysed recruitment of tSTAT2, pSTAT2 and IRF9 to ISRE-containing regions of *Ifit1, Mx2, Oas2, Cxcl10* and *Irf7* genes (Fig.2.14A-B). As such we could observe increased binding of tSTAT2 and pSTAT2 upon IFNα treatment, but surprisingly also in response to IFNγ. Similarily to pSTAT1, pSTAT2 binding pattern correlated with pSTAT2 protein enrichment examined upon stimulation with both IFN types (Fig.2.12B). Unexpectedly, pSTAT2 protein could be detected not only upon stimulation with IFNα and IFNα+LPS, but also IFNγ and IFNγ+LPS (Fig.2.12B). IRF9 binding pattern resembled that of pSTAT2 and correlated with IRF9 protein levels (Fig.2.14B, Fig.2.12B). Thus, Western blot followed by ChIP-PCR indicated simultaneous formation and recruitment of tSTAT1/pSTAT1, tSTAT2/pSTAT2 and IRF9 upon stimulation with both IFNα and IFNγ. This observation clearly suggests potential involvement of ISGF3 complex in ISRE-containing gene expression regulation. In order to investigate formation of ISGF3 complex upon IFN treatment, we performed a set of co-IP experiments. Proteins were isolated from VSMC treated with IFNα and IFNγ and co-immunoprecipitated with IRF9 antibody. Next, formed immunocomplexes were visualised by STAT1 and STAT2 Western blot, which confirmed assembly of ISGF3 complex in response to IFNα and IFNγ (Fig.2.14C).

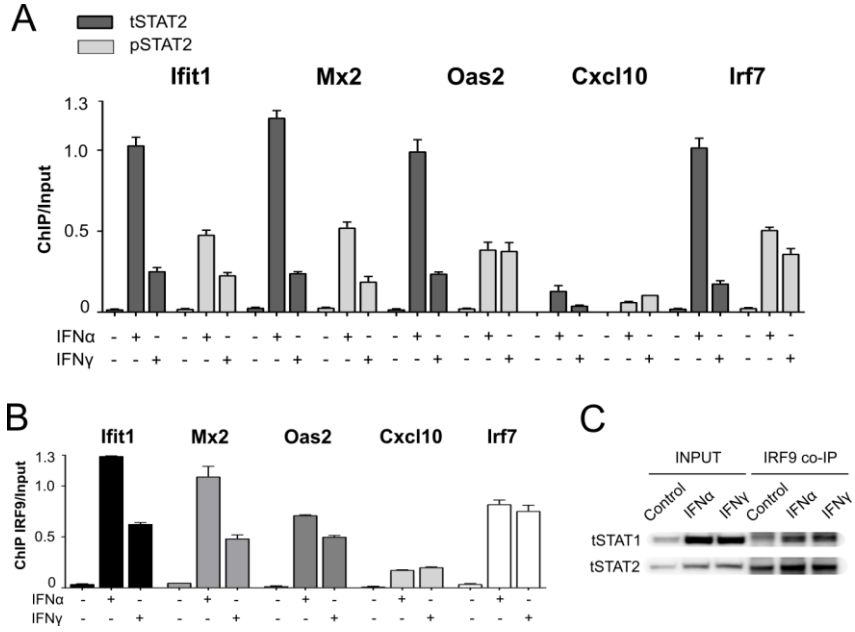

Figure 2. 14. STAT1, STAT2 and IRF9 in transcriptional regulation of ISRE-containing genes under stimulation with IFNα and IFNγ. (Figure description on the next page)

ChIP-PCR. VSMC were left untreated or stimulated with IFNα(8h) and IFNγ(8h), chromatin was isolated and immunoprecipitated with **(A)** tSTAT2, pSTAT2 and **(B)** IRF9 antibodies, followed by ChIP-PCR analysis of *Ifit1, Mx2, Oas2, Cxcl10* and *Irf7*. Mean ± s.e.m., n=2. Primers are listed in Table 2.2. **(C)** Co-IP. Protein extracts were isolated from VSMC untreated or treated with IFNα(8h) and IFNγ(8h), immunoprecipitated with IRF9 antibody and analysed by tSTAT1 and/or tSTAT2 Western blot. n=3, one representative blot is shown.

Yet if expression of ISRE-containing genes would be driven exclusively by ISGF3 complex, then the ratio between its components pSTAT1, pSTAT2 and IRF9 would be equal, which did not correlate with our results. Expression pattern of *Ifit1, Mx2, Oas2, Cxcl10* and *Irf7* resembled binding pattern of pSTAT2 and IRF9, being higher upon stimulation with IFNα in comparison to IFNγ (Fig.2.12A, Fig.2.14A-B). Surprisingly, it was not true for pSTAT1, which was more efficiently recruited in response to IFNγ as compared to IFNα (Fig.2.13B). This observation may imply STAT1 presence in an additional transcriptionally active complex to mediate IFNγ-driven expression of ISRE-containing genes. Elevated pSTAT1 and IRF9 levels upon type II IFN treatment could suggest potential involvement of STAT1-IRF9 complex, as reported previously (Bluyssen et al. 1995).

In order to characterize the nature of transcriptional complex potentially driving ISRE-containing gene expression in response to IFNγ, in addition to ISGF3, we examined expression pattern of *Ifit1, Mx2, Oas2, Cxcl10* and *Irf7* in STAT1, STAT2 and IRF9 depleted VSMC (Fig.2.15A-D). First, we confirmed expression pattern of these genes in WT VSMC (Fig.2.15A). *Ifit1, Mx2, Irf7* and to lesser extent *Oas2* gene expression was higher in response to IFNα in comparison to IFNγ (Fig.2.15A), what correlated with RNA-seq FC values (Fig.2.12A). Yet in case of *Cxcl10*, RT-PCR analysis resulted in the opposite results indicating higher responsiveness to IFNγ as compared to IFNα (Fig.2.15A). Next we evaluated ISRE-containing gene expression in VSMC STAT1 KO (Fig.2.15B). As expected, in the absence of STAT1, IFNγ-induced response was totally abrogated (Fig.2.15B), confirming crucial role of STAT1-containing complexes in type II IFN-driven gene activation. Yet, IFNα-dependent expression of ISRE-containing genes was sustained in these cells (Fig.2.15B). This could point to a regulatory role of STAT2-IRF9 complex in the absence of STAT1, as reported previously (Blaszczyk et al. 2015). In the next set of RT-PCR experiments we noticed that IFNα stimulation of VSMC STAT2 KO did not result in *Ifit1, Mx2, Oas2, Cxcl10* and *Irf7* transcriptional activation, proving critical role of STAT2-containing complexes in type I IFN-driven response. In contrast, these ISRE-containing gene expression was elevated upon IFNγ treatment (Fig.2.15C). This observation could serve as a

crucial evidence for the potential role of STAT1-IRF9 complex in IFNγ-dependent ISRE-containing gene expression. Remarkably, a similar gene expression pattern as in VSMC STAT2 KO was observed in VSMC IRF9 KO in response to both IFN (Fig.2.15D). As such, we could observe reduced or abrogated IFNα-dependent gene expression of *Ifit1*, *Mx2*, *Irf7* and *Oas2, Cxcl10*. At the same time, IFNγ-driven transcriptional response was sustained (Fig.2.15D). This notion may imply involvement of an additional TF/complex except ISGF3 and STAT1-IRF9 in the regulation of ISRE-containing gene expression upon IFNγ stimulation.

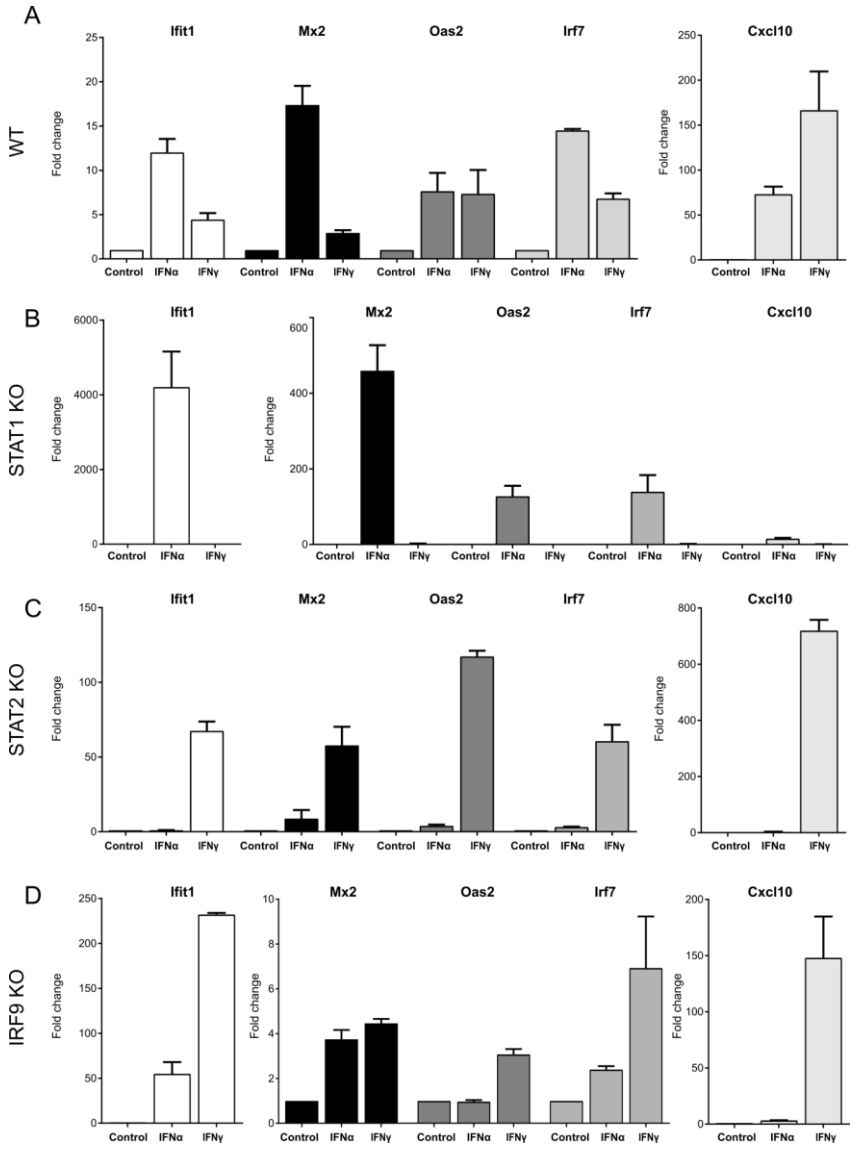

Figure 2. 15. ISRE-containing gene expression pattern upon stimulation with IFNα and IFNγ in WT, STAT1 KO, STAT2 KO and IRF9 KO VSMC.

Ifit1, *Mx2*, *Oas2*, *Cxcl10* and *Irf7* relative gene expression (over *β-Actin*) in **(A)** WT VSMC, **(B)** STAT1 KO VSMC, **(C)** STAT2 KO VSMC and **(D)** IRF9 KO VSMC stimulated with IFNα(8h) and IFNγ(8h), determined by RT-PCR. Primers listed in Table 2.1.

Since before mentioned Western blot analysis revealed that IFNγ treatment correlated with elevated IRF1 levels (Fig.2.12B), we speculated about the potential involvement of STAT1-IRF1 complexes in ISRE-containing gene regulation. Indeed, ChIP-PCR experiment provided evidence for IRF1 recruitment to ISRE-containing gene promoters upon stimulation with IFNγ, but only weakly with IFNα (Fig.2.16A). Significant IRF1 binding was observed especially at *Ifit1* and *Mx2* regulatory regions, in comparison to *Oas2*, *Cxcl10* and *Irf7*. In order to investigate formation of STAT1-IRF1 complex upon IFNγ stimulation, co-IP experiment was performed. We could not observe direct interaction between STAT1 and IRF1 under this treatment conditions (Fig.2.16B), what suggests STAT1-independent role of IRF1 in ISRE-containing gene expression regulation.

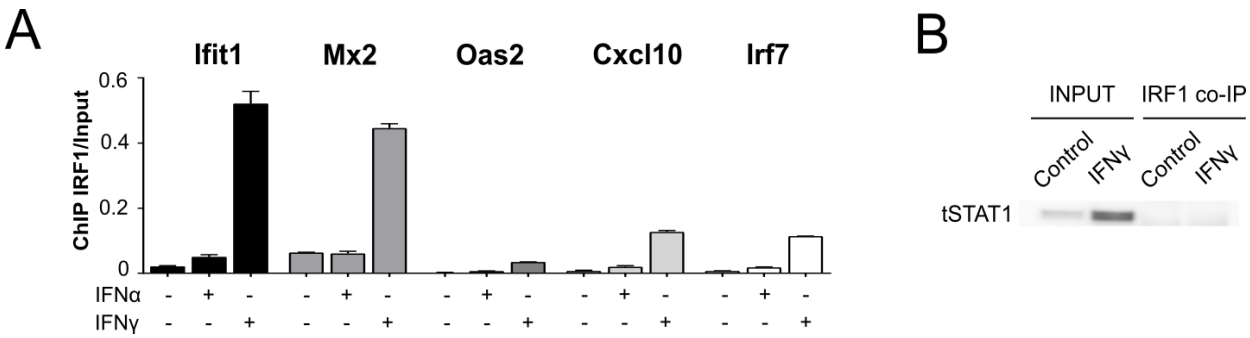

Figure 2. 16. Potential involvement of IRF1 in transcriptional regulation of ISRE-containing genes under stimulation with IFN.

(A) ChIP-PCR. VSMC were left untreated or stimulated with IFNα(8h) and IFNγ(8h), chromatin was isolated and immunoprecipitated with IRF1 antibody, followed by ChIP-PCR analysis of *Ifit1*, *Mx2*, *Oas2*, *Cxcl10* and *Irf7*. Mean ± s.e.m., n=2. Primers are listed in Table 2.2. **(B)** Co-IP. Protein extracts were isolated from VSMC untreated or treated with IFNα(8h) and IFNγ(8h), immunoprecipitated with IRF1 antibody and analysed by tSTAT1 Western blot. n=3, one representative blot is shown.

Collectively our results provide evidence for critical role of ISGF3 complex in IFNα- but also IFNγ-dependent transcriptional response in VSMC. Additionally, IFNγ-induced ISRE-containing gene expression involve STAT1-IRF9 complex. However, involvement of the other transcriptional complexes could not be excluded.

STAT1 and p65 are recruited to GAS/NFκB or ISRE/NFκB composite sites in response to IFNα+LPS or IFNγ+LPS

Since we characterized how GAF, ISGF3 and STAT1/IRF9 transcriptional complexes could be involved in IFNα- and IFNγ-dependent gene expression, afterwards we aimed at understanding how these STAT1-containing complexes mediate SI between IFN and LPS. For this purpose we focused on the genes which were representing STAT1-p65 'co-binding' modes under stimulation with IFNα+LPS- and IFNγ+LPS (Fig.2.17). Interestingly, analysis of genome-wide distance between the summits of STAT1 ChIP peak and the closest p65 ChIP peak summit, after combined stimulation with both IFN and LPS, revealed that great majority of STAT1-p65 peaks were occurring at a distance of not more than 200bp (marked by a dashed red line) (Fig.2.17).

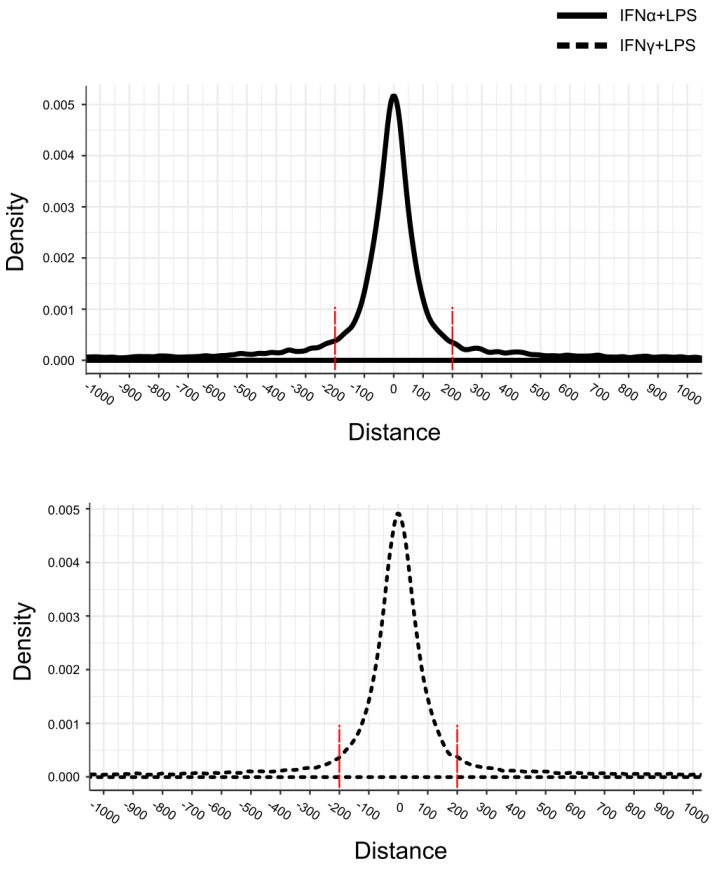

Figure 2. 17. Distribution of STAT1 and p65 ChIP-seq peak summits in IFNα+LPS and IFNγ+LPS-induced VSMC.

Peak distribution plots showing distances between STAT1 and the closest p65 peak summits resulting from ChIP-seq in VSMC upon stimulation with IFNα(8h)+LPS(4h) (upper panel, a solid black line) and IFNγ(8h)+LPS(4h) (lower panel, a dashed black line). Red dashed line marks 200bp (+/-) distance between STAT1 and p65 peak summit. *Graph was prepared based on the bioinformatic analysis performed by Lajos Széles and Attila Csermely (Department of Biochemistry and Molecular Biology, University of Debrecen).*

Next we determined how many of the genes which were assigned to one of the 'co-binding' modes: GAS-NFκB, ISRE-NFκB or GAS-ISRE-NFκB (Fig.2.11B), were affected by SI between IFN and LPS in terms of increased transcriptional activation. Thus, we identified 170 genes and 211 genes affected by SI between IFNα+LPS and IFNγ+LPS, respectively. As shown in Venn diagram (Fig.2.18A), 106 genes were commonly affected by SI between these two gene lists. Further, from the common gene list we selected the following STAT1-p65 'co-binding' modes examples. GAS-NFκB mode was represented by *Serpina3i*, *Steap4*, *Irf1*, ISRE-NFκB mode by *Ccl5*, *Ifit1*, *Gbp6* and GAS-ISRE-NFκB mode by *Cxcl10* and *Gbp7*. FC values resulting from RNA-seq experiment, reflecting transcriptional changes upon treatment with IFNα, IFNγ, LPS and IFNα+LPS, IFNγ+LPS, are presented in Figure 2.18B. Clearly, all selected genes were induced by at least one of IFNα, IFNγ or LPS and this response was elevated after combined treatment, reflecting SI between IFN and LPS (Fig.2.18B). Additionally, in Figure 2.18B there are presented FC values resulting from RNA-seq for two representatives of ISRE 'single' mode *Irf7* and NFκB 'single' mode *Saa1*. These two genes were used as a comparison in the downstream analysis of the mechanism driving expression of STAT1 and p65 'co-binding' mode.

A

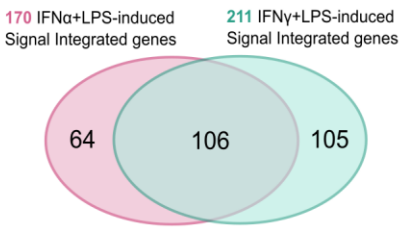

B

Binding mode	Gene name	Fold change					Binding site distance [bp]	
		IFNα	IFNγ	LPS	IFNα+LPS	IFNγ+LPS	GAS-NFκB	ISRE-NFκB
GAS-NFκB	*Serpina3i*	2,3	62,3	19,0	32,6	156,5	41	-
	Steap4	4,9	7,4	38,0	43,1	88,4	123	-
	Irf1	4,0	22,6	1,6	7,4	24,4	68	-
ISRE-NFκB	*Ccl5*	5,1	1,7	4,8	20,9	15,9	-	38
	Ifit1	113,3	40,1	11,1	153,6	59,2	-	46/65
	Gbp6	36,9	266,1	23,5	117,2	555,3	-	264
GAS-ISRE-NFκB	*Cxcl10*	75,9	49,8	4,6	312,1	364,9	52	44
	Gbp7	29,7	65,2	6,9	45,2	75,5	234	200
ISRE	*Irf7*	58,6	15,4	3,4	50,1	13,0	-	-
NFκB	*Saa1*	2,0	2,3	18,0	30,8	63,6	-	-

Figure 2. 18. Selected representatives of STAT1 and p65 'single' and 'co-binding' modes.

(A) Venn diagram showing the overlap between 170 IFNα(8h)+LPS(4h)- and 211 IFNγ(8h)+LPS(4h)-activated SI genes resulting from RNA-seq experiment. **(B)** Gene expression values (FC in comparison to control) for selected genes representing identified STAT1 and p65 'co-binding' modes: GAS-NFκB: *Serpina3i*, *Steap4*, *Irf1*; ISRE-NFκB: *Ccl5*, *Ifit1*, *Gbp6*; GAS-ISRE-NFκB: *Cxcl10*,

Gbp7; and 'single' modes: ISRE: *Irf7*; NFκB: *Saa1*, resulting from RNA-seq experiment in VSMC treated with IFNα(8h), IFNγ(8h), LPS(4h), IFNα(8h)+LPS(4h) and IFNγ(8h)+LPS(4h). Additionally, GAS-NFκB and ISRE-NFκB binding sites distances (bp) within selected STAT1 and p65 'co-binding' mode representative gene promoters are depicted in the table.

In the next step, we analysed recruitment of STAT1 and p65 to the promoters of pre-selected genes, being representatives of GAS-NFκB, ISRE-NFκB and GAS-ISRE-NFκB 'co-binding' modes as well as ISRE and NFκB 'single' modes. IGV genome browser views from STAT1 and p65 ChIP-seq experiments revealed binding pattern of these two TF under stimulation with single and combined treatment with IFNα, IFNγ and LPS. In general, STAT1 and p65 recruitment pattern (Fig.2.19) correlated with transcriptional activation identified by RNA-seq (Fig.2.18B).

Moreover, STAT1 and p65 binding peaks were closely aligned. Distance between ISRE/GAS and NFκB binding sites present in these gene promoters oscillated in a range of 38-264bp (Fig.2.18B). It correlated with previously mentioned observation, resulting from the analysis of the distances between summits of STAT1 and p65 peaks, which suggested prevalence of closely spaced peaks (~200bp) identified under stimulation with IFNα+LPS or IFNγ+LPS (Fig.2.17). Moreover analysis of the regulatory regions of top 30 IFNα+LPS- and IFNγ+LPS-dependent genes presented in Table 2.3-4 revealed the presence of GAS, ISRE and NFκB binding sites (indicated by a dot [•]). It suggests that presence and close binding sites distribution may be a pre-requisite for efficient STAT1 and p65 collaboration in driving IFN and LPS-dependent gene expression.

One striking observation resulting from IGV screenshots analysis, was noticed recruitment of p65 to NFκB sites present in the promoters of all 'co-binding' modes gene representatives *Serpina3i, Steap4, Irf1, Ccl5, Ifit1, Gbp6, Cxcl10* and *Gbp7*, after stimulation with IFNα and IFNγ single treatments (Fig.2.19). In contrast, p65 was not recruited to *Saa1* regulatory region containing solitary NFκB site under these conditions (Fig.2.19).

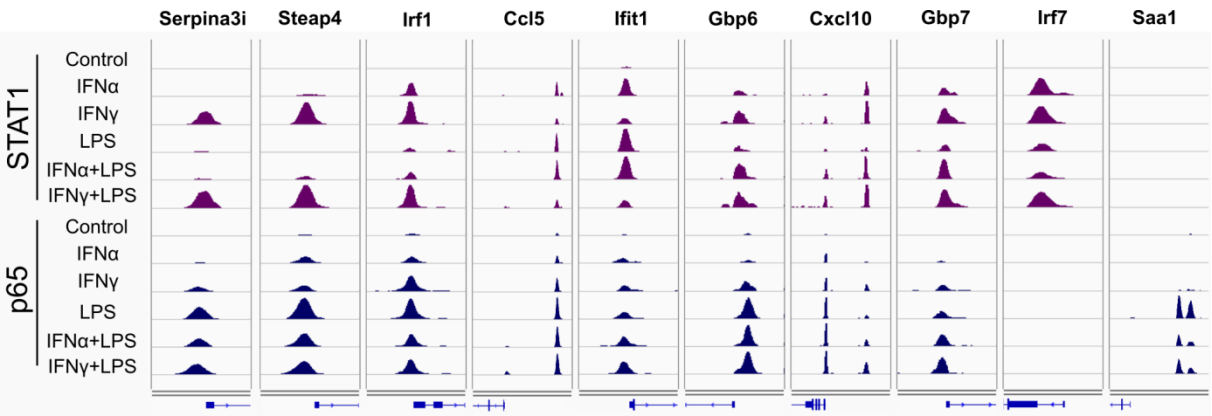

Figure 2. 19. STAT1 and p65 recruitment pattern to IFN+LPS-induced SI gene promoters.

Representative views of STAT1 and p65 ChIP-seq peaks (STAT1: violet peaks, p65: dark blue peaks) identified in the regulatory regions of *Serpina3i*, *Steap4*, *Irf1*, *Ccl5*, *Ifit1*, *Gbp6*, *Cxcl10*, *Gbp7*, *Irf7* and *Saa1* genes, in untreated or IFNα(8h), IFNγ(8h), LPS(4h), IFNα(8h)+LPS(4h), IFNγ(8h)+LPS(4h)-stimulated VSMC. STAT1- and p65-binding peaks were mapped onto the mouse reference genome mm10 and visualized using the IGV genome browser.

Initial recruitment of STAT1 to GAS/NFκB or ISRE/NFκB composites sites facilitates subsequent p65 binding to collaboratively mediate elevated transcription of IFNα+LPS- and IFNγ+LPS-activated genes in VSMC

In order to validate observations made upon STAT1 and p65 recruitment pattern analysis (Fig.2.19), we performed a set of ChIP-PCR experiments (Fig.2.20A-C). Indeed, STAT1 and p65 co-binding to the promoters of *Serpina3i*, *Steap4*, *Irf1*, *Ccl5*, *Ifit1*, *Gbp6*, *Cxcl10* and *Gbp7* identified by IGV screenshots analysis, correlated with that resulting from ChIP-PCR (Fig.2.20A-B). Similarly, we could confirm exclusive recruitment of STAT1 or p65 to the promoters of *Irf7* or *Saa1*, respectively (Fig.2.20C).

Worth mentioned, in case of *Cxcl10* there were reported two regulatory regions, where STAT1 and p65 were co-recruited upon stimulation. Proximal region is composed of ISRE-NFκB binding sites, while distal one contains GAS-ISRE-NFκB composite site (Ohmori and Hamilton 1993, Rauch et al. 2015). Therefore in this part of the study the latter region was chosen for further validation of STAT1 and p65 recruitment in the context of IFN and LPS mediated SI.

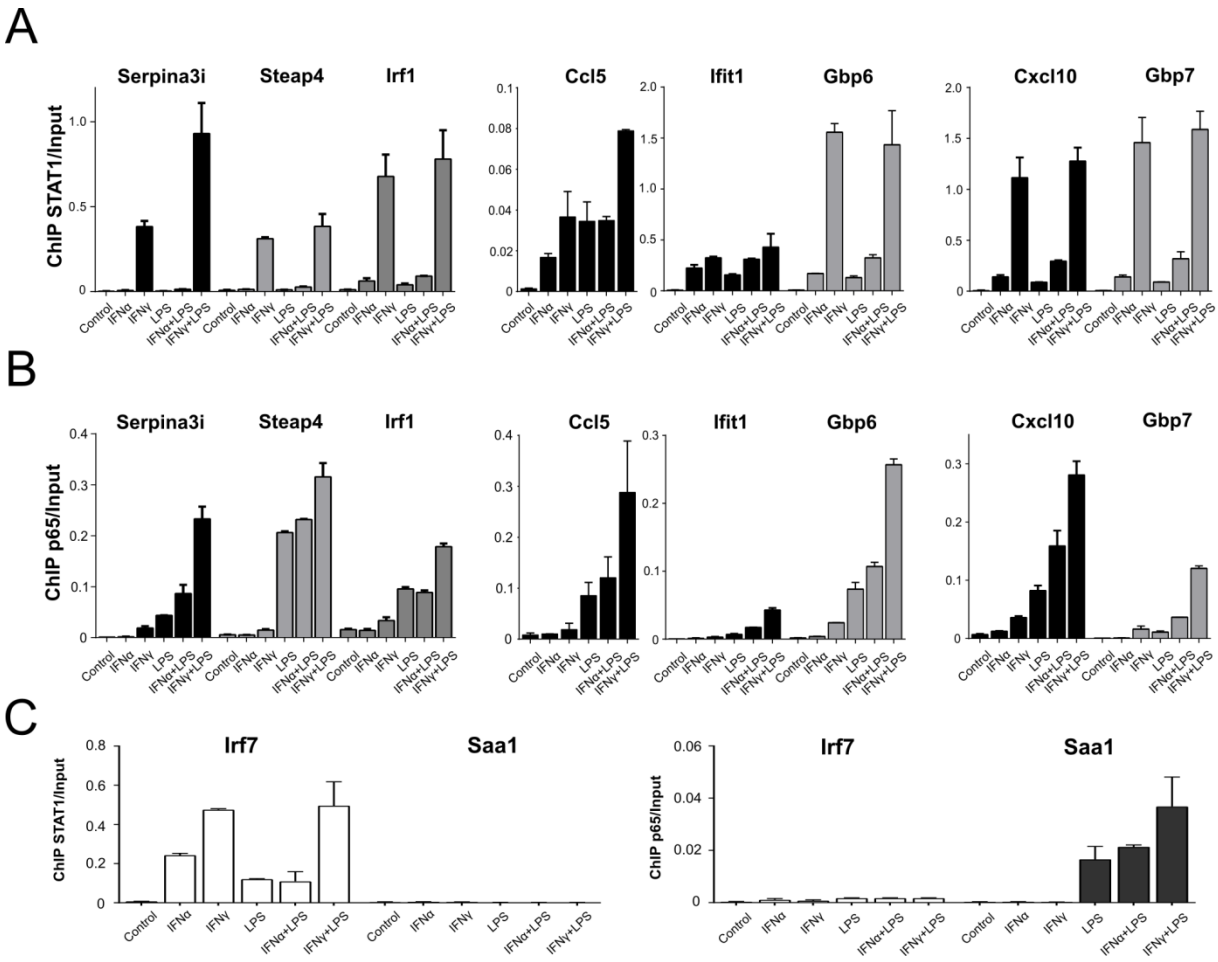

Figure 2. 20. STAT1 and p65 recruitment upon stimulation with IFN and LPS characterization by ChIP-PCR.

(A) ChIP-PCR of STAT1 at *Serpina3i*, *Steap4*, *Irf1*, *Ccl5*, *Ifit1*, *Gbp6*, *Cxcl10* and *Gbp7* gene promoters (primers listed in Table 2.2) in WT VSMC treated with IFNα(8h), IFNγ(8h), LPS(4h), IFNα(8h)+LPS(4h), IFNγ(8h)+LPS(4h). Mean ± s.e.m., n=2. **(B)** ChIP-PCR of p65 at *Serpina3i*, *Steap4*, *Irf1*, *Ccl5*, *Ifit1*, *Gbp6*, *Cxcl10* and *Gbp7* gene promoters in VSMC WT treated with IFNα(8h), IFNγ(8h), LPS(4h), IFNα(8h)+LPS(4h), IFNγ(8h)+LPS(4h). Mean ± s.e.m., n=2. **(C)** ChIP-PCR of STAT1 and p65 at *Irf7* and *Saa1* gene promoters (primers listed in Table 2.2) in WT VSMC treated with IFNα(8h), IFNγ(8h), LPS(4h), IFNα(8h)+LPS(4h), IFNγ(8h)+LPS(4h). Mean ± s.e.m., n=2.

STAT1 and p65 ChIP-PCR experiments supported also the following conclusions. First, STAT1 and p65 enlistment to their cognate binding sites was more abundant in response to IFNγ and IFNγ+LPS in comparison to IFNα and IFNα+LPS (Fig.2.20A-B). This correlated with FC values resulting from RNA-seq (Fig.2.18B), indicating higher responsiveness of *Serpina3i*, *Steap4*, *Irf1*, *Gbp6* and *Gbp7* to IFNγ in comparison to IFNα.

Second, we could confirm abovementioned striking observation of p65 binding to NFκB-GAS/ISRE composites sites in *Serpina3i*, *Steap4*, *Irf1*, *Ccl5*, *Ifit1*, *Gbp6*, *Cxcl10* and

Gbp7 promoters after single IFNα and IFNγ treatments, but not to solitary NFκB element present in *Saa1* promoter (Fig.2.19, Fig.2.20A-B).

Third, for all pre-selected genes representing different STAT1 and p65 'co-binding' modes, we noticed moderate increase in STAT1 recruitment after combined treatments with IFN and LPS in comparison to single ones (Fig.2.20A). The same observation was made for p65, which was even more potently recruited to gene promoters after combined treatments in comparison to LPS alone (Fig.2.20B). Closer examination revealed, that only in case of *Gbp6*, STAT1 recruitment after combined stimulation with IFN and LPS was not elevated in comparison to single IFNγ or IFNα (Fig.2.20A). Importantly, in general STAT1 binding was more potent after stimulation with IFNγ than IFNα, alike IFNγ+LPS in comparison to IFNα+LPS (Fig.2.20A).

Since VSMC were pre-treated with IFNα and IFNγ and then stimulated with LPS, we hypothesised that increased p65 recruitment after combined treatment could be STAT1-dependent. To validate this hypothesis we immunoprecipitated chromatin from STAT1 KO VSMC which were left untreated and IFNα, IFNγ, LPS, IFNα+LPS, IFNγ+LPS-treated with p65 antibody. Strikingly, previously observed increase in p65 binding to the regulatory regions of *Serpina3i, Steap4, Irf1, Ccl5, Ifit1, Gbp6, Cxcl10* and *Gbp7* after combined IFNα+LPS or IFNγ+LPS treatment in comparison to single LPS was totally abrogated in STAT1 KO VSMC (Fig.2.21). Moreover, surprising p65 recruitment after IFNα or IFNγ to gene promoters containing composite GAS/ISRE/NFκB sites in VSMC WT (Fig.2.20B), could not be observed anymore in STAT1 KO VSMC (Fig.2.21).

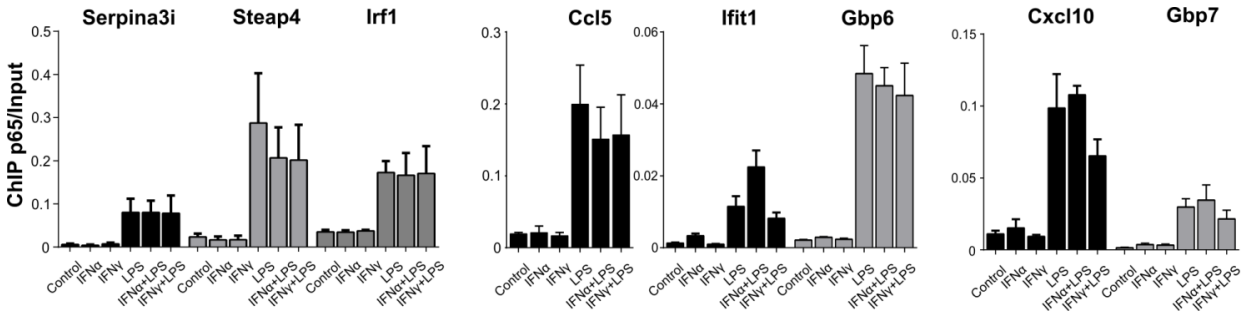

Figure 2. 21. STAT1-dependent p65 recruitment to GAS/NFκB or ISRE/NFκB composite sites upon stimulation with IFN and LPS.

ChIP-PCR of p65 at *Serpina3i, Steap4, Irf1, Ccl5, Ifit1, Gbp6, Cxcl10* and *Gbp7* gene promoters (primers listed in Table 2.2) in STAT1 KO VSMC treated with IFNα(8h), IFNγ(8h), LPS(4h), IFNα(8h)+LPS(4h), IFNγ(8h)+LPS(4h). Mean ± s.e.m., n=2.

Collectively, these results clearly suggest that STAT1-p65 co-binding plays a crucial role in transcriptional regulation of SI genes. Additionally, it seems that elevated gene expression is regulated in STAT1-depnedent manner, which in necessary for subsequent p65 recruitment via nearby located GAS and NFκB or ISRE and NFκB binding sites present in the regulatory regions of SI genes.

IFNα+LPS- and IFNγ+LPS-dependent transcriptional activation correlates with increased hitone acetylation and PolII recruitment in a STAT1-p65 co-binding dependent manner

In order to further understand potential mechanism of STAT1-dependent recruitment of p65 to SI gene promoters, we investigated epigenetic changes occurring upon IFN and LPS treatment. In this part of the study *Cxcl10* and *Gbp7* genes were selected as representatives of STAT1-p65 'co-binding' mode, while *Saa1* and *Irf7* genes exemplified NFκB and ISRE 'single' mode, respectively. Therefore, treatment with IFNα+LPS and IFNγ+LPS resulted in elevated enrichment of H3K27Ac (hisotne mark correlated with gene transcriptional activation) at *Cxcl10* and *Gbp7* gene promoters in comparison to single treatment with IFNα, IFNγ or LPS, which resulted in elevated H3K27Ac alike, yet to lower extent (Fig.2.22A). On the other hand, analysis of negative histone mark H3K27me3 at promoters of STAT1-p65 'co-binding' mode gene representatives presented the opposite pattern. As such, IFNα+LPS and IFNγ+LPS stimulation resulted in diminished level of H3K27me3 at *Cxcl10* and *Gbp7* gene promoters in comparison to IFNα, IFNγ or LPS alone (Fig.2.22A). These observations suggest that treatment with IFN and LPS results in overcoming of the chromatin permissive state and finally STAT1-p65 co-binding dependent gene transcriptional activation. As reported previously, epigenetic histone modifications directly correlate with PolII recruitment to actively transcribing genes (Miller and Grant 2013). Thus, we inspected recruitment of PolII to *Cxcl10* and *Gbp7* gene promoters, which reflected that of H3K27Ac mark, being elevated upon IFNα+LPS and IFNγ+LPS treatment (Fig.2.22A).

At this point we concluded, that SI gene transcriptional activation is mediated by the following order of events. First, IFNα or IFNγ pre-stimulation results in SI gene promoters epigenetic modification, thus increased H3K27Ac at STAT1 ISRE or GAS binding sites. Due to the close proximity of ISRE and GAS motifs to NFκB sites (<200bp, Fig.2.17), histone acetylation encompasses also the latter binding sites. Therefore, not only ISRE and GAS, but

also NFκB binding sites become accessible for TF binding. This hypothesis would explain unexpected p65 binding to NFκB upon stimulation with IFNα and IFNγ. However in order to obtain final proof for such scenario, we aimed to compare epigenetic modifications pattern and PolII recruitment at regulatory regions of STAT1-p65 'co-binding' modes with that of 'single' mode gene representatives. As mentioned before, *Saa1* and *Irf7* exemplified NFκB and ISRE 'single' mode, respectively. Indeed, single treatment with IFNα, IFNγ and LPS resulted in increased H3K27Ac as well as PolII recruitment and decreased H3K27me3 at *Saa1* and *Irf7* gene promoters (Fig.2.22B). In more detail, levels of H3K27Ac at *Saa1* promoter was increased after LPS stimulation, in contrast to IFN, while in case of *Irf7* this mark was enriched predominantly after IFN in comparison to LPS (Fig.2.22B). Opposite observations could be made for H3K27me3 negative mark. Combined stimulation with IFNα+LPS or IFNγ+LPS did not significantly alter neither H3K27Ac and H3K27me3 nor PolII recruitment at *Saa1* and *Irf7* gene promoters, in comparison to LPS only or IFNα, IFNγ only treatment, respectively (Fig.2.22B). This correlated with STAT1 and p65 recruitment to NFκB only and ISRE only gene promoters (Fig.2.20C) and gene expression level (Fig.2.18B).

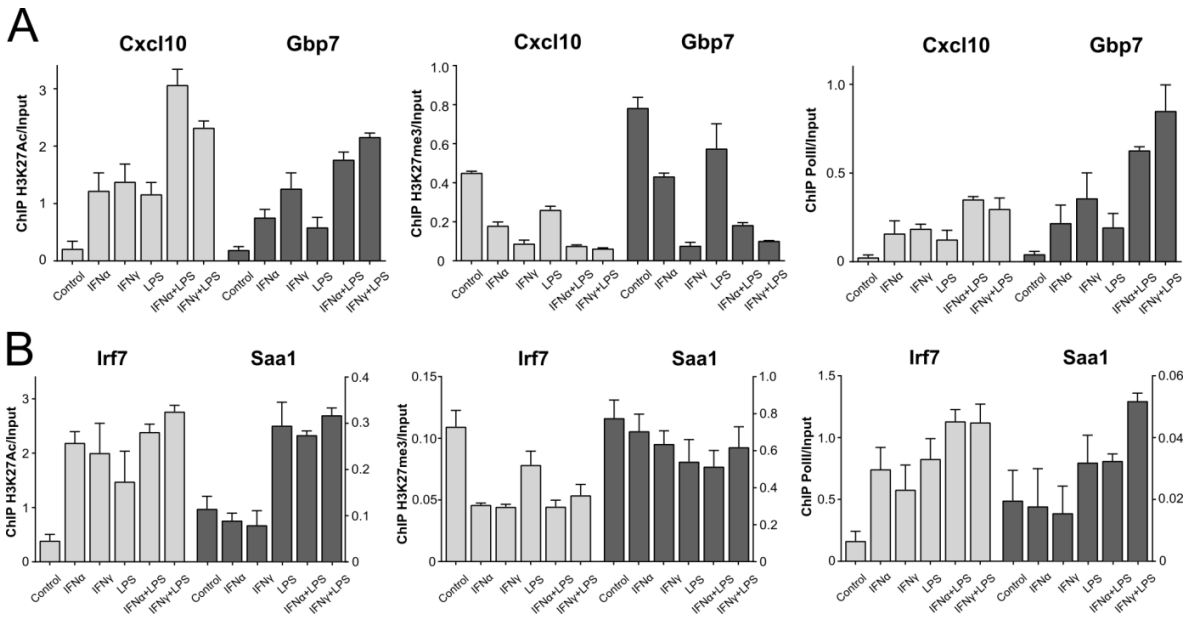

Figure 2. 22. PolII and histone modifications upon IFN and LPS treatment at promoters of STAT1 and p65 'co-binding' and 'single' modes gene representatives.

(A) ChIP-PCR of H3K27Ac, H3K27me3 and PolII at *Cxcl10* and *Gbp7* gene promoters (primers are listed in Table 2.2) in VSMC treated with IFNα(8h), IFNγ(8h), LPS(4h), IFNα(8h)+LPS(4h), IFNγ(8h)+LPS(4h). Mean ± s.e.m., n=2. **(B)** ChIP-PCR of H3K27Ac, H3K27me3 and PolII at *Irf7* and *Saa1* gene promoters (primers are listed in Table 2.2) in VSMC treated with IFNα(8h), IFNγ(8h), LPS(4h), IFNα(8h)+LPS(4h), IFNγ(8h)+LPS(4h). Mean ± s.e.m., n=2.

Collectively our results suggest that pre-treatment with IFNα or IFNγ followed by LPS results in introduction of chromatin modifications which allow for independent, yet sequential binding of STAT1 and p65 to closely spaced composite ISRE/GAS/NFκB sites present in SI gene promoters, resulting in robust transcriptional activation.

Discussion

Chronic, excessive and unresolved vascular inflammation lead to atherosclerotic plaque build-up within the arteries intima, mainly built of VSMC (van Thiel et al. 2017). As a consequence, due to vessel lumen narrowing, oxygen and nutrients supply to the body's tissues is diminished, being detrimental for the entire organism. Atherosclerosis-related diseases remain the leading cause of morbidity and mortality world-wide (WHO 2018). Therefore deciphering of the molecular mechanisms underlying inflammatory component of the disease is a crucial challenge, which may contribute to development of new diagnostic and treatment strategies.

Priming-induced SI between IFNγ, as well as potentially IFNα, and TLR4-activators (f.ex. LPS) is manifested by dramatically increased inflammatory gene transcriptional activation in response to pre-treatment with IFN followed by LPS, in comparison to single inflammatory cues. STAT1 and NFκB are crucial mediators of SI effect (Tamassia et al. 2007). This phenomenon was proposed as a mechanism utilized by atheroma interacting immune cells, including MΦ and DC, to elicit robust pro-inflammatory response. Yet it was not investigated previously if a similar mechanism could participate in pro-inflammatory response mediated by arterial VSMC.

In the current study we aimed to characterize the mechanism of priming-induced IFNα+LPS- and IFNγ+LPS-dependent SI in vascular cells as compared to immune cells. First, we performed genome-wide transcriptome analysis of mouse primary VSMC, MΦ and DC in response to single IFNα, IFNγ or LPS and combined treatment with IFNα+LPS or IFNγ+LPS, the latter conditions mimicking priming-induced SI. In all three cell types we observed SI effect after combined treatment with IFN and LPS as compared to single treatments, manifested by increased number of genes as well as an average gene expression levels, pointing to a common effect of SI mediated by IFNα and IFNγ. The potency of these responses was significantly lower in VSMC as compared to MΦ and DC (Fig.2.3). This correlated with the principal functions performed by the different cell types - VSMC mainly participate in the regulation of contraction, vessel tone and blood flow, while MΦ and DC are primarily involved in host inflammatory responses through antigen presentation, phagocytic clearance and immunomodulation, which functions are directly related with cellular responses to inflammatory stimuli such as IFN, TNFα, LPS and extracellular matrix proteins (O'Neill and Pearce 2016, Steucke et al. 2015).

Further RNA-seq analysis resulted in identification of 579 and 536 IFNα+LPS and IFNγ+LPS commonly up-regulated genes, respectively, suggesting existence of potentially common regulatory mechanism underlying SI in immune and vascular cells. Interestingly, comparing the expression pattern of these genes in the three different cell types, predicted greater similarity between VSMC and MΦ than between VSMC and DC (Fig.2.5A-B). Especially, the response of VSMC and MΦ was more directed towards IFNγ, whereas that of DC was primarily dependent on LPS (Fig.2.5A-B). Interestingly, Shankman et al. provided evidence suggesting that in the inflammatory milieu, VSMC are able to undergo a phenotypic switch to pro-inflammatory MΦ-like cells, which contribute to atherosclerotic plaque progression (Shankman et al. 2015). Similarly, in the presence of cholesterol, VSMC get a phenotype similar to MΦ characterized by increased phagocytic activity and further foam cell formation (Rong et al. 2003). Therefore although VSMC, MΦ and DC perform cell-type-specific functions in a healthy vessel, stimulation with pro-inflammatory stimuli might results in activation of partially common transcriptional programs and allow for concerted responses during vascular inflammation.

Next, we observed >64% overlap between commonly up-regulated genes in response to IFNα+LPS and IFNγ+LPS, which may suggest that IFNα and IFNγ share molecular mechanisms driving IFN-dependent gene transcription. Moreover GO analysis proved functional overlap between IFNα+LPS- and IFNγ+LPS-dependent genes, which seem to serve similar functions related with stress, immune and inflammatory response, response to cytokine, regulation of cell proliferation and migration, regulation of cell adhesion and chemotaxis, cell death and apoptotic process, response to lipid and ROS metabolic process, all reflecting pro-inflammatory and pro-atherogenic biological functions (Fig.2.7A).

Therefore we asked if such striking overlap in IFNα- and IFNγ-driven cell type-common gene expression pattern (>64%) and biological responses (GO analysis) would correlate with an overlap in IFN-activated TF complexes pools. Indeed, subsequent *in silico* promoter analysis revealed the presence of either single GAS, ISRE and NFκB sites or rather combinations of potential GAS-ISRE, GAS-NFκB, ISRE-NFκB or GAS-ISRE-NFκB binding motifs within regulatory regions of IFNα+LPS- and IFNγ+LPS-dependent genes. Importantly the distribution of abovementioned binding sites in IFNα+LPS-induced genes resembled that of IFNγ+LPS (Fig.2.7B). As reported previously, ISRE motifs may serve as binding sites either for ISGF3 complex (STAT1/STAT2-IRF9) or different IRF (IRF1, IRF7, IRF8, IRF9), GAS motifs recruit STAT1, while NFκB motifs may be occupied by NFκB-p65. Previously

our research group predicted presence of ISRE, GAS and NFκB sites in multiple combinations in gene promoters affected by SI between IFNγ and LPS, exemplified by *Cxcl9*, *Cxcl10* and *Nos2* (Chmielewski et al. 2014, Sikorski et al. 2014). The same genes were identified in the current study as the most commonly affected by SI, in terms of elevated gene expression, between IFNγ, but also IFNα and LPS, implying that type I and II IFN-driven responses may display regulatory overlap. Moreover there may exist a common regulatory SI mechanism shared by immune and vascular cells.

To further characterize the mechanism of SI between IFNα+LPS and IFNγ+LPS we particularly focused on the groups of commonly expressed genes between VSMC and immune cells. Next we performed STAT1 and p65 ChIP-seq in VSMC treated with IFN and LPS to characterize the genome-wide recruitment of STAT1 and NFκB (p65) to the regulatory regions of commonly expressed genes. This approach allowed for combining genome-wide expression and TF binding data to obtain full mechanistic model of SI regulation. STAT1 was predominantly recruited upon stimulation with IFNγ or IFNγ+LPS and to lower extent with IFNα and IFNα+LPS, while p65 binding was clearly LPS-dependent (Fig.2.8A-B). Interaction between IFNα+LPS and IFNγ+LPS increased the genome-wide number of STAT1 and p65 binding sites in comparison to individual treatments, correlating with the observed SI effect on gene transcription under the same conditions (Fig.2.8A-B). Both STAT1 and p65 were recruited to cognate GAS/ISRE and NFκB sites, respectively, distributed across the genome. Most of these sites were located within intronic and intergenic regions, but also as expected in gene promoters, corroborating previous *in silico* promoter analysis (Fig.2.11A, Fig.2.7B). Our data correlated with the observation made by others, that approximately 50% of the total STAT1-bound sites were intragenic and 25% intergenic (Robertson et al. 2007). Satoh et al. provided evidence for STAT1 recruitment to GAS motifs present in gene intronic regions in IFNγ stimulated HeLa S3 cells (Satoh and Tabunoki 2013). Similarly, 26% of NFκB-occupied binding sites upon LPS treatment of THP1 cells were located in upstream promoter, while 38% sites were found to be located within gene introns (Rao et al. 2011). In the other study, in TNFα-treated HeLa cells, just 7% of p65-bound sites were located within gene promoters, whereas 46% were intragenic (Lim et al. 2007). Such observations correlate with the general view of genome-wide TF occupancy, which mediate their functions not only through proximal, but also distal *cis*-regulatory elements (Spitz and Furlong 2012), the latter being related with mediation of cell-type-specific responses (Heinz et al. 2015). Therefore we could speculate that distal STAT1 and p65 binding sites might

correlate with VSMC cell type-exclusive functions. Accordingly, our further analysis were directed towards proximal gene regulatory regions occupied by STAT1 and p65, which could mediate common ISG expression in vascular and immune cells. Clustering analysis together with re-mapping of STAT1 and p65 recruitment to cognate ISRE/GAS and NFκB motifs, respectively, revealed stimuli-dependent enrolment of these two TF to distinct, but also overlapping genomic regions (Fig.2.9, Fig.2.11). As such we could distinguish different STAT1 and p65 binding modes, including: 'single' binding mode (STAT1 binding to solitary GAS and/or ISRE; p65 to solitary NFκB) or 'co-binding' mode (STAT1 binding to co-occuring GAS and/or ISRE+p65 to NFκB) (Fig.2.11B). We observed an overlap within each of 'single' and 'co-binding' modes between IFNα+LPS and IFNγ+LPS induced genes, what again indicated existence of regulatory overlap between IFN I and IFN II activated pathways. The most striking observation was 29.4% and 21.6% overlap within ISRE-only and ISRE-NFκB 'co-binding' mode (Fig.2.11B), respectively, since limited evidence exists for a role of ISGF3 complex in IFNγ-dependent gene expression regulation. More detailed characterization of classical ISRE-containing genes, *Ifit1*, *Mx2*, *Oas2*, *Irf7* and *Cxcl10*, revealed high gene transcriptional activation in response to IFNα and to lesser extent with IFNγ (Fig.2.12A). This observation correlated with tSTAT1 and pSTAT1 recruitment to ISRE motifs within these gene regulatory regions after stimulation not only with IFNα, but also with IFNγ (Fig.2.13). Moreover, we detected simultaneous recruitment of pSTAT2 and IRF9 to ISRE binding sites upon IFNα and IFNγ stimulation, together suggesting involvement of ISGF3 in the transcriptional regulation of *Ifit1, Mx2, Oas2, Irf7* and *Cxcl10* (Fig.2.14).

The expression pattern of examined ISRE-containing genes resembled the binding pattern of pSTAT2 and IRF9 alike pSTAT2 and IRF9 protein level, being higher after IFNα treatment in comparison to IFNγ (Fig.2.12A-B, Fig.2.14A-B). There is limited evidence for a direct role of STAT2 in the IFNγ-driven response. Yet it was reported that STAT2 tyrosine phosphorylation caused ISGF3 complex formation in IFNγ-treated wild-type primary MEF (Matsumoto et al. 1999). The same group observed that IRF9 KO mice suffer from impaired IFN I response, but also IFNγ-driven ISRE-dependent gene expression (Kimura et al. 1996). Alike, STAT2 phosphorylation was essential for the antiviral potency of IFNγ-treated MEF (Zimmermann et al. 2005). Together, this suggest the existence of ISGF3-dependent mechanism by which type I and II IFN can commonly elicit antiviral activities.

In contrast to pSTAT2 and IRF9, pSTAT1 was predominantly recruited upon IFNγ stimulation in comparison to IFNα (Fig.2.13). This may imply participation of STAT1 in an

additional transcriptionally active complex to mediate IFNγ-driven expression of ISRE-containing genes. Based on high pSTAT1 and IRF9 protein levels under type II IFN stimulation (Fig.2.12B) we speculated that this complex may consist of STAT1 homodimers together with IRF9. We verified this presumption by analysing gene transcriptional activation pattern of ISRE-containing genes in VSMC lacking STAT1, STAT2 and IRF9 (Fig.2.15). Remarkably, while the levels of IFNγ-dependent gene expression were abrogated in STAT1 KO VSMC, they were sustained in STAT2 KO VSMC (Fig.2.15B-C). This clearly lends support to the idea of STAT1-IRF9 involvement in ISRE-driven *Ifit1*, *Mx2*, *Oas2*, *Cxcl10* and *Irf7* in response to type II IFN. The very first evidence for STAT1-IRF9-dependent and STAT2-independent expression of IFNγ-induced gene expression came from the studies of *Ifit2* (Bluyssen et al. 1995) and *CXCL10* (Majumder et al. 1998). More recent analysis also confirmed formation of STAT1-IRF9 complexes in IFNγ-treated MΦ, which were recruited to ISRE motifs located in *Cxcl10* gene enhancers (Rauch et al. 2015). Moreover, the same authors showed that IFNγ-driven expression of *IRF7* and *DDX58* ISRE-containing genes depends on ISGF3 instead of STAT1-IRF9. This conclusion corroborates our results and imply collaborative involvement of STAT1-IRF9 complexes either with or without the STAT2 subunit for the cellular response to IFNγ. Yet the mechanism of distinct transcriptional complexes recruitment in not clear and could be envisioned either as a competition between ISGF3 and STAT1-IRF9 or ISRE sequence selectivity. Remarkably, we observed a significant difference in the basal gene expression levels in VSMC KO versus STAT1, STAT2 and IRF9 KO cells, which resulted in dramatic change of measured FC values after IFN stimulation (Fig.2.15). There was established a link between IFN-dependent response and unphosphorylated(U)-STAT, which mediated prolonged expression of ISG group as a result of the accumulation of U-ISGF3 components (Majoros et al. 2017). Therefore abrogation of both U- and p-STAT in KO VSMC could affect the basal gene expression levels of some of ISRE-containing genes. Other explanation of various gene expression levels in KO cells, could come from the study of Vinkemeier et al. who alike us, observed increased expression of IFNγ-target genes *CxCl9*, *CxCl10*, *Irf1*, *Ido1*, *Il1β* and *Marco* in MΦ in the absence of STAT2. It was proposed that U-STAT2 acts as an inhibitor of STAT1, by modulating STAT1:STAT2 protein ratio and decreasing the availability of STAT2-free molecules to mediate cytokine functions (Ho et al. 2016).

Interestingly, ISRE-containing gene expression pattern upon IFNγ treatment in IRF9 KO VSMC resembled that observed in STAT2 KO VSMC (Fig.2.15C-D), which could

suggest involvement of an additional TF/complex except ISGF3 and STAT1-IRF9 in regulation of ISRE-containing gene expression upon IFNγ stimulation. In addition to STAT1, STAT2 and IRF9 we could detect IRF1 recruitment to ISRE binding sites within gene promoters, predominantly in response to IFNγ, but weakly upon IFNα (Fig.2.16). Since no direct STAT1 protein-IRF1 protein interaction was detected (Fig.2.16B), we propose that IRF1 may participate in ISRE-containing gene expression regulation in STAT1-independent manner. However others identified direct interaction between U-STAT1-IRF1 and argued for the role of this complex in regulation of *LMP2* constitutive gene expression, this result was obtained only in U3A cells overexpressing STAT1 tyrosine 701 (Chatterjee-Kishore et al. 2000). Examination of detailed IRF1 role in transcriptional regulation of ISRE-containing genes in response to IFNγ, next to ISGF3 and STAT1-IRF9 complexes, would require additional experiments in double IRF9-IRF1 KO VSMC.

Collectively, our results together with discussed literature evidence suggest, that IFNα-dependent gene expression of ISRE-containing genes is predominantly driven by ISGF3 complex. In contrast, IFNγ-dependent response is mediated by collaborative action of ISGF3 and STAT1-IRF9 transcriptional complexes. Based on the common transcription pattern identified between VSMC and immune cells in response to IFNα and IFNγ, it is tempting to speculate that the regulatory mechanisms identified in VSMC may be extrapolated to MΦ and DC. Moreover, ISGF3 and STAT1-IRF9 binding to ISRE together with STAT1 homodimers recruited to GAS, provide an additional twist to the canonical IFNγ signaling pathway, which could explain some of the overlapping responses to IFNα and IFNγ in these cells.

Since we better understood the regulatory overlap between the two IFN driven by STAT1-containing complexes, we wanted to use this knowledge to further characterize the mechanism of SI between IFN and LPS. Therefore we concentrated on the genes which were identified within STAT1-p65 'co-binding' modes (Fig.2.11B). For the majority of IFNα+LPS and IFNγ+LPS up-regulated genes which were commonly affected by SI in the three cell types, STAT1 and p65 peak summits were spaced by less than 200bp (Fig.2.17). Obviously this correlated with close proximity of ISRE-NFκB (38-264bp) and GAS-NFκB (41-234bp) motifs within regulatory regions of these genes (Fig.2.18B), which distribution may be a pre-requisite for effective STAT1 and p65 collaboration. This presumption is supported by evidence from IRF3 and NFκB co-occupancy studies in the context of Sendai virus-induced gene activation, where cognate TF binding sites were spaced by ~50bp (Freaney et al. 2013). Moreover, others shown that STAT1 and IRF1 were co-recruited to closely spaced GAS and

ISRE motifs in response to type II IFN treatment (Abou El Hassan et al. 2017, Michalska et al. 2018).

Stimuli-dependent binding of two proteins to closely spaced DNA motifs, could assume occurrence of direct protein-protein interaction. Importantly, if the distance exceeds 20bp, interaction between TF would require DNA looping (Heinz and Glass 2012). There is mixed evidence on whether STAT1 and NFκB could directly cooperate. Ganster et al. and Kramer et al. proved direct protein-protein interaction between STAT1 and NFκB (Ganster et al. 2005, Krämer et al. 2006). In contrast, although mutual recruitment of STAT1 and NFκB was necessary for maximal *Cxcl9*, *IP-10*, *Becn1* and *NOS2* gene transcriptional activation, no direct interaction between these two TF was detected (Ohmori and Hamilton 1993, Ganster et al. 2001, Hiroi and Ohmori 2003, Zhu et al. 2013). These results are in line with our STAT1-NFκB co-IP experiment performed on protein extracts isolated from IFNα+LPS and IFNγ+LPS-treated VSMC, where we did not observe interaction between STAT1 and p65 protein (data not shown).

Further examination of STAT1 and p65 driven mechanism of SI gene expression, revealed recruitment of STAT1 to gene promoters containing either GAS-NFκB (*Serpina3i, Steap4, Irf1*), ISRE-NFκB (*Ccl5, Ifit1, Gbp6*) or GAS-ISRE-NFκB (*Cxcl10, Gbp7*) motifs upon treatment with IFNγ, to a lesser extent with IFNα and only weakly with LPS (Fig.2.19). STAT1 binding pattern mirrored the transcriptional activation of SI genes, which expression was primarily driven by IFN (Fig.2.18B). The most striking result which emerged during subsequent p65 recruitment analysis was detection of its binding to SI gene promoters upon IFNα or IFNγ treatment. Remarkably, this could not be observed at regulatory regions of *Saa1*, which has a solitary NFκB binding site (Fig.2.19). Moreover, subsequent LPS exposure resulted in increased STAT1-p65 co-binding, mainly driven by enhanced p65 recruitment (Fig.2.19). Increased binding of p65 after combined treatment with IFN+LPS in comparison to single stimuli and p65 recruitment upon stimulation with IFN only, were abrogated in VSMC STAT1 KO (Fig.2.21). This finding would seem to imply STAT1-dependent role in recruitment of p65 to combined GAS-NFκB or ISRE-NFκB binding sites present in SI gene regulatory regions. We thus hypothesise that IFN I and IFN II stimulation results in STAT1 recruitment to ISRE and/or GAS motifs due to potential chromatin modifications which subsequently increase nearby located NFκB sites accessibility.

To validate such possibility we analysed the pattern of histone active mark together with PolII recruitment in VSMC treated with IFN and LPS. Indeed, IFNα and IFNγ priming

followed by LPS stimulation resulted in increased histone acetylation and PolII recruitment in comparison to single stimuli (Fig.2.22). This data correlate with previous studies on STAT1 and NFκB mutual involvement in gene transcriptional activation, in the context of bacterial or viral infection. As such it was shown that initial NFκB binding was necessary for preparation of open chromatin state to enhance subsequent ISGF3 recruitment, regulating PolII recruitment and *Nos2, Il6* gene expression in MΦ infected with bacterial pathogen *Listeria monocytogenes* (Farlik et al. 2010, Wienerroither et al. 2015). Similarly, combined stimulation with TNFα and IFNγ correlated with elevated histone H4 acetylation at distinct NFκB sites and PolII recruitment to the PreproET-1 promoter region in primary HPASM cells (Wort et al. 2009). Several studies provided evidence for the opposite scenario, when NFκB recruitment was facilitated by initial pre-treatment, alike in our experimental setup. As such, IL10-dependent STAT3 binding resulted in increased acetylation of *IL1ra* gene promoter region, facilitating the latter NFκB binding (Tamassia et al. 2010). Alike in the context of virus-dependent IRF3 assembly in the gene promoters resulted in the recruitment of PolII, associated machinery and NFκB to stimulate efficient elongation and activation of antiviral genes (Freaney et al. 2013). On the other hand, p65 showed ability to additively recruit PolII to its cognate sites within gene promoters to induce transcriptional activation (Giorgetti et al. 2010). Within the criteria of priming-induced SI, IFNγ pre-stimulation correlated with elevated histone acetylation being inevitable for STAT1 and IRF1 binding at gene promoters. Afterwards, NFκB recruitment was significantly increased and prolonged, what corresponded with PolII recruitment to gene promoters and enhancers (Ramsauer et al. 2007).

Collectively our results offer compelling evidence that gene expression directed by type I or II IFN treatment followed by LPS stimulation, depends on STAT1-p65 co-binding in sequential manner, which correlates with increased histone acetylation and PolII recruitment to amplify target gene transcription.

Detailed predictive mechanism of STAT1-NFκB co-binding involved in SI of IFNα and IFNγ with TLR4 in VSMC, MΦ and DC is depicted in Figure 2.23. Initially, IFNα-induced STAT1 is recruited to closely spaced ISRE-NFκB or GAS-NFκB binding sites in the form of ISGF3 or GAF, respectively. Alike, IFNγ triggers binding of STAT1-complexes ISGF3, STAT1-IRF9 and GAF to the cognate sites. In first wave of stimulation, IFN-driven STAT1 binding elevated histone acetylation which facilitates subsequent p65 binding to adjacent (~200bp) NFκB sites upon type II IFN and to a lesser extent IFN I stimulation. In the second wave of LPS treatment, STAT1-p65 recruitment is increased, mainly due to elevated

NFκB (p65-p50 dimers) formation. This coincides with enhanced histone acetylation and PolII recruitment which finally result in robust expression of IFNα+LPS- and IFNγ+LPS-activated pro-inflammatory genes, the latter one being higher affected by the SI effect.

Collectively, IFNα and IFNγ together with the following LPS treatment results in activation of TF pool, which mediates robust transcriptional activation of pro-inflammatory genes. GAF, ISGF3, STAT1-IRF9 are recruited to their cognate binding sites in IFN-specific or -common manner, what provides an explanation for comparable effects of IFNα or IFNγ priming on TLR4-induced activation in vascular and immune cells and allow for driving important biological functions of both IFN in the context of vascular inflammation. Although our model provides a comprehensive explanation of priming-dependent SI mechanism, we can not exclude the possibility of other TF and TF complexes regulatory involvement, which would require further investigation.

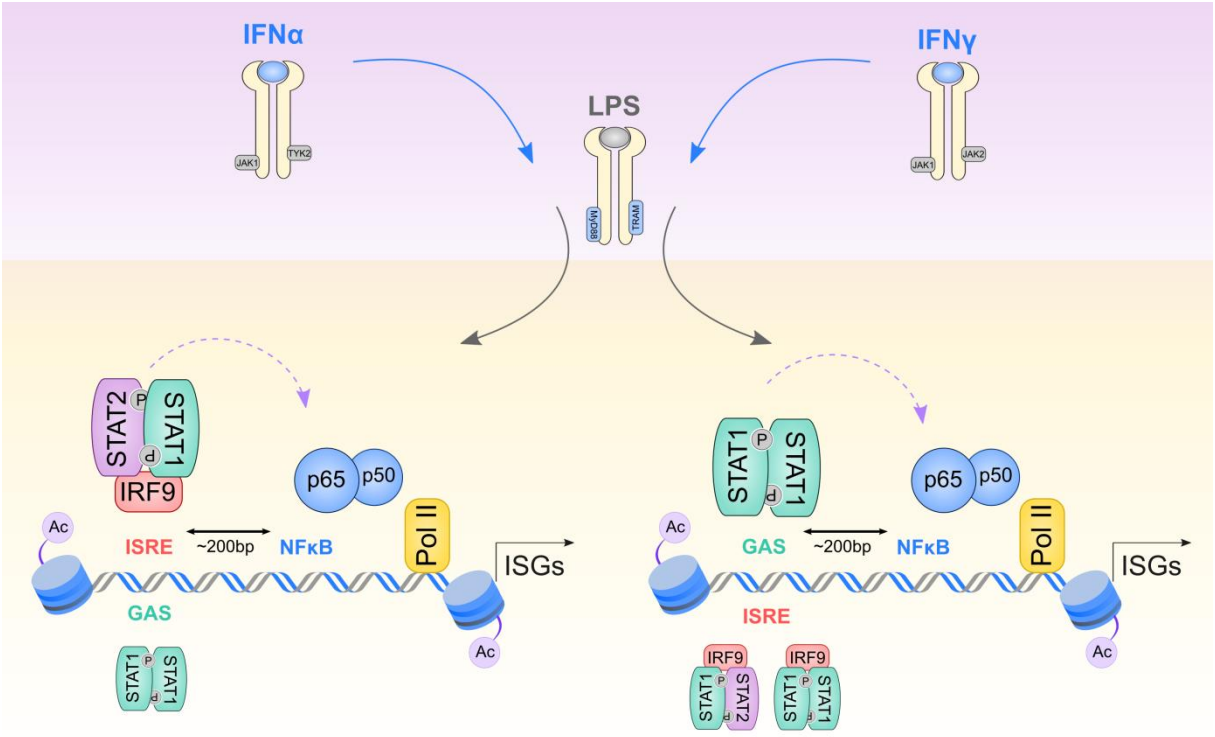

Figure 2. 23. Model describing transcriptional regulation of SI genes by STAT1-dependent preceding of p65 and PolII to acetylated GAS/NFκB or ISRE/NFκB composite sites.

1st wave of stimulation: After initial cell exposure to IFNα or IFNγ, receptors dimerize and facilitate transphosphorylation of the receptor-bound JAK1/TYK2 kinases for IFNα and JAK1/JAK2 kinases for IFNγ. Next STAT proteins are recruited, phosphorylated and dimerized, either in a form of ISGF3 complex (STAT1-STAT2 together with IRF9), GAF (STAT1 homodimers) or STAT1/IRF9 complex

(STAT1 homodimers together with IRF9. Activated TF supply a platform for 2nd wave of stimulation: LPS stimulates TLR4 receptor associated with adapter molecules MyD88 and TRAM and activates NFκB, as well as STAT1-containing transcriptional complexes. IFNα stimulation results in recruitment of ISGF3 to ISRE sites and GAF to GAS sites present in ISG promoters. IFNγ initiates binding of GAF to GAS sites as well as ISGF3 and possibly STAT1/IRF9 to ISRE elements. Initial binding of STAT1-containing complexes followed by subsequent p65-p50 heterodimers binding (indicated by a violet curved arrow) to NFκB sites closely spaced to ISRE and GAS sites (~200bp), together results in histone acetylation enrichment and PolII recruitment to ISG promoters. For a detailed explanation, see the text.

Chapter 3. STAT1 mediates IFNγ+LPS-dependent transcriptional gene down-regulation

Introduction

Every living organism is exposed to the multiple external stimuli, including pro-inflammatory cues, which are a constant obstacle on the way to keep the tissue homeostasis and contribute to the development of inflammatory diseases, such as atherosclerosis. Hence, stimuli-dependent transcriptional programmes have to either become activated or repressed in order to mediate cell response adequate to the current biological context. Gene transcriptional networks activated in response to the pro-inflammatory stimuli, like IFNγ or LPS, were broadly examined and shown to be dependent on the collaborative action of STAT, IRF and NFκB. Downstream ISG up-regulation was previously correlated with pathophysiology of various inflammatory diseases, including CVD (Mehra et al. 2005). Remarkably, elevated pro-inflammatory gene expression was shown to rely on the phenomenon of priming-induced SI between IFN and TLR4-activators. Within the mechanism of SI, IFNα- or IFNγ-activated STAT1-containing transcriptional complexes ISGF3 or GAF collaborate with LPS-dependent NFκB (p65-p50 heterodimers) on cognate ISRE, GAS and NFκB DNA binding motifs, respectively, present in ISG promoters.

Remarkably, evidence for the potential role of IFN- and LPS-mediated priming-induced SI in the context of pro-inflammatory gene down-regulation was not examined before. However, there exists some reports which provide evidence for the involvement of STAT1 and NFκB in gene transcriptional suppression. As such, STAT1-dependent down-regulation was reported for genes including *Skp2*, *ABC1*, *Bcl-2*, *Bcl-x*, *Bax*, *CXCR4*, *c-myc*, *CSF1* in multiple cell types (Wang et al. 2010, Wang et al. 2002, Stephanou et al. 2000, Cao et al. 2015, Soond et al. 2007, Hiroi et al. 2009, Ramana et al. 2000, Horvai et al. 1997). Similarly, NFκB was shown to play regulatory role in transcriptional repression of *IL8*, *Bcl-2*, *IL4* and *Sp1* (Oliveira et al. 1994, Chu et al. 2011, Casolaro et al. 1995, Ye et al. 2015).

Therefore in this study we aimed to examine if priming-induced SI between IFNγ and LPS, resulting in gene transcriptional repression identified by comprehensive genome-wide transcriptome analysis (RNA-seq) in VSMC, could be regulated in STAT1- and/or NFκB-dependent manner. We hypothesised that STAT1- and/or NFκB-containing transcriptional complexes would collaborate to mediate gene transcriptional repression, alike in the mechanism characterized in the context of priming-induced SI-dependent gene up-regulation.

This could be achieved either by TF-dependent recruitment of HDAC, which would deposit repressive histone marks or transcriptional co-repressors as well as removal of transcriptional co-activators. Elucidation of the potential mechanism underlying transcriptional repression in response to the pro-inflammatory cues in the cells from the vasculature, would be crucial for better understanding of atherosclerosis pathophysiology. Moreover, this might help to identify potential therapeutical targets against the disease in the future.

Material and Methods

Primary VSMC isolation

Mice. WT mice, strain background C57BL/6 were provided by Charles River Laboratories, while STAT1 KO mice (on the same strain background as WT mice), were provided by Thomas Decker (Department of Microbiology, Immunobiology and Genetics, University of Vienna). First, animals underwent euthanasia by cervical dislocation under isoflurane anaesthesia. Next, aortas were isolated. All performed experimental procedures which required involvement of the mice were performed according to good animal practice and local law. Accordingly, no medical ethical approval was necessary for tissue isolation procedures.

Detailed information regarding primary VSMC isolation procedure and cell culture protocol is available in Material and Methods section, Chapter 2.

Briefly, after 24 hour starvation, VSMC were treated with: a single stimulus: 10ng/ml of IFNγ (PMC4031, TFS) for 8 hours or 1μg/ml of LPS (L4391, Sigma-Aldrich) for 4 hours. To further study the effect of IFN priming on LPS signaling, VSMC were first treated with IFNγ for 8 hours followed by LPS stimulation for 4 hours, at concentrations listed above. Described treatment strategy was applied in RT-PCR, RNA-seq, ChIP-PCR and ChIP-seq experiments presented in this study.

Promoter analysis

Filtered list of down-regulated (FC≤-3; raw counts in control sample≥500) genes (288 genes) in response to combined stimulation with IFNγ+LPS in VSMC resulting from RNA-seq experiment was subjected to *in silico* promoter analysis. In order to estimate gene promoter (5000bp upstream/2000bp downstream from the nearest gene TSS) enrichment in potential STAT1 binding sites (GAS and ISRE) and p65 binding sites (NFκB), oPPOSUM web-based system (Kwon et al. 2012) was used. Single Site Analysis were performed using either GAS (STAT1, JASPAR CORE Profiles), ISRE (Isgf3g_1, JASPAR PBM Profiles) or NFκB (RELA, JASPAR CORE Profiles) matrix. Applied conservation cut-off: 0.4 and matrix threshold: ≥ 0.85 were selected during promoter analysis.

RNA isolation and RT-PCR

RNA isolation. Total RNA from WT and STAT1 KO VSMC was isolated with GeneMATRIX Universal RNA Purification Kit (E3598, EURx) according to the

manufacturer's guidance. Total RNA concentration was measured with NanoDrop 2000 spectrophotometer (TFS).

Reverse transcription. 1µg of total RNA isolated from WT and STAT1 KO VSMC untreated and stimulated with IFNγ(8h)+LPS(4h) was used to synthesize cDNA. First, RNA was mixed with DNAseI-buffer solution (EN0521, TFS) and incubated for 30 minutes at 37°C in order to remove DNA from the sample. This reaction was stopped by addition of 1µl of 50mM EDTA (EN0521, TFS) for 10 minutes at 65°C. Next, random hexamers (1µl, 100µM, [SO142, TFS]) were ligated to mRNA (5 minutes, 65°C). In the end, cDNA was synthesized in C1000 Touch Thermal Cycler (Bio-Rad) for 10 minutes at 25°C, 1h at 42°C and then 10 minutes at 70°C. To the reaction mix the following reagents were added: 0.75µl of 10mM dNTPs (10297018, TFS), 9.75µl of NFW, 0.5µl of RiboLock RNase Inhibitor 40U/µl (EO0381, TFS), 3µl of 5x RT buffer and 1µl of RevertAid Reverse Transcriptase (200U/µl, [EP0442, TFS]). Obtained cDNA was stored at -20°C or diluted and proceeded for RT-PCR analysis.

RT-PCR. RT-PCR was performed with Maxima SYBR Green/ROX qPCR Master Mix (K0223, TFS) on the CFX Connect Thermal Cycler System (Bio-Rad). In detail, the reaction mix consisted of: 3µl of 25x diluted cDNA, 5µl of Maxima SYBR (K0223, TFS), 1.2µl of forward and reverse primers mix and 0.8µl of NFW. PCR product amplification was performed in the following steps: 10 minutes at 95°C, followed by 40 cycles of: 10 seconds denaturation step at 95°C and 1 minute primer annealing step at 60°C, then 15 seconds at 95°C, 5 seconds at 55°C and 1 minute 95°C was done as final amplification step. The amount of target gene in each sample was normalized to endogenous control *β-actin* (*β-Actb*), according to the formula: Q = 2^(-ΔCt) where ΔCt = Ct target of interest – Ct housekeeping gene, or with the formula: Q = 2^(-ΔΔCt) where ΔΔCt =ΔCt control – ΔCt sample. Transcript quantification is presented as mean ± SEM for three independent biological repeats, compared by two-way ANOVA and unpaired two-tailed student T-test using GraphPad Prism v.7 software. The sequences of the primers are listed in Table 3.1.

Table 3. 1. List of primers used for RT-PCR analysis in Chapter 3.

Gene name	Primer sequence	
	Forward	Reverse
Adamtsl3	CCAGAAGTCTCTAATCCAGTGGG	AATGAGCTTGAGAACGACCGT
Angpt2	CCGTGGGAGTTCAGCAGTAA	GCCCACCACTTAGAAGTCCC
Cd248	CAACGGGCTGCTATGGATTG	GCAGAGGTAGCCATCGACAG
Dusp1	GTTGTTGGATTGTCGCTCCTT	TTGGGCACGATATGCTCCAG
Fads2	CAGCCCCTTGAGTATGGCAA	TAGTAGCTGATGGCCCAAGC
Igf1	CTGAGCTGGTGGATGCTCT	CACTCATCCACAATGCCTGT
Insig1	GTCTTACCTTGCTCCCCCAC	CCCCCTTACCCGACTTTCAC
Maf	GAGGTGATCCGACTGAAGCA	CTCCTTGTAGGCGTCCCTTT
Mvd	TCCTGAAGGGCTGCTTGATG	GAGGCACTTGAGAGGGGTTC
Npr3	CAAGCATACTCGTCCCTCCAA	GGCGATACCTTCAAATGTCCTG
Pbx1	GCCAGACAGGAGGATACAGTG	CTGCCAACCTCCATTAGCAC
Rab3il1	GAAGAGTGTGAACGGCTTTGC	GCTTCCCGAACCATCTTGTGA
Scel	CTTCAATGCAAACACTACCGC	ATGGTTTAGGAGAAGCAATGGG
Slc5a3	CGGGGTTGGTACAGTAGGC	CTCTCCACAAGACCATCAGCA
Sox4	CGCCTTTATGGTGTGGTCGC	CCCGACTTCACCTTCTTTCGC
Spon2	GCAACTATCCCACAAGACACAG	TGAGGCGTGGGTAGTAGAATG
Sspn	CGTTGGGCATCGCGG	ATGTCCTCTCGTCAACTTGG
Thbd	CTCTGTGCGTCACGGTCTC	GTCTCAGTCTCGCATGGCTT
β-Actb	CCACACCCGCCACCAGTTCG	TAGGGCGGCCCACGATGGAG

RNA-seq experimental procedure and data analysis

Detailed information regarding RNA-seq experiment performed in VSMC treated with IFN and LPS together with general in silico data analysis is available in Material and Methods section, Chapter 2.

BioVenn web tool (Hulsen et al. 2008) was used to generate Venn diagram illustrating overlap between down-regulated gene (FC≤-2) lists resulting from RNA-seq differential gene expression analysis (1 cell type: VSMC, 3 conditions: IFNγ[8h], LPS[4h], IFNγ[8h]+LPS[4h]) performed in Chapter 3.

ChIP-seq experimental procedure and data analysis

Detailed description of STAT1 and p65 ChIP-seq experiment performed in WT VSMC treated with IFN and LPS together with general in silico data analysis is available in Material and Methods section, Chapter 2.

ChIP-PCR. ChIP was carried according to the modified protocol previously described by Siersbaek and colleagues (Siersbæk et al. 2012). First, WT VSMC were left untreated or treated with IFNγ (8h), LPS (4h) or IFNγ(8h)+LPS(4h). DNA and protein were cross-linked directly on cell culture plates in double step procedure: with 0.5M DSG (80424, Sigma-Aldrich) for 45 minutes and 1% formaldehyde (28906, TFS) for 10 minutes. To stop fixation step, glycine (G7126, Sigma-Aldrich) at 125mM concentration was added. Cell pellet was suspended in ChIP Lysis Buffer (1% Triton X-100 [TRX777, Bio-Shop], 0.1% SDS [SDS001, Bio-Shop], 150mM NaCl [S9888, Sigma-Aldrich], 1mM EDTA [15575-038, TFS] and 20mM Tris, pH 8.0 [15568-025, TFS]) to disrupt the cells and free nuclei. Next, chromatin was sonicated with Diagenode Bioruptor Plus to generate fragments in a range of 100-2000bp. Chromatin was immunoprecipitated overnight at 4°C with:

- tSTAT1 (Santa Cruz, sc-346),
- tp65 (CST, 6956, L8F6),
- RNA Polymerase II (Merck Millipore, 05-623, CTD4H8),
- Acetyl-Histone H3 (Lys27) (CST, 8173, D5E4) antibodies.

Afterwards, formed antibody coupled DNA-protein complexes were precipitated with anti-IgA and anti-IgG Dynabeads (10008D[A], 10009D[G], TFS) for 6 hours at 4°C. Next, beads were subjected to series of washes at 4°C: once with IP Wash Buffer 1 (1% Triton X-100 [TRX777, Bio-Shop], 0.1% SDS [SDS001, Bio-Shop], 150 mM NaCl [S9888, Sigma-Aldrich], 1mM EDTA [15575-038, TFS], 20mM Tris, pH 8.0 [15568-025, TFS], 0.1% NaDOC [DCA33, Bio-Shop]), twice with IP Wash Buffer 2 (1% Triton X-100 [TRX777, Bio-Shop], 0.1% SDS [SDS001, Bio-Shop], 500mM NaCl [S9888, Sigma-Aldrich], 1mM EDTA [15575-038, TFS], 20mM Tris, pH 8.0 [15568-025, TFS] and 0.1% NaDOC [DCA33, Bio-Shop]), once with IP Wash Buffer 3 (0.25M LiCl [1056790256, Sigma-Aldrich], 0.5% NP-40 [NON505, Bio-Shop], 1mM EDTA [15575-038, TFS], 20mM Tris, pH 8.0 [15568-025, TFS], 0.5% NaDOC [DCA33, Bio-Shop]) and two times with TE buffer (10mM EDTA [15575-038, TFS] and 200mM Tris, pH 8.0 [15568-025, TFS]). Finally, beads were incubated for 30 minutes in Elution Buffer (1%SDS [SDS001, Bio-Shop], 0.1M NaHCO3 [S5761, Sigma-Aldrich]) to release beads-bound DNA-protein complexes. DNA was de-cross-linked by overnight incubation with high salt (0.2M NaCl [S9888, Sigma-Aldrich]) at 65°C. DNA was purified using MinElute PCR Purification kit (28006, Qiagen). DNA concentration was measured with Qubit fluorometer (TFS). All ChIP-PCR assays were performed in biological duplicates with primers listed in Table 3.2.

Table 3. 2. List of primers used for ChIP-PCR analysis in Chapter 3.

Gene name	Primer sequence	
	Forward	Reverse
Angpt2	TTCAGTCAGAGCCAACAAGC	GCTGCTAGAGAGGAACAAACC
Igf1	TCTGAAAGGGGTGAAGTCGC	CCCTGCCAAAGTCAGCATTC
Pbx1	CCCACCCCTCGTTCGTCTA	TTCAACAGTTTCCCTGAGGTCT
Rab3il1	TCAGGAGCCCAGAGGTTGT	CCAGACAATGTGAGCAAAGGG
Scel	TGCTTGCCAGTATTGTGCGT	ACAGTCTCATTCACAGGACGG
Sox4	CCAAACGCAAGTTTCTCGCC	GCTCTCGTGAACTGCAATCG
Spon2	CTCTATCCAGTGAGCAAGGC	TGAGGCTTCTTGCTCTCACTT

Integrative RNA-seq and ChIP-seq analysis

The closest gene for each STAT1 ChIP-seq peak presented in Figure 3.5A was identified using annotatePeaks.pl (HOMER). Consensus STAT1 (GAS, ISRE) and p65 (NFκB) motifs re-mapping analysis (Fig.3.5B) was performed using HOMER database available GAS – motif273, ISRE – motif140, NFκB – motif208 (Motif logos presented in Chapter 2, Fig. 2.10A-C). Motif matrix were re-mapped to STAT1 and p65 peaks detected after WT VSMC stimulation with IFNγ+LPS. *This ChIP-seq bioinformatic analysis was performed by Lajos Széles and Attila Csermely (Department of Biochemistry and Molecular Biology, University of Debrecen).* Next, lists of GAS, ISRE and NFκB re-mapped genomic regions were filtered according to the motif distance from the closest annotated gene TSS (-/+100kb) and according to MST (GAS - MST 6, ISRE - MST 6, NFκB - MST 7). Gene list of 1102 down-regulated genes in VSMC after treatment with IFNγ+LPS resulting from RNA-seq was overlapped with lists of STAT1 and p65 ChIP-seq genomic regions containing re-mapped motifs.

Integrative GO and network-based analysis

Filtered list of VSMC down-regulated (FC≤-3; raw counts in control sample≥500) genes (288 genes) and commonly up-regulated (FC≥3) genes (398 genes) in response to combined stimulation with IFNγ+LPS resulting from RNA-seq experiment was used for GO analysis. This examination was performed with online NetworkAnalyst 3.0 platform (Zhou et al. 2019). Built-in GO:Biological Process Database and *Mus musculus* gene background list was used to perform integrative gene ontology analysis and network-based data visualisation. Overrepresented GO terms with assigned p-value of less than 0.05 were identified as

statistically significant. GO records which were represented by the highest number of enriched genes (uniquely enriched for down-regulated gene list) within individual GO category were selected for graphical presentation. Commonly enriched terms for both up- and down-regulated analysed gene lists were marked by a blue circle around a GO term bubble. Increasing orange colour of the bubble reflects the higher GO term p-value.

Results

Extensive genome-wide transcriptome analysis (RNA-seq), which aimed to study the regulatory mechanism of priming-induced SI between IFNγ and LPS, revealed gene transcriptional patterns repressed upon stimulation with pro-inflammatory stimuli in VSMC. Cells were treated with IFNγ (8h), LPS (4h) alone or IFNγ(8h)+LPS(4h) together and proceeded to RNA-seq experiment. Subsequent differential gene expression analysis identified fraction of down-regulated genes (FC≤-2) in response to IFN and LPS. As such, IFNγ lowered expression of 267 genes, while LPS treatment resulted in down-regulation of 279 genes (Fig.3.1). Pre-stimulation with IFNγ, followed by LPS resulted in altered expression of 1102 genes (Fig.3.1). Thus, although VSMC stimulation with IFNγ or LPS alone resulted in a repression of similar gene number, combined stimulation caused an obvious elevation of the number of down-regulated genes as compared to single stimuli. It suggests that combined stimulation with IFNγ and LPS affect VSMC negative transcriptional response, yet the mechanism of priming-induced SI in this context remains unknown.

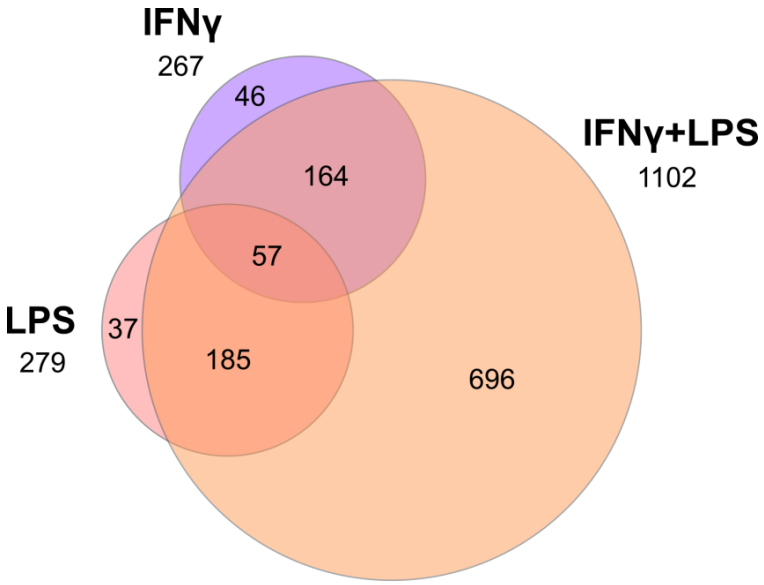

Figure 3. 1. Characterization of gene down-regulation patterns in VSMC in response to IFNγ and LPS.

Venn diagram presenting overlap between lists of down-regulated genes (FC≤-2) in response to IFNγ(8h), LPS(4h) and IFNγ(8h)+LPS(4h) resulting from RNA-seq.

Initially, detailed analysis of 1102 down-regulated genes upon IFNγ+LPS stimulation in VSMC were performed. Figure 3.2A reveals FC values (FC≤-2) distribution of 1102 IFNγ+LPS-repressed genes in VSMC. Strikingly, only 9.5% of genes (94 genes in a range <-12.49;-5> and 11 genes in a range <-12.5) took the FC value lower than (-5), while 997 out of 1102 genes (90.5%) fit within a FC value range of <-4.99;-2>. Closer examination of the latter gene group indicated that most of the genes (659 genes) were classified within the lowest FC value range of <-2.99;-2>. 90 and 248 genes fit within <-4.99;-4> and <-3.99;-3> FC value ranges, respectively (Fig.3.2A). Moreover we characterized the distribution of raw values (represented as RPKM) in the control sample to estimate a basal gene expression level of 1102 IFNγ+LPS-down-regulated genes in VSMC. As depicted in Figure 3.2B only 8.3% genes (62 genes in a range 4000-7999; 23 genes in a range 8000-15999; 7 genes in a range >16000) took raw value higher than 4000 in the control sample. The other 91.7% of genes (1010 genes) fit within a raw value range of (0-3999). Most of these genes (394 genes) took the raw value of less than 499 in the control sample. Rest of the genes fit within the raw value ranges of 500-999 (280 genes), 1000-1999 (207 genes) and 2000-3999 (129 genes) (Fig.3.2B).

Collectively, the great majority of the analysed 1102 IFNγ+LPS-dependent genes in VSMC showed very low level of transcriptional down-regulation accompanied by low basal gene expression level. In order to fish out a list of the genes which would serve as a reliable tool for further analysis of IFNγ-dependent gene down-regulation mechanism, we performed 2-step gene list filtering. Accordingly, we removed from 1102 gene list the ones which took FC value higher than -3 and raw value in control sample lower than 500. Finally, we obtained a list of 288 genes which was subjected for further analysis. Top 30 genes from this list are presented in Table 3.3, depicting ascribed FC values and raw counts after single IFNγ, LPS and combined IFNγ+LPS treatment.

Next, we asked a question about the potential function of the down-regulated genes in the context of vascular inflammation. Performed integrative GO and network-based analysis revealed possible functions of 288 IFNγ+LPS repressed genes in VSMC. Among the most enriched GO terms, there were distinguished the following categories formulating a network depicted in Figure 3.3A: Vasculature development, Angiogenesis, Tissue development, Cell development; Cell cycle, Cell division, Cytoskeleton organisation, Positive regulation of cell cycle, Negative regulation of cell cycle; Regulation of lipid biosynthetic process; Cell Proliferation; Cell migration; Regulation of cell adhesion. Enrichment of the down-regulated

genes in the abovementioned processes suggests potential inhibition of these pathways upon stimulation with pro-inflammatory stimuli. Inhibited vascular cell divisions and angiogenesis may correlate with limitation of abnormal cell proliferation, migration and adhesion, which processes are characteristic for inflamed vessels, while limited lipid biosynthesis may correlate with restricted atherosclerotic plaque lipid core formation. Therefore this GO analysis results could imply that IFNγ+LPS-dependent selected gene group down-regulation potentially participate in vascular cell survival against vascular inflammation.

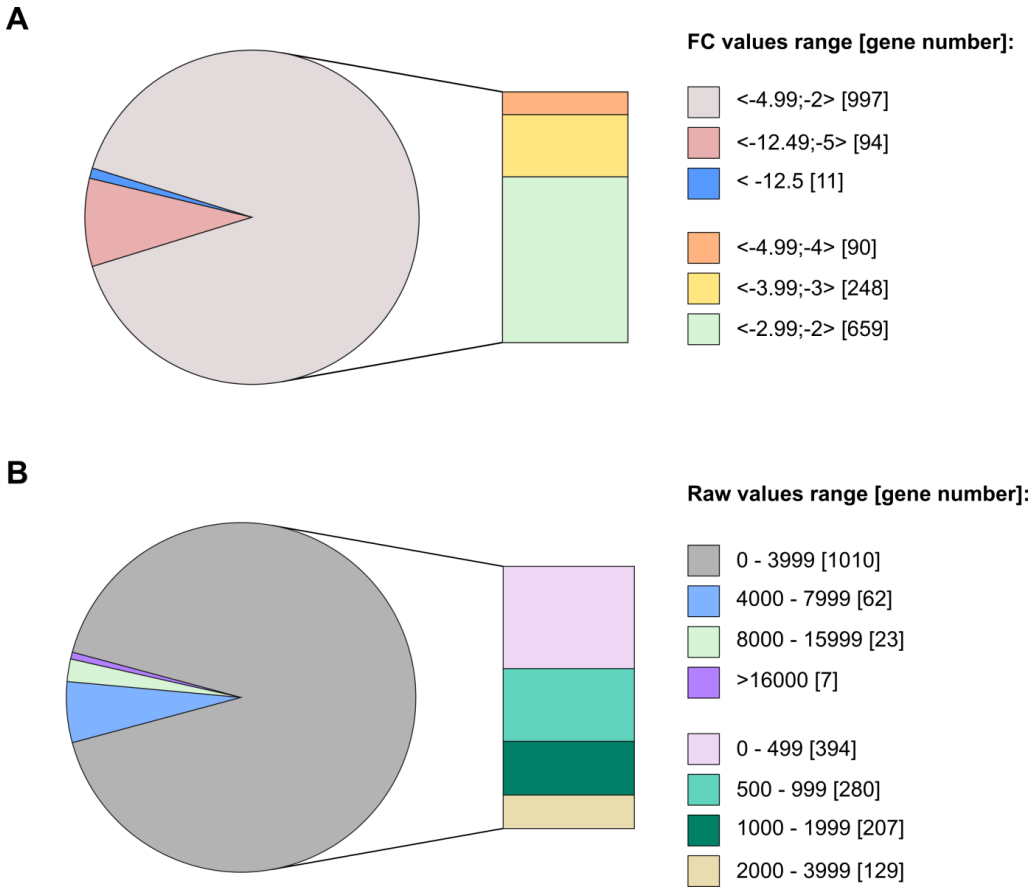

Figure 3. 2. Characterization of FC values and raw values for IFNγ+LPS-repressed genes in VSMC.

(A) 1102 IFNγ+LPS-down-regulated genes in VSMC were sub-classified into presented FC value ranges. Gene expression levels were presented as FC IFNγ(8h)+LPS(4h) relative to control sample in VSMC. For more detail see the text. **(B)** Next, 1102 IFNγ+LPS-down-regulated genes in VSMC were sub-classified into presented raw values ranges in control sample. Raw counts, control and IFNγ(8h)+LPS(4h), are presented as RPKM values. For more detail see the text.

Table 3. 3. Representative top-30 genes down-regulated (FC≤-3; raw counts≥500) by IFNγ+LPS in VSMC.

No.	Gene name	FC			Raw counts			
		IFNγ	LPS	IFNγ+LPS	Control	IFNγ	LPS	IFNγ+LPS
1	**Angpt2**	-2,8	-8,9	-33,4	2604,2	652,4	292,3	69,1
2	**Nr4a1**	-3,6	-3,2	-20,7	1847,9	364,1	585,7	79,3
3	**Shisa2**	-2,8	-4,7	-19,6	749,8	187,5	158,6	34,0
4	**Cdh3**	-5,0	-3,8	-18,6	1691,8	238,8	442,3	80,9
5	**Daam2**	-3,0	-4,5	-18,4	4504,2	1050,7	990,9	217,8
6	**Fam189a2**	-2,8	-4,8	-17,3	610,3	156,0	126,4	31,3
7	**Aff3**	-1,8	-3,1	-14,1	595,0	228,3	193,1	37,5
8	**AI646023**	-3,2	-3,2	-13,6	622,2	139,9	192,0	40,5
9	**Mn1**	-2,1	-2,5	-13,0	719,6	244,4	293,1	49,2
10	**Rab3il1**	-1,1	-4,5	-12,0	545,6	352,6	120,2	40,5
11	**Spon2**	-2,2	-4,0	-11,3	2190,7	715,3	542,5	171,5
12	**Ctgf**	-2,4	-2,4	-11,2	8314,6	2498,5	3508,3	656,1
13	**Megf9**	-2,5	-2,6	-11,1	652,7	184,1	248,5	52,0
14	**Npr3**	-3,8	-4,5	-10,7	967,3	181,2	216,1	80,4
15	**Fam180a**	-3,0	-1,8	-10,7	1359,2	322,0	750,2	113,2
16	**Sdpr**	-1,7	-3,1	-10,3	5243,7	2201,7	1695,0	451,9
17	**Jag1**	-3,7	-1,8	-10,3	1070,5	202,3	610,8	92,3
18	**Irs1**	-3,2	-2,4	-10,3	1141,5	248,9	476,1	98,6
19	**Ctnnal1**	-2,5	-2,8	-10,1	689,7	191,7	246,1	60,5
20	**Tfcp2l1**	-5,7	-2,9	-10,1	501,6	62,4	175,9	44,1
21	**Cd248**	-1,8	-4,1	-9,7	2539,8	1024,7	616,7	231,9
22	**Jup**	-2,0	-3,3	-9,6	3908,9	1396,1	1195,4	361,7
23	**Fhl1**	-3,1	-2,8	-9,5	1705,8	391,9	619,0	159,8
24	**Ano1**	-4,2	-2,4	-9,2	559,4	95,1	237,6	54,1
25	**Hoxa5**	-2,0	-4,0	-9,2	910,0	327,7	230,0	88,2
26	**Cdon**	-2,2	-3,7	-9,1	3726,9	1191,2	1007,5	364,5
27	**Dusp1**	-2,7	-2,2	-9,1	5613,5	1472,6	2522,2	550,5
28	**Sema3d**	-2,5	-3,1	-8,6	3195,6	887,8	1033,0	329,3
29	**Scel**	-1,6	-3,2	-8,6	1555,0	687,3	492,3	160,6
30	**Ntn4**	-2,4	-2,8	-8,3	1066,8	314,6	381,4	113,8

Gene expression levels were presented as FC IFNγ(8h), LPS(4h) and IFNγ(8h)+LPS(4h) relative to control in VSMC. Raw counts control, IFNγ(8h), LPS(4h) and IFNγ(8h)+LPS(4h) are presented as RPKM values.

However, some of enriched GO terms, related to cell migration, cell proliferation, cell adhesion and cell response to lipid, were previously identified during GO analysis of IFNγ+LPS-dependent up-regulated genes (Chapter 2, Fig.2.7A; Chapter 3, Fig.3.3A, marked by blue circles). This observation prompt us to re-analyse the same list of commonly IFNγ+LPS-up-regulated genes (398 genes FC≥3 filtered from 536 commonly up-regulated genes) together with a list of down-regulated genes (288 genes FC≤-3 filtered from 1102 VSMC down-regulated genes), what confirmed existance of the functional overlap between up- and down-regulated genes (reflected by the enrichment of GO terms related with cell migration, cell proliferation, cell adhesion and lipid biosynthetic process). Yet GO term

enrichment does not clearly indicate the direction of individual process regulation. It was previously reported that IFN-dependent gene up-regulation positively correlated with cell proliferation and migration in the context of vascular inflammation. However not much is known about the correlation of these processes with IFN-dependent gene down-regulation. Therefore we took a closer look at genes representing two example GO terms, commonly enriched between up- and down-regulated genes: Cell proliferation and Cell migration. Surprisingly, both GO terms were represented by the genes involved in the positive (green dots), negative (red dots) and not directed (grey dots) regulation of these processes (Fig.3.3B). In detail, for Cell proliferation GO term there were enriched 11 genes, 7 genes and 18 genes representing positive, negative and not directed regulation of the process, respectively. Cell migration GO term was represented by 26 positive correlated genes, 22 negative and 5 not clearly indicating process regulation (Fig.3.3B). Remarkably, some of the genes were correlated with both positive and negative process direction, like *Bmp4*, *Efnb2*, *Esr1*, *F2r*, *Fgfr2*, *Igf1*, *Sox4* and *Tgfb3* for Cell proliferation (Fig.3.3B). Hence, indicating a precise direction of the processes mediated by IFNγ+LPS-repressed genes is challenging and potentially highly depends on cell biological context.

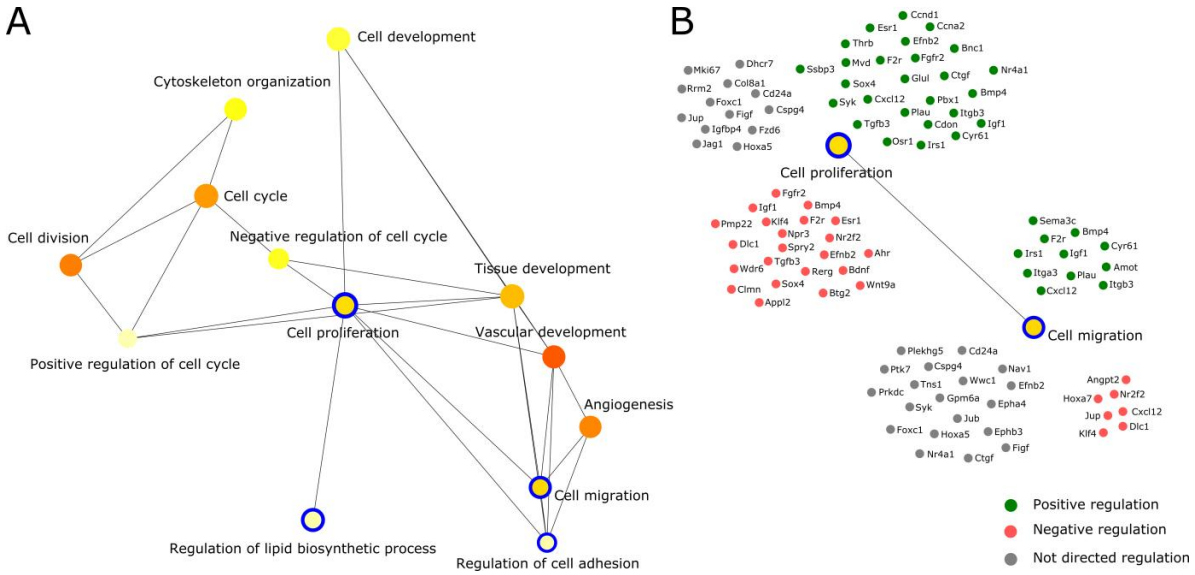

Figure 3. 3. Integrative GO and network-based analysis of IFNγ+LPS-repressed genes in VSMC.

(A) Network of enriched GO terms identified for IFNγ(8h)+LPS(4h)-down-regulated genes in VSMC (RNA-seq). Increasing orange colour of the GO term bubble reflects higher p-value (p-value<0.05). GO records commonly identified for both 288 down-regulated genes in VSMC (FC≤-3; raw counts in control sample≥500) and 398 commonly up-regulated (FC≥3) genes under stimulation with IFNγ+LPS

are marked by a blue ring around the GO term bubble. **(B)** Detailed gene characterization of Cell proliferation and Cell migration GO terms. Genes reflecting 'positive regulation of a process' are marked by a green dot, 'negative regulation of a process' are marked by a red dot and 'not directed regulation of a process' are marked by a grey dot.

Since STAT1 and NFκB are widely involved in IFNγ- and LPS-dependent gene up-regulation, we hypothesized on their role in the opposite scenario of gene transcriptional suppression. To verify such possibility, during subsequent *in silico* promoter analysis, consensus GAS, ISRE and NFκB binding motifs were screened in the final list of 288 gene promoter regions. 116 GAS, 36 ISRE and 99 NFκB binding sites were identified (Fig.3.4). Recognition of a low number of ISRE binding motifs as compared to GAS sites in repressed gene promoters suggests that STAT1 may be predominantly recruited in a form of GAF homodimer to GAS motifs, while STAT1 binding in a form of ISGF3 complex to ISRE sequence seems to be limited in case of gene down-regulation. Moreover, there was found relatively low overlap between ISRE and NFκB binding sites (4 genes) or ISRE and GAS binding sites (5 genes) or all three motifs (14 genes). The most represented were solitary GAS and NFκB motifs occuring in 54 and 38 gene promoters, respectively and combination of GAS-NFκB sites in case of 43 genes (Fig.3.4). Hence, we could speculate that STAT1 and NFκB could collaborate on GAS-NFκB sites to regulate transcriptional suppression in response to IFNγ and LPS in VSMC.

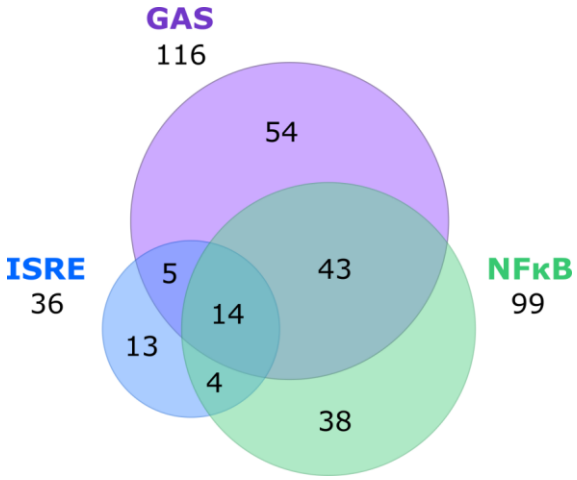

Figure 3. 4. Promoter analysis of down-regulated genes by IFNγ+LPS in VSMC.

Venn diagram presenting distribution of promoter located (-5000bp/+2000bp) GAS, ISRE and NFκB binding sites among 288 down-regulated genes in VSMC by IFNγ(8h)+LPS(4h) resulting from RNA-seq experiment.

In order to experimentally validate involvement of STAT1 in gene transcriptional repression, STAT1 ChIP-seq experiment in VSMC treated with IFNγ (8h), LPS (4h) and IFNγ(8h)+LPS(4h) was conducted. Results of the genome-wide recruitment of STAT1 to the regulatory regions of the down-regulated genes in response to IFNγ and combined treatment with LPS, resulting from RNA-seq are depicted in Figure 3.5A. Bars represent the total number of transcriptionally repressed genes upon stimulation with IFNγ and LPS in VSMC. Blue colour refers to the number of the genes which regulatory regions were STAT1-occupied, while red one identifies STAT1-binding depleted genes (Fig.3.5A). Therefore, it is clearly visible that IFNγ was more potent single stimuli in terms of STAT1 recruitment (242 genes), as compared to LPS (103 genes). Combined IFNγ+LPS stimulation resulted in an increase in the total number of STAT1-bound repressed genes up 1102 (Fig.3.5A). Based on the results of abovementioned *in silico* promoter analysis, further we anticipated on the potential collaborative NFκB role in gene transcriptional repression, beside STAT1. To further study this concept p65(NFκB) ChIP-seq in VSMC treated with IFNγ (8h), LPS (4h) or IFNγ(8h)+LPS(4h) was performed. Subsequent GAS, ISRE and NFκB consensus motif re-mapping to IFNγ+LPS suppressed gene regulatory regions analysis revealed diverse STAT1 and p65 binding pattern (Fig.3.5B). Upon IFNγ+LPS stimulation STAT1 bound to 479 GAS and 327 ISRE motifs, while p65 was recruited to 473 cognate NFκB sites and 177 gene regions were STAT1 and p65 depleted (Fig.3.5B). Moreover the sum of GAS, ISRE and NFκB binding sites and non occupied regions in response to IFNγ+LPS stimulation exceeded 1102 genes (1456 genes) (Fig.3.5B). This clearly implies that IFNγ+LPS-dependent STAT1 and p65 recruitment is directed towards gene promoters potentially containing more than one binding site, such as composite GAS-ISRE, GAS-NFκB, ISRE-NFκB and GAS-ISRE-NFκB sites.

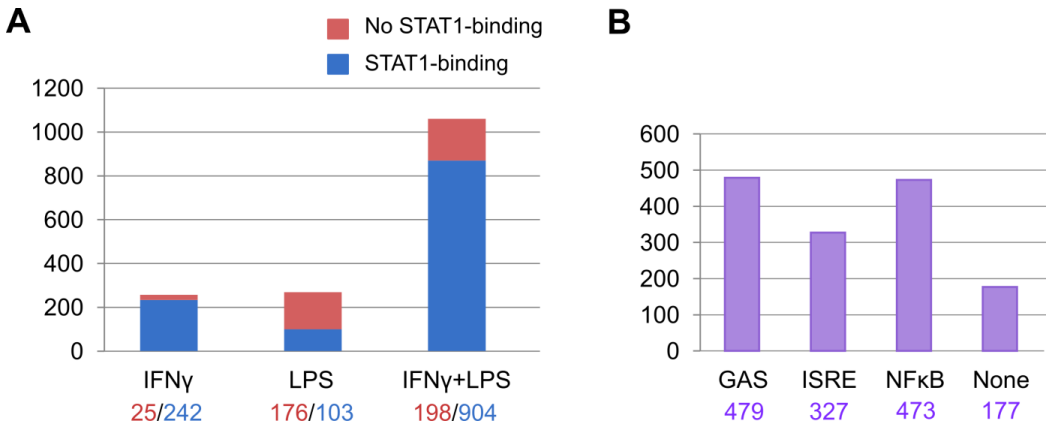

Figure 3. 5. STAT1 and p65 ChIP-seq gene annotation and re-mapping analysis in VSMC treated with IFNγ and LPS. (Figure description on the next page)

(A) Number of down-regulated genes annotated to STAT1-occupied (blue bars) and not occupied (red bars) regions resulting from ChIP-seq in VSMC stimulated with IFNγ(8h), LPS(4h) and IFNγ(8h)+LPS(4h). **(B)** Number of genes characterized by STAT1 and p65 recruitment (ChIP-seq) to GAS/ISRE and NFκB consensus sites, respectively, upon stimulation with IFNγ(8h)+LPS(4h) in VSMC.

During subsequent analysis, STAT1 and p65 recruitment pattern to suppressed gene regulatory regions upon VSMC stimulation with IFNγ (8h), LPS (4h) or IFNγ(8h)+LPS(4h) was analysed. Sequencing results in a form of STAT1 and p65 ChIP-seq peaks for the selected group of genes are depicted in Figure 3.6. IGV screenshots are presented for 18 genes (*Angpt2*, *Rab3il1*, *Spon2*, *Npr3*, *Cd248*, *Dusp1*, *Scel*, *Sox4*, *Thbd*, *Igf1*, *Slc5a3*, *Maf*, *Adamtsl3*, *Insig1*, *Pbx1*, *Fads2*, *Mvd* and *Sspn*) which were characterized by the lowest gene expression (the lowest FC value) and surprisingly co-occuring STAT1 recruitment to the gene regulatory regions upon IFNγ+LPS stimulation. FC values for all 18 genes in response to IFNγ, LPS and IFNγ+LPS in VSMC (resulting from RNA-seq) are depicted in Table 3.4. Stimulation with IFNγ and IFNγ+LPS resulted in potent STAT1 recruitment to the regulatory regions of all 18 down-regulated genes (Fig.3.6). Moreover for *Angpt2*, *Spon2*, *Scel*, *Igf1*, *Fads2* and *Mvd*, there could be observed p65 binding upon LPS and IFNγ+LPS treatment, yet much weaker in comparison to STAT1. Interestingly, p65 recruitment was detected in the region overlapping with STAT1 binding.

Further we aimed to validate a startling observation of STAT1 binding to the regulatory regions of the down-regulated genes in response to IFNγ+LPS in VSMC. Hence, STAT1 ChIP-PCR experiment in control and IFNγ+LPS-treated VSMC was conducted. STAT1 recruitment to the promoters of 7 example genes which showed the strongest TF recruitment based on IGV screenshots analysis: *Angpt2*, *Rab3il1*, *Spon2*, *Scel*, *Sox4*, *Igf1* and *Pbx1* was examined. Certainly, ChIP-PCR results corroborated observations formulated based on ChIP-seq experiment analysis, since STAT1 was efficiently recruited to all 7 down-regulated gene promoters (Fig.3.7).

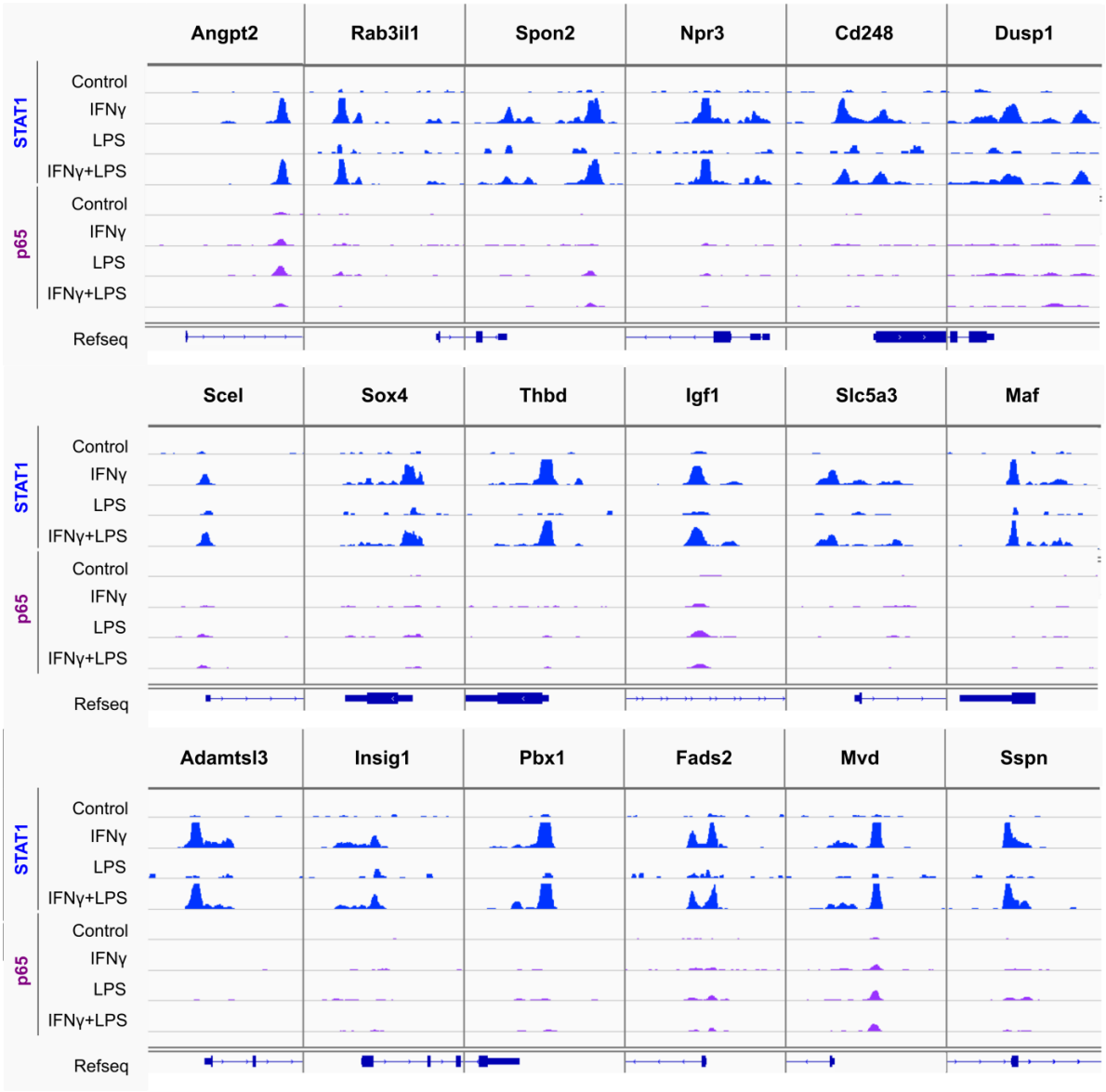

Figure 3. 6. STAT1 and p65 recruitment pattern to IFNγ+LPS down-regulated gene promoters in VSMC.

Representative views of STAT1 and p65 ChIP-seq peaks (STAT1: blue peaks, p65: violet peaks) identified in the regulatory regions of *Angpt2*, *Rab3il1*, *Spon2*, *Npr3*, *Cd248*, *Dusp1*, *Scel*, *Sox4*, *Thbd*, *Igf1*, *Slc5a3*, *Maf*, *Adamtsl3*, *Insig1*, *Pbx1*, *Fads2*, *Mvd* and *Sspn* in untreated or IFNγ(8h), LPS(4h), IFNγ(8h)+LPS(4h)-stimulated VSMC. STAT1- and p65-binding peaks were mapped onto the mouse reference genome mm10 and visualized using the IGV genome browser.

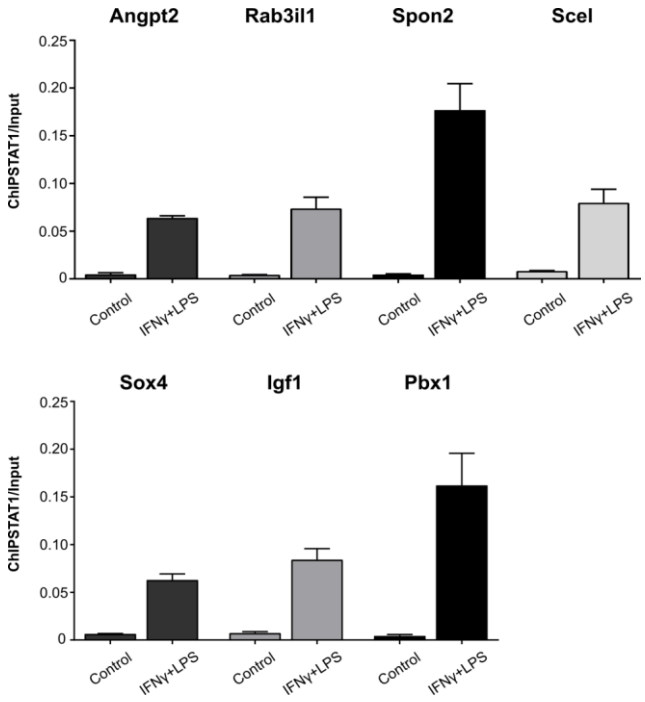

Figure 3. 7. Characterization of STAT1 recruitment upon stimulation with IFNγ+LPS in VSMC by ChIP-PCR.

ChIP-PCR of STAT1 at *Angpt2*, *Rab3il1*, *Spon2*, *Scel*, *Sox4*, *Igf1* and *Pbx1* gene promoters (primers listed in Table 3.2) in VSMC untreated and stimulated with IFNγ(8h)+LPS(4h). Mean ± s.e.m., n=2.

Although in general TF recruitment to the gene regulatory regions correlates with its transcriptional activation, in case of down-regulated genes this has not to be true due to involvement of more complex regulatory mechanisms. Accordingly, we examined which of 18 STAT1-bound gene (*Angpt2*, *Rab3il1*, *Spon2*, *Npr3*, *Cd248*, *Dusp1*, *Scel*, *Sox4*, *Thbd*, *Igf1*, *Slc5a3*, *Maf*, *Adamtsl3*, *Insig1*, *Pbx1*, *Fads2*, *Mvd* and *Sspn*) expression rely on STAT1. WT and STAT1 KO VSMC were left untreated or stimulated with IFNγ+LPS and gene transcriptional decrease level was analysed by RT-PCR. Thus, for 15 genes (*Angpt2*, *Rab3il1*, *Spon2*, *Npr3*, *Cd248*, *Dusp1*, *Scel*, *Sox4*, *Thbd*, *Igf1*, *Slc5a3*, *Adamtsl3*, *Pbx1*, *Fads2* and *Sspn*) there was identified clear expression decrease upon stimulation with IFNγ+LPS in WT VSMC (Fig.3.8). In case of *Maf*, *Insig1* and *Mvd* genes, treatment-dependent down-regulation was not clearly visible (Fig.3.8). Further, IFNγ+LPS-induced gene down-regulation was not affected in STAT1 KO VSMC in comparison to WT VSMC in case of 6 out of 15 genes: *Spon2*, *Npr3*, *Dusp1*, *Thbd*, *Slc5a3* and *Pbx1* (Fig.3.8, gene names marked in red). In contrast, other 9 gene expression: *Angpt2*, *Rab3il1*, *Cd248*, *Scel*, *Sox4*, *Igf1*, *Adamtsl3*, *Fads2* and *Sspn* was abrogated in STAT1 KO VSMC upon IFNγ+LPS treatment (Fig.3.8, gene names marked in green). Remarkably, the effect of applied treatment in STAT1 KO VSMC on the level of

gene down-regulation varied between examined genes. Almost total gene expression alteration could be observed in case of *Rab3il1*, *Scel*, *Sox4* and *Igf1*. On the other hand, although *Angpt2*, *Cd248*, *Adamtsl3*, *Fads2* and *Sspn* transcriptional regulation was STAT1-dependent, observed effect of gene repression was not as strong as in case of abovementioned 4 genes (Fig.3.8). This observation may suggest involvement of some additional factor collaborating with STAT1 in mediating selected gene repression. Together, this data supports the concept of a crucial STAT1 role in gene-specific priming-induced SI between IFNγ and LPS and pro-inflammatory stimuli-dependent transcriptional down-regulation.

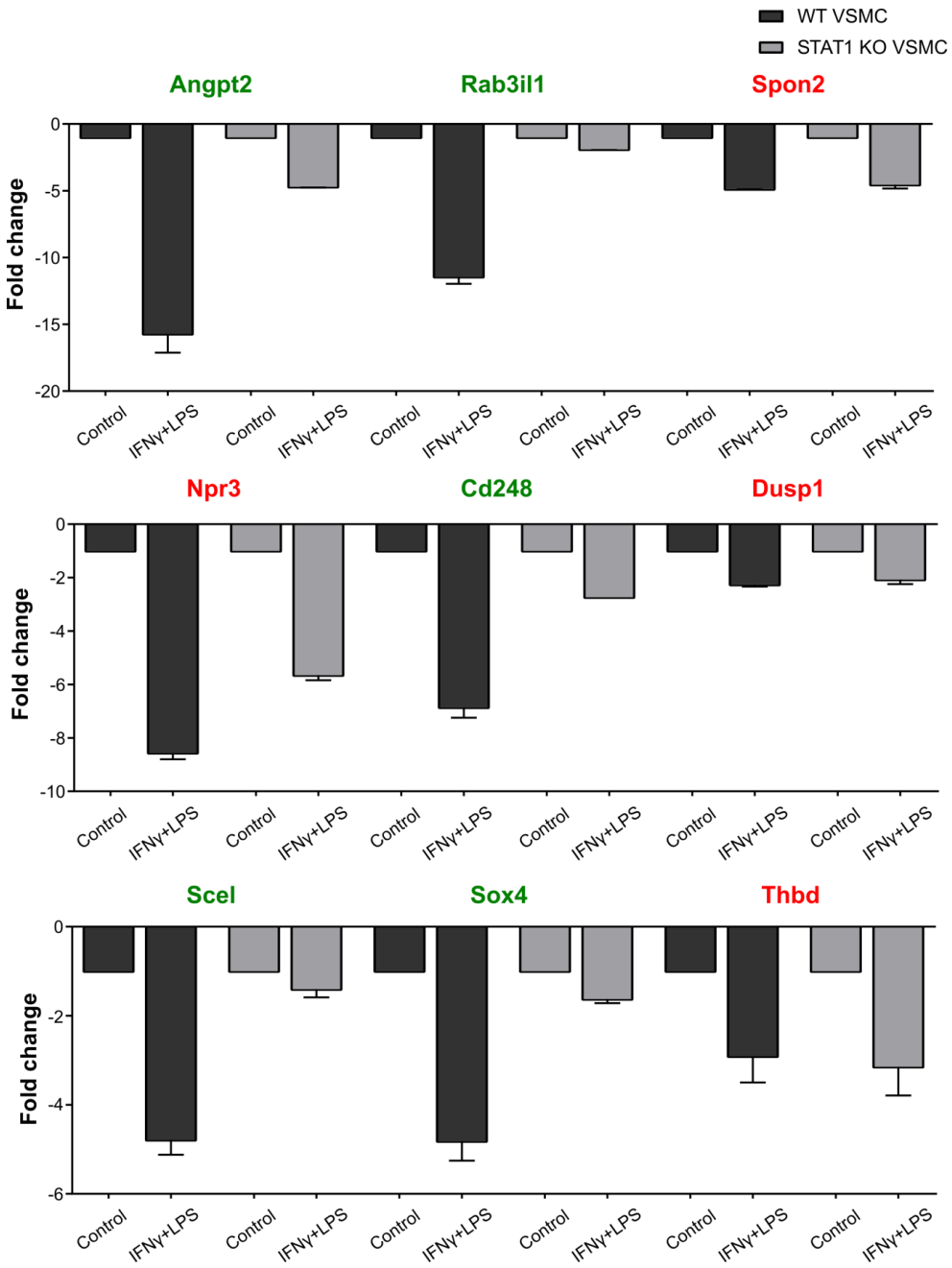

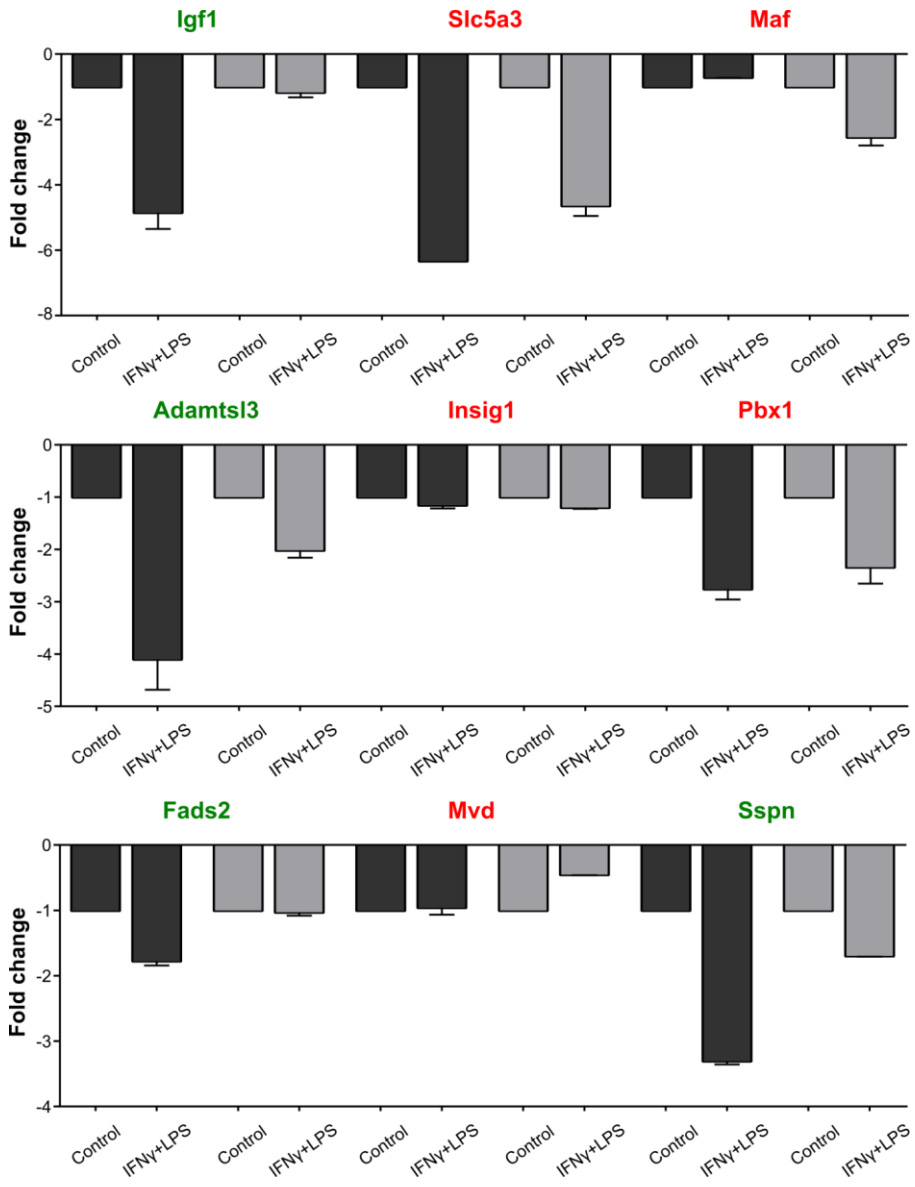

Figure 3. 8. Relative expression (over β-actin) of IFNγ+LPS down-regulated genes in WT and STAT1 KO VSMC.

Angpt2, *Rab3il1*, *Spon2*, *Npr3*, *Cd248*, *Dusp1*, *Scel*, *Sox4*, *Thbd*, *Igf1*, *Slc5a3*, *Maf*, *Adamtsl3*, *Insig1*, *Pbx1*, *Fads2*, *Mvd* and *Sspn* enrichment in untreated and IFNγ(8h)+LPS(4h) stimulated WT and STAT1 KO VSMC examined by RT-PCR.

Table 3.4 offers a summary of the above-mentioned 18 IFNγ+LPS-repressed gene analysis results. FC values in response to IFNγ, LPS and IFNγ+LPS in VSMC (resulting from RNA-seq) are presented together with an indication of gene down-regulation dependence on STAT1 (Table 3.4, Fig.3.8). Moreover, there is illustrated STAT1 and p65 recruitment pattern to the gene regulatory regions and corresponding GAS or NFκB binding sites presence. Remarkably, STAT1 binding correlated with the presence of GAS motif in all 18 gene promoters (Table 3.4, Fig.3.6). Interestingly, NFκB binding site was recognized in 12 gene

promoters (*Rab3il1*, *Sox4*, *Adamtsl3*, *Sspn*, *Angpt2*, *Igf1*, *Fads2*, *Npr3*, *Thbd*, *Slc5a3*, *Insig1*, *Mvd*), corresponding to p65 recruitment only in case of 4 genes, *Angpt2*, *Igf1*, *Fads2* and *Mvd* (Table 3.4, Fig.3.6). Together, based on gene repression STAT1 dependence, STAT1 and p65 binding pattern and promoter binding site composition, 18 IFNγ+LPS down-regulated gene examples were divided into 4 groups presenting similar features (Table 3.4). Thus, we could identify 2 gene groups (Table 3.4, Group I and Group II, marked in orange) which may correspond to STAT1-dependent gene repression regulatory mechanisms, while the rest of the gene expression was not STAT1-dependent (Table 3.4, Group III and Group IV, marked in blue). We further aimed to anticipate on the potential mechanism of STAT1-dependent gene repression in the context of priming-induced SI between IFNγ and LPS. Gene Group I (*Rab3il1*, *Cd248*, *Sox4*, *Adamtsl3* and *Sspn*) was characterized by STAT1-dependent gene expression, STAT1 recruitment to GAS binding site and lack of p65 binding, yet presence of NFκB binding site (NFκB binding site not identified for *Cd248*). Gene Group II (*Angpt2*, *Scel*, *Igf1*, *Fads2)* was characterized alike by STAT1-dependent gene expression and STAT1 recruitment to GAS motif, but p65 recruitment to NFκB binding site (NFκB binding site not identified for *Scel*) (Table 3.4).

Table 3. 4. Characteristics summary of 18 IFNγ+LPS-repressed gene representatives in VSMC.

Gene group	Gene name	FC			STAT1-dependence	STAT1 binding	p65 binding	Binding site		
		IFNγ	LPS	IFNγ+LPS				GAS	ISRE	NFκB
Group I	Rab3il1	-1,1	-4,5	-12,0	+	+	-	•	-	•
	Cd248	-1,8	-4,1	-9,7	+	+	-	•	-	-
	Sox4	-2,1	-1,7	-8,0	+	+	-	•	•	•
	Adamtsl3	-1,8	-2,8	-4,1	+	+	-	•	-	•
	Sspn	-1,4	-1,9	-3,1	+	+	-	•	•	•
Group II	Angpt2	-2,8	-8,9	-33,4	+	+	+	•	•	•
	Scel	-1,6	-3,2	-8,6	+	+	+	•	-	-
	Igf1	-2,5	-2,3	-5,0	+	+	+	•	-	•
	Fads2	-2,0	-1,7	-3,2	+	+	+	•	-	•
Group III	Npr3	-3,8	-4,5	-10,7	-	+	-	•	-	•
	Dusp1	-2,7	-2,2	-9,1	-	+	-	•	-	-
	Thbd	-1,1	-3,5	-5,4	-	+	-	•	-	•
	Slc5a3	-2,4	-1,9	-4,5	-	+	-	•	-	•
	Maf	-1,7	-1,8	-4,4	-	+	-	•	-	-
	Insig1	-1,7	-1,9	-3,6	-	+	-	•	-	•
	Pbx1	-1,4	-2,1	-3,3	-	+	-	•	-	-
Group IV	Spon2	-2,2	-4,0	-11,3	-	+	+	•	-	-
	Mvd	-1,7	-1,6	-3,1	-	+	+	•	-	•

Gene expression levels were presented as FC IFNγ(8h), LPS(4h) and IFNγ(8h)+LPS(4h) relative to control in VSMC. STAT1-dependence of listed gene expression was marked by a plus (+). STAT1 or p65 recruitment to listed gene promoter was marked by a plus (+). Presence of GAS, ISRE or NFκB binding sites in the promoters of listed genes was indicated by a dot (•).

In order to further understand the potential mechanism of STAT1-dependent gene transcriptional repression, we examined epigenetic changes and PolII recruitment occurring upon IFNγ and LPS VSMC treatment. Two genes representing Group I and Group II (Table 3.4) *Rab3il1* and *Angpt2*, respectively, were selected for further examination. Additionally, one representative of IFNγ+LPS-driven STAT1-independent gene down-regulation, *Spon2* was chosen. First, we analysed recruitment of PolII to the regulatory regions of these genes upon IFNγ+LPS stimulation by ChIP-PCR. As depicted in Figure 3.9 in case of *Rab3il1* PolII was less efficiently enrolled after IFNγ+LPS treatment in comparison to the control, which result correlates with gene transcriptional down-regulation. Oppositely, we observed increased PolII recruitment to *Angpt2* and *Spon2* gene promoter (Fig.3.9). Moreover, enrichment level of H3K27Ac histone mark, which in general corresponds with gene transcriptional activation, was measured. As such, for *Rab3il1*, *Angpt2* and *Spon2* we could observe decrease in histone acetylation upon IFNγ+LPS treatment in VSMC, which correlated with all gene transcriptional down-regulation.

Together, IFNγ+LPS-dependent STAT1 may participate in selected gene group down-regulation in VSMC. Pro-inflammatory stimuli-repressed genes in VSMC reflect biological processes related with cell survival against vascular inflammation. Mechanism of STAT1-mediated gene repression in the context of priming-induced SI between IFNγ and LPS might be highly gene-specific, depends predominantly on STAT1 and correlate with decreased H3K27Ac.

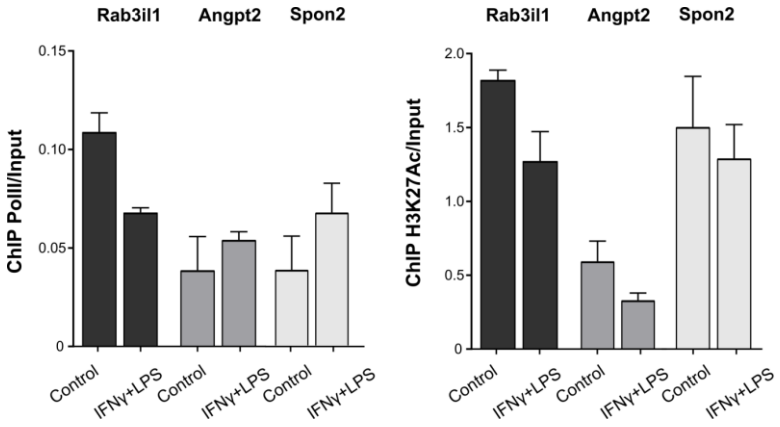

Figure 3. 9. Characterization of PolII recruitment and H3K27Ac enrichment upon stimulation with IFNγ+LPS in VSMC by ChIP-PCR.

ChIP-PCR of PolII and H3K27Ac at *Rab3il1*, *Angpt2* and *Spon2* gene promoters (primers listed in Table 3.2) in VSMC untreated and stimulated with IFNγ(8h)+LPS(4h). Mean ± s.e.m., n=2.

Discussion

Genome-wide RNA-seq analysis of VSMC response to single and combined treatment with IFNγ(8h) and LPS(4h), let for characterization of transcriptional down-regulation occurring in response to pro-inflammatory stimuli. Combined stimulation of VSMC with IFNγ+LPS resulted in suppression of 1102 genes (Fig.3.1). One of the crucial aims of this study was to decipher the mechanism of VSMC gene repression in the context of priming-induced SI between IFNγ and LPS.

First, we asked a question about the potential role of gene down-regulation in connection with IFNγ- or LPS-driven vascular inflammation. As presented in Figure 3.3A, performed integrative GO and network-based analysis, indicated possible functions of 288 IFNγ+LPS repressed genes (after filtering) in VSMC related with: Vasculature development, Angiogenesis, Tissue development, Cell development; Cell cycle, Cell division, Cytoskeleton organisation, Positive regulation of cell cycle, Negative regulation of cell cycle; Regulation of lipid biosynthetic process; Cell Proliferation; Cell migration; Regulation of cell adhesion. Interestingly, terms including cell migration, cell proliferation, cell adhesion and cell response to lipid, were identified alike during GO analysis of IFNγ+LPS-dependent up-regulated genes (Chapter 2, Fig.2.7A; Chapter 3, Fig.3.3A, marked by blue circles). It could suggest existance of the partial functional overlap between IFNγ+LPS-driven up- and down-regulated genes. Yet, although performed integrative GO and network-based analysis let for identification of crucial processes affected by IFNγ+LPS stimulation, it is challenging to indicate an overall effect of gene up- or down-regulation on the progression of vascular inflammation.

Next, we aimed to study the regulatory mechanism of IFNγ+LPS-driven priming-induced SI in the context of gene down-regulation in VSMC. Since STAT1 and NFκB are involved in pro-inflammatory stimuli-dependent gene activation, we hypothesized on their role in the opposite scenario of gene repression. However there is limited evidence for a role of these TF in gene transcriptional repression and an exact mechanism of neither STAT1- nor NFκB-dependent gene down-regulation is known. Worthmentioned, supression of genes including *Skp2*, *ABC1*, *Bcl-2*, *Bcl-x, Bax, CXCR4, c-myc, CSF1* was shown previously to be directly dependent on STAT1 in various cell types (Wang et al. 2010, Wang et al. 2002, Stephanou et al. 2000, Cao et al. 2015, Soond et al. 2007, Hiroi et al. 2009, Ramana et al. 2000, Horvai et al. 1997). Similarly, repressory effect of NFκB was observed in case of *IL8*, *Bcl-2*, *IL4* and *Sp1* (Oliveira et al. 1994, Chu et al. 2011, Casolaro et al. 1995, Ye et al. 2015).

In silico promoter analysis performed in our study, predicted presence of GAS (116 genes) and NFκB (99 genes) binding sites in the regulatory regions of IFNγ+LPS-dependent repressed genes (Fig.3.4). Moreover, experimental validation of the potential involvement of STAT1 and NFκB in gene supression was performed by ChIP-seq in IFNγ (8h) and/or LPS (4h)-treated VSMC. STAT1 and p65 recruitment to the regulatory regions of IFNγ+LPS-repressed genes in VSMC was visualised by IGV screenshots for 18 selected genes: *Angpt2*, *Rab3il1*, *Spon2*, *Npr3*, *Cd248*, *Dusp1*, *Scel*, *Sox4*, *Thbd*, *Igf1*, *Slc5a3*, *Maf*, *Adamtsl3*, *Insig1*, *Pbx1*, *Fads2*, *Mvd* and *Sspn* (Fig.3.6). Table 3.4 presents negative FC values for all 18 genes in response to treatment with IFNγ, LPS and IFNγ+LPS in VSMC, illustrating an effect of transcriptional SI (resulting from RNA-seq). STAT1 was recruited to all 18 down-regulated gene regulatory regions upon stimulation with IFNγ and IFNγ+LPS. In case of *Angpt2*, *Spon2*, *Scel*, *Igf1*, *Fads2* and *Mvd* we observed STAT1 co-occuring weak binding of p65 within the same gene regulatory regions (Fig.3.6). Unexpected observation of STAT1 recruitment to the regulatory regions of 7 selected (*Angpt2*, *Rab3il1*, *Spon2*, *Scel*, *Sox4*, *Igf1* and *Pbx1*) gene promoters of transcriptionally repressed genes was further validated by ChIP-PCR (Fig.3.7).

In the next step, dependence of of the down-regulated gene expression on STAT1 was evaluated by RT-PCR in VSMC WT versus VSMC STAT1 KO. Among 18 analysed genes, clear gene down-regulation upon WT VSMC stimulation with IFNγ+LPS could be confirmed in case of 15 genes: *Angpt2*, *Rab3il1*, *Spon2*, *Npr3*, *Cd248*, *Dusp1*, *Scel*, *Sox4*, *Thbd*, *Igf1*, *Slc5a3*, *Adamtsl3*, *Pbx1*, *Fads2* and *Sspn* (Fig.3.8). Moreover, 9 (*Angpt2*, *Rab3il1*, *Cd248*, *Scel*, *Sox4*, *Igf1*, *Adamtsl3*, *Fads2* and *Sspn*) out of 15 gene repression was abrogated in IFNγ+LPS-treated STAT1 KO VSMC (Fig.3.8, gene names marked in green). Importantly, gene down-regulation was almost totally dependent on STAT1 in case of *Rab3il1*, *Scel*, *Sox4* and *Igf1*, while just altered for *Angpt2*, *Cd248*, *Adamtsl3*, *Fads2* and *Sspn* (Fig.3.8). This result may imply involvement of some other STAT1-collaborating factors, participating in gene repression regulation. As shown previously, priming-induced SI between IFN and LPS resulting in robust pro-inflammatory gene up-regulation, relies on cooperative action of STAT1-containing transcriptional complexes and NFκB (p65-p50 heterodimers). For instance, STAT1 collaboration with NFκB was inevitable for transcriptional activation of *Cxcl9*, *IP-10*, *Becn1* and *NOS2* (Ohmori and Hamilton 1993, Ganster et al. 2001, Hiroi and Ohmori 2003, Zhu et al. 2013). Remarkably, some TF may perform a bi-directional action depending on the biological context. Thus such TF could participate both in gene activation

by collaboration with GTM or gene down-regulation by recruitment of the relevant repressors. Hence, we could speculate that in case of *Angpt2* and *Fads2* which promoters were co-bound by STAT1 and p65 (Table 3.4), these two TF could coact to regulate gene down-regulation. On the other hand, *Sspn* promoter contains ISRE binding site (Table 3.4), which could directly point to the involvement of IRF1 in STAT1 collaborative gene down-regulation. Mutual action of these two TF was essential for IFNγ-dependent *Gbp2* transcription (Ramsauer et al. 2007). Moreover, STAT1 and IRF1 were co-recruited to closely spaced GAS and ISRE motifs in response to IFNγ (Abou El Hassan et al. 2017). Mottet et al. reported that cooperative action of STAT1, IRF1 and USF-1 was necessary for activation of CIITA promoter IV by type II IFN (Muhlethaler-Mottet et al. 1998). On the other hand, STAT1 required BRCA1 acting as a co-activator, to regulate expression of a subset of IFNγ-dependent genes and finally p21WAF1-mediated growth inhibition (Ouchi et al. 2000). Remarkably, although a positive action of the abovementioned TF was broadly studied in the context of IFN-induced gene transcriptional activation, evidence for their involvement in mediating gene down-regulation is limited.

Table 3.4 offers an insight in the characteristics of 18 down-regulated genes in VSMC upon stimulation with IFNγ+LPS. The gene list was divided into 4 main gene groups, which could represent two different STAT1-dependent gene down-regulation regulatory mechanisms (Table 3.4, marked in orange) and two distinct STAT1-independent mechanisms (Table 3.4, marked in blue). 1st Group of genes (*Rab3il1*, *Cd248*, *Sox4*, *Adamtsl3* and *Sspn)* representing potential STAT1-dependent mechanism was characterized by STAT1-dependent gene expression, STAT1 recruitment to GAS and/or ISRE binding site and lack of p65 binding, yet presence of NFκB binding site. 2nd Group of genes (*Angpt2*, *Scel*, *Igf1*, *Fads2)*, illustrating different potential STAT1-dependent mechanism, was characterized by STAT1-dependent gene expression and STAT1 recruitment to GAS and/or ISRE binding site, alike, however accompanied by p65 recruitment to NFκB binding site.

As mentioned before, although STAT1- or NFκB-dependent gene repression was previously observed in several studies, the potential explanation of their action is not known, especially in the context of SI between IFNγ and LPS. Few mechanism which could underlie STAT1-dependent gene transcriptional down-regulation are described below. Yet it is much more challenging to speculate about the role of NFκB transcriptional complexes in the mechanism of STAT1-dependent priming-induced SI. One possibility could be that both STAT1- and NFκB would collaborate to promote gene transcriptional repression. On the

other hand, STAT1 activated during first phase of IFNγ-dependent stimulation might serve a predominant role in mediating SI-dependent gene down-regulation. First, STAT1 might sequester gene transcriptional co-activators, like CBP/p300 which drive gene activation. Indeed, Ma et al. reported that IFNγ induced association of STAT1α and CBP resulted in decreased association of CBP with *MMP9* promoter. Finally, transcriptional activation of *MMP9* was abrogated due to suppressed H3/H4 acetylation and PolII recruitment (Ma et al. 2005). Similar mechanism involving competition between STAT1 and CBP/p300 was shown to be involved in the PPARγ-dependent transcriptional down-regulation of *iNOS* (Li et al. 2000). Second, in the opposite scenario, STAT1 could associate with gene transcriptional co-repressors to down-regulate gene expression. As such, co-repressor SMRT was found to associate with STAT5 to repress *Cis* and *OSM* target genes (Nakajima et al. 2001). Moreover, association between STAT4 and co-repressor PIASx resulted in inhibited gene activation in human T cells after stimulation with IL12 (Arora et al. 2003). Others characterized SLFN5 as STAT1 co-repressor, which could negatively control STAT1 target gene expression (Arslan et al. 2017). Third, STAT1 binding to its cognate motif within gene promoter could mask a binding site of other positively acting TF, thus inhibit its potentially positive effect on gene transcription. Alike, TNFα-induced NFκB-dependent *MMP9* transcriptional activation was blocked by IRF1, acting as a competitive inhibitor, binding to the gene promoter at a position that overlaps with NFκB motif. Thus, NFκB could not gain access to *MMP9* promoter, what resulted in gene transcriptional repression (Sancéau et al. 2002). Fourth, STAT1 might participate in the recruitment of enzymes establishing histone modifications negatively affecting gene transcription and finally enabling PolII recruitment or its elongation. It was shown previously, that STAT could recruit chromatin-modifying enzymes via their TAD domains. As such, all STAT are likely to interact with with CBP/p300 (Levy and Darnell 2002). STAT1 also functionally synergized with pCIP, other known Histone Acetyltransferase (HAT) (Korzus et al. 1998). On the other hand there is limited evidence for STAT association with the enzymes introducing modifications determining negative transcriptional outcomes. STAT5-dependent transcription was negatively affected by HDAC and co-repressor SMRT (Nakajima et al. 2001). Interestingly, HDAC was required as a co-activator for STAT1-, STAT2- and STAT5-dependent gene expression (Nusinzon and Horvath 2005). Although in this study STAT1-HDAC interaction was correlated with gene transcriptional activation, it provides a prove for such association and let to speculate, that it could affect gene repression-related events in the other biological context.

In order to determine how H3K27Ac enrichment and PolII recruitment varied upon stimulation with IFNγ+LPS in the regulatory regions of the down-regulated genes, we examined the following 3 gene examples. *Rab3il1*, representing Group I, characterized by STAT1 solitary binding, *Angpt2* being example of Group II, simultaneously bound by STAT1 and p65 and *Spon2* IFNγ+LPS-repressed gene in STAT1-independent manner (Table 3.4). H3K27Ac histone mark enrichment levels corresponded with gene transcriptional repression, thus were lowered upon IFNγ+LPS treatment in VSMC in *Rab3il1*, *Angpt2* and *Spon2* gene promoters (Fig.3.9). Interestingly, while PolII recruitment was decreased in case of *Rab3il1*, it presented the opposite tendency in case of the other two genes, *Angpt2* and *Spon2* (Fig.3.9). The latter observation was very surprising, because transcriptional repression correlated with moderate increase in PolII recruitment. This result could be explained by the phenomena of PolII early elongation pausing. Upon stimulation, promoter recruited PolII is kept in a form of unstable initiation transcribing complex and cannot become a processive elongation complex, depending on the interplay between recruited positive and negative factors (Nechaev and Adelman 2011). As a consequence PolII pausing could be a rate-limiting step during early elongation for multiple genes (Jonkers et al. 2014). PolII pausing-dependent premature transcription termination was shown to determine down-regulation of *c-myc* in differentiating HL60 cells (Strobl and Eick 1992). Hence, moderately increased recruitment of PolII to *Angpt2* and *Spon2* gene promoters could not reflect an actual direction of gene expression.

Together, we propose a model illustrating the potential mechanism underlying STAT1-dependent priming-induced SI between IFNγ and LPS in the context of gene down-regulation (Fig.3.10). Table 3.4 summarizes characteristics of the two gene groups, which transcriptional repression was STAT1-dependent (Table 3.4, orange colour). Group I is characterized by STAT1 recruitment to predominantly GAS cognate motif co-localizing with p65 unbound NFκB motifs within gene regulatory regions (Fig.3.5, Table 3.4). This observation could suggest that STAT1 masks closely spaced NFκB binding site, preventing p65 access, in order to mediate STAT1-dependent gene repression. Additionally, we could speculate that STAT1 might act as a co-repressor and mediate recruitment of repressory mechinery to drive gene down-regulation. Moreover, gene transcriptional repression correlates with decreased H3K27Ac enrichment, potentially mediated by STAT1-recruited HDAC. Finally, PolII recruitment was limited, what together correlates with the negative direction of transcriptional regulation. Group II (Table 3.4) is characterized by STAT1 and p65 co-binding to predominantly GAS and NFκB motifs. The fact that this group gene

repression was STAT1-dependent, we could speculate on crucial STAT1 role in repressor recruitment. Similar role could be served by p65, yet effect of this TF depletion on gene expression was not studied (due to the lethal effect of p65 KO in mouse embryos). Gene down-regulation correlated with decreased H3K27Ac enrichment, which again could be mediated by STAT1- and/or NFκB recruited HDAC. Interestingly, gene down-regulation correlated with moderately increased PolII recruitment, which could be explained by the potential phenomena of PolII pausing.

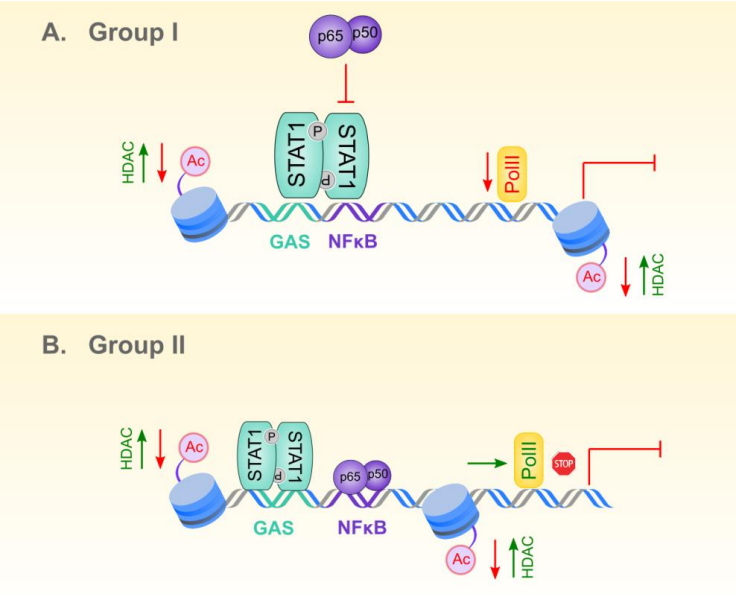

Figure 3. 10. Model of the potential mechanisms driving STAT1-dependent transcriptional gene repression in the context of SI between IFNγ and LPS.

(A) Group I of STAT1-dependent genes is characterized by STAT1 recruitment to predominantly GAS cognate motifs upon stimulation with IFNγ+LPS. Due to the close distance to adjacent NFκB site, STAT1 masks NFκB motif, enabling p65 to bind. Gene transcriptional repression correlates with decreased H3K27Ac enrichment and PolII recruitment. **(B)** Group II of STAT1-dependent genes is characterized by STAT1 and p65 co-binding to predominantly GAS and NFκB motifs upon stimulation with IFNγ+LPS. Gene down-regulation correlated with decreased H3K27Ac enrichment and moderately increased PolII recruitment, which could be caused by PolII pausing. For more details, see the text.

Table 3.4 also offers an insight in the characteristics of STAT1-independent IFNγ+LPS down-regulated genes. Therefore one could ask about the role of STAT1 recruited to these gene promoters, if its depletion did not alter gene transcriptional repression. Interplay between TF and their DNA binding motifs play a crucial role in mediating gene expression outputs. Remarkably, recent genome-wide studies let to formulate a conclusion, that TF

binding does not always correlate with gene transcription. Transcriptome analysis of 59 TF and chromatin modifiers depletion in lymphoblastoid cell line combined with ChIP-seq and DNAse-seq data revealed that ~85.3% of binding events did not result in significant putative target gene expression changes (Cusanovich et al. 2014). Based on multiple studies which lead to the same findings, there arouse a term of 'non-functional' or 'spurious' TF binding, which in contrast to the 'functional' binding does not occur when and where necessary (Spivakov 2014). Thus, there exists a possibility, that discussed STAT1-independent group of genes exemplifies such scenario. Additionally, we could consider a concept when unknown co-repressor binds in the close vicinity of GAS/ISRE binding site, making it accidentally accessible for IFNγ+LPS-activated, thus available STAT1. Co-repressor would collaborate with repressor to regulate gene transcriptional down-regulation, independently on STAT1. STAT1 could serve as transcription co-activator in the other biological context and act autonomously or represent redundant binding.

Abovementioned integrative GO and network-based analysis indicated enrichment of 288 IFNγ+LPS repressed genes in VSMC in the processes characteristic for inflammatory vascular disease. Finally, we aimed to anticipate on the potential functions served by a selected group of STAT1-dependent IFNγ+LPS down-regulated genes (Table 3.4, Group I) in context of vascular inflammation. Few gene examples are discussed below. As such, RAB3A interacting protein (rabin3)-like 1 (Rab3il1) acts as a binding partner for GTPases Rab11a and Rab11b (Horgan et al. 2013). Interestingly, anti-atherosclerotic effect of statins, the most powerful among available drugs against atherosclerosis, is mediated via inhibition of GTPases and subsequent cell proliferation, vascular inflammation and oxidative stress restriction (Babelova et al. 2013). Thus, we could speculate that *Rab3il1* IFNγ+LPS-dependent down-regulation could be beneficial and result in alleviated vascular inflammation. Endosialin (Cd248) is a marker of activated VSMC, which might regulate VSMC synthetic phenotype, thus contribute to the pathogenesis of atherosclerosis (Volobueva et al. 2018). *CD248* was found to be up-regulated in ApoE KO mice and human atherosclerotic plaques. On the contrary, Oil Red O staining of aortas from ApoE/CD248 KO mice revealed reduction of atherosclerotic lesions (Hasanov et al. 2017). Moreover targeting Cd248 is considered as a promising strategy to fight against cancer and fibrosis-related diseases (Teicher 2019). Angiopoietin 2 (Angpt2) contributes to the vessel destabilization, angiogenesis and neovascularization, especially in the presence of angiogenic factor Vascular Endothelial Growth Factor (VEGF). Interestingly, IFNγ-dependent STAT1 activation in Human

Umbilical Vein EC (HUVEC), mediated suppression of pro-angiogenic VEGF effect by *ANGPT2* repression (Battle et al. 2006). Whatsmore Angpt-2 was correlated with an early onset and development of CVD in patients with chronic inflammatory disease, rheumatoid arthritis (López-Mejías et al. 2013). Oppositely, in the angiotensin II (AngII)-infused Apolipoprotein E deficient mice, administration of recombinant Angpt2 significantly inhibited aortic inflammation and angiogenesis (Yu et al. 2016). Angpt2 is also known as a biomarker of activated endothelium, which makes it responsive to various pro-inflammatory cytokines (López-Mejías et al. 2014). Insulin-like growth factor 1 (Igf1) was reported to play pleiotropic effects on vascular inflammation. Low IGF1 levels were correlated with an increased risk of ischemic heart disease and high mortality rates, due to potentially antiapoptotic, antioxidant and plaque stabilization actions of IGF1 (Juul et al. 2002, Laughlin et al. 2004). Moreover, Sukhanov et al. reported that recombinant IGF1 infusion in ApoE KO mouse model fed on high fat diet decreased atherosclerotic plaque progression, immune cell infiltration, pro-inflammatory cytokines release and oxidative stress (Sukhanov et al. 2007). Reduced expression of IGF1, accompanied by IGF2, IGFBP-3, -4, -5, and -6 repression, was found in human carotid plaques (Wang et al. 2012). However in strike contrast, Zhu et al. showed that targeted overexpression of IGF1 in VSMC increased neointimal formation causing abrogated cell proliferation and migration after intraarterial injury (Zhu et al. 2001). In double-KO mice depleted of ApoE and pregnancy associated plasma protein-A (Pappa), a metalloproteinase that degrades IGFBP-4, Harrington et al. observed decreased atherosclerotic plaques size and lowered expression of IGF1 target genes. Since Pappa depletion increases IGFBP-4 levels and lower IGF1 synthesis, authors proposed that these data may imply pro-atherogenic role of IGF1 (Harrington et al. 2007).

Although it is not possible to estimate the general effect of IFNγ+LPS-dependent gene down-regulation in the context of vascular inflammation, gene-specific analysis suggests that STAT1 might participate in vascular cell survival mechanism against vascular inflammation. In this study, we provide evidence for STAT1 involvement in transcriptional regulation of IFNγ+LPS SI-dependent gene repression via two potential distinct mechanisms. First, STAT1 might act as a possible competitive inhibitor of p65 and recruit transcriptional repressors to mediate gene down-regulation. Second, STAT1 could potentially collaborae with p65 to recruit transcriptional repressors and regulate gene supression. Hovewer elucidation of the details of proposed STAT1-dependent mechanisms underlying SI between IFNγ and LPS would require further experimental investigation.

Chapter 4. STAT1 acts as a mediator of MΦ- and VSMC-specific IFNγ-dependent gene expression

Introduction

MΦ and VSMC are crucial cell types which mediate tissue homeostasis by performing partially overlapping, but mostly cell type-unique functions in a healthy vessel. Pro-inflammatory stimuli-dependent alteration of the original cell function and gene expression may contribute to the development of various inflammatory diseases, like atherosclerosis (Hoeksema and Glass 2019). Elucidation of the molecular mechanisms driving MΦ- and VSMC-specific gene expression in the context of vascular inflammation would be crucial for better understanding of atherosclerosis pathogenesis.

According to the most recent data, cell type-specific responses are mediated by a hierarchical collaboration between cell type-specific LDTF which have an ability to bind cognate sequences in the context of closed chromatin and subsequently recruited SDTF in stimuli-dependent manner. Indeed, it was shown that MΦ-specific transcriptional responses are widely regulated by cell type specific LDTF, like PU.1 and IRF8, directing IFNγ-induced STAT and IRF to their genome-wide cognate binding sites in a cell type-specific manner to activate gene expression (Platanitis and Decker 2018). It is tempting to speculate that a similar mechanism could underlie VSMC-unique gene expression in response to pro-inflammatory cues, yet this concept was not examined before. It may be caused by a challenging identification of an exclusive LDTF crucial for VSMC differentiation and maturation (Owens et al. 2004).

Therefore the aim of this study was to characterize the mechanism of cell type-specific IFNγ-dependent gene expression in VSMC as compared to MΦ. We hypothesized that unknown VSMC-unique LDTF would be bound to the regions of condensed chromatin and initiate its relaxation to allow subsequent IFNγ-dependent STAT1 recruitment in cell type-specific manner. Identification of VSMC-specific master regulator and the mechanism driving cell type-specific gene expression in the context of vascular inflammation could help to develop new therapeutic strategies, which could precisely target unbalanced cell type-specific transcriptional responses.

Material and Methods

Primary VSMC, MΦ and DC isolation

Mice. WT mice strain background C57BL/6 were obtained from Charles River Laboratories. Euthanasia performed by cervical dislocation under isoflurane anaesthesia, preceded aortas and bones (femur and tibia) isolation. All the animal experimental procedures were carried out in accordance with good animal practice and applicable local law. Any medical ethical approval was necessary for tissue isolation procedures.

Detailed information regarding primary VSMC, MΦ and DC isolation procedure and cell culture protocol is available in Material and Methods section, Chapter 2.

In short, after 24 hour starvation in 2% (10500-064, TFS) DMEM medium (11, IITD PAN Wrocław), VSMC, MΦ and DC were treated with IFNγ (PMC4031, TFS) for 8 hours. Described treatment strategy was applied in RNA-seq and ChIP-seq experiments presented in Chapter 4.

RNA-seq experimental procedure and data analysis

Detailed information regarding RNA-seq experiment performed in VSMC, MΦ and DC treated with IFNγ with general in silico data analysis is available in Material and Methods section, Chapter 2.

BioVenn web tool (Hulsen et al. 2008) was used to generate Venn diagram illustrating an overlap between IFNγ(8h)-dependent up-regulated gene (FC≥2) lists resulting from RNA-seq differential gene expression analysis in VSMC, MΦ and DC.

Before subsequent analysis, IFNγ(8h)-up-regulated unique genes in VSMC (266 genes) and MΦ (982 genes) were filtered in two steps procedure. First, cut-off FC≥3 was applied in VSMC (result: 111 genes) and MΦ (result: 435 genes) gene lists. Second, these lists were filtered according to the expression in the opposite cell type: FC<2 and FC>-2. Finally two gene lists were obtained, for VSMC (81 genes) and MΦ (417 genes), which were subjected for further analysis.

Promoter analysis - all TF profiles

In silico promoter analysis were performed to anticipate on the potential STAT1-collaborating TF involved in the regulation of the cell type-specific gene expression in VSMC or MΦ. Four gene lists were subjected for the analysis in oPPOSUM web-based system (Kwon et al. 2012): IFNγ-dependent VSMC-specific group of genes (9 genes, Table 4.4) and MΦ-specific group

of genes (10 genes, Table 4.5) as well as expressed in the control VSMC-specific group of genes (892 genes, Fig.4.2) and MΦ-specific group of genes (531 genes, Fig.4.2). All JASPAR Core Profiles and JASPAR PBM Profiles were re-mapped for the four gene lists within the region of 10 000bp upstream/5000bp downstream from the nearest gene TSS. Conservation cut-off: 0.4 and matrix threshold: ≥ 0.85 were applied. Finally, from the lists of enriched TF, there were selected the ones which were uniquely expressed (Raw values in Control <50 RPKM) in MΦ or VSMC (Table 4.1 and Table 4.6).

Promoter analysis - STAT1 binding sites

In order to predict enrichment of the potential STAT1 (GAS and/or ISRE) binding sites within the regulatory regions of uniquely up-regulated genes in VSMC or MΦ, *in silico* promoter analysis were performed. Filtered list of uniquely up-regulated genes (FC≥3 in one cell type [VSMC or MΦ]; FC<2 and FC>-2 in the other cell type [MΦ or VSMC, respectively]) in VSMC (81 genes) and MΦ (417 genes) in response to stimulation with IFNγ(8h) resulting from RNA-seq experiment were used. Employing oPPOSUM web-based system (Kwon et al. 2012), Single Site Analysis were performed examining either GAS (matrix: STAT1, JASPAR CORE Profiles) or ISRE (matrix: Isgf3g_1, JASPAR PBM Profiles) motif enrichment within the region of 10 000bp upstream/5000bp downstream from the nearest gene TSS. Conservation cut-off: 0.4 and matrix threshold: ≥ 0.85 were applied during the promoter analysis.

Chromatin Immunoprecipitation (ChIP)-seq experimental procedure and data analysis

Detailed description of STAT1 ChIP-seq experiment performed in WT VSMC treated with IFNγ with general in silico data analysis is available in Material and Methods section, Chapter 2.

The closest gene for each STAT1 ChIP-seq peak and its genomic location (promoter and other region) presented in Figure 4.3C was identified using annotatePeaks.pl (HOMER).

Additionally, in Chapter 4 there were used the following external ChIP-seq datasets to perform peak visualisation in IGV Genome Browser: GSE115435 (MΦ untreated/IFNγ(1.5h) treated); GSE112417 (VSMC untreated H3K27Ac, VSMC untreated H4K4me3); GSE113226 (MΦ untreated H3K27Ac); GSE91009 (MΦ untreated PU.1).

Results

Genome-wide transcriptome (RNA-seq) comparative analysis between gene expression profiles induced in VSMC, MΦ and DC in response to pro-inflammatory IFNγ (8h), revealed cell type-specific differences. As such, IFNγ stimulation resulted in elevated expression of 752, 1630 and 437 genes in VSMC, MΦ and DC, respectively. Among these up-regulated genes, 266, 982 and 34 were expressed in VSMC-, MΦ- and DC-specific manner, respectively (Fig.4.1). Clearly, DC-specific response to type II IFN seems to be marginal as compared to VSMC- or MΦ-unique transcriptional response. Therefore, further analysis focused on the characterization of the regulatory mechanism underlying VSMC-specific transcriptional response to the pro-inflammatory stimuli IFNγ, as compared to the mechanism regulating MΦ-unique gene expression.

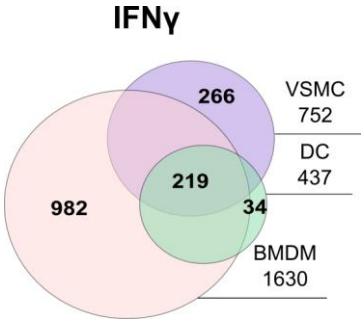

Figure 4. 1. Characterization of gene up-regulation patterns in vascular and immune cells in response to IFNγ.

Venn diagram presenting overlap between the lists of up-regulated genes (FC≥2) in response to IFNγ(8h) in VSMC (violet circle), MΦ (pink circle) and DC (green circle) resulting from RNA-seq.

Cell type-specific identity is pre-determined by LDTF which have an ability to mark the genome in cell type-unique manner and open chromatin fractions to be ready for binding by upcoming SDTF and to finally regulate cell type-specific gene expression (Heinz and Glass 2012). Thus, taking into consideration the fact that cell type-specific identity is pre-determined by LDTF before cell exposition to the external stimuli, all the genes which presented basal gene expression (raw counts, RPKM>20) in untreated VSMC and MΦ were filtered out. There were identified 892 genes uniquely expressed in VSMC, 531 genes uniquely expressed in MΦ and 9938 genes which presented common basal gene expression in immune and vascular untreated cells (Fig.4.2). Next we aimed to identify potential LDTF which could mediate MΦ- or VSMC-unique gene expression. For that, the lists of 531 MΦ- and 892 VSMC-specific basal genes were used to perform genome-wide *in silico* distal

promoter analysis. Since most of the cell type-specific TF assembly was shown to occur at distally located enhancers from gene TSS, 10 000bp upstream and 5000bp downstream region was analyzed. From the resulting lists of enriched TF, there were selected uniquely expressed TF either in MΦ or VSMC. In case of the former cell type, there were identified 3 potential LDTF: PU.1, NFATc2 and CEBP (Fig.4.2, Table 4.1). In case of VSMC, analogical analysis resulted in identification of 9 potential LDTF: Gata6, Tead1, Zeb1, Glis2, Nr2f2, Sox12, Foxa2, Sox9, and Hoxa5 (Fig.4.2, Table 4.1). Table 4.1 offers an insight into the detailed characteristics of the identified potential LDTF. Among 3 identified MΦ-specific TF, PU.1 showed the highest basal gene expression in MΦ (9369,7 RPKM), as well as statistical significance reflected by Z-score and Fisher score (35,1 and 8,4, respectively). Yet the highest number of target gene hits was identified for NFATc2 (380 genes). On the other hand, in case of VSMC-specific TF, Gata6 presented the highest basal gene expression (3933,6 RPKM). Remarkably, this result did not correlate with the topmost target gene hits and Z-score or Fisher score. Abovementioned parameters took the highest values in case of Hoxa5 (Table 4.1). Thus this data suggest a few potential LDTF, yet does not clearly indicate which of them could be the strongest candidate for either MΦ- or VSMC-specific LDTF.

Finally, we hypothesised that any of the recognized potential LDTF candidates in MΦ and VSMC, could be recruited to the regions of condensed chromatin in a cell type-specific manner to open the chromatin and together with IFNγ-activated STAT1 drive cell type-specific gene expression (Fig.4.2).

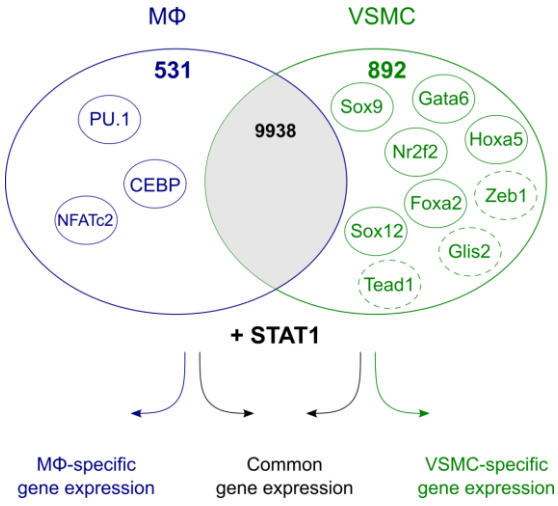

Figure 4. 2. Genome-wide prediction of potential cell type-specific LDTF and their role in common and unique gene expression.

Promoter analysis of gene showing unique basal gene expression (raw counts, RPKM>20) in MΦ resulting from RNA-seq (531 genes) predicted PU.1, CEBP and NFATc2 as potential MΦ LDTF.

Promoter analysis of gene showing unique basal gene expression (raw counts, RPKM>20) in VSMC resulting from RNA-seq (892 genes) predicted Gata6, Nr2f2, Sox12, Foxa2, Sox9, Hoxa5, Zeb1, Glis2 and Tead1 as potential VSMC LDTF (TF marked by a dashed line were not enriched anymore in the subsequent promoter analysis depicted in Table 4.5). In proposed model, cell type-specific TF establish regions of an open chromatin, which upon activation of SDTF by external cues (like IFNγ-dependent STAT1) activate common by also cell type-specific gene expression patterns.

Table 4. 1. Genome-wide *in silico* promoter analysis-based prediction of potential MΦ- and VSMC-specific LDTF.

TF name		Raw value in control [RPKM]		Target gene hits	Z-score	Fisher score
		MΦ	VSMC			
MΦ-specific	**PU.1**	9369,7	28,3	363	35,1	8,4
	NFATc2	3538,0	44,2	380	-8,4	0,7
	CEBP	1478,6	3,0	196	-5,4	0,1
VSMC-specific	**Gata6**	3,2	3933,6	382	3,9	36,6
	Tead1	4,0	2455,2	444	22,4	83,0
	Zeb1	43,1	1747,8	845	-2,8	84,0
	Glis2	13,6	1681,3	234	9,0	42,4
	Nr2f2	1,2	1323,9	410	8,3	37,8
	Sox12	5,0	1203,9	340	2,3	34,9
	Foxa2	1,4	1166,6	465	-0,5	47,3
	Sox9	2,0	1051,9	726	14,0	70,1
	Hoxa5	5,7	910,0	855	25,5	71,4

Raw counts (Control) are presented as RPKM values in MΦ and VSMC.

In order to verify this hypothesis, the lists of uniquely activated genes in VSMC and MΦ in response to IFNγ (resulting from RNA-seq) (Fig.4.1) were used for further analysis. Initially, gene lists of VSMC- and MΦ-uniquely up-regulated genes by IFNγ, underwent the double step filtering. First, the list of 266 VSMC- and 982 MΦ-specific genes were filtered by the FC value, with an applied cut-off FC≥3. Second, the two gene lists resulting from the previous filtering step were subsequently filtered according to the FC value in the opposite cell type, cut-off FC<2 and FC>-2. This step resulted in elimination of the oppositely regulated genes in one cell type as compared to the other (f.ex. gene up-regulated in VSMC and down-regulated in MΦ). Finally, the filtering procedure resulted in generation of the two gene lists, 81 VSMC-specific genes and 417 MΦ-specific genes. Top 30 genes from VSMC-uniquely IFNγ up-regulated genes are presented in Table 4.2, while 30 the most up-regulated MΦ-unique genes upon IFNγ are listed in Table 4.3. Table 4.2 and 4.3 present gene lists with ascribed FC values together with raw counts after IFNγ treatment in VSMC and MΦ resulting from RNA-seq.

Table 4. 2. Representative top-30 genes uniquely up-regulated (FC≥3 in VSMC; FC<2 and FC>-2 in MΦ) by IFNγ in VSMC.

No	Gene name	IFNγ FC		VSMC Raw values		MΦ Raw values	
		VSMC	MΦ	Control	IFNγ	Control	IFNγ
1	**Gm6654**	270,6	-1,1	570,4	670,3	359,9	221,6
2	**Chl1**	46,6	1,4	3,8	95,1	0,0	1,4
3	**Mpeg1**	34,3	1,4	297,0	7206,0	116488,4	114029,2
4	**H2-Eb1**	16,9	2,0	101,7	1218,2	5975,5	8281,3
5	**Neurl3**	15,8	-1,5	18,3	205,3	4598,0	2122,2
6	**Batf3**	15,4	1,1	2,8	34,2	75,0	59,5
7	**Tmtc1**	11,8	-1,1	82,1	683,6	1,2	0,0
8	**Ikzf4**	11,7	1,1	25,8	213,0	1,0	1,0
9	**Mt3**	9,3	1,1	1,6	11,3	1,0	1,0
10	**Trim5**	9,2	1,9	38,7	251,2	274,8	372,7
11	**Lmo2**	8,2	-1,5	3,5	23,3	2781,0	1335,8
12	**Pla1a**	7,3	1,7	9,3	48,3	1,3	2,0
13	**Ccr1**	7,2	-1,9	9,7	49,6	486,5	184,3
14	**Mreg**	6,7	1,8	24,9	118,3	10,1	12,5
15	**Csf2rb2**	6,0	1,9	33,9	145,4	5904,9	7938,2
16	**Nuak2**	5,7	1,9	38,7	155,1	757,6	1025,8
17	**H2-Q2**	5,3	2,0	16,1	60,9	256,1	357,7
18	**Gm9574**	5,2	2,0	18,9	70,1	320,5	440,7
19	**H2-M3**	5,1	1,7	137,5	500,1	804,4	940,0
20	**H2-Q7**	4,9	1,8	76,6	263,6	1488,1	1876,3
21	**Cnr2**	4,8	1,2	1,0	67,0	1164,2	956,4
22	**Greb1l**	4,8	-1,7	283,7	961,8	2,4	1,0
23	**Rab19**	4,7	1,9	5,1	17,1	196,5	256,1
24	**Xdh**	4,7	1,3	5349,8	17861,9	4923,1	4397,4
25	**H2-Q5**	4,7	1,9	53,9	178,0	870,5	1189,4
26	**H2-Q10**	4,5	1,9	48,4	154,6	773,3	1023,2
27	**Ptpn18**	4,5	-1,3	3,0	11,0	1489,9	800,3
28	**9930023K05Rik**	4,4	-1,0	1,2	9,1	1,0	0,0
29	**H2-K2**	4,4	1,9	58,4	181,6	514,4	701,5
30	**H2-Q1**	4,4	1,9	81,2	251,8	1505,6	1966,7

Gene expression levels were presented as FC (IFNγ[8h]) relative to control in VSMC and MΦ. Raw counts (Control, IFNγ[8h]) are presented as RPKM values in VSMC and MΦ.

Table 4. 3. Representative top-30 genes uniquely up-regulated (FC≥3 in МΦ; FC<2 and FC>-2 in VSMC) by IFNγ in МΦ.

No	Gene name	IFNγ FC		МΦ Raw values		VSMC Raw values	
		МΦ	VSMC	Control	IFNγ	Control	IFNγ
1	**Clvs1**	333,8	1,1	0,0	282,1	83,8	66,4
2	**Lhx2**	190,5	1,0	5,7	773,0	17,2	12,3
3	**Slc4a11**	64,7	-1,1	5,5	257,1	45,5	28,1
4	**Kdr**	59,3	-1,5	57,8	2409,8	491,2	227,0
5	**Prrg4**	40,8	1,5	5,9	169,6	86,2	92,3
6	**Tnfaip8l3**	35,3	1,2	1,4	33,1	4,1	4,6
7	**Kalrn**	33,9	-1,2	4,2	102,5	326,8	198,6
8	**Vcan**	31,2	1,4	109,3	2394,4	6667,4	6502,3
9	**Akap2**	25,8	1,5	7,4	134,7	3349,1	3547,0
10	**Gm20459**	24,1	1,5	8,4	141,8	3515,2	3723,8
11	**Spsb1**	22,4	1,9	11,3	178,1	228,1	302,8
12	**Bcl2a1b**	21,6	-1,1	70,2	1063,5	16,2	10,6
13	**Mycl1**	19,3	1,0	33,2	451,2	23,1	17,0
14	**Gm20547**	19,2	1,8	219,8	2961,0	787,4	1013,6
15	**Hbegf**	19,2	-2,0	6,8	90,9	413,4	146,5
16	**Csf1**	19,1	-1,1	53,1	712,0	5270,7	3450,3
17	**Slc2a6**	18,8	1,0	766,5	10144,4	135,5	96,5
18	**Bcl2a1c**	18,3	1,1	2,0	30,1	1,9	5,6
19	**Rap1gap2**	18,2	1,4	45,9	585,4	177,2	172,8
20	**Stk39**	18,2	1,0	3,3	43,1	570,4	405,3
21	**Tmtc2**	17,5	-1,6	36,5	448,8	177,7	79,5
22	**Armcx6**	16,9	-1,1	60,6	718,4	214,7	143,6
23	**Ifnb1**	16,6	-1,0	2,0	15,1	1,4	0,0
24	**Arhgef3**	16,1	1,0	282,1	3197,6	495,7	359,8
25	**G530011O06Rik**	16,0	1,2	55,6	626,3	6,7	5,9
26	**Procr**	15,3	1,1	390,1	4188,5	623,3	469,2
27	**Bcl2a1a**	15,0	-1,1	47,2	497,6	12,4	5,4
28	**Ccl5**	14,9	1,7	583,3	6100,9	152,4	178,7
29	**Trp53i11**	14,6	-1,4	7,4	75,5	104,4	52,2
30	**Plagl1**	14,0	-1,6	2,6	26,7	2,7	1,7

Gene expression levels were presented as FC (IFNγ[8h]) relative to control in МΦ and VSMC. Raw counts (Control, IFNγ[8h]) are presented as RPKM values in МΦ and VSMC.

Since it was widely proved that IFNγ-dependent gene expression is mainly driven by STAT1, the regulatory regions of IFNγ-dependent 81 VSMC-specific and 417 МΦ-specific genes were analyzed for the presence of potential STAT1 binding sites. GAS and ISRE motifs enrichment was estimated within the region of 10 000 bp upstream and 5000bp downstream to the nearest gene TSS. Relatively long distance selected for this analysis was motivated by

the fact, that cell type-specific gene expression is coordinated by concerted action of the proximal promoters together with the multiple distal *cis*-regulatory modules located up to hundreds of bases from gene TSS (Spitz and Furlong 2012). Therefore we could anticipate that STAT1 binding sites present in the regulatory regions of VSMC- and MΦ-specific genes would not be limited to the proximal promoter gene region. Figure 4.3A-B shows the predicted representation of individual or combinations of ISRE and GAS binding sites in the regulatory regions of VSMC- and MΦ-specific genes. Thus, there were identified 16 and 2 solitary GAS and ISRE sites, respectively, and 8 GAS-ISRE combined motifs in the regulatory regions of 81 VSMC-uniquely expressed genes (Fig.4.3A). Similar distribution of STAT1 binding motifs was identified in the list of MΦ-specific genes. Alike most of the genes contained a solitary GAS site (153 genes), a combination of GAS-ISRE sites was predicted for 66 genes, while only 25 genes had a single ISRE motif (Fig.4.3B). Low number of the genes containing a single ISRE binding site and moderate overlap between GAS and ISRE motifs within the regulatory regions of cell type-specific genes may suggest that STAT1 involved in regulation of VSMC- and MΦ-unique gene expression may be predominantly recruited in a form of GAF homodimer, as compared to ISGF3 complex. *In silico* promoter analysis which predicted potential involvement of STAT1 in the transcriptional regulation of IFNγ-dependent VSMC- and MΦ-specific responses (Fig.4.3A-B) was further corroborated by the analysis of the genome-wide recruitment of STAT1 (ChIP-seq) to the regulatory regions of VSMC-unique genes in response to IFNγ. Figure 4.3C shows, that out of 81 IFNγ-driven VSMC-specific genes resulting from RNA-seq experiment, 51 gene regulatory regions were STAT1-occupied upon treatment with IFNγ in our ChIP-seq experiment. 36 genes were STAT1-bound in the promoter region, while 15 genes outside this genomic region. Therefore the results of *in vitro* experiment exceeded *in silico* promoter prediction and confirmed involvement of STAT1 in VSMC-specific IFNγ-dependent gene expression regulation.

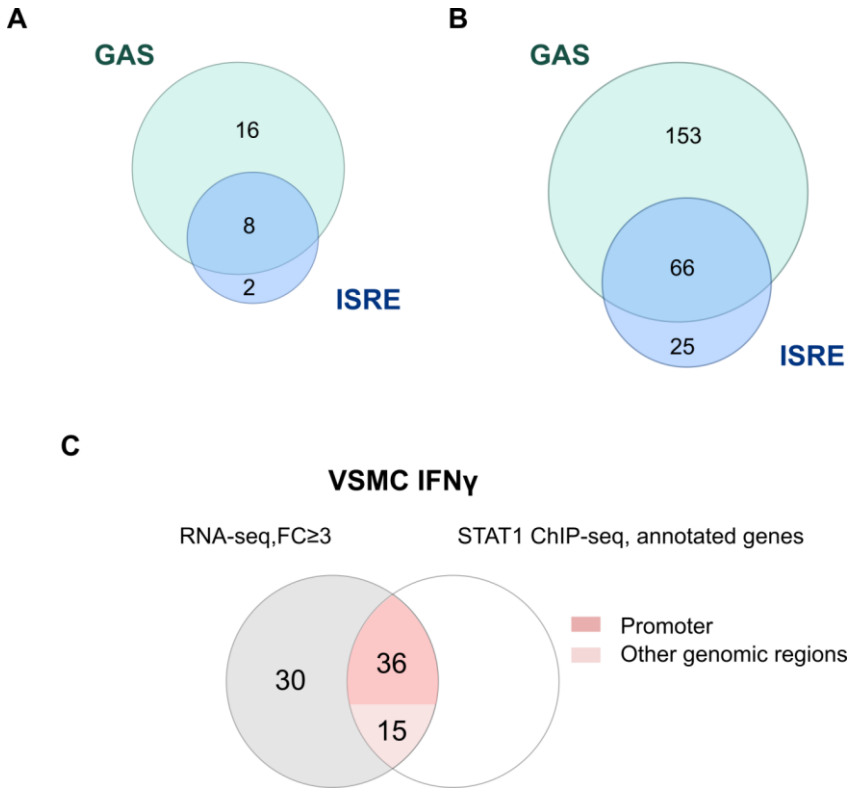

Figure 4. 3. STAT1 enrichment analysis of uniquely up-regulated genes by IFNγ in VSMC and MΦ.

Venn diagrams presenting distribution of GAS and ISRE binding sites (-10 000bp/+5000bp) among **(A)** 81 uniquely up-regulated genes in VSMC by IFNγ(8h) resulting from RNA-seq. **(B)** 417 uniquely up-regulated genes in MΦ by IFNγ(8h) resulting from RNA-seq **(C)** Venn diagram presenting uniquely up-regulated genes in VSMC by IFNγ(8h) annotated to STAT1-occupied (pink color) and not occupied (grey color) regions resulting from ChIP-seq in VSMC stimulated with IFNγ(8h). Dark pink refers to STAT1-occupied promoter regions, while light pink refers to the other genomic regions bound by STAT1.

In the attempt to elucidate how STAT1 could mediate cell type-specific gene expression, we analyzed STAT1 binding pattern upon stimulation with IFNγ to the regulatory regions of VSMC-uniquely expressed genes. IGV screen shots examination resulted in identification of 22 VSMC-specific genes which were uniquely bound by STAT1 in VSMC and not bound by STAT1 in MΦ (MΦ external dataset source: GSE115435) upon stimulation with IFNγ (Fig.4.4 and Fig.4.5). According to the current literature view, TF binding is determined mainly by the chromatin state, which if 'opened' allows for TF binding at the current biological context (Heinz and Glass 2012). This idea could also explain TF recruitment in cell type-specific manner, like it was observed in our experiment. Therefore, next we intended to determine the chromatin state of 22 VSMC-unique STAT1-bound genes.

H3K27Ac histone mark is widely associated with gene transcriptional activation and chromatin accessibility (Creyghton et al. 2010). As such, H3K27Ac enrichment was analyzed for abovementioned 22 genes both in VSMC and MΦ untreated cells (VSMC and MΦ external dataset source: GSE112417, GSE113226). Additionally, H4K4me3 histone positive mark was analyzed in untreated VSMC (VSMC external dataset source: GSE112417), which in general resembled the pattern of the positive histone acetylation mark. Strikingly, in case of 13 genes: *Neurl3*, *Batf3*, *H2-M3*, *Tmem106a*, *Adc*, *Slc26a2*, *Runx1*, *Txnip*, *Fmnl1*, *Trib3*, *Tlr2*, *Inpp5d* and *Rbm47*, H3K27Ac was enriched in both cell types, what suggested an 'open' chromatin state not only in VSMC, but also in MΦ (Fig.4.4). In contrast, in case of 9 genes: *Tmtc1*, *Ikzf4*, *Pla1a*, *Mreg*, *Greb1l*, *Has1*, *Nsg1*, *Nav3*, *Vegfc*, H3K27Ac enrichment could be observed just in case of VSMC, while not in MΦ (Fig.4.5). Hence these results clearly imply, that two described gene groups are regulated by two distinct STAT1-dependent mechanisms. Table 4.4 summarizes information collected for the two VSMC-specific gene groups, depicting gene FC values upon stimulation with IFNγ in VSMC and MΦ (RNA-seq) as well as raw values in control and IFNγ in VSMC and MΦ (RNA-seq), STAT1 binding pattern and chromatin state characterization (ChIP-seq). Remarkably, there is visible an evident difference in the basal gene expression levels (RPKM) between Group 1 and 2 gene representatives (Table 4.4). Although Group 1 gene examples showed lack of gene expression upon stimulation with IFNγ in MΦ as compared to VSMC (FC≥3), the basal gene expression levels were detected in both cell types. It suggests that this group of genes is not 'turned off' in MΦ, but rather not responsive to IFNγ in the STAT1-dependent manner. In striking contrast, Group 2 gene representatives showed lack of gene expression upon stimulation with IFNγ in MΦ as compared to VSMC (FC≥3), what correlated with no basal gene expression levels in MΦ, while high basal gene expression in VSMC. Hence, second group of genes is clearly VSMC-specific and not dedicated for an activation in MΦ. The difference between Group 1 and Group 2 basal gene expression levels in VSMC and MΦ, correlated with the state of the chromatin, which was opened in both cell types or just in VSMC, respectively (Table 4.4; Fig.4.4; Fig.4.5).

Together, we propose that in case of Group 1, although the chromatin is opened in both cell types, IFNγ-dependent VSMC-specific gene expression is mediated by STAT1 in cell type-specific manner. In case of Group 2, in untreated cells chromatin is closed in MQ, but opened in VSMC, which mechanism allow for IFNγ-dependent STAT1 recruitment in VSMC and subsequent gene expression in VSMC-specific manner.

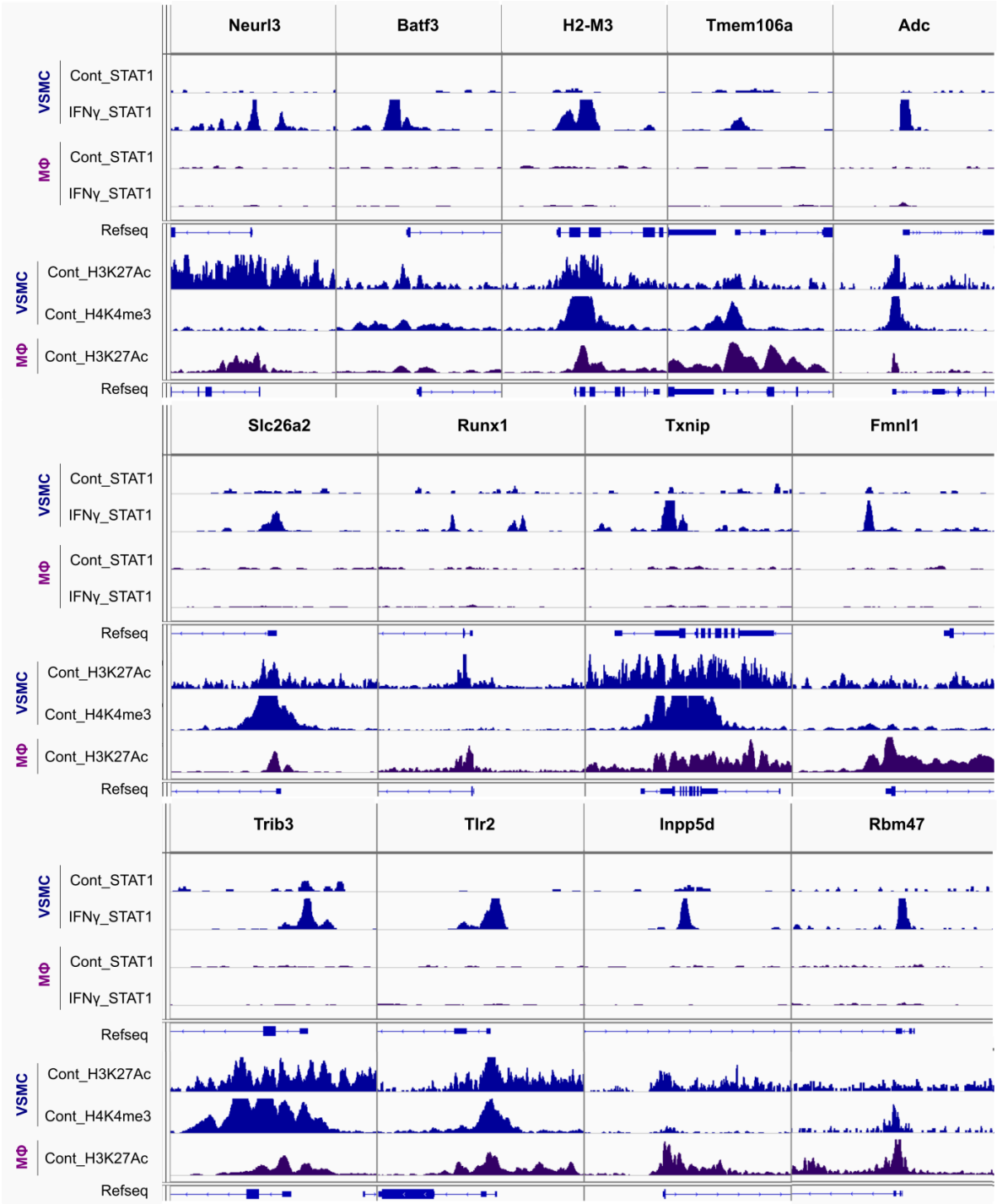

Figure 4. 4. STAT1 and histone marks enrichment pattern for uniquely IFNγ up-regulated genes in VSMC (Group 1).

Representative views of STAT1 ChIP-seq peaks identified in the regulatory regions of *Neurl3*, *Batf3*, *H2-M3*, *Tmem106a*, *Adc*, *Slc26a2*, *Runx1*, *Txnip*, *Fmnl1*, *Trib3*, *Tlr2*, *Inpp5d* and *Rbm47* in untreated or IFNγ(8h)-stimulated VSMC (blue peaks) and untreated or IFNγ(1.5h)-stimulated MΦ (violet peaks). Below, representative views of H3K27Ac (VSMC and MΦ) and H4K4me3 (VSMC) ChIP-seq peaks identified in the regulatory regions of the same genes in untreated VSMC (blue peaks) and MΦ (violet peaks). STAT1- or histone marks-binding peaks were mapped onto the mouse reference genome mm10 or mm9, respectively and visualized using the IGV genome browser.

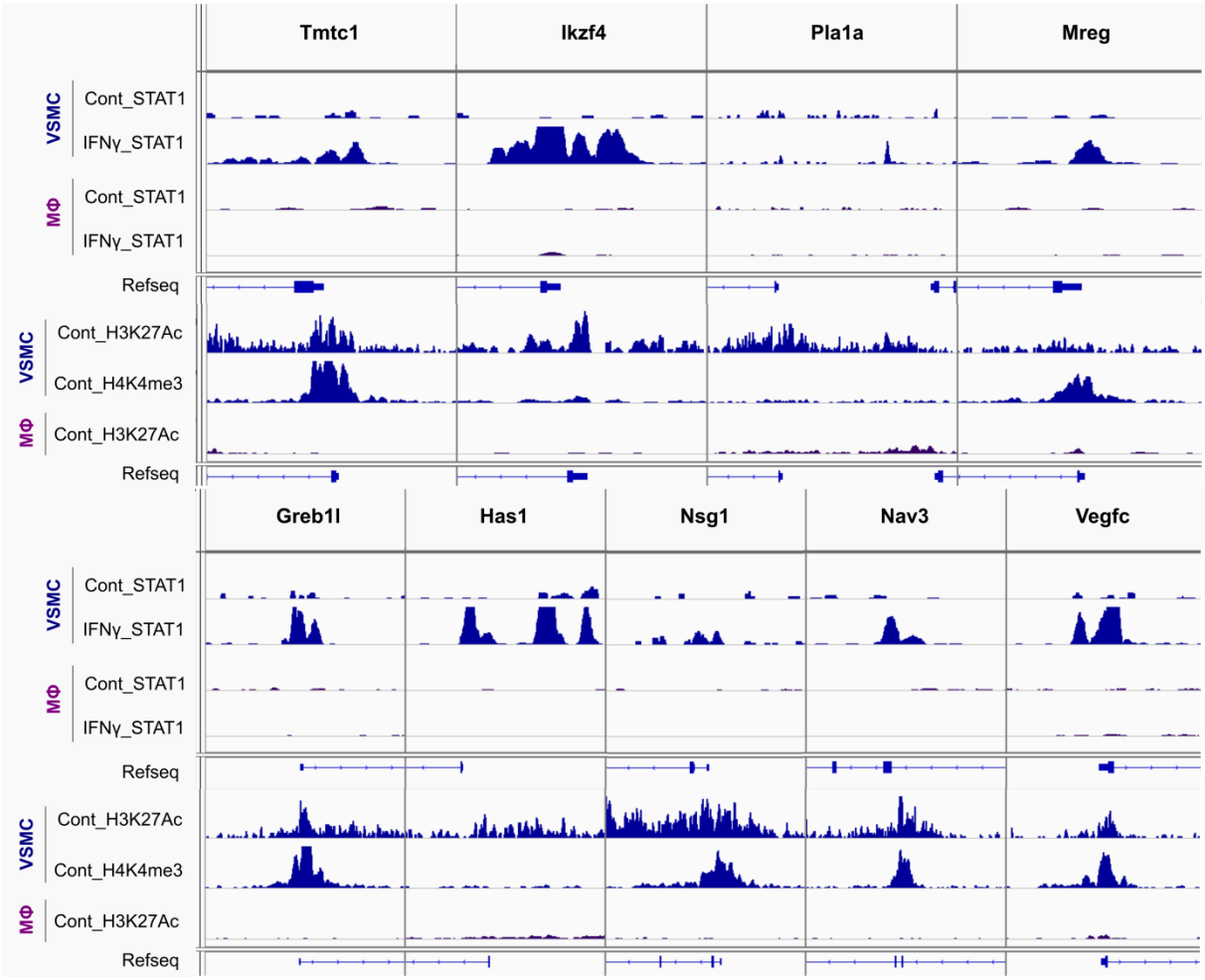

Figure 4. 5. STAT1 and histone marks enrichment pattern for uniquely IFNγ up-regulated genes in VSMC (Group 2).

Representative views of STAT1 ChIP-seq peaks identified in the regulatory regions of *Tmtc1*, *Ikzf4*, *Pla1a*, *Mreg*, *Greb1l*, *Has1*, *Nsg1*, *Nav3* and *Vegfc* in untreated or IFNγ(8h)-stimulated VSMC (blue peaks) and untreated or IFNγ(1.5h)-stimulated MΦ (violet peaks). Below, representative views of H3K27Ac (VSMC and MΦ) and H4K4me3 (VSMC) ChIP-seq peaks identified in the regulatory regions of the same genes in untreated VSMC (blue peaks) and MΦ (violet peaks). STAT1- and histone marks-binding peaks were mapped onto the mouse reference genome mm10 or mm9, respectively and visualized using the IGV genome browser.

Table 4. 4. Characteristics summary of 22 uniquley IFNγ up-regulated gene representatives in VSMC.

	Gene name	IFNγ FC		VSMC Raw values		MΦ Raw values		STAT1 binding				H3K27Ac		PU.1 binding	
		VSMC	MΦ	Control	IFNγ	Control	IFNγ	VSMC	MΦ	GAS	ISRE	VSMC	MΦ	MΦ	PU-box
Group 1	Neurl3	15,8	-1,5	18,3	205,3	4598,0	2122,2	+	-	•	•	+	+	+	•
	Batf3	15,4	1,1	2,8	34,2	75,0	59,5	+	-	•	-	+	+	+	•
	H2-M3	5,1	1,7	137,5	500,1	804,4	940,0	+	-	-	•	+	+	+	•
	Tmem106a	4,0	1,1	174,6	499,0	7509,7	5650,6	+	-	-	•	+	+	+	•
	Adc	4,0	1,9	223,8	627,9	26,8	35,7	+	-	•	-	+	+	+	•
	Slc26a2	3,8	1,4	960,9	2604,0	1345,9	1277,6	+	-	•	-	+	+	+	-
	Runx1	3,6	-1,1	144,1	367,2	2177,3	1361,3	+	-	•	-	+	+	+	•
	Txnip	3,6	-1,2	1057,5	2673,1	14777,5	8344,0	+	-	•	-	+	+	+	•
	Fmnl1	3,6	-1,3	15,7	39,7	7416,0	3969,0	+	-	•	-	+	+	+	•
	Trib3	3,4	1,8	198,1	480,9	43,0	53,9	+	-	•	-	+	+	+	•
	Tlr2	3,2	-1,2	160,7	369,0	2489,1	1466,3	+	-	•	•	+	+	+	•
	Inpp5d	3,1	-1,3	8,7	19,2	5825,1	3160,4	+	-	•	-	+	+	+	•
	Rbm47	3,0	1,4	66,1	141,0	1503,7	1480,0	+	-	•	-	+	+	+	•
Group 2	Tmtc1	11,8	-1,1	82,1	683,6	1,2	0,0	+	-	•	-	+	-	-	-
	Ikzf4	11,7	1,1	25,8	213,0	1,0	1,0	+	-	•	-	+	-	-	-
	Pla1a	7,3	1,7	9,3	48,3	1,3	2,0	+	-	•	-	+	-	+	•
	Mreg	6,7	1,8	24,9	118,3	10,1	12,5	+	-	•	-	+	-	+	•
	Greb1l	4,8	-1,7	283,7	961,8	2,4	1,0	+	-	•	-	+	-	-	-
	Has1	4,4	-1,0	169,2	524,5	1,0	0,0	+	-	•	-	+	-	-	-
	Nsg1	3,5	1,7	717,6	1760,8	7,0	8,6	+	-	•	-	+	-	-	-
	Nav3	3,3	-1,0	41,3	97,4	1,0	0,0	+	-	•	•	+	-	-	-
	Vegfc	3,0	1,5	173,5	367,8	13,0	13,5	+	-	•	-	+	-	-	-

Gene expression levels were presented as FC (IFNγ[8h]) relative to control in VSMC. Raw counts (Control, IFNγ[8h]) were presented as RPKM values in VSMC and MΦ. STAT1 recruitment in VSMC and MΦ to listed gene promoters was marked by a plus (+). Presence of GAS or ISRE binding sites in the promoters of listed genes was indicated by a dot (•). H3K27Ac enrichment in VSMC and MΦ in listed gene promoters was marked by a plus (+). PU.1 recruitment in MΦ to listed gene promoters was marked by a plus (+). Presence of PU-box binding site in the promoters of listed genes was indicated by a dot (•).

Further, we aimed to study if an analogous gene group as Group 2 in VSMC, could be identified among MΦ-specific genes. This finding would support an idea that STAT1 involvement in cell type-specific gene expression stands for a more universal mechanism. Since the idea of LDTF-SDTF collaboration in the context of MΦ-specific gene expression was widely reported before, similar mechanism could be extrapolated and used to explain VSMC-specific response. Indeed, among 417 IFNγ-dependent MΦ-unique genes there were identified 10 genes (*Cacng8*, *Creb5*, *AB124611*, *Ikzf1*, *Aoah*, *Gna15*, *Tnfsf8*, *Slamf7*, *Ms4a6c*, *Adap2*) which were uniquely bound by STAT1 in MΦ, but not in VSMC (Fig.4.6). Additionally, all these genes presented open chromatin state in MΦ, but not in VSMC, reflected by enriched H3K27Ac mark in immune cells (Fig.4.6). All the information collected during analysis of this gene group is presented in Table 4.5. Alike VSMC-specific gene Group 2 (Table 4.4), in case of 10 MΦ-specific genes, closed chromatin conformation in VSMC correlated with the lack of basal gene expression, in contrast to MΦ (Table 4.5).

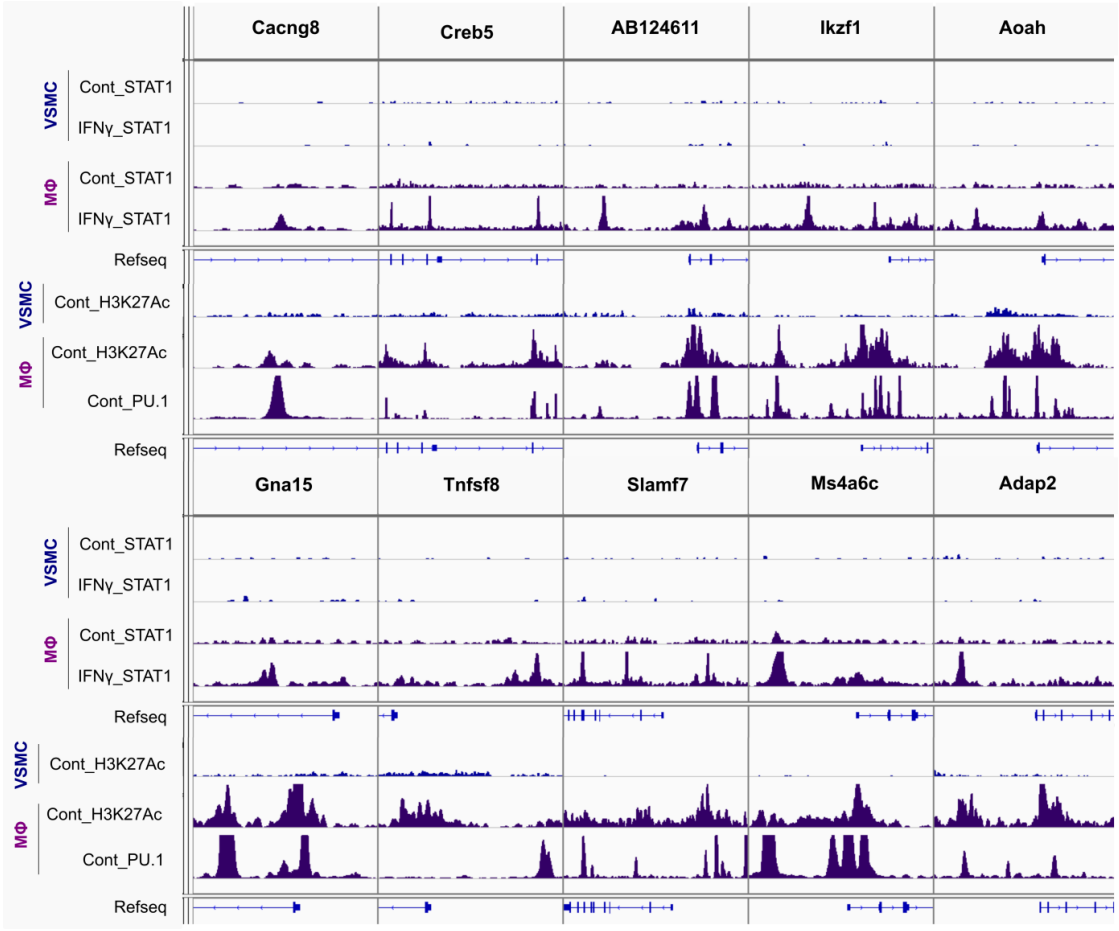

Figure 4. 6. STAT1, PU.1 and histone marks enrichment pattern for uniquely IFNγ up-regulated genes in MΦ.

Representative views of STAT1 ChIP-seq peaks identified in the regulatory regions of *Cacng8*, *Creb5*, *AB124611*, *Ikzf1*, *Aoah*, *Gna15*, *Tnfsf8*, *Slamf7*, *Ms4a6c* and *Adap2* in untreated or IFNγ(8h)-stimulated VSMC (blue peaks) and untreated or IFNγ(1.5h)-stimulated MΦ (violet peaks). Below, representative views of H3K27Ac (VSMC and MΦ) and PU.1 (MΦ) ChIP-seq peaks identified in the regulatory regions of the same genes in untreated VSMC (blue peaks) and MΦ (violet peaks). STAT1- and histone marks/PU.1-binding peaks were mapped onto the mouse reference genome mm10 or mm9, respectively and visualized using the IGV genome browser.

Table 4. 5. Characteristics summary of 10 uniquley IFNγ up-regulated gene representatives in MΦ.

Gene name	IFNγ FC		MΦ Raw values		VSMC Raw values		STAT1 binding				H3K27Ac		PU.1 binding	
	MΦ	VSMC	Control	IFNγ	Control	IFNγ	MΦ	VSMC	GAS	ISRE	MΦ	VSMC	MΦ	PU-box
Cacng8	6,3	-1,0	10,2	45,1	5,8	4,2	+	-	-	•	+	-	+	•
Creb5	6,1	1,7	160,6	686,0	4,3	11,6	+	-	•	-	+	-	+	•
AB124611	5,6	1,3	1045,1	4090,6	6,3	5,5	+	-	•	-	+	-	+	•
Ikzf1	4,5	-1,4	1867,6	5866,8	15,6	5,6	+	-	•	-	+	-	+	•
Aoah	4,2	1,5	1273,0	3772,0	8,6	12,2	+	-	•	-	+	-	+	•
Gna15	3,9	-1,0	342,5	930,8	17,8	12,6	+	-	•	-	+	-	+	•
Tnfsf8	3,8	1,1	5,3	14,1	3,1	4,0	+	-	•	-	+	-	+	•
Slamf7	3,6	1,0	1555,1	3884,9	11,4	7,6	+	-	•	•	+	-	+	•
Ms4a6c	3,1	-1,5	3257,9	7148,5	11,6	4,4	+	-	•	-	+	-	+	•
Adap2	3,1	-1,4	1136,6	2466,6	11,6	4,0	+	-	•	-	+	-	+	•

Gene expression levels were presented as FC (IFNγ[8h]) relative to control in MΦ. Raw counts (Control, IFNγ[8h]) were presented as RPKM values in MΦ and VSMC. STAT1 recruitment in MΦ

and VSMC to listed gene promoters was marked by a plus (+). Presence of GAS or ISRE binding sites in the promoters of listed genes was indicated by a dot (•). H3K27Ac enrichment in MΦ and VSMC in listed gene promoters was marked by a plus (+). PU.1 recruitment in MΦ to listed gene promoters was marked by a plus (+). Presence of PU-box binding site in the promoters of listed genes was indicated by a dot (•).

Therefore there arouse a question how STAT1 recruitment could be directed to precise genomic sites in cell type-specific manner, either in MΦ (Table 4.5) or VSMC (Table 4.4, Group 2). Multiple studies regarding cell type-specific gene expression regulation were performed in immune cells, like B cells, T cells or MΦ, but not VSMC. As mentioned before, it was reported that cell type-unique gene expression in response to external cues is mediated by collaboration between LDTF and SDTF (like IFNγ-activated STAT1). As depicted in Figure 4.2 and Table 4.1, *in silico* promoter analysis of the genes presenting basal expression in MΦ or VSMC, predicted a number of potential LDTF which could mediate cell type-specific identity. Similar analysis performed on two gene lists of 10 MΦ-specific (*Cacng8*, *Creb5*, *AB124611*, *Ikzf1*, *Aoah*, *Gna15*, *Tnfsf8*, *Slamf7*, *Ms4a6c*, *Adap2*) (Table 4.5) and 9 VSMC-specific (*Tmtc1*, *Ikzf4*, *Pla1a*, *Mreg*, *Greb1l*, *Has1*, *Nsg1*, *Nav3*, *Vegfc*) (Table 4.4, Group 2) IFNγ-activated genes corroborated the previous results. As such, from the list of enriched TF, there were selected the ones which were uniquely expressed either in MΦ or VSMC as compared to the opposite cell type. MΦ-specific gene list analysis revealed enrichment of 3 MΦ-specific TF: PU.1, CEBP and NFATc2, and 6 potential VSMC-specific TF: Gata6, Nr2f2, Sox12, Foxa2, Sox9, Hoxa5 (Table 4.6). All the potential TF were identified during previous *in silico* promoter analysis (Fig.4.2, Table 4.1). The highest basal gene expression of PU.1 in MΦ did not correlate with the highest number of target gene hits and Z-score or Fisher score values, which were ascribed to NFATc2 (Table 4.6). Alike in VSMC, the highest basal gene expression of Gata6 did not correlate with the highest number of target gene hits or statistical significance. Oppositely, binding site for Hoxa5 (910 RPKM) was found to be enriched in 9 gene promoters with Z-score value of 10 (Table 4.6).

Table 4. 6. *In silico* promoter analysis-based prediction of cell type-specific LDTF in MΦ and VSMC.

	TF name	Raw value in control [RPKM]		Target gene hits	Z-score	Fisher score
		MΦ	VSMC			
MΦ-specific	**PU.1**	9369,7	28,3	5	3,4	0,2
	NFATc2	3538,0	44,2	9	2,9	2,3
	CEBP	1478,6	3,0	5	-4,5	0,1
VSMC-specific	**Gata6**	3,2	3933,6	3	2,4	0,6
	Nr2f2	1,2	1323,9	5	5,7	2,0
	Sox12	5,0	1203,9	4	2,3	0,4
	Foxa2	1,4	1166,6	6	0,9	0,5
	Sox9	2,0	1051,9	6	5,6	0,5
	Hoxa5	5,7	910,0	9	10,0	1,3

Raw counts (Control) were presented as RPKM values in VSMC and MΦ.

Among identified potential MΦ-specific LDTF (Table 4.6), PU.1 is a known master regulator which determines MΦ cell identity, as previously reported in multiple studies (Feng et al. 2008). To verify if indeed this factor could be recruited into the regulatory regions of MΦ-uniquely expressed genes and involved in MΦ-specific gene expression, we analyzed PU.1 binding (MΦ external dataset source: GSE91009) to the regulatory regions of 10 MΦ-specific genes (Fig.4.6). Indeed, in case of all 10 MΦ-specific genes, PU.1 was pre-bound in untreated cells (Fig.4.6, Table 4.5). This result supports an idea of PU.1-dependent opening of the chromatin and subsequent STAT1 recruitment in MΦ. This scenario could not be realised for the same genes in VSMC, because these cells do not express MΦ-specific LDTF PU.1 (Table 4.6). We propose that VSMC-specific expression of gene Group 2 in VSMC (Fig.4.5, Table 4.4) could be mechanistically explained by the similar mechanism. Thus, a unknown VSMC-specific LDTF would open the chromatin in the genomic regulatory regions of VSMC-uniquely expressed genes and allow for further recruitment of STAT1 in VSMC, but not in MΦ. However, due to the lack of available ChIP-seq binding data for any of identified potential LDTF in VSMC, we could not verify recruitment of these TF to the regulatory regions of VSMC-unique genes.

As shown in Table 4.4, in case of Group 2 VSMC-specific genes, the chromatin is closed and not accessible for STAT1 in MΦ, due to lack of PU.1 recruitment. Interestingly, in case of Group 1 VSMC-specific genes (Fig.4.4, Table 4.4), open chromatin state in both cell

types, correlates with PU.1 recruitment in MΦ. It seems that in case of Group 1 genes even though PU.1 binds, it does not promote gene expression in MΦ by itself. Consequently, we asked a question how LDTF could participate in gene expression regulation of the common transcriptional targets which are activated in more than a one cell type. Figure 4.7 depicts IGV screenshots for 6 example genes commonly activated by IFNγ in MΦ and VSMC (from the list of 9938 genes, Fig.4.2). As presented, STAT1 was commonly recruited to the regulatory regions of *Irf1*, *Cxcl10*, *Gbp6*, *Gbp7*, *Igtp* and *Oas2* upon stimulation with IFNγ in both vascular and immune cells. This observation correlated with enriched H3K27Ac in both cell types. Moreover, binding of PU.1 could be detected to all 6 genes promoters in MΦ. Table 4.7 summarizes all collected information.

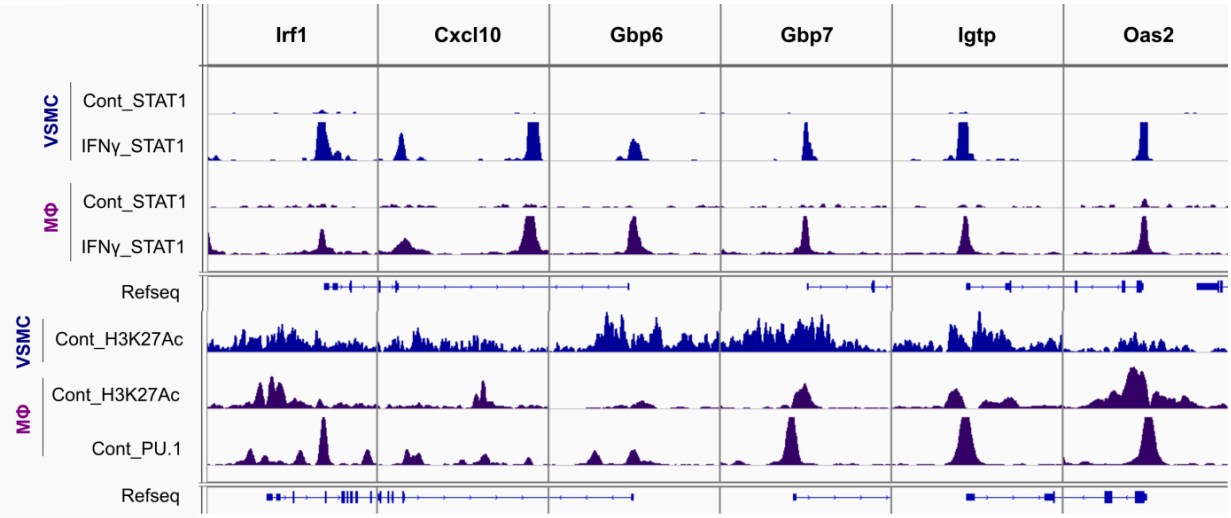

Figure 4. 7. STAT1, PU.1 and histone marks enrichment pattern for commonly IFNγ up-regulated genes in VSMC and MΦ.

Representative views of STAT1 ChIP-seq peaks identified in the regulatory regions of *Irf1*, *Cxcl10*, *Gbp6*, *Gbp7*, *Igtp* and *Oas2* in untreated or IFNγ(8h)-stimulated VSMC (blue peaks) and untreated or IFNγ(1.5h)-stimulated MΦ (violet peaks). Below, representative views of H3K27Ac (VSMC and MΦ) and PU.1 (MΦ) ChIP-seq peaks identified in the regulatory regions of the same genes in untreated VSMC (blue peaks) and MΦ (violet peaks). STAT1- and histone marks/PU.1-binding peaks were mapped onto the mouse reference genome mm10 or mm9, respectively and visualized using the IGV genome browser.

Table 4. 7. Characteristics summary of 6 commonly IFNγ up-regulated gene representatives in VSMC and MΦ.

Gene name	IFNγ FC		MΦ Raw values		VSMC Raw values		STAT1 binding				H3K27Ac		PU.1 binding	
	MΦ	VSMC	Control	IFNγ	Control	IFNγ	MΦ	VSMC	GAS	ISRE	MΦ	VSMC	MΦ	PU-box
Irf1	14,7	22,6	1584,5	16406,8	651,2	10444,2	+	+	•	-	+	+	+	•
Cxcl10	211,7	49,8	324,7	48289,1	154,3	5436,8	+	+	•	•	+	+	+	•
Gbp6	181,8	266,1	67,1	8566,5	53,8	10141,7	+	+	•	•	+	+	+	•
Gbp7	36,8	65,2	274,9	7099,4	109,0	5034,5	+	+	•	•	+	+	+	•
Igtp	36,4	328,8	732,9	18713,2	135,2	31502,3	+	+	•	•	+	+	+	•
Oas2	5,5	19,1	496,1	1927,6	23,3	315,5	+	+	-	•	+	+	+	•

Gene expression levels were presented as FC (IFNγ[8h]) relative to control in MΦ and VSMC. Raw counts (Control, IFNγ[8h]) were presented as RPKM values in MΦ and VSMC. STAT1 recruitment in MΦ and VSMC to listed gene promoters was marked by a plus (+). Presence of GAS or ISRE binding sites in the promoters of listed genes was indicated by a dot (•). H3K27Ac enrichment in MΦ and VSMC in listed gene promoters was marked by a plus (+). PU.1 recruitment in MΦ to listed gene promoters was marked by a plus (+). Presence of PU-box binding site in the promoters of listed genes was indicated by a dot (•).

Discussion

Data presented in Chapter 4 focused on the characterization of the regulatory mechanism underlying MΦ- and VSMC-specific transcriptional response to IFNγ, a potent pro-inflammatory stimuli contributing to the progression of vascular inflammation.

MΦ are phagocytic monocyte-derived cells, which fight against invading microbes by the recognition of PAMP. Moreover, they act at the border of innate and adaptive immunity, by presenting antigens to T cells. MΦ alert and protect other cells by releasing plethora of pro-inflammatory cytokines, chemokines and matrix metalloproteinases, but also participate in the processes of tissue healing and repair (Frodermann and Nahrendorf 2018, Shirai et al. 2015). However, if immune system barrier is not efficient enough, MΦ-dependent unresolved inflammation may underlie the pathophysiology of multiple diseases, like CVD (Tabas and Glass 2013). Indeed, MΦ were found in the area of atherosclerotic lesions, correlating with robust secretion of pro-inflammatory mediators, finally leading to endothelium activation, monocytes recruitment and oxidative stress (Shirai et al. 2015, Hansson and Hermansson 2011, Moore et al. 2013, Waldo et al. 2008). Moreover, MΦ excessive lipoprotein accumulation leads to cholesterol-laden foam cells formation, which form lipid lesion in the artery lumen (Yu et al. 2013). In contrast, main function of VSMC in a healthy vessel is to regulate vessel wall structure, lumen dimension, vessel tone and blood pressure. However, VSMC exposition to the pro-inflammatory cues, alter their phenotype and contribute to the pathophysiology of atherosclerosis (van Thiel et al. 2017). Synthetic VSMC identified within the atherosclerotic lesions are characterized by redundant cell proliferation and migration, but also extracellular matrix production (Lutgens et al. 2017). Moreover, VSMC are a potent source of multiple pro-inflammatory cytokines and matrix metalloproteinases, as well as VSMC-derived foam cells (Lin et al. 2008, Allahverdian et al. 2014).

Therefore, although there exists some overlap between the functions performed by both MΦ and VSMC, these two distinct cell types mostly perform cell type-specific roles, both in a healthy and inflamed vessel. Any abrogation in transcriptional activation of MΦ- or VSMC-unique transcriptional networks may contribute to alteration of cell homeostasis, and finally be a culprit for a wide range of inflammatory diseases, including CVD (Hoeksema and Glass 2019). Better understanding of the changes in MΦ- and VSMC-specific gene expression in a steady-state versus inflammatory state, could help to elucidate the molecular basis of atherosclerosis. Hence, we decided to investigate the potential regulatory mechanism

which could underlie VSMC- as compared to MΦ-unique gene expression in response to IFNγ.

According to the recent data, cell type-specific responses are shaped by a hierarchical collaboration between LDTF and SDTF. The former ones frequently display pioneering functions, thus have an ability to bind cognate sequences in cell type-specific manner, in the context of closed chromatin (Heinz et al. 2015). Therefore first, context-specific combinations of LDTF mark the genome in a cell type-unique manner, which code is further read by general sequence-specific TF (SDTF), activated among others by the pro-inflammatory stimuli, to drive gene transcriptional activation (Gosselin and Glass 2014, Phanstiel et al. 2017). Although MΦ-specific transcriptional response to inflammatory stimuli, was broadly studied and proven to be regulated by hierarchical cooperation between LDTF and SDTF, the molecular mechanism regulating VSMC-specific responses in the context of vascular inflammation remains unknown. This may be due to the challenging identification of TF playing exclusive role in VSMC differentiation, since many TF being crucial for VSMC development and cell type-specific gene expression, were found to be expressed, at least at some developmental stage, in the other cell types (Owens et al. 2004). Yet we hypothesized that a similar mechanism could drive both MΦ- and VSMC-specific transcriptional response.

In order to identify potential LDTF specific for MΦ or VSMC which could potentially drive unique transcriptional response, we performed genome-wide *in silico* distal promoter (+10 000/-5000bp) analysis of the genes presenting cell type-specific basal gene expression. Finally, it resulted in identification of 3 potential MΦ-specific factors: PU.1, C/EBP, NFATc2 and 9 potential VSMC-specific factors: Gata6, Nr2f2, Sox12, Foxa2, Sox9, Hoxa5, Zeb1, Glis2 and Tead1 (Table 4.1; Fig.4.2). Obtained results were corroborated and narrowed down by a similar analysis performed on further identified two gene lists of 10 MΦ-specific (Table 4.5) and 9 VSMC-specific (Table 4.4, Group 2) IFNγ-activated genes. There were characterized 3 potential MΦ-specific TF: PU.1, CEBP and NFATc2 and 6 potential VSMC-specific TF: Gata6, Nr2f2, Sox12, Foxa2, Sox9, Hoxa5 (Table 4.6). Indeed both PU.1 and CEBP were widely identified on MΦ enhancers to regulate cell differentiation and identity (Hoeksema and Glass 2019). Moreover PU.1 and CEBPα/β co-localized in cell type-specific fashion in MΦ, as compared to adipocytes (Lefterova et al. 2010). Others shown that PU.1 depletion in MΦ leads to decreased H3K4me3 at cell type-specific enhancers resulting in abrogated gene expression (Ghisletti et al. 2010). Interestingly, yet there is no evidence for NFATc2 role in MΦ cell type-specific gene expression, it was found to be crucial in the

regulation of immune response or B cell and T cell differentiation (Peng et al. 2001). Among potential VSMC LDTF there was identified Gata6, which in many reports was proposed as a master regulator of VSMC-specific gene expression. As such, differentiated phenotype VSMC-specific marker genes, *Smooth Muscle Myosin Heavy Chain* (*Sm-MHC*) and *α1-integrin* gene, remain under transcriptional control of Gata6 (Wada et al. 2000, Obata et al. 1997). Additionally, myocardin is a inevitable co-activator which associates with SRF to regulate VSMC differentiation and gene expression (Li et al. 2003). Gata6 can selectively modulate myocardin-SRF complexes activity to induce, but also inhibit VSMC-specific gene expression (Yin and Herring 2005). Moreover, GATA6 overexpression elevated expression of VSMC marker genes and prevented VSMC de-differentiation to the synthetic phenotype in the rat model of carotid balloon catheter injury (Mano et al. 1999). Although Nr2f2 was not reported as a crucial TF for mediating VSMC identity, it was previously characterized as a master regulator of vein EC, the cells of similar origin. Nr2f2 determined expression of arterial markers NP-1 and Notch, hence set the identity of vein versus artery endothelium (You et al. 2005). Further, two representatives of SOX gene family, which represents important developmental cascades regulators, were identified in our study (Prior and Walter 1996). Interestingly, Sox9 is a master regulator of VSMC phenotype change to chondrogenic cells, a process which contributes to vascular calcification during atherosclerosis. Sox9 activation correlated with myocardin, a master regulator of VSMC gene expression, and VSMC differentiation markers SM22, α-actin and SM-MHC repression. By direct association with myocardin, Sox9 counteracted its activity and modulated VSMC-specific gene expression, being important modulator of VSMC fate (Xu et al. 2012). However, no clear correlation between the other potential LDTF and VSMC-specific differentiation or transcriptional scenarios was reported in the literature before, it is worth mention that all these factors or families they belong to, were involved in mediating other cell types identity during embryonic and postnatal life. Therefore it is highly likely that due to lack of an experimental evidence these TF were not previously studied in the context of VSMC-specific gene expression.

Considering the abovementioned data, we hypothesised that any of the identified potential LDTF in MΦ or VSMC, could mediate chromatin opening in a cell type-specific manner to allow for subsequent recruitment of IFNγ-activated STAT1. To verify involvement of STAT1 in IFNγ-dependent cell type-specific gene expression, regulatory regions of filtered 81 VSMC-specific (top 30 genes presented in Table 4.2) and 417 MΦ-specific (top 30 genes

presented in Table 4.3) genes were analyzed for the presence of potential STAT1 binding sites by *in silico* promoter analysis. Indeed, predominantly solitary GAS, as compared to ISRE or GAS/ISRE, motifs were found to be enriched in the regulatory regions of both VSMC and MΦ-specific genes (Fig.4.3A-B), implying a dominant regulatory role of GAF homodimers, but not ISGF3 complex. This observation correlates with the general view of crucial GAF complexes involvement in IFN II-dependent gene expression, while rather limited role for ISGF3 complex (Decker et al. 1989).

Yet there arouse a question if STAT1 could be recruited to precise genomic locations via cell type-specific LDTF. Indeed, Aittomaki et al. showed that expression of FcγRI cell-type specific receptor requires DNA-binding as well as transactivation functions of both PU.1 and STAT1 (Aittomäki et al. 2004). Moreover, IFNγ-dependent MΦ-specific *Fgl2/Fibroleukin* expression involved collaboration between the composite *cis* elements Sp1/Sp3 and GAS/PU.1 (Liu et al. 2006). Wang et al. reported that GATA4 transcription factor was able to recruit STAT1 to target gene promoters and cooperate through direct physical interaction in myoblasts (Wang et al. 2005). Thus, abovementioned data provide evidence for a collaborative interaction between LDTF and STAT1 in the context of cell-type specific gene expression, existing in different cell types.

In order to validate cell type-specific IFNγ-dependent STAT1 recruitment, we performed STAT1 ChIP-seq IGV screenshots analysis. There were identified 22 VSMC-specific genes which were uniquely bound by STAT1 in VSMC, but not in MΦ upon stimulation with IFNγ (Fig.4.4 and Fig.4.5). One of the crucial factors which determine the selective recruitment of TF to their cognate motifs is the current chromatin accessibility state, which was associated with enrichment of H3K27Ac histone mark in gene promoters and enhancers (Creyghton et al. 2010). Thus its binding pattern was analysed in untreated VSMC and MΦ, for 22 STAT1-bound VSMC-uniquely expressed genes. Remarkably, in case of 13 genes: *Neurl3*, *Batf3*, *H2-M3*, *Tmem106a*, *Adc*, *Slc26a2*, *Runx1*, *Txnip*, *Fmnl1*, *Trib3*, *Tlr2*, *Inpp5d* and *Rbm47*, H3K27Ac was enriched in both cell types, suggesting an 'open' chromatin state not only in VSMC, but also in MΦ (Fig.4.4). In contrast, in case of other 9 genes: *Tmtc1*, *Ikzf4*, *Pla1a*, *Mreg*, *Greb1l*, *Has1*, *Nsg1*, *Nav3*, *Vegfc*, H3K27Ac enrichment was identified just in case of VSMC, while not in MΦ (Fig.4.5). Strikingly, chromatin accessibility state correlated with the basal gene expression levels (RPKM) just in case of Group 2 gene representatives (Table 4.4). Hence, for Group 1 genes we identified basal gene expression levels in both cell types. In striking contrast, for genes from Group 2 lack of gene expression

upon stimulation with IFNγ in MΦ, correlated with no basal gene expression levels in this cell type (Table 4.4).

Therefore, we concluded that in case of Group 2, VSMC-specific STAT1 recruitment is determined by a chromatin accessibility state. An analogical group of 10 genes (*Cacng8*, *Creb5*, *AB124611*, *Ikzf1*, *Aoah*, *Gna15*, *Tnfsf8*, *Slamf7*, *Ms4a6c*, *Adap2*) was identified among MΦ-specific IFNγ-activated genes (Fig.4.6, Table 4.5). Cell type-specific gene expression correlated with unique STAT1 recruitment in MΦ, but not in VSMC (Fig.4.6). Moreover, H3K27Ac enrichment was detected in untreated MΦ, while not in VSMC (Fig.4.6), correlating with undetectable basal gene expression levels in this cell type (Table 4.5). Therefore we speculated that a similar mechanism, in which STAT1 binding in a cell type-specific manner is determined by the chromatin accessibility state, could drive both VSMC- and MΦ-specific IFNγ-dependent gene expression.

Literature evidence suggest that a process of cell type-specific chromatin opening could be mediated by LDTF-dependent H3K27Ac mark deposition. The most broadly described HAT, p300 and CBP, were fund at active gene enhancers to introduce histone acetylation on highly conserved lysine residues (Tie et al. 2009). TF such as HNF1-α, HNF4, PU.1, Zta, NF-E2, C/EBP, Elk1, c-Fos, and NFAT were shown to stimulate activity of p300/CBP and increase histone acetylation at target gene regulatory elements (Legube and Trouche 2003, Liu et al. 2004). On the other hand, LDTF may also participate in the recruitment of HDAC, to remove histone acetylation marks and inhibit gene transcription, as reported for C/EBP (Di-Poï et al. 2005). This data suggest that LDTF may actively determine the pattern of histone code and in this way shape cell type-specific gene transcription.

Since PU.1 is a known MΦ LDTF (Feng et al. 2008), we characterized its recruitment into the regulatory regions of 10 MΦ-uniquely expressed genes (Fig.4.6). Identified PU.1 pre-binding in unstimulated MΦ supports the concept of LDTF-dependent chromatin opening allowing for further IFNγ-dependent STAT1 binding in this group of genes. A similar mechanism involving cooperation between one of the potential VSMC-specific TF (Table 4.6) opening the chromatin to make STAT1 binding sites accessible for binding upon IFNγ stimulation, could underlie expression of Group 2 VSMC-specific genes (Fig.4.5, Table 4.4). Remarkably, in case of Group 1 VSMC-uniquely expressed genes (Table 4.4), open chromatin state in both cell types, correlated with PU.1 recruitment in MΦ. Therefore it seems that solitary PU.1 binding is not sufficient to promote this group gene expression in MΦ. Interestingly, detailed analysis of 6 genes commonly up-regulated by IFNγ in both MΦ and

VSMC (selected from the list of 9938 genes, Fig.4.2), revealed a similar STAT1 and PU.1 binding pattern. In detail, regulatory regions of *Irf1*, *Cxcl10*, *Gbp6, Gbp7*, *Igtp* and *Oas2* were pre-bound by PU.1 in MΦ and bound by STAT1 in IFNγ-dependent manner in the regions of the open chromatin in both cell types (Fig.4.7, Table 4.7). Thus we could speculate, that Group 1 of VSMC-specific genes would need to be pre-bound by an additional MΦ-specific TF to recruit STAT1 and become active. The other possibility assumes involvement of cell type-specific epigenetic modifications which would allow for STAT1 binding in VSMC or inhibit its recruitment in MΦ, regardless of H3K27Ac enrichment. Similarly, in case of commonly expressed genes, cell type-specific LDTF could be recruited to its cognate motifs distributed in the regulatory regions of all genes expressed in a distinct cell type. Yet just in case of cell type-specific gene transcriptional activation, LDTF could be directed towards cell type-specific enhancers by cell-unique epigenetic modifications.

Based on abovementioned results collected for VSMC as compared to MΦ, combined with the literature data, we propose a model which explains the potential regulatory mechanism of 4 identified scenarios: (1) basally active genes in VSMC or MΦ, (2) Group 1 uniquely activated genes in VSMC or MΦ, (3) Group 2 uniquely activated genes in VSMC or MΦ and (4) commonly activated genes in VSMC and MΦ. As depicted in Figure 4.8A-B, in untreated VSMC or MΦ cell type-specific enhancers of basally active genes are pre-bound by LDTF X or PU.1, respectively, which have an unique ability to recognize and gain access to their binding sites in the context of closed chromatin. As a consequence, the chromatin structure is reorganised to a form of less tightly packed and transcription-friendly. Subsequently, LDTF may recruit HAT which introduces acethyl group on lysine residues present in histone tails. HAT p300/CBP was identified at active gene enhancers, being responsible for H3K27Ac histone mark deposition (Tie et al. 2009). Additionally, LDTF accompanied by collaborating chromatin-modifying and remodeling enzymes, possess an exclusive ability to prime cell type-specific enhancers with H3K4me1 for future activation (Zhang and Glass 2013). Next, (Fig.4.8C/E) VSMC or (Fig.4.8D/F) MΦ IFNγ treatment results in STAT1 homodimers (GAF) recruitment to cognate GAS motifs present in the regions of an open chromatin (pre-bound by LDTF X in VSMC or PU.1 in MΦ). Subsequently, this leads to cell type-specific gene transcriptional activation. Group 1 VSMC-specific genes (Fig.4.8C) or MΦ-specific genes (Fig.4.8D) are characterized by an open chromatin state in both cell types correlating with LDTF X or PU.1 pre-binding, respectively. Yet STAT1 recruitment occurs in cell type-specific manner, potentially due to involvement of

an additional LDTF or cell type-specific epigenetic modifications. Except H3K4me1 also H3K4me2 was reported among potential histone marks associated with cell type-unique enhancer selection (Zhang and Glass 2013). In contrast, Group 2 VSMC-specific genes (Fig.4.8E) or MΦ-specific genes (Fig.4.8F) are characterized by the chromatin accessibility just in one cell type. As presented in Figure 4.8E, LDTF X pre-binding in VSMC mediates chromatin opening and subsequent STAT1 recruitment to drive VSMC-specific gene expression. Although STAT1 homodimers are formed upon IFNγ stimulation in both cell types, it cannot bind to GAS sites hidden in the regions of MΦ condensed chromatin (due to lack of PU.1 binding). Closed chromatin state correlates with the deposition of H3K27me3 repressive mark (Zhang and Glass 2013). Oppositely, PU.1 opens the chromatin in MΦ to recruit STAT1 and drive MΦ-specific gene expression. The same genes remain silent in VSMC, due to closed chromatin state and lack of LDTF X binding (Fig.4.8F). Finally, Figure 4.8G-H illustrate that STAT1-bound regulatory regions of commonly IFNγ-activated genes both in VSMC and MΦ are pre-bound by LDTF X or PU.1, respectively, alike in case of Group 1 cell type-specific genes (Fig.4.8C-D). Active gene promoters involved in the regulation of common gene expression between VSMC and MΦ are associated with different histone signatures, exemplified not only by H3K27Ac, but also H3K4me3 (Zhang and Glass 2013). Thus, binding of cell type-specific TF seems to be necessary to maintain particular cell type identity, yet in case of cell type-specific gene expression, LDTF recruitment to cell type-specific enhancer would potentially require guidance by cell-unique epigenetic modifications.

Finally, there arises a question about the role of the genes expressed in a cell type-specific manner. As mentioned before, any abrogation in transcriptional activation of VSMC- or MΦ-unique programmes may contribute to altered resident tissue homeostasis and unresolved IFNγ-dependent vascular inflammation. Therefore we analysed potential contribution of VSMC or MΦ cell type-specific gene expression in the pathophysiology of vascular inflammation. In Table 4.4 (Group 2) and Table 4.5 were presented VSMC- and MΦ-uniquely expressed genes in response to IFNγ, respectively. Some of these genes which present the strongest correlation between reported gene function and its potential role in vascular inflammation are briefly discussed below.

TMTC1 (Transmembrane and Tetratricopeptide repeat Containing 1) is a known regulator of calcium homeostasis, which overexpression caused a reduction of calcium release, whereas KO increased the carbachol and ATP stimulated calcium release (Sunryd et al. 2014). Moreover, *TMTC1* has been associated with a risk of incident heart failure (Smith et al. 2010).

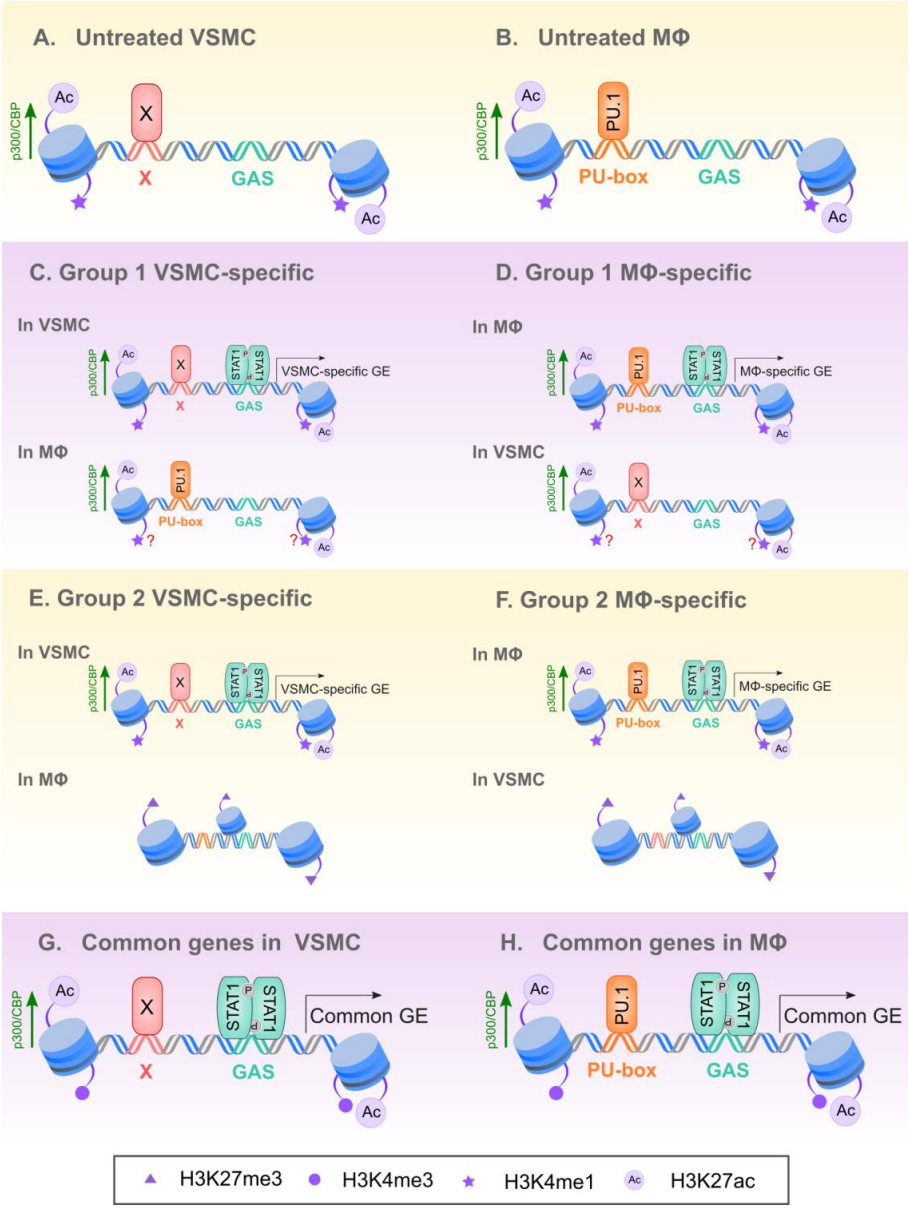

Figure 4. 8. Model of VSMC and MΦ cell type-specific gene expression regulation.

(A) In untreated VSMC regulatory regions of genes showing basal activity are marked by LDTF (potential TF X) which opens the chromatin structure and deposits H3K27Ac and H3K4me1 marks. **(B)** Alike, regulatory regions of basally active genes in MΦ are marked by PU.1. **(C/E)** VSMC or **(D/F)** MΦ exposition to IFNγ treatment results in recruitment of STAT1 homodimers to GAS sites exposed in the region of the open chromatin (pre-bound by LDTF X in VSMC or PU.1 in MΦ), what leads to VSMC- or MΦ-specific gene expression. In case of **(C)** Group 1 VSMC-specific genes or **(D)** Group 1 MΦ-specific genes the chromatin is opened in both cell types, thus pre-bound by both LDTF X and PU.1 in the opposite cell type. In case of **(E)** Group 2 VSMC-specific genes or **(F)** Group 2 MΦ-specific genes the chromatin is opened just in VSMC (by LDTF X) or MΦ (by PU.1), respectively. Although STAT1 homodimers are formed upon IFNγ stimulation in both cell types, it cannot bind to GAS sites hidden in the regions of condensed chromatin, characterized by the deposition of H3K27me3 repressive mark. Promoters of commonly IFNγ-activated genes both in **(G)** VSMC and **(H)** MΦ are pre-bound by LDTF X or PU.1, respectively and marked by H3K27Ac and H3K4me3. For more detail, see the text.

Pla1a (Phospholipase A1 member A) is a phospholipase which catalyze the degradation of phospholipids liberating 2-acyl-lysophospholipids and free fatty acids. Others provided evidence for a role of the lipoprotein-associated PLA2 in atherogenesis, which could represent risk factors for coronary heart disease (Tselepis and John Chapman 2002). Additionally, *Pla1a* was found to be up-regulated in mineralizing VSMC induced by chondrocyte-derived factors, suggesting that this gene may play a role in vascular calcification (Mikhaylova et al. 2007). *MREG* (Melanoregulin) was significantly up-regulated in atherosclerotic patient aortas versus healthy controls and proposed as a novel atherosclerosis marker (Aldi et al. 2015). During early stages of atherosclerosis, VSMC migrate to *tunica intima* and start releasing excessive amount of extracellular matrix, including hyaluronic acid, to attract circulating leukocytes (Evanko et al. 1999). *HAS1* (Hyaluronan Synthase 1) overexpressing VSMC produced cable-like structures in the extracellular matrix, involved in leukocyte adhesion (Sadowitz et al. 2012). Thus, VSMC-produced *HAS1* could accelerate the early pro-inflammatory stage of vascular inflammation. The family of VEGF and their receptors have a beneficial role in healthy vessels, by mediating vascular protection and survival, however they were shown to contribute to acceleration of the inflammatory processes, arterial wall thickening and angiogenesis, during atherosclerosis. *VEGFC*-expressing cells were identified in the atherosclerotic lesions in the intima of human coronary arteries (Nakano et al. 2005). Additionally, Masunaga et al. demonstrated that *VEGFC* plays a vital role in angiogenesis and dyslipidaemia in atherosclerosis (Nobutoyo et al. 2018). Moreover, *VEGFC* overexpression in mouse model induced growth of functional lymphatic vessels, which might promote vascular hyperplasia (Xu et al. 2007).

Alike, functions of MΦ-uniquely expressed genes in response to IFNγ could be associated with immune cell type-specific functions in the context of vascular inflammation. *Aoah* (Acyloxyacyl Hydrolase) was found to be up-regulated in MΦ derived from large-lesion group of atherosclerosis-sensitive mice (Smith et al. 2006). Moreover, *AOAH* was activated in ischemic stroke patients suffering from atherosclerosis (Lee et al. 2014). In the other study *Aoah* was involved in the process of inflammatory response and increased atherogenesis in ApoE KO mice (Xu et al. 2009). Treatment against Tnfsf8 (TNF Superfamily Member 8) was shown to inhibit atherosclerotic plaques progression and prevention of acute cardiovascular symptoms in mice. Anti-Tnfsf8 antibody reduced lesion size by 35% in LDLR KO mice fed with a Western diet for 8 weeks (Foks et al. 2012). Other MΦ-uniquely expressed gene,

SLAMF7 (Signaling Lymphocytic Activation Molecule 7) was identified as a key regulator of carotid atherosclerosis progression. Hypo-methylation of SLAMF7 promoter correlated with high gene expression levels in cartoid plaques. SLAMF7 depleted plaque-derived MΦ reduced release of pro-inflammatory cytokines, but also abrogated VSMC proliferation. Together, SLAMF7 was proposed as a potential therapeutical target in carotid atherosclerosis (Xia et al. 2018). Others reported that *Adap2* (ArfGAP with dual PH domains 2) plays a role in heart development and could contribute to occurrence of cardiovascular defects in patients with NF1 microdeletion syndrome (Venturin et al. 2014).

Together, these reports clearly suggest that VSMC- and MΦ-specific gene expression activated by IFNγ, corresponds to cell type-specific functions potentially performed in the inflamed vessel. Collected transcriptomic and genomic data allowed to propose a model of hierarchical involvement of PU.1 and STAT1 in MΦ-specific IFNγ-dependent gene expression. Explanation of the mechanism of gene transcriptional regulation is depicted in Figure 4.8. Further, we extrapolated this model to VSMC-specifically expressed gene regulation. By performing genome-wide *in silico* promoter analysis of VSMC-uniquely expressed gene regulatory regions we could appoint potential VSMC LDTF. However in order to obtain a direct proof for potential VSMC-specific LDTF involvement in cell type-specific gene expression, additional ChIP-seq experiments in WT and LDTF KO VSMC need to be performed. As mentioned before, better understanding of MΦ- and VSMC-specific gene expression regulation in a healthy vessel versus inflamed one, could help to elucidate atherosclerosis pathophysiology. Moreover genes expressed in a cell-specific manner could serve as potential vascular inflammation therapeutical targets.

Chapter 5. STAT1-dependent transcriptional mechanisms in vascular inflammation

IFN mediate their downstream transcriptional effects via activation of JAK-STAT signaling pathway. As such, IFNα binding to its cognate receptor results in predominant formation of STAT1/STAT2 heterodimers together with IRF9, forming ISGF3 complex recruited to ISRE sequence present in the target gene promoters (Darnell et al. 1994). IFNγ-induced canonical pathway results in formation of STAT1 homodimers (GAF), binding to GAS consensus sequence present in the gene regulatory regions (Decker et al. 1989). However transcriptional regulation of IFN-dependent pathways seems to be much more complex, since other non-canonical complexes were shown to be functional in the context of ISG expression. Thus, it was reported previously, that IFNα stimulation results in formation not only of ISGF3 complex, but also GAF (Pilz et al. 2003), STAT1/STAT2 heterodimers (Li et al. 1996, Ghislain et al. 2001) or STAT2 homodimers associated with IRF9 (ISGF3-like) (Bluyssen and Levy 1997, Kraus et al. 2003, Poat et al. 2010, Blaszczyk et al. 2015). In contrast, limited evidence was provided in the context of IFNγ-dependent non-canonical signaling. Single reports support a role of ISGF3 (Matsumoto et al. 1999, Zimmermann et al. 2005) or an alternative complex consisting of STAT1 homodimers coupled with IRF9 in the regulation of IFNγ-stimulated gene expression (Bluyssen et al. 1995, Kimura et al. 1996, Majumder et al. 1998). Importantly, the data presented in Chapter 2 of this thesis shed a new light on the non-canonical mechanisms of IFNγ-dependent ISG expression. As such, ISRE-containing gene expression analysis combined with characterization of STAT1, STAT2 and IRF9 recruitment to the gene promoters (ChIP) let to conclude, that ISGF3 complex is formed and potentially transcriptionally functional upon stimulation not only with IFNα, but also IFNγ in VSMC. Moreover, RT-PCR experiments performed in STAT2 KO VSMC provided evidence for a role of an additional STAT1-IRF9 complex, since IFNγ-dependent gene expression was still observed in these cells. Yet, subsequent analysis of IFNγ-mediated response in IRF9 KO VSMC suggested involvement of the other TF complex in ISRE-containing gene transcriptional regulation, which potentially could be IRF1, also recruited to these gene promoters. Therefore further experiments will be necessary to study the detailed mechanism of IFN II-induced gene transcriptional regulation. It would be beneficial to examine ISRE-containing gene expression patterns upon IFNγ treatment in IRF1 KO VSMC as well as double IRF1-IRF9 KO VSMC, to further prove our assumptions, characterize and

study a mutual role of IRF- and STAT-containing transcriptional complexes in the underlying mechanism.

Interestingly, it was suggested before that there exist a signaling synergy between JAK-STAT and TLR4 pathways. Phenomenon of priming-induced SI between IFNγ and LPS, results in STAT1- and NFκB-dependent robust pro-inflammatory response of monocytes or MΦ (Hayes et al. 1995, Qiao et al. 2013). Initially it was proposed, that underlying mechanism depends on IFNγ-mediated increase in STAT1 availability for TLR4 stimulation and subsequent STAT1 phosphorylation (Hayes et al. 1995). However, STAT1 phosphorylation is not exclusively type II IFN-dependent and could be induced by LPS (Hu et al. 2008). Moreover, TLR4 signaling activates not only STAT1, but also other TF, like NFκB, IRF1 or IRF8. Thus, although collaboration between all these TF was shown to be necessary for SI-dependent gene transcriptional activation of *Cxcl10*, *Nos2*, *IL1*, *IL6*, *IL12*, *TNFα* and *Ccl5*, precise molecular mechanism remained unclear (Ganster et al. 2005, Clarke et al. 2010, Zhao et al. 2006, Liu and Ma 2006).

Since recently, more attention has been paid to the immune component of atherosclerosis, SI-dependent pro-inflammatory gene expression in MΦ and DC was linked with the process of vascular inflammation. Thus in our study we hypothesised that a similar mechanism to priming induced-SI in immune cells, could underlie inflammatory stimuli-dependent gene expression in the other crucial atheroma-interacting cells, like VSMC. Indeed, data presented in Chapter 2 showed that comparison of VSMC, MΦ and DC transcriptome, resulted in an identification of a group of commonly activated genes between vascular and immune cells in response not only to IFNγ+LPS, but also IFNα+LPS treatments, mimicking SI conditions. Results provided in Chapter 2 present the novel mechanism of priming-induced SI, in which IFNα- or IFNγ-activated STAT1-containing transcriptional complexes ISGF3, GAF or ISGF3, STAT1-IRF9, GAF, respectively, are recruited to closely spaced ISRE-NFκB or GAS-NFκB binding sites. Remarkably, our results for the first time provide evidence for both IFNγ-, but also surprisingly IFNα-dependent common SI gene expression in the cells from the vasculature. Partial overlap between these two signaling pathways could be explained by both IFN-dependent activation of mutual-exclusive pool of ISGF3, GAF and STAT1-IRF9 transcriptional complexes. In our model of priming-induced SI, STAT1-containing complexes recruitment to closely spaced ISRE-NFκB or GAS-NFκB binding sites correlates with increased histone acetylation of adjacent region. Subsequent LPS-induced p65 binding is facilitated due to the open chromatin conformation in the region of composite sites,

which coincides with enhanced histone acetylation and PolII recruitment, finally resulting in robust pro-inflammatory SI gene expression. Crucial role of acetylation-primed chromatin in enabling of increased transcriptional response to TLR4 signaling was also observed by others in connection with IFNγ+LPS SI-dependent gene expression in MΦ, obviously corroborating our results (Qiao et al. 2013).

Although single studies provide evidence for the involvement of STAT1 or NFκB in the regulation of gene suppression, the underlying mechanism was not elucidated. Moreover, to the best of our knowledge, role of these TF in the context of priming-induced SI between IFNγ and LPS was not examined before. Therefore in Chapter 3 we hypothesised that alike in case of SI-dependent gene up-regulation, STAT1 and NFκB dependent mechanism could drive IFNγ+LPS-dependent gene suppression in VSMC. In the attempt to elucidate how these two TF could actually collaborate within the mechanism of priming-induced SI, we defined a model for two identified gene groups. In Group I STAT1 binding could mask closely located NFκB site within repressed gene promoter to inhibit positively acting TF, what together with STAT1-dependent recruitment of repressory machinery or sequestering gene transcriptional co-activators, could result in gene suppression. A similar mechanism was reported in case of *MMP9* gene and competitive binding of IRF1 and NFκB (Sancéau et al. 2002). For Group II, we propose a different scenario, in which STAT1 and NFκB co-binding is necessary to recruit repressor or alter transcriptional co-activators assembly, in a collaborative manner. Therefore it seems that there exist both common and individual aspects of priming induced SI in case of gene activation or suppression. Hence, both STAT1 and NFκB could either collaborate or antagonise each other within the mechanism of SI-dependent gene down-regulation, in contrast to the mechanism of SI-dependent gene up-regulation, where this two TF collaboration is necessary for maximal gene expression. Moreover, it looks like a specific promoter organisation of closely spaced ISRE-GAS-NFκB motifs is crucial for SI-induced gene up-regulation, while not necessarily in case of gene suppression. On the other hand, it occurs that STAT1-containing GAF complexes play predominant role in SI-driven both gene up- or down-regulation, as compared to an alternative ISGF3 or STAT1-IRF9. Importantly, a series of additional experiments will be necessary to obtain further proof for functionality of the predicted mechanisms. Importantly, ability of STAT1 or NFκB to recruit candidate repressors, like SMRT, PIASx or SLNF5 should be validated together with these TF effect on gene activators, like CBP/p300 and PolII assembly, upon IFNγ+LPS stimulation. Since we observed a big overlap between the lists of down-regulated genes in response to IFNγ+LPS in

VSMC, MΦ and DC (data not shown), next, it would be important to examine if identified potential mechanism of SI-dependent gene repression in VSMC, would be rather cell type-specific or shared in various cell types, alike the common mechanism of SI-dependent gene up-regulation in VSMC, MΦ and DC.

Results provided in Chapter 2 confirmed existence of a huge functional and regulatory overlap between VSMC and immune cells. Indeed, both these cell types were shown to be involved in pathogenesis of vascular inflammation, by participation in release of pro-inflammatory cytokines, chemokines, metalloproteinases and cholesterol-laden foam cell formation (Shirai et al. 2015, Allahverdian et al. 2014). Yet subsequent RNA-seq data analysis revealed a fraction of genes expressed in cell type-specific manner upon stimulation with pro-inflammatory IFNγ. As reported before, immune cell type-unique gene expression depends on hierarchical collaboration between master regulators (LDTF) which mark a genome in cell type-specific way and stimuli-induced SDTF, subsequently recruited to LDTF pre-bound genomic regions (Heinz and Glass 2012). In Chapter 4 we showed that indeed for selected group of genes, cooperation between PU.1 and STAT1 was prerequisite to mediate chromatin opening and histone acetylation enrichment in MΦ-specific regions which further could bind STAT1 upon IFNγ-stimulation. Since no comprehensive mechanism was provided before to explain VSMC-specific gene expression, we hypothesised that the abovementioned one could be functional not only in MΦ, but also VSMC. *In silico* promoter analysis were applied to anticipate on PU.1-analogue (Gata6, Nr2f2, Sox12, Foxa2, Sox9, Hoxa5) in VSMC to drive cell type-unique type II IFN-driven gene activation. Together with the analysis of VSMC-specific chromatin opening and histone acetylation these results let to speculate about the involvement of LDTF-SDTF-dependent mechanism of VSMC-specific gene expression. Yet in order to obtain a definitive proof for a role of a specific LDTF in VSMC-specific transcriptional activation, there need to be generated VSMC depleted of potential LDTF candidates. Next the effect of LDTF depletion on IFNγ-induced VSMC-specific gene expression should be examined. Other interesting new observation presented in Chapter 4 is that MΦ-specific master regulator PU.1 was recruited to the accessible regulatory regions of commonly expressed genes. Therefore there arises a question about a role of PU.1 in the mechanism of transcriptional regulation and STAT1 TF recruitment to the promoters of ubiquitously expressed genes, since to the best of our knowledge it was not addressed in the literature before. Thus it seems that LDTF recruitment itself is some circumstances in not sufficient to mediate cell type-specific outcomes. Therefore we could speculate about a

crucial role of epigenetic modifications which serve as an additional layer of gene expression regulation and affect LDTF performance. Chromatin accessibility was previously associated with enrichment of different histone acetylation and methylation marks, deposited in the gene promoters and enhancers. Importantly, H3K27Ac, H3K4me1 also H3K4me2 were correlated with cell type-unique enhancer selection, while genomic regions dedicated for common activation correlate predominantly with H3K27Ac and H3K4me3 marks (Zhang and Glass 2013). Hence, further epigenome analysis (ChIP-seq for selected histone marks) of VSMC and MΦ will be necessary to decipher the histone code potentially regulating cell type-specific as well as common gene expression.

It is worth mentioned that the number of the genes expressed in VSMC- and MΦ-specific manner identified in our study was relatively low as compared to the total number of expressed genes. It might be caused by the fact that cell stimulation with a general pro-inflammatory factor, as IFNγ, results in robust pro-inflammatory response of mostly universal gene targets. Moreover, VSMC and MΦ coexist within inflamed vessel, thus huge overlap between the pools of activated transcriptional targets in both cell types, is not a surprising observation. On the other hand, the selection performed in this study, which was made among IFNγ-induced genes only, might narrow down the number of uniquely expressed genes in VSMC and MΦ. Since LDTF are crucial not only for cell type-specific response to the external cues, but also maintenance of cell differentiation and identity, the selection method could be further extended on the genes which present basal gene expression in a given cell type. This could help to verify the role of identified potential VSMC-specific LDTF in the context of VSMC response to a broader spectrum of pro-inflammatory stimuli and help to understand the role of cell type-unique LDTF in the regulation of common gene expression between various cell types.

Together, data presented in this thesis as well as collected by others, emphasises a crucial role of STAT1 together with NFκB in mediating pro-inflammatory and immune response, which could play a critical role during pathogenesis of inflammatory diseases, such as CVD. Thus, detailed investigation of the molecular mechanisms underlying its pathology, holds promise for the development of new diagnostic tools and therapeutical strategies to fight against the disease.

Potential application of STAT1-dependent mechanisms in diagnostics of vascular diseases

According to World Health Organisation (WHO), CVD including heart and blood vessels disorders, are the leading cause of morbidity and mortality world-wide (WHO 2018). Therefore it is a huge challenge for a modern diagnostics to develop new tools which could detect early signs of the disease onset to prevent its progression. Yet currently, atherosclerosis diagnostics is based on a series of blood tests (mainly lipid profile measuring levels of HDL, LDL and triglycerides), electrocardiogram (EKG), ankle/brachial index calculation, an exercise stress test, an angiogram or a chest x-ray test. Remarkably, all abovementioned tests may detect advanced symptoms of the disease, which subsequently require invasive surgical intervention or constant drug administration. Instead, if diagnosed at early stage, atherosclerosis progression could be targeted by less intrusive methods, like dietary changes (more fiber, healthy fats, fruit and vegetables), calories restriction, quitting smoking or alcohol intake and introduction of physical activity. This would allow to reduce CVS-related morbidity rates as well as tremendous annual cost of CVD treatment, which reached $351.2 billion in 2014-2015, only in USA (Benjamin et al. 2019).

A biomarker is defined as 'characteristic that is measured as an indicator of normal biological processes, pathogenic processes or responses to an exposure or intervention' (FDA-NIH 2016). Importantly, this definition covers also established risk factors, encompassing smoking, hypertension, dyslipidaemia, familial history of coronary heart disease or diabetes, in case of atherosclerosis. However, 10-15% of CVD patients do not present any of these symptoms (Montgomery and Brown 2013, Vasan 2006). Diagnostic biomarkers, measured in the body fluids or tissues, play crucial role in diagnostics of multiple diseases, due to opening of the possibility for early, precise and reliable, not invasive and low cost diagnostics (Califf 2018). Despite increasing number of the reports proposing new potential biomarkers, the European Society of Cardiology (ESC) approves only one, troponin, for the diagnosis of acute coronary syndromes, so far (Hamm et al. 2011). Therefore, there is an urgent need to identify more disease-specific biomarkers which could find their way to clinics soon. For that, new genome-wide technologies have to be enrolled to perform efficient screening of multiple molecules at once.

Currently, such strategy was applied in two European collaborative research projects, EPIC-CVD study23 and the Biomarker for Cardiovascular Risk Assessment in Europe

(BiomarCaRE), which aims for clinical and epidemiological biomarker identification and validation in large patient cohorts (EPIC-CVD 2015, Zeller et al. 2014). Also in our study, there was used genome-wide approach of combined transcriptomics (RNA-seq) and genomics (ChIP-seq) to characterize pro-inflammatory gene expression profiles and their regulatory mechanisms in response to IFN and LPS in the atheroma interacting cells. Data presented in Chapter 2 proved collaborative involvement of STAT1 and NFκB in transcriptional regulation of the genes commonly affected by the phenomena of priming-induced SI between IFNα or IFNγ and LPS, in VSMC, MΦ and DC. Among these up-regulated genes, there were identified multiple chemokines, cytokines, adhesion molecules, matrix metalloproteinases and other pro-inflammatory mediators. GO analysis revealed involvement of these genes in the processes crucial for atherosclerotic plaque formation and disease progression, such as immune and inflammatory response, cell proliferation, migration, adhesion, chemotaxis, apoptosis, response to lipid and ROS. Interestingly, integrative GO and network-based analysis of IFNγ+LPS-repressed genes in VSMC, suggested potential involvement of these genes in the negative regulation of vasculature development, angiogenesis, cell cycle, lipid biosynthetic process, cell proliferation, migration and adhesion. As such, although it would require further validation, it is tempting to suggest that a selection of SI-dependent both up- and down-regulated genes could serve as diagnostic biomarkers of vascular inflammation. Indeed, a role of STAT1-NFκB-dependent gene expression in the context of atherosclerosis was suggested by others. Chmielewski et al. found that STAT1-NFκB-dependent SI gene up-regulation of *CXCL9*, *CXCL10*, *CCL5*, *CCL8*, *CRCL2*, *Cd74*, *GBP5*, *UBD*, *SECTM1*, *IFI16*, *UPP1*, *FAM26F* and *IRF8* could be identified in human cartoid and coronary plaques, confirming importance of SI in atherosclerosis pathophysiology (Chmielewski et al. 2014). However, despite the fact that commonly expressed pro-inflammatory genes in various atheroma interacting cells definitely reflect ongoing inflammation, one could argue that their potential to become diagnostic biomarkers of atherosclerosis is limited. It is due to systemic activation of cytokines, chemokines and other pro-inflammatory mediators by many inflammatory disorders, also unrelated to atherosclerosis. Such concerns were previously reported in case of C-reactive protein (CRP), IL-6 and TNF-α, some of the most widely described potential biomarkers of CVD. F.ex CRP is released in response to the acute inflammation, but also infection, injury or tissue damage, obesity, old age, diabetes or hypertension, thus conditions related with pathophysiology of multiple diseases (Soeki and Sata 2016). Hence recently, more attention has been paid to the concept of cell type-specific biomarkers, which might more accurately reflect locally ongoing inflammation. In Chapter 4

we identified IFNγ-induced genes activated in VSMC- or MΦ-specific manner, as compared to the other cell type, in STAT1-dependent way. VSMC gene-specific analysis revealed involvement of these STAT1-dependent genes in the regulation of calcium homeostasis, degradation of phospholipids, excessive ECM production, arterial wall thickening and angiogenesis, which correspond to cell type-specific functions served by VSMC in an inflamed vessel. Together, it is tempting to speculate, that such cell type-specific gene expression products could serve as precise indicators of atherosclerosis-related inflammation. Although extensive validation will be necessary to estimate clinical potential of identified pro-inflammatory genes expressed in cell-type specific manner as potential biomarkers of atherosclerosis, the data provided by others seems to support the proposed concept. In order to overcome arterial tissue heterogenity, proteomics coupled with laser capture microdissection was used to identify potential biomarkers of CVD, specific for various cell types isolated from tissue sections (Li et al. 2004). Cell type-specific analysis were applied to fish out prostate cancer-associated biomarkers, allowing for identification of male individuals suffering from this particular cancer type (Nelson and Montgomery 2006). Similarly, in case of breast cancer which mainly occurs in women, cell-specific biomarkers were used to classify cancer subtypes as well as direct generic-targeted biopharmaceuticals (Liu et al. 2016). In the field of renal medicine, nephron section-specific biomarkers were reported to be utilized to precisely localize the area of renal injury (Shaw 2010).

Considering increasing impact of cell type-specific markers in the field of diagnostics of various diseases, it is tempting to speculate that STAT1-dependent cell type-specific target genes expressed in the cells from the vasculature in the process of arterial inflammation could serve as promising diagnostic biomarkers of atherosclerosis. However as abovementioned, additional analysis will be inevitable to validate a diagnostic potential of identified cell type-specific genes as biomarkers. First, this could be obtained by an extensive comparison of the external transcriptomic and genomic datasets, coming either from the vasculature-related cell type-specific material or clinical studies of atherosclerosis. This analysis would help to verify cell type-specificity of the potential biomarkers, confirm its clinical association with the particular vascular disease and validate STAT1-dependent transcriptional cascades regulating vascular pro-inflammatory gene expression. Further, identified STAT1-mediated gene signatures could be validated in the experimental animal models of atherosclerosis, like ApoE KO or LDRL KO.

Potential application of STAT1-dependent mechanisms in the development of therapeutical strategies against vascular diseases

The data presented in Chapters 2-4 as well as published by others imply that an abnormal regulation of STAT1- and NFκB-dependent gene expression could be considered as valuable therapeutical target in many inflammatory diseases, including CVD. Although there are not available FDA approved drugs which would directly target STAT1 or NFκB, there are known several ways to inhibit these TF and consequently their downstream target genes.

STAT inhibitory strategies are based either on direct or indirect protein inhibition. Direct STAT inhibitors encompass oligomerization inhibitors, dimerization inhibitors, which block the STAT SH2 domain, thus subsequent phosphorylation and dimer formation or DNA-binding competitive inhibitors. Indirect STAT inhibition is achieved by antisense oligonucleotides- or siRNA-dependent arrest of STAT expression, blocking of the signaling pathway (receptor or ligand) upstream to STAT or inhibition of JAK kinases-mediated STAT phosphorylation or nuclear translocation (Miklossy et al. 2013, Kortylewski and Nechaev 2014, Turkson and Jove 2000). Alike, NFκB inhibition may be achieved by similar strategies, of which the most targeted ones are Iκκ activation, IκB degradation and NFκB nuclear translocation and DNA binding (Lin et al. 2010). Yet a major molecular target for NFκB inhibition is Iκκ activity, resulting in an inhibition of inactive NFκB/IκB kinase-mediated phosphorylation to prevent polyubiquitination of IκB proteins and subsequent NFκB release.

Although all abovementioned inhibitory strategies are extensively studied in the context of inflammatory diseases, especially cancer, resulting in identification of numerous potential STAT or NFκB inhibitors, just few of them are accepted for clinical trials. As described, most of inhibitors indirectly block an upstream signaling pathway, thus may affect numerous molecules unrelated with an actual target. In turn, such multi-inhibition may result in increased toxicity and low specificity of selected inhibitory strategy. Indeed, data published by our group and others proved that some inhibitors originally characterized as STAT3-specific, also potently affect other STAT activity. This was true for known STAT3 inhibitors STATTIC and STX-0119, as well as newly identified multi-STAT inhibitor C01L_F03, all of which targeted the SH2 domain of STAT1, STAT2 and STAT3. It resulted in an inhibition of all STAT phosphorylation, DNA-binding and subsequent IFNα-dependent target gene expression (Plens-Galaska et al. 2018). Also known anti-inflammatory drugs, like sulindac, aspirin, ibuprofen, indomethacin or COX-2 inhibitors, which were not initially identified as

NFκB inhibitors, apparently blocks its activity in addition to their original inflammatory targets (Lin et al. 2010).

Such multi-inhibitory approach could be considered as a promising strategy in the treatment of CVD and other inflammation-driven conditions, due to its wide spectrum of action. On the other hand it seems that the new inhibitory strategies, which would result in more precise and targeted effects, are needed. One possibility would be to link known functional inhibitors to new cell, tissue or disease type-specific delivery systems, like nanoparticles, molecular aptamers or DNA-micelles (Pang et al. 2017, Tan et al. 2011). This could reduce the systemic effect of a multi-inhibitor, both considering its toxicity and wide downstream effects. Alternatively, epigenetic-based targeted therapies are recently proposed as a new treatment strategy for CVD. Results presented in Chapter 2-4 provided evidence for a crucial role of histone acetylation and methylation in the regulation of the mechanism underlying IFN+LPS SI-dependent pro-inflammatory gene expression in VSMC, MΦ and DC. Moreover, VSMC- or MΦ-specific genetic programmes activated in response to IFNγ, were dependent of epigenetically modified accessibility of the chromatin and subsequent collaboration between LDTF and SDTF. Also other reports suggest, that epigenetic regulation of pro-inflammatory genes relate to increased CVD risk (Ordovás and Smith 2010, Abi Khalil 2014). Optimistically, post-translational modifications of histone tails could be potentially reversed by treatment with epidrugs. Especially modulating an activity of the enzymes responsible for histone modifications introduction or removal, like HAT, HDAC or histone methyltransferases or demetylases, seems to be promising way to alter transcription of the pro-inflammatory genes induced during vascular inflammation (Ghosh and Vaughan 2018). Two HDAC inhibitors, scriptaid and tubacin, were tested in animal models and shown to block atherosclerosis-related events. Scriptaid treatment resulted in the suppression of mitogen-activated cyclin D1 and subsequent inhibition of SMC proliferation, involved in pathophysiology of atherosclerosis (Findeisen et al. 2011). Other group showed that tubacin-dependent inhibition of HDAC6 could control atherosclerosis initiation and progression via increasing levels of cardiovascularprotective enzyme CSEg in EC (Leucker et al. 2017). This data holds promise for the development of a novel, epigenetic-based target-specific treatment strategies, yet still better characterization of the epigenome underlying CVD is necessary.

References

Abi Khalil, C. (2014) 'The emerging role of epigenetics in cardiovascular disease', *Ther Adv Chronic Dis,* 5(4), 178-87.

Abou El Hassan, M., Huang, K., Eswara, M. B., Xu, Z., Yu, T., Aubry, A., Ni, Z., Livne-Bar, I., Sangwan, M., Ahmad, M. and Bremner, R. (2017) 'Properties of STAT1 and IRF1 enhancers and the influence of SNPs', *BMC Mol Biol,* 18(1), 6.

Agalioti, T., Lomvardas, S., Parekh, B., Yie, J., Maniatis, T. and Thanos, D. (2000) 'Ordered recruitment of chromatin modifying and general transcription factors to the IFN-beta promoter', *Cell,* 103(4), 667-78.

Aggarwal, B. B. (2003) 'Signalling pathways of the TNF superfamily: a double-edged sword', *Nat Rev Immunol,* 3(9), 745-56.

Aittomäki, S., Yang, J., Scott, E. W., Simon, M. C. and Silvennoinen, O. (2004) 'Molecular basis of Stat1 and PU.1 cooperation in cytokine-induced Fcgamma receptor I promoter activation', *Int Immunol,* 16(2), 265-74.

Aldi, S., Perisic, L., Lengquist, M., Kronqvist, M., Roy, J., Backlund, A., Ketelhuth, D. F., Lindeman, J. H., Hansson, G. K., Paulsson-Berne, G. and Hedin, U. (2015) 'Identification of Melanoregulin as Novel Marker for Atherosclerosis', *Arteriosclerosis, Thrombosis, and Vascular Biology*.

Allahverdian, S., Chehroudi, A. C., McManus, B. M., Abraham, T. and Francis, G. A. (2014) 'Contribution of intimal smooth muscle cells to cholesterol accumulation and macrophage-like cells in human atherosclerosis', *Circulation,* 129(15), 1551-9.

Arnosti, D. (2004) 'Multiple Mechanisms of Transcriptional Repression in Eukaryotes' in *Handbook of Experimental Pharmacology*.

Arora, T., Liu, B., He, H., Kim, J., Murphy, T. L., Murphy, K. M., Modlin, R. L. and Shuai, K. (2003) 'PIASx is a transcriptional co-repressor of signal transducer and activator of transcription 4', *J Biol Chem,* 278(24), 21327-30.

Arslan, A. D., Sassano, A., Saleiro, D., Lisowski, P., Kosciuczuk, E. M., Fischietti, M., Eckerdt, F., Fish, E. N. and Platanias, L. C. (2017) 'Human SLFN5 is a transcriptional co-repressor of STAT1-mediated interferon responses and promotes the malignant phenotype in glioblastoma', *Oncogene,* 36(43), 6006-6019.

Babelova, A., Sedding, D. G. and Brandes, R. P. (2013) 'Anti-atherosclerotic mechanisms of statin therapy', *Curr Opin Pharmacol,* 13(2), 260-4.

Barta, E. (2011) 'Command line analysis of ChIP-seq results', *EMBnet.journal*

Battle, T. E., Lynch, R. A. and Frank, D. A. (2006) 'Signal transducer and activator of transcription 1 activation in endothelial cells is a negative regulator of angiogenesis', *Cancer Res,* 66(7), 3649-57.

Benjamin, E. J., Muntner, P., Alonso, A., Bittencourt, M. S., Callaway, C. W., Carson, A. P., Chamberlain, A. M., Chang, A. R., Cheng, S., Das, S. R., Delling, F. N., Djousse, L., Elkind, M. S. V., Ferguson, J. F., Fornage, M., Jordan, L. C., Khan, S. S., Kissela, B. M., Knutson, K. L., Kwan, T. W., Lackland, D. T., Lewis, T. T., Lichtman, J. H., Longenecker, C. T., Loop, M. S., Lutsey, P. L., Martin, S. S., Matsushita, K., Moran, A. E., Mussolino, M. E., O'Flaherty, M., Pandey, A., Perak, A. M., Rosamond, W. D., Roth, G. A., Sampson, U. K. A., Satou, G. M., Schroeder, E. B., Shah, S. H.,

Spartano, N. L., Stokes, A., Tirschwell, D. L., Tsao, C. W., Turakhia, M. P., VanWagner, L. B., Wilkins, J. T., Wong, S. S., Virani, S. S. and Subcommittee, A. H. A. C. o. E. a. P. S. C. a. S. S. (2019) 'Heart Disease and Stroke Statistics-2019 Update: A Report From the American Heart Association', *Circulation,* 139(10), e56-e528.

Besançon, F., Przewlocki, G., Baró, I., Hongre, A. S., Escande, D. and Edelman, A. (1994) 'Interferon-gamma downregulates CFTR gene expression in epithelial cells', *Am J Physiol,* 267(5 Pt 1), C1398-404.

Blaszczyk, K., Nowicka, H., Kostyrko, K., Antonczyk, A., Wesoly, J. and Bluyssen, H. A. (2016) 'The unique role of STAT2 in constitutive and IFN-induced transcription and antiviral responses', *Cytokine Growth Factor Rev,* 29, 71-81.

Blaszczyk, K., Olejnik, A., Nowicka, H., Ozgyin, L., Chen, Y. L., Chmielewski, S., Kostyrko, K., Wesoly, J., Balint, B. L., Lee, C. K. and Bluyssen, H. A. (2015) 'STAT2/IRF9 directs a prolonged ISGF3-like transcriptional response and antiviral activity in the absence of STAT1', *Biochem J,* 466(3), 511-24.

Bluyssen, A. R., Durbin, J. E. and Levy, D. E. (1996) 'ISGF3 gamma p48, a specificity switch for interferon activated transcription factors', *Cytokine Growth Factor Rev,* 7(1), 11-7.

Bluyssen, H. A. and Levy, D. E. (1997) 'Stat2 is a transcriptional activator that requires sequence-specific contacts provided by stat1 and p48 for stable interaction with DNA', *J Biol Chem,* 272(7), 4600-5.

Bluyssen, H. A., Muzaffar, R., Vlieststra, R. J., van der Made, A. C., Leung, S., Stark, G. R., Kerr, I. M., Trapman, J. and Levy, D. E. (1995) 'Combinatorial association and abundance of components of interferon-stimulated gene factor 3 dictate the selectivity of interferon responses', *Proc Natl Acad Sci U S A,* 92(12), 5645-9.

Buono, C., Come, C. E., Stavrakis, G., Maguire, G. F., Connelly, P. W. and Lichtman, A. H. (2003) 'Influence of interferon-gamma on the extent and phenotype of diet-induced atherosclerosis in the LDLR-deficient mouse', *Arterioscler Thromb Vasc Biol,* 23(3), 454-60.

Califf, R. M. (2018) 'Biomarker definitions and their applications', *Exp Biol Med (Maywood),* 243(3), 213-221.

Campbell, L. A. and Rosenfeld, M. E. (2015) 'Infection and Atherosclerosis Development', *Arch Med Res,* 46(5), 339-50.

Cao, Z. H., Zheng, Q. Y., Li, G. Q., Hu, X. B., Feng, S. L., Xu, G. L. and Zhang, K. Q. (2015) 'STAT1-mediated down-regulation of Bcl-2 expression is involved in IFN-γ/TNF-α-induced apoptosis in NIT-1 cells', *PLoS One,* 10(3), e0120921.

Casbon, A. J., Long, M. E., Dunn, K. W., Allen, L. A. and Dinauer, M. C. (2012) 'Effects of IFN-γ on intracellular trafficking and activity of macrophage NADPH oxidase flavocytochrome b558', *J Leukoc Biol,* 92(4), 869-82.

Casolaro, V., Georas, S. N., Song, Z., Zubkoff, I. D., Abdulkadir, S. A., Thanos, D. and Ono, S. J. (1995) 'Inhibition of NF-AT-dependent transcription by NF-kappa B: implications for differential gene expression in T helper cell subsets', *Proc Natl Acad Sci U S A,* 92(25), 11623-7.

Chatterjee-Kishore, M., Wright, K. L., Ting, J. P. and Stark, G. R. (2000) 'How Stat1 mediates constitutive gene expression: a complex of unphosphorylated Stat1 and IRF1 supports transcription of the LMP2 gene', *EMBO J,* 19(15), 4111-22.

Chmielewski, S., Olejnik, A., Sikorski, K., Pelisek, J., Błaszczyk, K., Aoqui, C., Nowicka, H., Zernecke, A., Heemann, U., Wesoly, J., Baumann, M. and Bluyssen, H. A. (2014) 'STAT1-dependent signal integration between IFNγ and TLR4 in vascular cells reflect pro-atherogenic responses in human atherosclerosis', *PLoS One,* 9(12), e113318.

Chmielewski, S., Piaszyk-Borychowska, A., Wesoly, J. and Bluyssen, H. A. (2016) 'STAT1 and IRF8 in Vascular Inflammation and Cardiovascular Disease: Diagnostic and Therapeutic Potential', *Int Rev Immunol,* 35(5), 434-454.

Chu, S. H., Lim, J. W., Kim, D. G., Lee, E. S., Kim, K. H. and Kim, H. (2011) 'Down-regulation of Bcl-2 is mediated by NF-κB activation in Helicobacter pylori-induced apoptosis of gastric epithelial cells', *Scand J Gastroenterol,* 46(2), 148-55.

Chung, H. Y., Cesari, M., Anton, S., Marzetti, E., Giovannini, S., Seo, A. Y., Carter, C., Yu, B. P. and Leeuwenburgh, C. (2009) 'Molecular inflammation: underpinnings of aging and age-related diseases', *Ageing Res Rev,* 8(1), 18-30.

Clarke, D. L., Clifford, R. L., Jindarat, S., Proud, D., Pang, L., Belvisi, M. and Knox, A. J. (2010) 'TNFα and IFNγ synergistically enhance transcriptional activation of CXCL10 in human airway smooth muscle cells via STAT-1, NF-κB, and the transcriptional coactivator CREB-binding protein', *J Biol Chem,* 285(38), 29101-10.

Consortium, E. P. (2012) 'An integrated encyclopedia of DNA elements in the human genome', *Nature,* 489(7414), 57-74.

Creyghton, M. P., Cheng, A. W., Welstead, G. G., Kooistra, T., Carey, B. W., Steine, E. J., Hanna, J., Lodato, M. A., Frampton, G. M., Sharp, P. A., Boyer, L. A., Young, R. A. and Jaenisch, R. (2010) 'Histone H3K27ac separates active from poised enhancers and predicts developmental state', *Proc Natl Acad Sci U S A,* 107(50), 21931-6.

Cusanovich, D. A., Pavlovic, B., Pritchard, J. K. and Gilad, Y. (2014) 'The functional consequences of variation in transcription factor binding', *PLoS Genet,* 10(3), e1004226.

Cutter, A. R. and Hayes, J. J. (2015) 'A brief review of nucleosome structure', *FEBS Lett,* 589(20 Pt A), 2914-22.

Darnell, J. E., Kerr, I. M. and Stark, G. R. (1994) 'Jak-STAT pathways and transcriptional activation in response to IFNs and other extracellular signaling proteins', *Science,* 264(5164), 1415-21.

Decker, T., Lew, D. J., Cheng, Y. S., Levy, D. E. and Darnell, J. E. (1989) 'Interactions of alpha- and gamma-interferon in the transcriptional regulation of the gene encoding a guanylate-binding protein', *EMBO J,* 8(7), 2009-14.

Denny, M. F., Thacker, S., Mehta, H., Somers, E. C., Dodick, T., Barrat, F. J., McCune, W. J. and Kaplan, M. J. (2007) 'Interferon-alpha promotes abnormal vasculogenesis in lupus: a potential pathway for premature atherosclerosis', *Blood,* 110(8), 2907-15.

Di-Poï, N., Desvergne, B., Michalik, L. and Wahli, W. (2005) 'Transcriptional repression of peroxisome proliferator-activated receptor beta/delta in murine keratinocytes by CCAAT/enhancer-binding proteins', *J Biol Chem,* 280(46), 38700-10.

Doran, A. C., Meller, N. and McNamara, C. A. (2008) 'Role of smooth muscle cells in the initiation and early progression of atherosclerosis', *Arterioscler Thromb Vasc Biol,* 28(5), 812-9.

Edfeldt, K., Swedenborg, J., Hansson, G. K. and Yan, Z. Q. (2002) 'Expression of toll-like receptors in human atherosclerotic lesions: a possible pathway for plaque activation', *Circulation*, 105(10), 1158-61.

EPIC-CVD (2015) '*http://www.epiccvd.eu/frontpage/the-epic-cvd-study.html* ', [online], available].

Evanko, S. P., Angello, J. C. and Wight, T. N. (1999) 'Formation of hyaluronan- and versican-rich pericellular matrix is required for proliferation and migration of vascular smooth muscle cells', *Arterioscler Thromb Vasc Biol*, 19(4), 1004-13.

Farlik, M., Reutterer, B., Schindler, C., Greten, F., Vogl, C., Müller, M. and Decker, T. (2010) 'Nonconventional initiation complex assembly by STAT and NF-kappaB transcription factors regulates nitric oxide synthase expression', *Immunity*, 33(1), 25-34.

FDA-NIH, B. W. G. (2016) *BEST (Biomarkers, EndpointS, and other Tools) Resource*.

Feng, R., Desbordes, S. C., Xie, H., Tillo, E. S., Pixley, F., Stanley, E. R. and Graf, T. (2008) 'PU.1 and C/EBPalpha/beta convert fibroblasts into macrophage-like cells', *Proc Natl Acad Sci U S A*, 105(16), 6057-62.

Findeisen, H. M., Gizard, F., Zhao, Y., Qing, H., Heywood, E. B., Jones, K. L., Cohn, D. and Bruemmer, D. (2011) 'Epigenetic regulation of vascular smooth muscle cell proliferation and neointima formation by histone deacetylase inhibition', *Arterioscler Thromb Vasc Biol*, 31(4), 851-60.

Firestein, G. S. and McInnes, I. B. (2017) 'Immunopathogenesis of Rheumatoid Arthritis', *Immunity*, 46(2), 183-196.

Foks, A. C., Bot, I., Frodermann, V., de Jager, S. C., Ter Borg, M., van Santbrink, P. J., Yagita, H., Kuiper, J. and van Puijvelde, G. H. (2012) 'Interference of the CD30-CD30L pathway reduces atherosclerosis development', *Arterioscler Thromb Vasc Biol*, 32(12), 2862-8.

Freaney, J. E., Kim, R., Mandhana, R. and Horvath, C. M. (2013) 'Extensive cooperation of immune master regulators IRF3 and NFκB in RNA Pol II recruitment and pause release in human innate antiviral transcription', *Cell Rep*, 4(5), 959-73.

Frodermann, V. and Nahrendorf, M. (2018) 'Macrophages and Cardiovascular Health', *Physiol Rev*, 98(4), 2523-2569.

Galasko, D. and Montine, T. J. (2010) 'Biomarkers of oxidative damage and inflammation in Alzheimer's disease', *Biomark Med*, 4(1), 27-36.

Ganster, R. W., Guo, Z., Shao, L. and Geller, D. A. (2005) 'Differential effects of TNF-alpha and IFN-gamma on gene transcription mediated by NF-kappaB-Stat1 interactions', *J Interferon Cytokine Res*, 25(11), 707-19.

Ganster, R. W., Taylor, B. S., Shao, L. and Geller, D. A. (2001) 'Complex regulation of human inducible nitric oxide synthase gene transcription by Stat 1 and NF-kappa B', *Proc Natl Acad Sci U S A*, 98(15), 8638-43.

Garber, M., Yosef, N., Goren, A., Raychowdhury, R., Thielke, A., Guttman, M., Robinson, J., Minie, B., Chevrier, N., Itzhaki, Z., Blecher-Gonen, R., Bornstein, C., Amann-Zalcenstein, D., Weiner, A., Friedrich, D., Meldrim, J., Ram, O., Cheng, C., Gnirke, A., Fisher, S., Friedman, N., Wong, B., Bernstein, B. E., Nusbaum, C., Hacohen, N., Regev, A. and Amit, I. (2012) 'A high-throughput chromatin immunoprecipitation approach reveals principles of dynamic gene regulation in mammals', *Mol Cell*, 47(5), 810-22.

Ghislain, J. J., Wong, T., Nguyen, M. and Fish, E. N. (2001) 'The interferon-inducible Stat2:Stat1 heterodimer preferentially binds in vitro to a consensus element found in the promoters of a subset of interferon-stimulated genes', *J Interferon Cytokine Res*, 21(6), 379-88.

Ghisletti, S., Barozzi, I., Mietton, F., Polletti, S., De Santa, F., Venturini, E., Gregory, L., Lonie, L., Chew, A., Wei, C. L., Ragoussis, J. and Natoli, G. (2010) 'Identification and characterization of enhancers controlling the inflammatory gene expression program in macrophages', *Immunity*, 32(3), 317-28.

Ghosh, A. and Vaughan, D. (2018) 'Epigenetic Treatment Approaches to Cardiovascular Disease' in *Epigenetics in Human Disease*.

Gilmore, T. D. (2006) 'Introduction to NF-kappaB: players, pathways, perspectives', *Oncogene*, 25(51), 6680-4.

Gimbrone, M. A., Topper, J. N., Nagel, T., Anderson, K. R. and Garcia-Cardeña, G. (2000) 'Endothelial dysfunction, hemodynamic forces, and atherogenesis', *Ann N Y Acad Sci*, 902, 230-9; discussion 239-40.

Giorgetti, L., Siggers, T., Tiana, G., Caprara, G., Notarbartolo, S., Corona, T., Pasparakis, M., Milani, P., Bulyk, M. L. and Natoli, G. (2010) 'Noncooperative interactions between transcription factors and clustered DNA binding sites enable graded transcriptional responses to environmental inputs', *Mol Cell*, 37(3), 418-28.

Goossens, P., Gijbels, M. J., Zernecke, A., Eijgelaar, W., Vergouwe, M. N., van der Made, I., Vanderlocht, J., Beckers, L., Buurman, W. A., Daemen, M. J., Kalinke, U., Weber, C., Lutgens, E. and de Winther, M. P. (2010) 'Myeloid type I interferon signaling promotes atherosclerosis by stimulating macrophage recruitment to lesions', *Cell Metab*, 12(2), 142-53.

Gosselin, D. and Glass, C. K. (2014) 'Epigenomics of macrophages', *Immunol Rev*, 262(1), 96-112.

Gough, D. J., Levy, D. E., Johnstone, R. W. and Clarke, C. J. (2008) 'IFNgamma signaling-does it mean JAK-STAT?', *Cytokine Growth Factor Rev*, 19(5-6), 383-94.

Grivennikov, S. I., Greten, F. R. and Karin, M. (2010) 'Immunity, inflammation, and cancer', *Cell*, 140(6), 883-99.

Gupta, S., Pablo, A. M., Jiang, X., Wang, N., Tall, A. R. and Schindler, C. (1997) 'IFN-gamma potentiates atherosclerosis in ApoE knock-out mice', *J Clin Invest*, 99(11), 2752-61.

Hamm, C. W., Bassand, J. P., Agewall, S., Bax, J., Boersma, E., Bueno, H., Caso, P., Dudek, D., Gielen, S., Huber, K., Ohman, M., Petrie, M. C., Sonntag, F., Uva, M. S., Storey, R. F., Wijns, W., Zahger, D. and Guidelines, E. C. f. P. (2011) 'ESC Guidelines for the management of acute coronary syndromes in patients presenting without persistent ST-segment elevation: The Task Force for the management of acute coronary syndromes (ACS) in patients presenting without persistent ST-segment elevation of the European Society of Cardiology (ESC)', *Eur Heart J*, 32(23), 2999-3054.

Hansson, G. K. (2005) 'Inflammation, atherosclerosis, and coronary artery disease', *N Engl J Med*, 352(16), 1685-95.

Hansson, G. K. and Hermansson, A. (2011) 'The immune system in atherosclerosis', *Nat Immunol*, 12(3), 204-12.

Harrington, S. C., Simari, R. D. and Conover, C. A. (2007) 'Genetic deletion of pregnancy-associated plasma protein-A is associated with resistance to atherosclerotic lesion development in apolipoprotein E-deficient mice challenged with a high-fat diet', *Circ Res,* 100(12), 1696-702.

Hasanov, Z., Ruckdeschel, T., König, C., Mogler, C., Kapel, S. S., Korn, C., Spegg, C., Eichwald, V., Wieland, M., Appak, S. and Augustin, H. G. (2017) 'Endosialin Promotes Atherosclerosis Through Phenotypic Remodeling of Vascular Smooth Muscle Cells', *Arterioscler Thromb Vasc Biol,* 37(3), 495-505.

Hayden, M. S. and Ghosh, S. (2012) 'NF-κB, the first quarter-century: remarkable progress and outstanding questions', *Genes Dev,* 26(3), 203-34.

Hayes, M. P., Freeman, S. L. and Donnelly, R. P. (1995) 'IFN-gamma priming of monocytes enhances LPS-induced TNF production by augmenting both transcription and MRNA stability', *Cytokine,* 7(5), 427-35.

Heinz, S., Benner, C., Spann, N., Bertolino, E., Lin, Y. C., Laslo, P., Cheng, J. X., Murre, C., Singh, H. and Glass, C. K. (2010) 'Simple combinations of lineage-determining transcription factors prime cis-regulatory elements required for macrophage and B cell identities', *Mol Cell,* 38(4), 576-89.

Heinz, S. and Glass, C. K. (2012) 'Roles of lineage-determining transcription factors in establishing open chromatin: lessons from high-throughput studies', *Curr Top Microbiol Immunol,* 356, 1-15.

Heinz, S., Romanoski, C. E., Benner, C. and Glass, C. K. (2015) 'The selection and function of cell type-specific enhancers', *Nat Rev Mol Cell Biol,* 16(3), 144-54.

Hertzog, P. J., O'Neill, L. A. and Hamilton, J. A. (2003) 'The interferon in TLR signaling: more than just antiviral', *Trends Immunol,* 24(10), 534-9.

Higashimori, M., Tatro, J. B., Moore, K. J., Mendelsohn, M. E., Galper, J. B. and Beasley, D. (2011) 'Role of toll-like receptor 4 in intimal foam cell accumulation in apolipoprotein E-deficient mice', *Arterioscler Thromb Vasc Biol,* 31(1), 50-7.

Hiroi, M., Mori, K., Sakaeda, Y., Shimada, J. and Ohmori, Y. (2009) 'STAT1 represses hypoxia-inducible factor-1-mediated transcription', *Biochem Biophys Res Commun,* 387(4), 806-10.

Hiroi, M. and Ohmori, Y. (2003) 'The transcriptional coactivator CREB-binding protein cooperates with STAT1 and NF-kappa B for synergistic transcriptional activation of the CXC ligand 9/monokine induced by interferon-gamma gene', *J Biol Chem,* 278(1), 651-60.

Ho, J., Pelzel, C., Begitt, A., Mee, M., Elsheikha, H. M., Scott, D. J. and Vinkemeier, U. (2016) 'STAT2 Is a Pervasive Cytokine Regulator due to Its Inhibition of STAT1 in Multiple Signaling Pathways', *PLoS Biol,* 14(10), e2000117.

Hoeksema, M. A. and Glass, C. K. (2019) 'Nature and nurture of tissue-specific macrophage phenotypes', *Atherosclerosis,* 281, 159-167.

Horgan, C. P., Hanscom, S. R. and McCaffrey, M. W. (2013) 'GRAB is a binding partner for the Rab11a and Rab11b GTPases', *Biochem Biophys Res Commun,* 441(1), 214-9.

Horvai, A. E., Xu, L., Korzus, E., Brard, G., Kalafus, D., Mullen, T. M., Rose, D. W., Rosenfeld, M. G. and Glass, C. K. (1997) 'Nuclear integration of JAK/STAT and Ras/AP-1 signaling by CBP and p300', *Proc Natl Acad Sci U S A,* 94(4), 1074-9.

Hu, X., Chakravarty, S. D. and Ivashkiv, L. B. (2008) 'Regulation of interferon and Toll-like receptor signaling during macrophage activation by opposing feedforward and feedback inhibition mechanisms', *Immunol Rev*, 226, 41-56.

Hu, X., Chen, J., Wang, L. and Ivashkiv, L. B. (2007) 'Crosstalk among Jak-STAT, Toll-like receptor, and ITAM-dependent pathways in macrophage activation', *J Leukoc Biol*, 82(2), 237-43.

Hu, X. and Ivashkiv, L. B. (2009) 'Cross-regulation of signaling pathways by interferon-gamma: implications for immune responses and autoimmune diseases', *Immunity*, 31(4), 539-50.

Hulsen, T., de Vlieg, J. and Alkema, W. (2008) 'BioVenn - a web application for the comparison and visualization of biological lists using area-proportional Venn diagrams', *BMC Genomics*, 9, 488.

Ihle, J. N. (2001) 'The Stat family in cytokine signaling', *Curr Opin Cell Biol*, 13(2), 211-7.

ISAACS, A. and LINDENMANN, J. (1957) 'Virus interference. I. The interferon', *Proc R Soc Lond B Biol Sci*, 147(927), 258-67.

Jin, F., Li, Y., Ren, B. and Natarajan, R. (2011) 'PU.1 and C/EBP(alpha) synergistically program distinct response to NF-kappaB activation through establishing monocyte specific enhancers', *Proc Natl Acad Sci U S A*, 108(13), 5290-5.

Jonasson, L., Holm, J., Skalli, O., Bondjers, G. and Hansson, G. K. (1986) 'Regional accumulations of T cells, macrophages, and smooth muscle cells in the human atherosclerotic plaque', *Arteriosclerosis*, 6(2), 131-8.

Jonkers, I., Kwak, H. and Lis, J. T. (2014) 'Genome-wide dynamics of Pol II elongation and its interplay with promoter proximal pausing, chromatin, and exons', *Elife*, 3, e02407.

Juul, A., Scheike, T., Davidsen, M., Gyllenborg, J. and Jørgensen, T. (2002) 'Low serum insulin-like growth factor I is associated with increased risk of ischemic heart disease: a population-based case-control study', *Circulation*, 106(8), 939-44.

Kavurma, M. M., Rayner, K. J. and Karunakaran, D. (2017) 'The walking dead: macrophage inflammation and death in atherosclerosis', *Curr Opin Lipidol*, 28(2), 91-98.

Kawai, T. and Akira, S. (2010) 'The role of pattern-recognition receptors in innate immunity: update on Toll-like receptors', *Nat Immunol*, 11(5), 373-84.

Khansari, N., Shakiba, Y. and Mahmoudi, M. (2009) 'Chronic inflammation and oxidative stress as a major cause of age-related diseases and cancer', *Recent Pat Inflamm Allergy Drug Discov*, 3(1), 73-80.

Kimura, T., Kadokawa, Y., Harada, H., Matsumoto, M., Sato, M., Kashiwazaki, Y., Tarutani, M., Tan, R. S., Takasugi, T., Matsuyama, T., Mak, T. W., Noguchi, S. and Taniguchi, T. (1996) 'Essential and non-redundant roles of p48 (ISGF3 gamma) and IRF-1 in both type I and type II interferon responses, as revealed by gene targeting studies', *Genes Cells*, 1(1), 115-24.

Kiu, H. and Nicholson, S. E. (2012) 'Biology and significance of the JAK/STAT signalling pathways', *Growth Factors*, 30(2), 88-106.

Kleinert, H., Schwarz, P. M. and Förstermann, U. (2003) 'Regulation of the expression of inducible nitric oxide synthase', *Biol Chem*, 384(10-11), 1343-64.

Kobayashi, M., Inoue, K., Warabi, E., Minami, T. and Kodama, T. (2005) 'A simple method of isolating mouse aortic endothelial cells', *J Atheroscler Thromb*, 12(3), 138-42.

Kortylewski, M. and Nechaev, S. (2014) 'Cancer therapy using oligonucleotide-based STAT3 inhibitors: will they deliver?', *Ther Deliv,* 5(3), 239-42.

Korzus, E., Torchia, J., Rose, D. W., Xu, L., Kurokawa, R., McInerney, E. M., Mullen, T. M., Glass, C. K. and Rosenfeld, M. G. (1998) 'Transcription factor-specific requirements for coactivators and their acetyltransferase functions', *Science,* 279(5351), 703-7.

Kouzarides, T. (2007) 'Chromatin modifications and their function', *Cell,* 128(4), 693-705.

Kraus, T. A., Lau, J. F., Parisien, J. P. and Horvath, C. M. (2003) 'A hybrid IRF9-STAT2 protein recapitulates interferon-stimulated gene expression and antiviral response', *J Biol Chem,* 278(15), 13033-8.

Krämer, O. H., Baus, D., Knauer, S. K., Stein, S., Jäger, E., Stauber, R. H., Grez, M., Pfitzner, E. and Heinzel, T. (2006) 'Acetylation of Stat1 modulates NF-kappaB activity', *Genes Dev,* 20(4), 473-85.

Kumatori, A., Yang, D., Suzuki, S. and Nakamura, M. (2002) 'Cooperation of STAT-1 and IRF-1 in interferon-gamma-induced transcription of the gp91(phox) gene', *J Biol Chem,* 277(11), 9103-11.

Kusaba, K., Kai, H., Koga, M., Takayama, N., Ikeda, A., Yasukawa, H., Seki, Y., Egashira, K. and Imaizumi, T. (2007) 'Inhibition of intrinsic interferon-gamma function prevents neointima formation after balloon injury', *Hypertension,* 49(4), 909-15.

Kwon, A. T., Arenillas, D. J., Worsley Hunt, R. and Wasserman, W. W. (2012) 'oPOSSUM-3: advanced analysis of regulatory motif over-representation across genes or ChIP-Seq datasets', *G3 (Bethesda),* 2(9), 987-1002.

Kwon, H., Thierry-Mieg, D., Thierry-Mieg, J., Kim, H. P., Oh, J., Tunyaplin, C., Carotta, S., Donovan, C. E., Goldman, M. L., Tailor, P., Ozato, K., Levy, D. E., Nutt, S. L., Calame, K. and Leonard, W. J. (2009) 'Analysis of interleukin-21-induced Prdm1 gene regulation reveals functional cooperation of STAT3 and IRF4 transcription factors', *Immunity,* 31(6), 941-52.

Langlais, D., Barreiro, L. B. and Gros, P. (2016) 'The macrophage IRF8/IRF1 regulome is required for protection against infections and is associated with chronic inflammation', *J Exp Med,* 213(4), 585-603.

Laughlin, G. A., Barrett-Connor, E., Criqui, M. H. and Kritz-Silverstein, D. (2004) 'The prospective association of serum insulin-like growth factor I (IGF-I) and IGF-binding protein-1 levels with all cause and cardiovascular disease mortality in older adults: the Rancho Bernardo Study', *J Clin Endocrinol Metab,* 89(1), 114-20.

Lee, H. B., Kim, Y., Yoo, H., Lee, J. M., Kim, Y. K., Kim, N. K., Kim, J. K. and Oh, S. H. (2014) 'Blood genomic profiling in extracranial- and intracranial atherosclerosis in ischemic stroke patients', *Thromb Res,* 134(3), 686-92.

Lefterova, M. I., Steger, D. J., Zhuo, D., Qatanani, M., Mullican, S. E., Tuteja, G., Manduchi, E., Grant, G. R. and Lazar, M. A. (2010) 'Cell-specific determinants of peroxisome proliferator-activated receptor gamma function in adipocytes and macrophages', *Mol Cell Biol,* 30(9), 2078-89.

Legube, G. and Trouche, D. (2003) 'Regulating histone acetyltransferases and deacetylases', *EMBO Rep,* 4(10), 944-7.

Leon, M. L. and Zuckerman, S. H. (2005) 'Gamma interferon: a central mediator in atherosclerosis', *Inflamm Res,* 54(10), 395-411.

Leucker, T. M., Nomura, Y., Kim, J. H., Bhatta, A., Wang, V., Wecker, A., Jandu, S., Santhanam, L., Berkowitz, D., Romer, L. and Pandey, D. (2017) 'Cystathionine γ-lyase protects vascular endothelium: a role for inhibition of histone deacetylase 6', *Am J Physiol Heart Circ Physiol,* 312(4), H711-H720.

Levine, M. (2010) 'Transcriptional enhancers in animal development and evolution', *Curr Biol,* 20(17), R754-63.

Levy, D. E. and Darnell, J. E. (2002) 'Stats: transcriptional control and biological impact', *Nat Rev Mol Cell Biol,* 3(9), 651-62.

Levy, Z., Rachmani, R., Trestman, S., Dvir, A., Shaish, A., Ravid, M. and Harats, D. (2003) 'Low-dose interferon-alpha accelerates atherosclerosis in an LDL receptor-deficient mouse model', *Eur J Intern Med,* 14(8), 479-483.

Li, C., Hong, Y., Tan, Y. X., Zhou, H., Ai, J. H., Li, S. J., Zhang, L., Xia, Q. C., Wu, J. R., Wang, H. Y. and Zeng, R. (2004) 'Accurate qualitative and quantitative proteomic analysis of clinical hepatocellular carcinoma using laser capture microdissection coupled with isotope-coded affinity tag and two-dimensional liquid chromatography mass spectrometry', *Mol Cell Proteomics,* 3(4), 399-409.

Li, H., Cybulsky, M. I., Gimbrone, M. A. and Libby, P. (1993) 'Inducible expression of vascular cell adhesion molecule-1 by vascular smooth muscle cells in vitro and within rabbit atheroma', *Am J Pathol,* 143(6), 1551-9.

Li, H. and Durbin, R. (2009) 'Fast and accurate short read alignment with Burrows-Wheeler transform', *Bioinformatics,* 25(14), 1754-60.

Li, H., Freeman, M. W. and Libby, P. (1995) 'Regulation of smooth muscle cell scavenger receptor expression in vivo by atherogenic diets and in vitro by cytokines', *J Clin Invest,* 95(1), 122-33.

Li, J., Fu, Q., Cui, H., Qu, B., Pan, W., Shen, N. and Bao, C. (2011) 'Interferon-α priming promotes lipid uptake and macrophage-derived foam cell formation: a novel link between interferon-α and atherosclerosis in lupus', *Arthritis Rheum,* 63(2), 492-502.

Li, M., Pascual, G. and Glass, C. K. (2000) 'Peroxisome proliferator-activated receptor gamma-dependent repression of the inducible nitric oxide synthase gene', *Mol Cell Biol,* 20(13), 4699-707.

Li, S., Wang, D. Z., Wang, Z., Richardson, J. A. and Olson, E. N. (2003) 'The serum response factor coactivator myocardin is required for vascular smooth muscle development', *Proc Natl Acad Sci U S A,* 100(16), 9366-70.

Li, X., Leung, S., Qureshi, S., Darnell, J. E. and Stark, G. R. (1996) 'Formation of STAT1-STAT2 heterodimers and their role in the activation of IRF-1 gene transcription by interferon-alpha', *J Biol Chem,* 271(10), 5790-4.

Libby, P. (2006) 'Inflammation and cardiovascular disease mechanisms', *Am J Clin Nutr,* 83(2), 456S-460S.

Lim, C. A., Yao, F., Wong, J. J., George, J., Xu, H., Chiu, K. P., Sung, W. K., Lipovich, L., Vega, V. B., Chen, J., Shahab, A., Zhao, X. D., Hibberd, M., Wei, C. L., Lim, B., Ng, H. H., Ruan, Y. and Chin, K. C. (2007) 'Genome-wide mapping of RELA(p65) binding identifies E2F1 as a transcriptional activator recruited by NF-kappaB upon TLR4 activation', *Mol Cell,* 27(4), 622-35.

Lin, C. C., Tseng, H. W., Hsieh, H. L., Lee, C. W., Wu, C. Y., Cheng, C. Y. and Yang, C. M. (2008) 'Tumor necrosis factor-alpha induces MMP-9 expression via p42/p44 MAPK, JNK, and nuclear factor-kappaB in A549 cells', *Toxicol Appl Pharmacol*, 229(3), 386-98.

Lin, Y., Bai, L., Chen, W. and Xu, S. (2010) 'The NF-kappaB activation pathways, emerging molecular targets for cancer prevention and therapy', *Expert Opin Ther Targets*.

Liu, C., Lu, J., Tan, J., Li, L. and Huang, B. (2004) 'Human interleukin-5 expression is synergistically regulated by histone acetyltransferase CBP/p300 and transcription factors C/EBP, NF-AT and AP-1', *Cytokine*, 27(4-5), 93-100.

Liu, J. and Ma, X. (2006) 'Interferon regulatory factor 8 regulates RANTES gene transcription in cooperation with interferon regulatory factor-1, NF-kappaB, and PU.1', *J Biol Chem*, 281(28), 19188-95.

Liu, M., Li, Z., Yang, J., Jiang, Y., Chen, Z., Ali, Z., He, N. and Wang, Z. (2016) 'Cell-specific biomarkers and targeted biopharmaceuticals for breast cancer treatment', *Cell Prolif*, 49(4), 409-20.

Liu, M., Mendicino, M., Ning, Q., Ghanekar, A., He, W., McGilvray, I., Shalev, I., Pivato, D., Clark, D. A., Phillips, M. J. and Levy, G. A. (2006) 'Cytokine-induced hepatic apoptosis is dependent on FGL2/fibroleukin: the role of Sp1/Sp3 and STAT1/PU.1 composite cis elements', *J Immunol*, 176(11), 7028-38.

Lu, Z., Zhang, X., Li, Y., Jin, J. and Huang, Y. (2013) 'TLR4 antagonist reduces early-stage atherosclerosis in diabetic apolipoprotein E-deficient mice', *J Endocrinol*, 216(1), 61-71.

Lutgens, E., Bochaton-Piallat, M.-L. and Weber, C. (2017) '*Atherosclerosis: cellular mechanisms*' in *The ESC Textbook of Vascular Biology*.

Lutz, M. B., Kukutsch, N., Ogilvie, A. L., Rössner, S., Koch, F., Romani, N. and Schuler, G. (1999) 'An advanced culture method for generating large quantities of highly pure dendritic cells from mouse bone marrow', *J Immunol Methods*, 223(1), 77-92.

López-Mejías, R., Corrales, A., Genre, F., Hernández, J. L., Ochoa, R., Blanco, R., González-Juanatey, C., Martín, J., Llorca, J. and González-Gay, M. A. (2013) 'Angiopoietin-2 serum levels correlate with severity, early onset and cardiovascular disease in patients with rheumatoid arthritis', *Clin Exp Rheumatol*, 31(5), 761-6.

López-Mejías, R., Genre, F., González-Juanatey, C. and González-Gay, M. A. (2014) 'Autoantibodies and biomarkers of endothelial cell activation in atherosclerosis', *Vasa*, 43(2), 83-5.

Ma, Z., Chang, M. J., Shah, R. C. and Benveniste, E. N. (2005) 'Interferon-gamma-activated STAT-1alpha suppresses MMP-9 gene transcription by sequestration of the coactivators CBP/p300', *J Leukoc Biol*, 78(2), 515-23.

Mahlakõiv, T., Hernandez, P., Gronke, K., Diefenbach, A. and Staeheli, P. (2015) 'Leukocyte-derived IFN-α/β and epithelial IFN-λ constitute a compartmentalized mucosal defense system that restricts enteric virus infections', *PLoS Pathog*, 11(4), e1004782.

Majoros, A., Platanitis, E., Kernbauer-Hölzl, E., Rosebrock, F., Müller, M. and Decker, T. (2017) 'Canonical and Non-Canonical Aspects of JAK-STAT Signaling: Lessons from Interferons for Cytokine Responses', *Front Immunol*, 8, 29.

Majumder, S., Zhou, L. Z., Chaturvedi, P., Babcock, G., Aras, S. and Ransohoff, R. M. (1998) 'p48/STAT-1alpha-containing complexes play a predominant role in induction of IFN-gamma-

inducible protein, 10 kDa (IP-10) by IFN-gamma alone or in synergy with TNF-alpha', *J Immunol,* 161(9), 4736-44.

Mallat, Z., Taleb, S., Ait-Oufella, H. and Tedgui, A. (2009) 'The role of adaptive T cell immunity in atherosclerosis', *J Lipid Res,* 50 Suppl, S364-9.

Manduteanu, I. and Simionescu, M. (2012) 'Inflammation in atherosclerosis: a cause or a result of vascular disorders?', *J Cell Mol Med,* 16(9), 1978-90.

Mano, T., Luo, Z., Malendowicz, S. L., Evans, T. and Walsh, K. (1999) 'Reversal of GATA-6 downregulation promotes smooth muscle differentiation and inhibits intimal hyperplasia in balloon-injured rat carotid artery', *Circ Res,* 84(6), 647-54.

Manzi, S. and Wasko, M. C. (2000) 'Inflammation-mediated rheumatic diseases and atherosclerosis', *Ann Rheum Dis,* 59(5), 321-5.

Matsumoto, M., Tanaka, N., Harada, H., Kimura, T., Yokochi, T., Kitagawa, M., Schindler, C. and Taniguchi, T. (1999) 'Activation of the transcription factor ISGF3 by interferon-gamma', *Biol Chem,* 380(6), 699-703.

Mehra, V. C., Ramgolam, V. S. and Bender, J. R. (2005) 'Cytokines and cardiovascular disease', *J Leukoc Biol,* 78(4), 805-18.

Meraz, M. A., White, J. M., Sheehan, K. C., Bach, E. A., Rodig, S. J., Dighe, A. S., Kaplan, D. H., Riley, J. K., Greenlund, A. C., Campbell, D., Carver-Moore, K., DuBois, R. N., Clark, R., Aguet, M. and Schreiber, R. D. (1996) 'Targeted disruption of the Stat1 gene in mice reveals unexpected physiologic specificity in the JAK-STAT signaling pathway', *Cell,* 84(3), 431-42.

Methe, H., Kim, J. O., Kofler, S., Weis, M., Nabauer, M. and Koglin, J. (2005) 'Expansion of circulating Toll-like receptor 4-positive monocytes in patients with acute coronary syndrome', *Circulation,* 111(20), 2654-61.

Methe, H., Zimmer, E., Grimm, C., Nabauer, M. and Koglin, J. (2004) 'Evidence for a role of toll-like receptor 4 in development of chronic allograft rejection after cardiac transplantation', *Transplantation,* 78(9), 1324-31.

Mi, H., Huang, X., Muruganujan, A., Tang, H., Mills, C., Kang, D. and Thomas, P. D. (2017) 'PANTHER version 11: expanded annotation data from Gene Ontology and Reactome pathways, and data analysis tool enhancements', *Nucleic Acids Res,* 45(D1), D183-D189.

Michalska, A., Blaszczyk, K., Wesoly, J. and Bluyssen, H. A. R. (2018) 'A Positive Feedback Amplifier Circuit That Regulates Interferon (IFN)-Stimulated Gene Expression and Controls Type I and Type II IFN Responses', *Front Immunol,* 9, 1135.

Michelsen, K. S., Wong, M. H., Shah, P. K., Zhang, W., Yano, J., Doherty, T. M., Akira, S., Rajavashisth, T. B. and Arditi, M. (2004) 'Lack of Toll-like receptor 4 or myeloid differentiation factor 88 reduces atherosclerosis and alters plaque phenotype in mice deficient in apolipoprotein E', *Proc Natl Acad Sci U S A,* 101(29), 10679-84.

Mikhaylova, L., Malmquist, J. and Nurminskaya, M. (2007) 'Regulation of in vitro vascular calcification by BMP4, VEGF and Wnt3a', *Calcif Tissue Int,* 81(5), 372-81.

Miklossy, G., Hilliard, T. S. and Turkson, J. (2013) 'Therapeutic modulators of STAT signalling for human diseases', *Nat Rev Drug Discov,* 12(8), 611-29.

Miller, J. L. and Grant, P. A. (2013) 'The role of DNA methylation and histone modifications in transcriptional regulation in humans', *Subcell Biochem,* 61, 289-317.

Minghetti, L. (2005) 'Role of inflammation in neurodegenerative diseases', *Curr Opin Neurol,* 18(3), 315-21.

Monaco, C. and Lutgens, E. (2017) '*Atherosclerosis - a short history*' in *The ESC Textbook of Vascular Biology*.

Montgomery, J. E. and Brown, J. R. (2013) 'Metabolic biomarkers for predicting cardiovascular disease', *Vasc Health Risk Manag,* 9, 37-45.

Moore, K. J. and Freeman, M. W. (2006) 'Scavenger receptors in atherosclerosis: beyond lipid uptake', *Arterioscler Thromb Vasc Biol,* 26(8), 1702-11.

Moore, K. J., Sheedy, F. J. and Fisher, E. A. (2013) 'Macrophages in atherosclerosis: a dynamic balance', *Nat Rev Immunol,* 13(10), 709-21.

Muhlethaler-Mottet, A., Di Berardino, W., Otten, L. A. and Mach, B. (1998) 'Activation of the MHC class II transactivator CIITA by interferon-gamma requires cooperative interaction between Stat1 and USF-1', *Immunity,* 8(2), 157-66.

Naik, V., Leaf, E. M., Hu, J. H., Yang, H. Y., Nguyen, N. B., Giachelli, C. M. and Speer, M. Y. (2012) 'Sources of cells that contribute to atherosclerotic intimal calcification: an in vivo genetic fate mapping study', *Cardiovasc Res,* 94(3), 545-54.

Nakajima, H., Brindle, P. K., Handa, M. and Ihle, J. N. (2001) 'Functional interaction of STAT5 and nuclear receptor co-repressor SMRT: implications in negative regulation of STAT5-dependent transcription', *EMBO J,* 20(23), 6836-44.

Nakano, T., Nakashima, Y., Yonemitsu, Y., Sumiyoshi, S., Chen, Y. X., Akishima, Y., Ishii, T., Iida, M. and Sueishi, K. (2005) 'Angiogenesis and lymphangiogenesis and expression of lymphangiogenic factors in the atherosclerotic intima of human coronary arteries', *Hum Pathol,* 36(4), 330-40.

Nathan, C. and Ding, A. (2010) 'Nonresolving inflammation', *Cell,* 140(6), 871-82.

Nechaev, S. and Adelman, K. (2011) 'Pol II waiting in the starting gates: Regulating the transition from transcription initiation into productive elongation', *Biochim Biophys Acta,* 1809(1), 34-45.

Negishi, H., Fujita, Y., Yanai, H., Sakaguchi, S., Ouyang, X., Shinohara, M., Takayanagi, H., Ohba, Y., Taniguchi, T. and Honda, K. (2006) 'Evidence for licensing of IFN-gamma-induced IFN regulatory factor 1 transcription factor by MyD88 in Toll-like receptor-dependent gene induction program', *Proc Natl Acad Sci U S A,* 103(41), 15136-41.

Nelson, P. S. and Montgomery, B. (2006) 'Cell type-specific analyses for identifying prostate cancer biomarkers', *Curr Urol Rep,* 7(1), 57-63.

Nobutoyo, M., Shuichi, U., Mitsuru, I., Takashi, U., Daisuke, T., Moritake, I., Kensuke, T., Yugo, Y., Yasuhiro, H., Hisashi, O., Noriko, S.-A., Akira, S., Mitsuru, A., Masaharu, A., Koji, H. and Hiromichi, W. (2018) 'Relationship Between VEGF-C Levels and Mortality in Patients with Peripheral Artery Disease', *European Cardiology Review*.

Nusinzon, I. and Horvath, C. M. (2005) 'Unexpected roles for deacetylation in interferon- and cytokine-induced transcription', *J Interferon Cytokine Res,* 25(12), 745-8.

O'Neill, L. A. and Pearce, E. J. (2016) 'Immunometabolism governs dendritic cell and macrophage function', *J Exp Med,* 213(1), 15-23.

Obata, H., Hayashi, K., Nishida, W., Momiyama, T., Uchida, A., Ochi, T. and Sobue, K. (1997) 'Smooth muscle cell phenotype-dependent transcriptional regulation of the alpha1 integrin gene', *J Biol Chem,* 272(42), 26643-51.

Ohmori, Y. and Hamilton, T. A. (1993) 'Cooperative interaction between interferon (IFN) stimulus response element and kappa B sequence motifs controls IFN gamma- and lipopolysaccharide-stimulated transcription from the murine IP-10 promoter', *J Biol Chem,* 268(9), 6677-88.

Ohmori, Y. and Hamilton, T. A. (2001) 'Requirement for STAT1 in LPS-induced gene expression in macrophages', *J Leukoc Biol,* 69(4), 598-604.

Oliveira, I. C., Mukaida, N., Matsushima, K. and Vilcek, J. (1994) 'Transcriptional inhibition of the interleukin-8 gene by interferon is mediated by the NF-kappa B site', *Mol Cell Biol,* 14(8), 5300-8.

Ordovás, J. M. and Smith, C. E. (2010) 'Epigenetics and cardiovascular disease', *Nat Rev Cardiol,* 7(9), 510-9.

Ouchi, T., Lee, S. W., Ouchi, M., Aaronson, S. A. and Horvath, C. M. (2000) 'Collaboration of signal transducer and activator of transcription 1 (STAT1) and BRCA1 in differential regulation of IFN-gamma target genes', *Proc Natl Acad Sci U S A,* 97(10), 5208-13.

Owens, G. K., Kumar, M. S. and Wamhoff, B. R. (2004) 'Molecular regulation of vascular smooth muscle cell differentiation in development and disease', *Physiol Rev,* 84(3), 767-801.

Ozato, K., Tailor, P. and Kubota, T. (2007) 'The interferon regulatory factor family in host defense: mechanism of action', *J Biol Chem,* 282(28), 20065-9.

Packard, R. R., Maganto-García, E., Gotsman, I., Tabas, I., Libby, P. and Lichtman, A. H. (2008) 'CD11c(+) dendritic cells maintain antigen processing, presentation capabilities, and CD4(+) T-cell priming efficacy under hypercholesterolemic conditions associated with atherosclerosis', *Circ Res,* 103(9), 965-73.

Pai, S. Y., Truitt, M. L. and Ho, I. C. (2004) 'GATA-3 deficiency abrogates the development and maintenance of T helper type 2 cells', *Proc Natl Acad Sci U S A,* 101(7), 1993-8.

Palii, C. G., Perez-Iratxeta, C., Yao, Z., Cao, Y., Dai, F., Davison, J., Atkins, H., Allan, D., Dilworth, F. J., Gentleman, R., Tapscott, S. J. and Brand, M. (2011) 'Differential genomic targeting of the transcription factor TAL1 in alternate haematopoietic lineages', *EMBO J,* 30(3), 494-509.

Pang, L., Zhang, C., Qin, J., Han, L., Li, R., Hong, C., He, H. and Wang, J. (2017) 'A novel strategy to achieve effective drug delivery: exploit cells as carrier combined with nanoparticles', *Drug Deliv,* 24(1), 83-91.

Paun, A. and Pitha, P. M. (2007) 'The IRF family, revisited', *Biochimie,* 89(6-7), 744-53.

Peng, S. L., Gerth, A. J., Ranger, A. M. and Glimcher, L. H. (2001) 'NFATc1 and NFATc2 together control both T and B cell activation and differentiation', *Immunity,* 14(1), 13-20.

Peri, F. and Calabrese, V. (2014) 'Toll-like receptor 4 (TLR4) modulation by synthetic and natural compounds: an update', *J Med Chem,* 57(9), 3612-22.

Phanstiel, D. H., Van Bortle, K., Spacek, D., Hess, G. T., Shamim, M. S., Machol, I., Love, M. I., Aiden, E. L., Bassik, M. C. and Snyder, M. P. (2017) 'Static and Dynamic DNA Loops form AP-1-Bound Activation Hubs during Macrophage Development', *Mol Cell*, 67(6), 1037-1048.e6.

Piaszyk-Borychowska, A., Széles, L., Csermely, A., Chiang, H. C., Wesoły, J., Lee, C. K., Nagy, L. and Bluyssen, H. A. R. (2019) 'Signal Integration of IFN-I and IFN-II With TLR4 Involves Sequential Recruitment of STAT1-Complexes and NFκB to Enhance Pro-inflammatory Transcription', *Front Immunol*, 10, 1253.

Pilz, A., Ramsauer, K., Heidari, H., Leitges, M., Kovarik, P. and Decker, T. (2003) 'Phosphorylation of the Stat1 transactivating domain is required for the response to type I interferons', *EMBO Rep*, 4(4), 368-73.

Platanitis, E. and Decker, T. (2018) 'Regulatory Networks Involving STATs, IRFs, and NFκB in Inflammation', *Front Immunol*, 9, 2542.

Plens-Galaska, M., Szelag, M., Collado, A., Marques, P., Vallejo, S., Ramos-González, M., Wesoly, J., Sanz, M. J., Peiró, C. and Bluyssen, H. A. R. (2018) 'Genome-Wide Inhibition of Pro-atherogenic Gene Expression by Multi-STAT Targeting Compounds as a Novel Treatment Strategy of CVDs', *Front Immunol*, 9, 2141.

Poat, B., Hazari, S., Chandra, P. K., Gunduz, F., Alvarez, X., Balart, L. A., Garry, R. F. and Dash, S. (2010) 'Intracellular expression of IRF9 Stat fusion protein overcomes the defective Jak-Stat signaling and inhibits HCV RNA replication', *Virol J*, 7, 265.

Prior, H. M. and Walter, M. A. (1996) 'SOX genes: architects of development', *Mol Med*, 2(4), 405-12.

Proost, P., Verpoest, S., Van de Borne, K., Schutyser, E., Struyf, S., Put, W., Ronsse, I., Grillet, B., Opdenakker, G. and Van Damme, J. (2004) 'Synergistic induction of CXCL9 and CXCL11 by Toll-like receptor ligands and interferon-gamma in fibroblasts correlates with elevated levels of CXCR3 ligands in septic arthritis synovial fluids', *J Leukoc Biol*, 75(5), 777-84.

Qiao, Y., Giannopoulou, E. G., Chan, C. H., Park, S. H., Gong, S., Chen, J., Hu, X., Elemento, O. and Ivashkiv, L. B. (2013) 'Synergistic activation of inflammatory cytokine genes by interferon-γ-induced chromatin remodeling and toll-like receptor signaling', *Immunity*, 39(3), 454-69.

Quinlan, A. R. and Hall, I. M. (2010) 'BEDTools: a flexible suite of utilities for comparing genomic features', *Bioinformatics*, 26(6), 841-2.

Rai, V. and Agrawal, D. K. (2017) 'The role of damage- and pathogen-associated molecular patterns in inflammation-mediated vulnerability of atherosclerotic plaques', *Can J Physiol Pharmacol*, 95(10), 1245-1253.

Ramana, C. V., Grammatikakis, N., Chernov, M., Nguyen, H., Goh, K. C., Williams, B. R. and Stark, G. R. (2000) 'Regulation of c-myc expression by IFN-gamma through Stat1-dependent and -independent pathways', *EMBO J*, 19(2), 263-72.

Ramsauer, K., Farlik, M., Zupkovitz, G., Seiser, C., Kröger, A., Hauser, H. and Decker, T. (2007) 'Distinct modes of action applied by transcription factors STAT1 and IRF1 to initiate transcription of the IFN-gamma-inducible gbp2 gene', *Proc Natl Acad Sci U S A*, 104(8), 2849-54.

Rao, N. A., McCalman, M. T., Moulos, P., Francoijs, K. J., Chatziioannou, A., Kolisis, F. N., Alexis, M. N., Mitsiou, D. J. and Stunnenberg, H. G. (2011) 'Coactivation of GR and NFKB alters the repertoire of their binding sites and target genes', *Genome Res*, 21(9), 1404-16.

Rauch, I., Rosebrock, F., Hainzl, E., Heider, S., Majoros, A., Wienerroither, S., Strobl, B., Stockinger, S., Kenner, L., Müller, M. and Decker, T. (2015) 'Noncanonical Effects of IRF9 in Intestinal Inflammation: More than Type I and Type III Interferons', *Mol Cell Biol*, 35(13), 2332-43.

Robertson, G., Hirst, M., Bainbridge, M., Bilenky, M., Zhao, Y., Zeng, T., Euskirchen, G., Bernier, B., Varhol, R., Delaney, A., Thiessen, N., Griffith, O. L., He, A., Marra, M., Snyder, M. and Jones, S. (2007) 'Genome-wide profiles of STAT1 DNA association using chromatin immunoprecipitation and massively parallel sequencing', *Nat Methods*, 4(8), 651-7.

Robinson, J. T., Thorvaldsdóttir, H., Winckler, W., Guttman, M., Lander, E. S., Getz, G. and Mesirov, J. P. (2011) 'Integrative genomics viewer', *Nat Biotechnol*, 29(1), 24-6.

Rong, J. X., Shapiro, M., Trogan, E. and Fisher, E. A. (2003) 'Transdifferentiation of mouse aortic smooth muscle cells to a macrophage-like state after cholesterol loading', *Proc Natl Acad Sci U S A*, 100(23), 13531-6.

Ross, R. (1999) 'Atherosclerosis--an inflammatory disease', *N Engl J Med*, 340(2), 115-26.

Sadowitz, B., Seymour, K., Gahtan, V. and Maier, K. G. (2012) 'The role of hyaluronic acid in atherosclerosis and intimal hyperplasia', *J Surg Res*, 173(2), e63-72.

Saliba, D. G., Heger, A., Eames, H. L., Oikonomopoulos, S., Teixeira, A., Blazek, K., Androulidaki, A., Wong, D., Goh, F. G., Weiss, M., Byrne, A., Pasparakis, M., Ragoussis, J. and Udalova, I. A. (2014) 'IRF5:RelA interaction targets inflammatory genes in macrophages', *Cell Rep*, 8(5), 1308-17.

Samuel, C. E. (2001) 'Antiviral actions of interferons', *Clin Microbiol Rev*, 14(4), 778-809, table of contents.

Sancéau, J., Boyd, D. D., Seiki, M. and Bauvois, B. (2002) 'Interferons inhibit tumor necrosis factor-alpha-mediated matrix metalloproteinase-9 activation via interferon regulatory factor-1 binding competition with NF-kappa B', *J Biol Chem*, 277(38), 35766-75.

Satoh, J. and Tabunoki, H. (2013) 'A Comprehensive Profile of ChIP-Seq-Based STAT1 Target Genes Suggests the Complexity of STAT1-Mediated Gene Regulatory Mechanisms', *Gene Regul Syst Bio*, 7, 41-56.

Schindler, C., Levy, D. E. and Decker, T. (2007) 'JAK-STAT signaling: from interferons to cytokines', *J Biol Chem*, 282(28), 20059-63.

Schindler, C. and Plumlee, C. (2008) 'Inteferons pen the JAK-STAT pathway', *Semin Cell Dev Biol*, 19(4), 311-8.

Schroder, K., Hertzog, P. J., Ravasi, T. and Hume, D. A. (2004) 'Interferon-gamma: an overview of signals, mechanisms and functions', *J Leukoc Biol*, 75(2), 163-89.

Schroder, K., Sweet, M. J. and Hume, D. A. (2006) 'Signal integration between IFNgamma and TLR signalling pathways in macrophages', *Immunobiology*, 211(6-8), 511-24.

Shankman, L. S., Gomez, D., Cherepanova, O. A., Salmon, M., Alencar, G. F., Haskins, R. M., Swiatlowska, P., Newman, A. A., Greene, E. S., Straub, A. C., Isakson, B., Randolph, G. J. and Owens, G. K. (2015) 'KLF4-dependent phenotypic modulation of smooth muscle cells has a key role in atherosclerotic plaque pathogenesis', *Nat Med*, 21(6), 628-37.

Shaw, M. (2010) 'Cell-specific biomarkers in renal medicine and research', *Methods Mol Biol*, 641, 271-302.

Shimokado, K., Yokota, T., Kato, N., Kosaka, C., Sasaguri, T., Masuda, J., Ogata, J. and Numano, F. (1994) 'Bidirectional regulation of smooth muscle cell proliferation by IFN-gamma', *J Atheroscler Thromb*, 1 Suppl 1, S29-33.

Shirai, T., Hilhorst, M., Harrison, D. G., Goronzy, J. J. and Weyand, C. M. (2015) 'Macrophages in vascular inflammation--From atherosclerosis to vasculitis', *Autoimmunity*, 48(3), 139-51.

Shlyueva, D., Stampfel, G. and Stark, A. (2014) 'Transcriptional enhancers: from properties to genome-wide predictions', *Nat Rev Genet*, 15(4), 272-86.

Siersbæk, M. S., Loft, A., Aagaard, M. M., Nielsen, R., Schmidt, S. F., Petrovic, N., Nedergaard, J. and Mandrup, S. (2012) 'Genome-wide profiling of peroxisome proliferator-activated receptor γ in primary epididymal, inguinal, and brown adipocytes reveals depot-selective binding correlated with gene expression', *Mol Cell Biol*, 32(17), 3452-63.

Sikorski, K., Chmielewski, S., Olejnik, A., Wesoly, J. Z., Heemann, U., Baumann, M. and Bluyssen, H. (2012) 'STAT1 as a central mediator of IFNγ and TLR4 signal integration in vascular dysfunction', *JAKSTAT*, 1(4), 241-9.

Sikorski, K., Wesoly, J. and Bluyssen, H. A. (2014) 'Data mining of atherosclerotic plaque transcriptomes predicts STAT1-dependent inflammatory signal integration in vascular disease', *Int J Mol Sci*, 15(8), 14313-31.

Slaton, J. W., Perrotte, P., Inoue, K., Dinney, C. P. and Fidler, I. J. (1999) 'Interferon-alpha-mediated down-regulation of angiogenesis-related genes and therapy of bladder cancer are dependent on optimization of biological dose and schedule', *Clin Cancer Res*, 5(10), 2726-34.

Smith, J. D., Peng, D. Q., Dansky, H. M., Settle, M., Baglione, J., Le Goff, W., Chakrabarti, E., Xu, Y. and Peng, X. (2006) 'Transcriptome profile of macrophages from atherosclerosis-sensitive and atherosclerosis-resistant mice', *Mamm Genome*, 17(3), 220-9.

Smith, N. L., Felix, J. F., Morrison, A. C., Demissie, S., Glazer, N. L., Loehr, L. R., Cupples, L. A., Dehghan, A., Lumley, T., Rosamond, W. D., Lieb, W., Rivadeneira, F., Bis, J. C., Folsom, A. R., Benjamin, E., Aulchenko, Y. S., Haritunians, T., Couper, D., Murabito, J., Wang, Y. A., Stricker, B. H., Gottdiener, J. S., Chang, P. P., Wang, T. J., Rice, K. M., Hofman, A., Heckbert, S. R., Fox, E. R., O'Donnell, C. J., Uitterlinden, A. G., Rotter, J. I., Willerson, J. T., Levy, D., van Duijn, C. M., Psaty, B. M., Witteman, J. C., Boerwinkle, E. and Vasan, R. S. (2010) 'Association of genome-wide variation with the risk of incident heart failure in adults of European and African ancestry: a prospective meta-analysis from the cohorts for heart and aging research in genomic epidemiology (CHARGE) consortium', *Circ Cardiovasc Genet*, 3(3), 256-66.

Soeki, T. and Sata, M. (2016) 'Inflammatory Biomarkers and Atherosclerosis', *Int Heart J*, 57(2), 134-9.

Soond, S. M., Carroll, C., Townsend, P. A., Sayan, E., Melino, G., Behrmann, I., Knight, R. A., Latchman, D. S. and Stephanou, A. (2007) 'STAT1 regulates p73-mediated Bax gene expression', *FEBS Lett*, 581(6), 1217-26.

Spilianakis, C. G. and Flavell, R. A. (2004) 'Long-range intrachromosomal interactions in the T helper type 2 cytokine locus', *Nat Immunol*, 5(10), 1017-27.

Spitz, F. and Furlong, E. E. (2012) 'Transcription factors: from enhancer binding to developmental control', *Nat Rev Genet*, 13(9), 613-26.

Spivakov, M. (2014) 'Spurious transcription factor binding: non-functional or genetically redundant?', *Bioessays,* 36(8), 798-806.

Stephanou, A., Brar, B. K., Knight, R. A. and Latchman, D. S. (2000) 'Opposing actions of STAT-1 and STAT-3 on the Bcl-2 and Bcl-x promoters', *Cell Death Differ,* 7(3), 329-30.

Steucke, K. E., Tracy, P. V., Hald, E. S., Hall, J. L. and Alford, P. W. (2015) 'Vascular smooth muscle cell functional contractility depends on extracellular mechanical properties', *J Biomech,* 48(12), 3044-51.

Strickland, I. and Ghosh, S. (2006) 'Use of cell permeable NBD peptides for suppression of inflammation', *Ann Rheum Dis,* 65 Suppl 3, iii75-82.

Strobl, L. J. and Eick, D. (1992) 'Hold back of RNA polymerase II at the transcription start site mediates down-regulation of c-myc in vivo', *EMBO J,* 11(9), 3307-14.

Sukhanov, S., Higashi, Y., Shai, S. Y., Vaughn, C., Mohler, J., Li, Y., Song, Y. H., Titterington, J. and Delafontaine, P. (2007) 'IGF-1 reduces inflammatory responses, suppresses oxidative stress, and decreases atherosclerosis progression in ApoE-deficient mice', *Arterioscler Thromb Vasc Biol,* 27(12), 2684-90.

Sunryd, J. C., Cheon, B., Graham, J. B., Giorda, K. M., Fissore, R. A. and Hebert, D. N. (2014) 'TMTC1 and TMTC2 are novel endoplasmic reticulum tetratricopeptide repeat-containing adapter proteins involved in calcium homeostasis', *J Biol Chem,* 289(23), 16085-99.

Swiecki, M. and Colonna, M. (2011) 'Type I interferons: diversity of sources, production pathways and effects on immune responses', *Curr Opin Virol,* 1(6), 463-75.

Tabas, I. and Glass, C. K. (2013) 'Anti-inflammatory therapy in chronic disease: challenges and opportunities', *Science,* 339(6116), 166-72.

Tamassia, N., Calzetti, F., Ear, T., Cloutier, A., Gasperini, S., Bazzoni, F., McDonald, P. P. and Cassatella, M. A. (2007) 'Molecular mechanisms underlying the synergistic induction of CXCL10 by LPS and IFN-gamma in human neutrophils', *Eur J Immunol,* 37(9), 2627-34.

Tamassia, N., Castellucci, M., Rossato, M., Gasperini, S., Bosisio, D., Giacomelli, M., Badolato, R., Cassatella, M. A. and Bazzoni, F. (2010) 'Uncovering an IL-10-dependent NF-kappaB recruitment to the IL-1ra promoter that is impaired in STAT3 functionally defective patients', *FASEB J,* 24(5), 1365-75.

Tan, W., Wang, H., Chen, Y., Zhang, X., Zhu, H., Yang, C., Yang, R. and Liu, C. (2011) 'Molecular aptamers for drug delivery', *Trends Biotechnol,* 29(12), 634-40.

Teicher, B. A. (2019) 'CD248: A therapeutic target in cancer and fibrotic diseases', *Oncotarget,* 10(9), 993-1009.

Thacker, S. G., Berthier, C. C., Mattinzoli, D., Rastaldi, M. P., Kretzler, M. and Kaplan, M. J. (2010) 'The detrimental effects of IFN-α on vasculogenesis in lupus are mediated by repression of IL-1 pathways: potential role in atherogenesis and renal vascular rarefaction', *J Immunol,* 185(7), 4457-69.

Thacker, S. G., Zhao, W., Smith, C. K., Luo, W., Wang, H., Vivekanandan-Giri, A., Rabquer, B. J., Koch, A. E., Pennathur, S., Davidson, A., Eitzman, D. T. and Kaplan, M. J. (2012) 'Type I interferons modulate vascular function, repair, thrombosis, and plaque progression in murine models of lupus and atherosclerosis', *Arthritis Rheum,* 64(9), 2975-85.

Thorvaldsdóttir, H., Robinson, J. T. and Mesirov, J. P. (2013) 'Integrative Genomics Viewer (IGV): high-performance genomics data visualization and exploration', *Brief Bioinform,* 14(2), 178-92.

Tie, F., Banerjee, R., Stratton, C. A., Prasad-Sinha, J., Stepanik, V., Zlobin, A., Diaz, M. O., Scacheri, P. C. and Harte, P. J. (2009) 'CBP-mediated acetylation of histone H3 lysine 27 antagonizes Drosophila Polycomb silencing', *Development,* 136(18), 3131-41.

Tselepis, A. D. and John Chapman, M. (2002) 'Inflammation, bioactive lipids and atherosclerosis: potential roles of a lipoprotein-associated phospholipase A2, platelet activating factor-acetylhydrolase', *Atheroscler Suppl,* 3(4), 57-68.

Turkson, J. and Jove, R. (2000) 'STAT proteins: novel molecular targets for cancer drug discovery', *Oncogene,* 19(56), 6613-26.

van Thiel, B. S., van der Pluijm, I., Kanaar, R., Danser, A. H. J. and Essers, J. (2017) '*Structure and cell biology of the vessel wall*' in *The ESC Textbook of Vascular Biology*.

Vasan, R. S. (2006) 'Biomarkers of cardiovascular disease: molecular basis and practical considerations', *Circulation,* 113(19), 2335-62.

Venkataraman, C., Leung, S., Salvekar, A., Mano, H. and Schindler, U. (1999) 'Repression of IL-4-induced gene expression by IFN-gamma requires Stat1 activation', *J Immunol,* 162(7), 4053-61.

Venturin, M., Carra, S., Gaudenzi, G., Brunelli, S., Gallo, G. R., Moncini, S., Cotelli, F. and Riva, P. (2014) 'ADAP2 in heart development: a candidate gene for the occurrence of cardiovascular malformations in NF1 microdeletion syndrome', *J Med Genet,* 51(7), 436-43.

Volger, O. L., Fledderus, J. O., Kisters, N., Fontijn, R. D., Moerland, P. D., Kuiper, J., van Berkel, T. J., Bijnens, A. P., Daemen, M. J., Pannekoek, H. and Horrevoets, A. J. (2007) 'Distinctive expression of chemokines and transforming growth factor-beta signaling in human arterial endothelium during atherosclerosis', *Am J Pathol,* 171(1), 326-37.

Volobueva, A., Zhang, D., Grechko, A. V. and Orekhov, A. N. (2018) 'Foam cell formation and cholesterol trafficking and metabolism disturbances in atherosclerosis', *Cor et Vasa*.

Wada, H., Hasegawa, K., Morimoto, T., Kakita, T., Yanazume, T. and Sasayama, S. (2000) 'A p300 protein as a coactivator of GATA-6 in the transcription of the smooth muscle-myosin heavy chain gene', *J Biol Chem,* 275(33), 25330-5.

Waldo, S. W., Li, Y., Buono, C., Zhao, B., Billings, E. M., Chang, J. and Kruth, H. S. (2008) 'Heterogeneity of human macrophages in culture and in atherosclerotic plaques', *Am J Pathol,* 172(4), 1112-26.

Wang, J., Paradis, P., Aries, A., Komati, H., Lefebvre, C., Wang, H. and Nemer, M. (2005) 'Convergence of protein kinase C and JAK-STAT signaling on transcription factor GATA-4', *Mol Cell Biol,* 25(22), 9829-44.

Wang, J., Razuvaev, A., Folkersen, L., Hedin, E., Roy, J., Brismar, K. and Hedin, U. (2012) 'The expression of IGFs and IGF binding proteins in human carotid atherosclerosis, and the possible role of IGF binding protein-1 in the regulation of smooth muscle cell proliferation', *Atherosclerosis,* 220(1), 102-9.

Wang, S., Raven, J. F. and Koromilas, A. E. (2010) 'STAT1 represses Skp2 gene transcription to promote p27Kip1 stabilization in Ras-transformed cells', *Mol Cancer Res,* 8(5), 798-805.

Wang, X. Q., Panousis, C. G., Alfaro, M. L., Evans, G. F. and Zuckerman, S. H. (2002) 'Interferon-gamma-mediated downregulation of cholesterol efflux and ABC1 expression is by the Stat1 pathway', *Arterioscler Thromb Vasc Biol,* 22(5), e5-9.

Wesoly, J., Szweykowska-Kulinska, Z. and Bluyssen, H. A. (2007) 'STAT activation and differential complex formation dictate selectivity of interferon responses', *Acta Biochim Pol,* 54(1), 27-38.

Whitman, S. C., Ravisankar, P., Elam, H. and Daugherty, A. (2000) 'Exogenous interferon-gamma enhances atherosclerosis in apolipoprotein E-/- mice', *Am J Pathol,* 157(6), 1819-24.

WHO (2018) 'World health statistics 2018: monitoring health for the SDGs, sustainable development goals',

Wienerroither, S., Shukla, P., Farlik, M., Majoros, A., Stych, B., Vogl, C., Cheon, H., Stark, G. R., Strobl, B., Müller, M. and Decker, T. (2015) 'Cooperative Transcriptional Activation of Antimicrobial Genes by STAT and NF-κB Pathways by Concerted Recruitment of the Mediator Complex', *Cell Rep,* 12(2), 300-12.

Witztum, J. L. and Lichtman, A. H. (2014) 'The influence of innate and adaptive immune responses on atherosclerosis', *Annu Rev Pathol,* 9, 73-102.

Wort, S. J., Ito, M., Chou, P. C., Mc Master, S. K., Badiger, R., Jazrawi, E., de Souza, P., Evans, T. W., Mitchell, J. A., Pinhu, L., Ito, K. and Adcock, I. M. (2009) 'Synergistic induction of endothelin-1 by tumor necrosis factor alpha and interferon gamma is due to enhanced NF-kappaB binding and histone acetylation at specific kappaB sites', *J Biol Chem,* 284(36), 24297-305.

Wu, W. Z., Sun, H. C., Shen, Y. F., Chen, J., Wang, L., Tang, Z. Y., Iliakis, G. and Liu, K. D. (2005) 'Interferon alpha 2a down-regulates VEGF expression through PI3 kinase and MAP kinase signaling pathways', *J Cancer Res Clin Oncol,* 131(3), 169-78.

Xia, Z., Gu, M., Jia, X., Wang, X., Wu, C., Guo, J., Zhang, L., Du, Y. and Wang, J. (2018) 'Integrated DNA methylation and gene expression analysis identifies SLAMF7 as a key regulator of atherosclerosis', *Aging (Albany NY),* 10(6), 1324-1337.

Xu, X., Lin, H., Lv, H., Zhang, M. and Zhang, Y. (2007) 'Adventitial lymphatic vessels -- an important role in atherosclerosis', *Med Hypotheses,* 69(6), 1238-41.

Xu, Z., Azordegan, N., Zhao, Z., Le, K., Othman, R. A. and Moghadasian, M. H. (2009) 'Pro-atherogenic effects of probucol in apo E-KO mice may be mediated through alterations in immune system: Parallel alterations in gene expression in the aorta and liver', *Atherosclerosis,* 206(2), 427-33.

Xu, Z., Ji, G., Shen, J., Wang, X., Zhou, J. and Li, L. (2012) 'SOX9 and myocardin counteract each other in regulating vascular smooth muscle cell differentiation', *Biochem Biophys Res Commun,* 422(2), 285-90.

Ye, X., Liu, H., Gong, Y. S. and Liu, S. F. (2015) 'LPS Down-Regulates Specificity Protein 1 Activity by Activating NF-κB Pathway in Endotoxemic Mice', *PLoS One,* 10(6), e0130317.

Yin, F. and Herring, B. P. (2005) 'GATA-6 can act as a positive or negative regulator of smooth muscle-specific gene expression', *J Biol Chem,* 280(6), 4745-52.

You, L. R., Lin, F. J., Lee, C. T., DeMayo, F. J., Tsai, M. J. and Tsai, S. Y. (2005) 'Suppression of Notch signalling by the COUP-TFII transcription factor regulates vein identity', *Nature,* 435(7038), 98-104.

Yu, H., Moran, C. S., Trollope, A. F., Woodward, L., Kinobe, R., Rush, C. M. and Golledge, J. (2016) 'Angiopoietin-2 attenuates angiotensin II-induced aortic aneurysm and atherosclerosis in apolipoprotein E-deficient mice', *Sci Rep*, 6, 35190.

Yu, X. H., Fu, Y. C., Zhang, D. W., Yin, K. and Tang, C. K. (2013) 'Foam cells in atherosclerosis', *Clin Chim Acta*, 424, 245-52.

Zambelli, F., Pesole, G. and Pavesi, G. (2009) 'Pscan: finding over-represented transcription factor binding site motifs in sequences from co-regulated or co-expressed genes', *Nucleic Acids Res*, 37(Web Server issue), W247-52.

Zaret, K. S. and Carroll, J. S. (2011) 'Pioneer transcription factors: establishing competence for gene expression', *Genes Dev*, 25(21), 2227-41.

Zeller, T., Hughes, M., Tuovinen, T., Schillert, A., Conrads-Frank, A., Ruijter, H., Schnabel, R. B., Kee, F., Salomaa, V., Siebert, U., Thorand, B., Ziegler, A., Breek, H., Pasterkamp, G., Kuulasmaa, K., Koenig, W. and Blankenberg, S. (2014) 'BiomarCaRE: rationale and design of the European BiomarCaRE project including 300,000 participants from 13 European countries', *Eur J Epidemiol*, 29(10), 777-90.

Zhang, D. X. and Glass, C. K. (2013) 'Towards an understanding of cell-specific functions of signal-dependent transcription factors', *J Mol Endocrinol*, 51(3), T37-50.

Zhang, Y., Liu, T., Meyer, C. A., Eeckhoute, J., Johnson, D. S., Bernstein, B. E., Nusbaum, C., Myers, R. M., Brown, M., Li, W. and Liu, X. S. (2008) 'Model-based analysis of ChIP-Seq (MACS)', *Genome Biol*, 9(9), R137.

Zhao, J., Kong, H. J., Li, H., Huang, B., Yang, M., Zhu, C., Bogunovic, M., Zheng, F., Mayer, L., Ozato, K., Unkeless, J. and Xiong, H. (2006) 'IRF-8/interferon (IFN) consensus sequence-binding protein is involved in Toll-like receptor (TLR) signaling and contributes to the cross-talk between TLR and IFN-gamma signaling pathways', *J Biol Chem*, 281(15), 10073-80.

Zhong, H., Voll, R. E. and Ghosh, S. (1998) 'Phosphorylation of NF-kappa B p65 by PKA stimulates transcriptional activity by promoting a novel bivalent interaction with the coactivator CBP/p300', *Mol Cell*, 1(5), 661-71.

Zhou, G., Soufan, O., Ewald, J., Hancock, R. E. W., Basu, N. and Xia, J. (2019) 'NetworkAnalyst 3.0: a visual analytics platform for comprehensive gene expression profiling and meta-analysis', *Nucleic Acids Res*, 47(W1), W234-W241.

Zhu, B., Zhao, G., Witte, D. P., Hui, D. Y. and Fagin, J. A. (2001) 'Targeted overexpression of IGF-I in smooth muscle cells of transgenic mice enhances neointimal formation through increased proliferation and cell migration after intraarterial injury', *Endocrinology*, 142(8), 3598-606.

Zhu, S., Cao, L., Yu, Y., Yang, L., Yang, M., Liu, K., Huang, J., Kang, R., Livesey, K. M. and Tang, D. (2013) 'Inhibiting autophagy potentiates the anticancer activity of IFN1@/IFNα in chronic myeloid leukemia cells', *Autophagy*, 9(3), 317-27.

Zimmermann, A., Trilling, M., Wagner, M., Wilborn, M., Bubic, I., Jonjic, S., Koszinowski, U. and Hengel, H. (2005) 'A cytomegaloviral protein reveals a dual role for STAT2 in IFN-{gamma} signaling and antiviral responses', *J Exp Med*, 201(10), 1543-53.

List of Figures

List of Tables

List of important Abbreviations

CVD	- Cardiovascular Disease(s)
ChIP	- Chromatin Immunoprecipitation
DC	- Dendritic Cell(s)
EC	- Endothelial Cell(s)
FC	- Fold Change
GO	- Gene Ontology
HAT	- Histone Acetyltransferase(s)
HDAC	- Histone Deacetylase(s)
IFN	- Interferon(s)
IRF	- IFN Regulatory Factor(s)
ISRE	- IFN-Stimulated Response Element
GAF	- Gamma-activated Factor
GAS	- IFN gamma-activated Sequence
ISG	- Interferon-stimulated Gene(s)
JAK-STAT	- Janus kinase-Signal Transducers and Activators of Transcription
LDTF	- Lineage-Determining TF
LPS	- Lipopolysaccharide
MΦ	- Macrophage(s)
ox-LDL	- Oxidized Low-density Lipoprotein(s)
PRR	- Pattern Recognition Receptor(s)
PAMP	- Pattern-Associated Molecular Pattern(s)
DAMP	- Damage-Associated Molecular Pattern(s)
ROS	- Reactive Oxygen Species
RPKM	- Reads Per Kilobase Million
RT-PCR	- Real-Time Polymerase Chain Reaction (RT-PCR)
SI	- Signal Integration
SDTF	- Signal-Dependent TF
TLR	- Toll-like Receptor(s)
TF	- Transcription Factor(s)
VSMC	- Vascular Smooth Muscle Cell(s)

List of publications

Piaszyk-Borychowska, A., Széles, L., Csermely, A., Chiang, H. C., Wesoły, J., Lee, C. K., Nagy, L. and Bluyssen, H. A. R. (2019) 'Signal Integration of IFN-I and IFN-II With TLR4 Involves Sequential Recruitment of STAT1-Complexes and NFκB to Enhance Pro-inflammatory Transcription', Front Immunol, 10, 1253.

Antonczyk, A., Krist, B., Sajek, M., Michalska, A., **Piaszyk-Borychowska, A.**, Plens-Galaska, M., Wesoly, J. and Bluyssen, H. A. R. (2019) 'Direct Inhibition of IRF-Dependent Transcriptional Regulatory Mechanisms Associated With Disease', Front Immunol, 10, 1176.

Szelag, M., **Piaszyk-Borychowska, A.**, Plens-Galaska, M., Wesoly, J. and Bluyssen, H. A. (2016) 'Targeted inhibition of STATs and IRFs as a potential treatment strategy in cardiovascular disease', Oncotarget, 7(30), 48788-48812.

Chmielewski, S., **Piaszyk-Borychowska, A.**, Wesoly, J. and Bluyssen, H. A. (2016) 'STAT1 and IRF8 in Vascular Inflammation and Cardiovascular Disease: Diagnostic and Therapeutic Potential', Int Rev Immunol, 35(5), 434-454.

Acknowledgments

I would like to thank my supervisor, Prof. Hans Bluyssen, for his constant support and priceless scientific advice throughout the whole period of my PhD studies.

Moreover, I would like to thank the reviewers of this thesis, Prof. Katarzyna Kwiatkowska and Prof. Alicja Józkowicz, for taking time to review my work.

Many thanks goes to the entire team at Department of Human Molecular Genetics and Laboratory of High Throughput Technologies for countless advice, help and fantastic atmosphere. In particular, my gratitude goes to: Agata Michalska, Martyna Plens-Gałąska, Aleksandra Antończyk, Hanna Nowicka and Katarzyna Błaszczyk, for everyday mental support, exchanging experience and sharing PhD student 'lablife'.

I would like to express my gratitude to the whole team of Prof. Laszlo Nagy from the University of Debrecen in Hungary (Department of Biochemistry and Molecular Biology) for their incredible support during my stay at their facilities and opportunity to learn new techniques and gain new laboratory skills.

Ponadto składam podziękowania moim Rodzicom za ich nieustanne wsparcie, motywację i bezgraniczną wiarę w moje możliwości. Specjalne podziękowania kieruję do moich przyjaciół, bez wsparcia których nie osiągnęłabym wyznaczonego celu. Na końcu dziękuję mojemu ukochanemu mężowi Michałowi - za codzienną troskę, dzielenie sukcesów i wsparcie w trudnych chwilach, ogromną motywację do działania oraz wyrozumiałość.

Streszczenie w języku polskim

Schorzenia układu sercowo-naczyniowego, w tym miażdżyca naczyń krwionośnych, stanowią główną przyczynę śmiertelności na świecie. Obecnie jako kluczowy czynnik etiologiczny miażdżycy wymienia się chroniczną aktywację odpowiedzi immunologicznej w obrębie naczyń krwionośnych. W reakcji na szereg czynników środowiskowych, dochodzi do uszkodzenia warstwy śródbłonka naczyń i nadmiernej ekspresji czynników prozapalnych takich jak chemokiny, cytokiny i cząsteczki adhezyjne, zarówno przez komórki budujące ścianę naczyń (komórki mięśniówki gładkiej naczyń krwionośnych), jak i komórki układu odpornościowego (makrofagi i komórki dendrytyczne), infiltrujące naczynia krwionośne. Wraz z akumulacją cząsteczek lipidowych, prowadzi to do powstania płytki miażdżycowej, zmniejszenia światła naczyń krwionośnych, a w konsekwencji ograniczonej dystrybucji tlenu i substancji odżywczych niesionych wraz z krwią do wszystkich organów ciała.

Istotną rolę w mediacji odpowiedzi zapalnej naczyń krwionośnych odgrywa integracja sygnałowa (SI) pomiędzy szlakami przekazywania sygnału aktywowanymi przez interferon gamma (IFNγ), alfa (IFNα) oraz czynniki wpływające na receptor Toll-podobny 4 (TLR4), jak lipopolisacharyd (LPS). Odpowiednio, szlaki JAK-STAT oraz TLR4 współdziałają ze sobą poprzez aktywację białek STAT1 oraz NFκB. Jak wykazały wcześniejsze badania, SI mediowana przez powyższe czynniki transkrypcyjne stanowi mechanizm indukujący silną i intensywną odpowiedź komórek układu immunologicznego.

Dane przedstawione w rozdziale drugim niniejszej pracy dowodzą, że podobna integracja sygnałowa zarówno pomiędzy IFNγ-, jak i IFNα-zależnym szlakiem JAK-STAT oraz LPS-zależnym szlakiem TLR4, mediuje synergiczną ekspresję genów prozapalnych za pośrednictwem kompleksów transkrypcyjnych STAT1 i NFκB, także w komórkach mięśniówki gładkiej naczyń krwionośnych. Całogenomowa analiza transkryptomu (RNA-seq) połączona z immunoprecypitacją chromatyny (ChIP-seq) w pierwotnych komórkach immunologicznych (makrofagach i komórkach dendrytycznych) oraz komórkach mięśniówki gładkiej naczyń krwionośnych traktowanych IFNα, IFNγ oraz LPS, pozwoliła na odkrycie nowego mechanizmu SI. Udowodniono, że kompleksy transkrypcyjne GAF, ISGF3 oraz STAT1-IRF9 współdziałają z kompleksami NFκB, wiążąc się do miejsc kompozytowych GAS/ISRE oraz NFκB znajdujących się w bliskiej odległości w łańcuchu DNA, dzięki STAT1-zależnej otwartej konformacji chromatyny.

W rozdziale trzecim podano natomiast argumenty na istnienie SI pomiędzy szlakami JAK-STAT i TLR4 w kontekście obniżonej ekspresji genów prozapalnych. Potwierdzono wiązanie IFNγ+LPS-zależnych czynników transkrypcyjnych STAT1 oraz NFκB w regionach regulatorowych genów o obniżonej ekspresji oraz wykazano zależność ekspresji od czynnika STAT1 w komórkach mięśniówki gładkiej naczyń krwionośnych pozbawionych STAT1 (STAT1 KO). Zaproponowano także potencjalny mechanizm leżący u podstaw powyższych obserwacji, w którym czynniki transkrypcyjne STAT1 oraz NFκB pośredniczą w negatywnym znakowaniu histonów oraz wiązaniu korepresorów transkrypcji lub usuwaniu jej koaktywatorów.

Rozdział czwarty zawiera serię eksperymentów, które potwierdziły rolę czynnika STAT1 w IFNγ-zależnej ekspresji genów, specyficznej dla komórek śródbłonka naczyń krwionośnych. Wcześniej dowiedziono, że komórkowo specyficzna regulacja transkrypcji w komórkach układu immunologicznego, takich jak makrofagi, mediowana jest poprzez hierarchiczne współdziałanie Komórkowo-specyficznych czynników transkrypcyjnch (np. PU.1), charakteryzujących się zdolnością do działania w kontekście zamkniętej chromatyny oraz indukowanych sygnałem, Sygnałowo-specyficznych czynników transkrypcyjnych (takich jak aktywowany IFNγ STAT1). W niniejszym rozdziale potwierdzono, że podobny mechanizm, oparty na działaniu analogicznego komórkowo-specyficznego czynnika może być funkcjonalny w komórkach śródbłonka naczyń krwionośnych i regulować dostępność chromatyny dla IFNγ-zależnego białka STAT1 w komórkowo-specyficznych regionach genomowych.

W rozdziale piątym wyniki przedstawionych badań zostały podsumowane oraz przeanalizowane pod kątem potencjalnych możliwości ich aplikacji w diagnostyce oraz terapii chorób układu sercowo-naczyniowego.

Summary in English

Cardiovascular diseases, including atherosclerosis, are the leading cause of mortality world-wide. Nowadays, chronic activation of immunological response in the vessels is considered as the main etiological factor of atherosclerosis. Exposition to the numerous external cues, leads to the endothelium damage and excessive expression of pro-inflammatory stimuli, including chemokines, cytokines and adhesion molecules by vascular cells (vascular smooth muscle cells), as well as immune cells (macrophages and dendritic cells), infiltrating inflamed vessels. Lipid particles accumulation, leads to atherosclerotic plaque build-up, narrowing of the vessel lumen, and limited distribution of an oxygen and nutrients carried with the blood to all organs in the body.

Signal Integration (SI) between molecular pathways activated by interferon gamma (IFNγ), alpha (IFNα) and Toll-like receptor 4(TLR4)-inducers, like lipopolisaccharide (LPS), plays crucial role in mediating vascular pro-inflammatory response. JAK-STAT and TLR4 signaling pathways collaborate through STAT1 and NFκB transcription factors. As shown previously, STAT1- and NFκB-dependent SI serves the mechanism inducing robust pro-inflammatory response of immune cells.

Data presented in chapter two of this thesis prove, that a similar SI between IFNγ-, but also IFNα-dependent JAK-STAT pathway and LPS-dependent TLR4 pathway, mediates synergistic expression of pro-inflammatory genes, through STAT1- and NFκB-containing transcriptional complexes also in vascular smooth muscle cells. Genome-wide transcriptome analysis (RNA-seq) combined with chromatin immunoprecipitation (ChIP-seq) in primary immune cells (macrophages and dendritic cells) and vascular smooth muscle cells, treated with IFNα, IFNγ and LPS let to identify a new mechanism of SI. It was shown that transcriptional complexes GAF, ISGF3 and STAT1-IRF9 collaborate with NFκB, binding to GAS/ISRE and NFκB composite sites, closely spaced on DNA, in the regions of an open chromatin in STAT1-dependent way.

In chapter three, there was provided evidence for the existence of SI between JAK-STAT and TLR4 pathways in the context of pro-inflammatory gene down-regulation. Binding of IFNγ+LPS-dependent STAT1 and NFκB in the regulatory regions of repressed genes and STAT1-dependence of gene expression in STAT1 KO vascular smooth muscle cells, was proven. Moreover, it was proposed a potential mechanism underlying abovementioned

observations, where STAT1 and NFκB mediate the negative histone mark deposition and recruitment of transcriptional co-repressors or removal of co-activators.

In chapter four, there were presented experiments, which confirmed a role of STAT1 in IFNγ-dependent vascular smooth muscle cell-specific gene expression. Previously it was reported, that cell type-specific gene expression in immune cells, like macrophages, is mediated through hierarchical collaboration of Lineage-determining transcription factors (f.ex. PU.1) characterized by an ability to act in the context of closed chromatin and Signal-dependent transcription factors (like IFNγ-dependent STAT1). In this chapter it was proved that a similar mechanism, based on collaboration of an analogical cell type-specific factor could be functional in vascular smooth muscle cells and regulate chromatin accessibility for IFNγ-dependent STAT1 in cell type-specific genomic regions.

In chapter five, presented results were summarized and analyzed in the context of their potential application in the development of diagnostics and therapies against cardiovascular diseases.